The Tensile Material Properties of Plastic Concrete and the Influence on Plastic Cracking

By:

Mohammed Yaseen Khan

Thesis presented in fulfilment of the requirements for the degree of

Master of Engineering in the Faculty of Engineering at

Stellenbosch University

Supervisor: Dr. Riaan Combrinck

March 2018

Declaration

By submitting this thesis electronically, I declare that the entirety of the work contained therein is my own, original work, that I am the sole author thereof (save to the extent explicitly otherwise stated), that reproduction and publication thereof by Stellenbosch University will not infringe any third party rights and that I have not previously in its entirety or in part submitted it for obtaining any qualification.

March 2018

Signature:

Summary

During the plastic state of concrete, two forms of volume change exist, namely: plastic settlement which refers to the gravitational settlement of solid particles, which in turn displaces bleed water to the surface of the concrete, as well as plastic shrinkage which occurs directly after plastic settlement and can be explained as the rapid removal of water from the capillary pores of concrete, due to ongoing evaporation. However, a change in volume is only detrimental to the concrete body if restrained, for example by reinforcing steel embedded within the concrete body.

Any hindrance or resistance of the free volume change in plastic concrete induces tensile stresses and or strains in the concrete element. Crack formation is expected to occur if the tensile stress and strain induced within the concrete is greater than the tensile strength or strain capacity of the concrete. Another often overlooked factor that also influences the plastic cracking potential of concrete is relaxation. However, performing relaxation tests on plastic concrete presents great difficulty. Due to this, literature on the tensile and relaxation behaviour of plastic concrete is scarce and therefore a significant knowledge gap exists on the influence of tensile properties on the cracking behaviour of plastic concrete.

In light of this, the main objectives of this study are to investigate the tensile behaviour and relaxation properties of plastic concrete as well as the rheological influence on these properties. Once the tensile properties are fundamentally understood, the influence of a viscosity modifying agent on the cracking behaviour of plastic concrete is addressed. Lastly the influence of initial curing on the cracking behaviour of plastic concrete is also investigated.

Investigation into the tensile properties and relaxation behaviour of plastic concrete was carried out using a direct tensile testing machine, on specimens at hourly intervals up to after the final setting time of the concrete. The tests showed that the tensile strength of plastic concrete increases exponentially from the initial setting time of the concrete, while a significant reduction in strain capacity was observed between initial and final setting times. Furthermore, results indicate that the relaxation behaviour of concrete is dependent on the rate of hydration, with maximum relaxation potential occurring during the stiffening phase of concrete and reducing significantly as the concrete enters the setting and hardening phases.

Multiple loading results showed the resilient nature of a still plastic concrete which is capable of withstanding multiple loading cycles. Capillary pressure measurements during tensile tests revealed that the mechanism behind relaxation is the negative capillary pressure build-up induced by the mechanical tensile strain.

The addition of the viscosity modifying agent (VMA) significantly reduced the tensile strength of the concrete during the setting and hardened phases. Furthermore, relaxation tests indicate that the addition of VMA increased both the relaxation potential, as well as the ability to complete multiple loading cycles, compared to the reference mix. The cracking behaviour after the addition of the VMA, displayed an increase in crack area. The lower tensile strength, the increase in slump and the slightly retarded setting time is believed to be the cause of this observation.

Initial curing results, indicate that curing applied before air entry, relieves a greater amount of stress build-up and therefore a larger reduction in crack area, compared to curing applied before the build-up in capillary pressure. The addition of a VMA resulted in a larger stress reduction, compared to the reference mix. Furthermore, results indicate that applying curing procedures only once is not sufficient in preventing plastic cracking. However, if this is the only option, curing applied just before point of air entry has greater benefits in terms of crack area reduction compared to curing applied before the build-up in capillary pressure.

Opsomming

Gedurende die plastiek toestand van beton is daar twee vorms van volume verandering, naamlik: plastiek versakking wat verwys na die versakking van soliede deeltjies weens gravitasie wat op sy beurt bloei water na die oppervlak van die beton verplaas sowel as plastiek krimping wat plaasvind direk na plastiek versakking en beskryf kan word as die vinnige verwydering van water uit die kapillêre porie van beton, as gevolg van voortdurende verdamping. ʼn Verandering in volume is egter slegs nadelig indien dit verhinder word, byvoorbeeld deur staal in die betonliggaam.

Enige hindernis van die vrye volume verandering in plastiek beton induseer trek spanning en vervormings in die beton element. Krake kom voor indien die gedurende trekspanning en vervormings groter is as die treksterkte en vervormings kapasiteit van die beton. Nog ʼn faktor wat dikwels oor die hoof gesien word en wil die plastiese kraak potensiaal van beton beïnvloed is ontspanning. Die uitvoering van ontspannings toetse op plastiek beton is egter ʼn groot uitdaging. As gevolg van hierdie is, literatuur oor die trek en ontspanninggedrag van plastiek beton is skaars en dus is daar 'n beduidende kennis gaping op die invloed van trek eienskappe op die kraakgedrag van plastiek beton.

In die lig hiervan, is die hoofdoelwitte van hierdie studie om die trekgedrag en ontspanning eienskappe van plastiek beton sowel as die reologiese invloed op dié eienskappe te ondersoek. Sodra die trek eienskappe fundamenteel verstaan word, kan die invloed van viskositeit op die kraakgedrag van plastiek beton aangespreek word. Laastens word die invloed van die aanvanklike kuring op die kraakgedrag van plastiek beton ook ondersoek.

Die trek eienskappe en ontspanning gedrag van plastiek beton is bepaal op monsters wat getoets is op uurlikse intervalle tot na die finale settyd met behulp van 'n direkte trek toetsmasjien. Die toetse het getoon dat die treksterkte van plastiese beton eksponensieel toeneem vanaf die aanvanklike settyd van die beton, terwyl 'n aansienlike vermindering in vervormings kapasiteit is plaasvind tussen die aanvanklike en finale settye. Verder resultate dui daarop dat die ontspanningsgedrag van beton afhang van die tempo van hidrasie, met 'n maksimum ontspannings potensiaal wat gedurende die verstywing fase van beton en aansienlik verminder tydens die set in verhoudings fases. Herhaalde belasting resultate dui op die soepelheid van plastiek beton wat verskeie belastings siklusse, kan weerstaan. Kapillêre

dru**k** lesing tydens trektoetse het gedui daarop dat die meganisme agter ontspanning die opbou van negatiewe kapillêre druk is.

Die byvoeging van die viskositeit verander agent (VMA) het die treksterkte van die beton gedurende die set en verharding fases aansienlik verminder. Verder onspannings toetse dui omgewing en geharde fases. Verder ontspanning toetse dui daarop dat die byvoeging van VMA beide die ontspannings potensiaal, sowel as die vermoë om verskeie belastings siklusse te voltooi verhoog, in vergelyking met die verwysing mengsel. Die kraakgedrag na die toevoeging van die VMA, het 'n toename in kraak area vertoon. Die laer treksterkte, die toename in uitsakking en die effens vertraagde settye is redes vir die waarneming.

Aanvanklike kuring resultate dui daarop dat kuring net voor lugtoegang ʼn groter hoeveelheid spanning en dus ook kraak verminder tot gevolg het in vergelyking met kuring voor dit ophou van kapillêre druk. Die byvoeging van VMA het gelei tot 'n groter spannings vermindering, in vergelyking met die verwysing mengsel. Verder wys die resultate daarop dat die eenmalige toepassing van kuring prosedures nie genoeg is vir die voorkoming van plastiese krake nie. Indien dit die enigste opsie is bied kuring net voor lugtoegang die grootste voordele in terme van kraak vermindering in vergelyking met kuring voordat kapillêre druk begin ophou.

Acknowledgements

I would like to thank the following people for their assistance and support during this study

- My supervisor, Dr. Riaan Combrinck for his continued support, guidance and assistance throughout this study.

- The laboratory and workshop staff at the Civil Engineering Department of Stellenbosch, for their assistance and conversation during the experimental portion of this study.

- The National Research Foundation for their financial support

- My Father, Mohammed Faizal Khan and Mother, Suhea Khan, for their continued support, motivation, encouragement, advice and giving me the opportunity to pursue my studies in Civil Engineering.

- My sister Ra'eesah Khan for her sense of humour and support during times of intense pressure and stress.

- Family and friends who have played a significant role throughout the study period

- My late grandfather, Yusuf Khan, whom I would like to present this study in honour of

- Finally, the Almighty for giving me the strength, will, ability and patience to conduct this study.

Table of Contents

DECLARATION .... **I**

SUMMARY .... **II**

OPSOMMING .... **IV**

ACKNOWLEDGEMENTS .... **VI**

TABLE OF CONTENTS .... **VII**

LIST OF FIGURES .... **XIV**

LIST OF TABLES .... **XIX**

CHAPTER 1: INTRODUCTION **1**

1.1 Objectives 3

1.2 Methodology 4

1.3 Research significance 4

1.4 Report outline 5

CHAPTER 2: BACKGROUND STUDY **7**

2.1 Concrete as a construction material 7

2.2 Concrete in its plastic state 9

2.2.1 Hydration of concrete 9

2.2.2 Setting times and finishing operations 12

2.2.3 Types of volume change in plastic concrete 13
2.3 RHEOLOGY 15
2.3.1 Defining Consistency 15
2.3.2 Factors relating to consistency 16
2.3.2.1 Shear stress 16
2.3.2.2 Rate of shear strain 17
2.3.2.3 Viscosity 17
2.3.2.4 Yield stress 17
2.3.3 Flow behaviour of Newtonian fluids 18
2.3.4 Flow behaviour of non-Newtonian fluids 19
2.3.4.1 Time independent fluids 19
2.3.4.2 Time dependent fluids 20
2.3.4.3 Viscoelastic fluids 21
2.3.5 The flow behaviour of fresh concrete 22
2.3.6 Viscosity modification agents 23
2.4 PLASTIC CRACKING OF CONCRETE 24
2.4.1 Plastic settlement cracking 25
2.4.2 Plastic shrinkage cracking 26
2.4.3 Influencing factors 30
2.4.4 Preventative measures 32
2.4.4.1 Plastic settlement cracking 33
2.4.4.2 Plastic shrinkage cracking 34
2.5 TENSILE MATERIAL PROPERTIES OF PLASTIC CONCRETE 35
2.5.1 Tensile Strength 36
2.5.2 Strain capacity 38

2.5.3 Elastic Modulus 39

2.5.4 Relaxation 41

2.6 Concluding summary 43

CHAPTER 3: EXPERIMENTAL FRAMEWORK 44

3.1 Environment simulation...44

3.2 Tensile tests 45

3.2.1 The tensile testing machine..45

3.2.1.1 The support beam...46

3.2.1.2 Mechanical actuator 47

3.2.1.3 Air bearing 48

3.2.1.4 Loading platforms...49

3.2.1.5 Tensile mould..50

3.2.1.6 Measurement devices..53

3.2.1.7 Data acquisition 58

3.2.2 Calibration..58

3.2.2.1 Calibration process...58

3.2.2.2 Calibration results 61

3.3 Plastic cracking tests 63

3.3.1 Influential factor tests 63

3.3.1.1 Plastic settlement, shrinkage and capillary pressure build-up moulds 63

3.3.1.2 Evaporation 67

3.3.1.3 Surface tension..67

3.3.1.4 Bleeding 68

3.3.1.5 Setting time 68

3.3.1.6 Rheology 69

3.3.2 Cracking tests 69

3.4 Mix specification 71

3.5 Material specifications 71

3.5.1 Viscosity modification agent 72

3.5.2 Water 72

3.5.3 Cement 72

3.5.4 Coarse aggregate 72

3.5.5 Fine aggregate 73

3.6 Experimental procedures 73

3.6.1 Climate conditions 74

3.6.2 Mixing procedures 75

3.6.3 Testing procedures 75

3.6.3.1 Tensile tests 76

3.6.3.2 Plastic cracking tests 77

3.7 Test program 83

3.8 Concluding summary 85

CHAPTER 4: TENSILE MATERIAL PROPERTIES - TEST RESULTS AND DISCUSSION 86

4.1 Influence of VMA on the mix properties of plastic concrete 86

4.1.1 Surface tension 87

4.1.2 Rheology 88

4.1.3 Setting time 90

4.2 TENSILE PROPERTIES 91

4.2.1 Stress versus strain 91

4.2.1.1 Stress versus Strain – Mix Ref 92

4.2.1.2 Stress versus Strain – Mix VMA 93

4.2.2 Tensile strength (Ft) 94

4.2.2.1 Tensile strength (Ft) – Mix Ref 95

4.2.2.2 Tensile strength (Ft) – Mix VMA 96

4.2.3 Strain capacity (ε_{cap}) 98

4.2.3.1 Strain capacity (ε_{cap}) – Mix Ref 98

4.2.3.2 Strain capacity (ε_{cap}) – Mix VMA 99

4.2.4 Young's modulus (E) 100

4.2.4.1 Young's modulus (E) – Mix Ref 101

4.2.4.2 Young's modulus – Mix VMA 102

4.2.5 Influence of capillary pressure on tensile behaviour 104

4.2.5.1 Influence of capillary pressure on tensile behaviour – Mix Ref 104

4.2.5.2 Influence of capillary pressure on tensile behaviour – Mix VMA 106

4.2.5.3 Development of capillary pressure with time 108

4.3 RELAXATION BEHAVIOUR UNDER SINGLE LOADING 111

4.3.1 Relaxation – Mix Ref 111

4.3.2 Relaxation – Mix VMA 114

4.4 RELAXATION BEHAVIOUR UNDER MULTIPLE LOADING 116

4.4.1 Multiple loading – Mix Ref 116

4.4.2 Multiple loading – Mix VMA 119

4.5 INFLUENCE OF CAPILLARY PRESSURE ON THE RELAXATION BEHAVIOUR OF CONCRETE 122

4.5.1 At 60 minutes 122

4.5.2 At 120 minutes 125

4.5.3 At 180 minutes 127

4.5.4 At 240 minutes 130

4.6 CONCLUDING SUMMARY 131

CHAPTER 5: CRACKING BEHAVIOUR – TEST RESULTS AND DISCUSSION .. 132

5.1 PLASTIC SHRINKAGE CRACKING BEHAVIOUR 132

5.1.1 Plastic cracking behaviour of Mix Ref 132

5.1.2 Plastic cracking behaviour of Mix VMA 135

5.2 INITIAL CURING PROCEDURES 143

5.2.1 Influence of initial curing on the build-up of capillary pressure 144

5.2.2 Influence of initial curing on plastic shrinkage 145

5.2.3 Influence of initial curing on crack area 147

5.3 INFLUENCE OF VISCOSITY AND CURING PROCEDURES ON THE CRACKING BEHAVIOUR OF CONCRETE 149

5.3.1 Influence of curing procedures on Mix Ref 149

5.3.2 Influence of curing procedures on Mix VMA 151

5.4 LINK BETWEEN THE TENSILE PROPERTIES AND CRACKING BEHAVIOUR OF PLASTIC CONCRETE 152

5.5 LINK BETWEEN THE RELAXATION BEHAVIOUR AND CURING BEHAVIOUR OF PLASTIC CONCRETE 153

5.6 CONCLUDING SUMMARY 155

CHAPTER 6: CONCLUSIONS AND RECOMMENDATIONS....................................156

6.1 INFLUENCE OF VMA ON THE RHEOLOGICAL PROPERTIES 156

6.2 THE TENSILE MATERIAL PROPERTIES OF PLASTIC CONCRETE 156

6.3 THE INFLUENCE OF VMA ON THE TENSILE MATERIAL PROPERTIES 158

6.4 THE RELAXATION BEHAVIOUR OF PLASTIC CONCRETE 159

6.5 THE INFLUENCE OF VMA ON THE RELAXATION BEHAVIOUR OF PLASTIC CONCRETE.....159

6.6 INFLUENCE OF VMA ON THE PLASTIC CRACKING BEHAVIOUR 160

6.7 INFLUENCE OF INITIAL CURING ON THE PLASTIC CRACKING BEHAVIOUR 161

6.8 INFLUENCE OF VMA ON CURING PROCEDURES 161

6.9 RECOMMENDATIONS 162

REFERENCES...163

List of figures

Figure 2-1: Stages of concrete hydration (Compiled by Combrinck 2016 as adapted from Powers, 1968; ACI 308R., 2001; Mehta & Monteiro, 2006; Sant et al., 2009; Domone & Illston, 2010) 10

Figure 2-2: Schematic representation of shear flow 16

Figure 2-3: Concrete yield stress 17

Figure 2-4: Relationship between yield stress and slump of fresh concrete (Domone et al., 1999) 18

Figure 2-5: Flow behaviour of fluids 19

Figure 2-6: Flow behaviour of time dependent fluids 20

Figure 2-7: The creep and relaxation behaviour of viscoelastic fluids 21

Figure 2-8: Bingham model representing the flow behaviour of fresh concrete (Coussot, 2012) 22

Figure 2-9: The mechanism behind settlement 26

Figure 2-10: Mechanism behind plastic shrinkage 27

Figure 2-11: Important stages and points during the build-up in capillary pressure, within the pore system of plastic concrete (Compiled by Combrinck 2016 as adapted from Slowik et al., 2008) 28

Figure 2-12: Pressure build-up due to the formation of water meniscus 29

Figure 2-13: Influence of shrinkage and viscoelasticity on concrete cracking (Troxell, 1956) 36

Figure 2-14: Comparison of tensile strength results by Nguyen et al. (2017). 37

Figure 2-15: Effectiveness of tensile strength models compared to experimental results by Nguyen et al. (2017) 37

Figure 2-16: (a) Strain capacity by Roziere et al. (2015) (b) Strain capacity by Nguyen et al. (2015) 39
Figure 2-17: Development of Elastic modulus with time by Dao et al. (2009) and Nguyen et al. (2017) 40
Figure 2-18: Relaxation phenomenon in concrete (Owens, 2009) 41
Figure 2-19: Influence of multiple loading on plastic concrete (Combrinck, 2016) 42
Figure 3-1: Climate chamber layout (Combrinck, 2012) 45
Figure 3-2: The tensile testing machine 46
Figure 3-3: Free loading platform attached to the mechanical linear actuator 47
Figure 3-4: Layout of support beam, loading platforms, actuator and air bearing 48
Figure 3-5: Aluminium tensile testing moulds 50
Figure 3-6: 1st and 2nd set of primary connectors 51
Figure 3-7: Mould assembly 52
Figure 3-8: Measuring apparatus 53
Figure 3-9: Side LVDT setup 54
Figure 3-10: Centre LVDT setup 55
Figure 3-11: Capillary pressure sensor layout 57
Figure 3-12: Setting up procedure 61
Figure 3-13: Dry run tensile test result 62
Figure 3-14: Capillary pressure, plastic shrinkage and plastic settlement test layout 64
Figure 3-15: Plastic settlement mould layout 65
Figure 3-16: Shrinkage mould layout 65
Figure 3-17: LVDT layout on shrinkage mould 66
Figure 3-18: Capillary pressure mould layout 67
Figure 3-19: Surface tension apparatus 68

Figure 3-20: Bleeding apparatus 68

Figure 3-21: Vicat needle apparatus 69

Figure 3-22: ICAR Rheometer 69

Figure 3-23: Cracking mould layout 70

Figure 3-24: Sand grading 73

Figure 3-25: Example of a cracked specimen analysed on CAD software 82

Figure 4-1: Effect of VMA concentration on surface tension 88

Figure 4-2: Bingham properties of plastic concrete with increasing dosages of VMA 89

Figure 4-3: The relationship between yield stress and slump of fresh concrete (Domone et al., 1999) 89

Figure 4-4: Setting times 91

Figure 4-5: Ascending part of stress versus strain curve, showing the definitions of the Young's modulus, tensile strength and strain capacity 92

Figure 4-6: Stress vs strain results for Mix Ref 93

Figure 4-7: Stress vs strain results for Mix VMA 94

Figure 4-8: Mix Ref Strength development with time 96

Figure 4-9: Strength development with time of Mix VMA vs Mix Ref 97

Figure 4-10: Strain capacity at different ages for Mix Ref 98

Figure 4-11: Strain capacity at different ages for Mix Ref vs Mix VMA 99

Figure 4-12: Method followed for the determination of the Young’s modulus in plastic concrete 101

Figure 4-13: Young’s modulus at different ages for Mix Ref 102

Figure 4-14: Young's modulus development with time for Mix VMA vs Mix Ref 103

Figure 4-15: Capillary pressure measurements for Mix Ref at 60, 120, 180 and 240 minute time periods 105

Figure 4-16: Capillary pressure measurements for Mix VMA at 60, 120, 180 and 240 minute time periods 107

Figure 4-17: influence of capillary pressure on internal concrete particles 109

Figure 4-18: Relaxation for test samples at 60 and 120 minute time periods 112

Figure 4-19: Relaxation for test samples at 180 and 360 minute time periods 113

Figure 4-20: Relaxation for test samples at 60 and 120 minute time periods (Mix VMA) .. 115

Figure 4-21: Relaxation for test samples at 180 and 240 minute time periods (Mix VMA) 115

Figure 4-22: Multiple loading results for test samples at 60 and 120 minute time periods (Mix Ref) 117

Figure 4-23: Multiple loading results for test samples at 180 and 240 minute time periods 118

Figure 4-24: Multiple loading results for test samples at 60 and 120 minute time periods (Mix VMA) 119

Figure 4-25: Multiple loading results for test samples at 180 and 240 minute (Mix VMA) 120

Figure 4-26: Multiple loading vs peak loads for Mix Ref and Mix VMA at 180 minutes ... 121

Figure 4-27: Relaxation behaviour of concrete and capillary pressure at 60 minutes 123

Figure 4-28: Relaxation behaviour during points of loading and unloading 124

Figure 4-29: The relaxation behaviour of concrete and capillary pressure at 120 minutes for Mix Ref 125

Figure 4-30: The relaxation behaviour of concrete and capillary pressure at 120 minutes for Mix VMA 127

Figure 4-31: The relaxation behaviour of concrete and capillary pressure at 180 minutes for Mix Ref 128

Figure 4-32: Relaxation behaviour of concrete and capillary pressure at 180 minutes for Mix VMA 129

Figure 4-33: The relaxation behaviour of concrete and capillary pressure at 240 minutes for Mix VMA 130

Figure 5-1: Plastic cracking behaviour for Mix Ref 133

Figure 5-2: Phenomenological plastic shrinkage cracking behaviour for Mix VMA 136

Figure 5-3: Comparison between Mix Ref and Mix VMA in terms of cumulative bleeding and evaporation 137

Figure 5-4: Settlement, shrinkage and capillary pressure build-up for Mix Ref and Mix VMA 139

Figure 5-5: Plastic shrinkage and capillary pressure build-up in both Mix Ref and Mix VMA 140

Figure 5-6: Measured crack areas for Mix Ref and Mix VMA 142

Figure 5-7: Identified critical points during capillary pressure build-up 143

Figure 5-8: Capillary pressure results at different initial curing critical points 145

Figure 5-9: Influence of initial curing on vertical shrinkage 146

Figure 5-10: Influence of initial curing on horizontal shrinkage 147

Figure 5-11: Influence of initial curing on crack area 148

Figure 5-12: Curing applied on Mix Ref at 165 minutes 150

Figure 5-13: Curing applied on Mix VMA at 165 minutes 151

List of tables

Table 1: Factors influencing the cracking behaviour of plastic concrete 31

Table 2: Material constituents, proportions and mix properties...71

Chapter 1: Introduction

Concrete can be defined as a composite material consisting of sand, stone, cement and water, which upon mixing, results in a stone-like mass once hardened (Owens, 2009). The use of concrete, dates back to as early as the third century BC where the Romans discovered that using volcanic ash with lime mortar, sand and gravel, produced a rock-hard substance, similar to modern concrete. Today concrete has evolved to one of the most widely used man made substances in the world. Its success is owed to its high compressive strength, permanence, durability, resistance to fire and water, as well as the ability to be mouldable into almost any shape (Shetty, 2008). These qualities allow for the innovative use of concrete as a structural material, giving rise to many structures around the world such as the Pantheon in Rome, Hoover dam in Nevada and Burj Khalifa in Dubai, to name a few.

The success of concrete as a construction material is often governed by its durability aspects. The durability of concrete is defined as the ability of the concrete to withstand the damaging effects associated with environmental conditions for a certain period of time (Zhao et al., 2004). Previous research studies indicate that crack openings in concrete structures, not only reduces the aesthetic appeal of the structure, but also accelerates the penetration of aggressive agents, deteriorating any reinforcing steel embedded within the concrete (Aldea et al., 1999). Crack openings in concrete structures are therefore imperative when dealing with the life expectancy of concrete structures, such as dams, tunnels, floor slabs, etc. (Tailhan et al., 2014). It can be argued that the earlier cracks occur, the larger the influence on the serviceability and durability aspects of the concrete element. Given this reasoning, addressing the crack potential during the earliest ages of concrete, can greatly improve the performance of the concrete structure during the later stages of its life cycle.

The first form of cracking occurs during the early ages of concrete, typically when concrete is still in the plastic state. The plastic state of concrete refers to the state of matter that the concrete is in and occurs as soon as water is added to the dry constituents. The exact point in time where the plastic period ends, is however debatable, since the transition from a fluid to a solid material does not occur instantly, and requires a certain amount of time to become fully rigid (Mehta & Monteiro, 2006). This transition however, is expected to fall somewhere around the final setting time of the concrete (Sant et al., 2009; ACI 231R, 2010).

During this plastic state, cracking is likely to occur due two forms of volumetric changes. The first volume change, namely plastic settlement, starts directly after the concrete is placed and can be described as the gravitational settlement of solid particles, which in turn displaces water to the surface of the concrete, leaving a concrete body with a reduced vertical dimension. The displaced water to the surface of the concrete is more commonly known as bleeding. The second volumetric change, namely plastic shrinkage, occurs due to the removal of water from the concrete's pores once the evaporation amount exceeds the bleeding. This in turn, results in both a vertical and horizontal dimensional change. In principal, cracking can only occur if any one of the two aforementioned volume changes are restrained.

Any restraint that prevents volume change is believed to induce tensile stresses in the concrete which leads to crack formation. However, crack formation is only expected to occur if the tensile stress induced within the concrete, is greater than the tensile strength of the concrete or if the tensile strain that develops in the concrete, is larger than the tensile strain capacity of the concrete at that point in time (CCIP-048, 2010). These two principles therefore highlight the importance of the tensile properties when investigating the cracking behaviour of plastic concrete. The tensile properties of plastic concrete remains largely scarce in literature and the majority of work that could be found failed to document the tensile behaviour of plastic concrete before 3 hours after casting (Kasai et al., 1972; Abel & Hover, 1998; Dao et al., 2009; Nguyen et al., 2017). This therefore leaves a significant knowledge gap in research, especially when considering that plastic shrinkage cracking often occurs within 3 hours after concrete placement.

Another important and often overlooked factor which influences the plastic cracking behaviour is the tensile creep or relaxation behaviour of concrete, which is of great significance especially for concrete loaded at early ages (Pane & Hansen, 2008). Relaxation is defined as a decrease in stress observed over time while under a constant induced tensile strain. Limited research regarding the relaxation behaviour of concrete is available in literature and the only research that could be found investigated relaxation after the setting period of concrete (Østergaard et al., 2001; Delsaute et al., 2016; Nguyen et al., 2017).

Therefore the relaxation behaviour of plastic concrete and its influence on the plastic cracking of concrete remains largely unknown.

During the early ages of concrete, the concrete element is likely to undergo multiple loading and unloading cycles. As ongoing evaporation continues to draw free water from the capillary pores of the concrete element, a negative capillary pressure build-up arises within the concrete element. This represents the internal loading aspect within the concrete element. Applying curing procedures, for example through the use of a fog spray to increase the humidity of the atmosphere above the surface of the concrete, reduces the build-up in capillary pressure. This is indicative of the unloading aspect of the concrete element. The behaviour of loading and unloading can be linked to the relaxation behaviour of concrete. However, curing has not been given much attention in literature and therefore a large knowledge gap exists on the influence of curing procedures on the cracking behaviour of plastic concrete. Furthermore, the lack of literature on the relaxation of plastic concrete and curing procedures shows that a large portion of knowledge on stress reduction in plastic concrete remains unknown.

The main reason behind the lack of literature on the relaxation and tensile properties of plastic concrete is mainly due to the difficulty in carrying out experimental tests on plastic concrete. The fluid nature and wide range of influential factors on plastic concrete, increases this difficulty further. Therefore there remains a need to investigate the tensile properties and relaxation behaviour of plastic concrete in order to provide new insight on the plastic cracking behaviour of concrete.

1.1 Objectives

This study sets out to achieve the following main objectives:

- Investigate the tensile behaviour of plastic concrete and its development with time.
- Identify and investigate the relaxation behaviour of plastic concrete and its development with time as well as its resistance to multiple loading.
- Identify the influence of an admixture based viscosity modifying agent on the tensile material properties and relaxation behaviour of plastic concrete.

- Identify the influence of initial curing procedures on the cracking behaviour of plastic concrete.
- Identify the influence of an admixture based viscosity modifying agent on the cracking behaviour of plastic concrete.
- Identify the influence of an admixture based viscosity modifying agent on initial curing procedures applied to plastic concrete.

1.2 Methodology

The methodology adopted to achieve the aforementioned objectives of this study is as follows:

- Conduct an in depth literature review to gain a fundamental understanding of plastic concrete as well as the associated forms of cracking. The literature study should also provide an understanding on the rheological behaviour of fresh concrete as well as the tensile material properties of plastic concrete.
- Conduct trial mixes to develop a control concrete mix as well as a viscosity modified concrete mix to use for several experiments.
- Conduct several tensile and relaxation tests on the developed concrete mixes.
- Conduct cracking, plastic shrinkage and settlement tests as well as tests associated with initial curing procedures.
- Finally, analyse all experimental results and draw suitable conclusions.

1.3 Research significance

The availability of literature on the tensile material properties of plastic concrete remains largely scarce. Available literature, either fails to capture the tensile properties of concrete earlier than 3 hours after casting or focuses on the tensile material properties of concrete after the setting time of concrete is reached. This creates a significant knowledge gap on the tensile behaviour of plastic concrete, especially considering that plastic shrinkage cracking usually occurs within 3 hours after placement. This study therefore focuses on providing insight into the tensile behaviour of plastic concrete during the stiffening, setting and hardening phases of concrete.

In addition, the relaxation behaviour of plastic concrete has not been given much attention in literature. Identifying the mechanism behind relaxation can help in explaining the relaxation phenomenon as well as why it occurs. Furthermore, the relaxation behaviour of concrete can help differentiate between pure elastic stresses induced by volume restraints as well as the actual stress induced within the concrete incorporating possible stress reduction. This therefore creates potential for future investigation in developing more accurate cracking models incorporating the relaxation phenomenon into the cracking behaviour of plastic concrete.

Initial curing is widely known to reduce the cracking potential in plastic concrete. However, the lack of literature on the influence of curing on the cracking potential of plastic concrete leaves a significant knowledge gap. Furthermore, possible links between the stress reduction associated with relaxation and the stress reduction associated with curing during the plastic state of concrete can help in controlling plastic shrinkage cracking.

1.4 Report outline

Chapter 1 provides an introduction to the current study and outlines the objectives used to conduct the study, methodology followed to achieve the set out objectives as well as the significance of the current study to the academic and construction field.

Chapter 2 provides a comprehensive literature review on plastic concrete. This includes a description on the hydration phases, definitions of setting times as well volume changes experienced during the plastic state of concrete. Thereafter the rheology of fresh concrete is explored in terms of definitions, factors affecting the rheology of fresh concrete, various flow behaviours as well as a brief discussion on the flow behaviour of plastic concrete. Furthermore, the use of viscosity modification agents in concrete to enhance the rheological properties of plastic concrete is addressed. Thereafter, the various cracking behaviour experienced in plastic concrete as well as influential factors and preventative measures are discussed. Lastly the tensile material properties of plastic concrete are researched and presented.

Chapter 3 describes the experimental framework of this study in terms of direct tensile tests as well as tests relating to the plastic cracking behaviour of concrete. This includes description of tests, test apparatus, test procedures, mix properties and a description of the mix constituents. Lastly a suitable test program is presented.

Chapter 4 provides and discusses the results obtained relating to the tensile properties of plastic concrete. This includes rheological tests, setting time tests, tensile strength development, strain capacity and the development of the elastic modulus with time. The relaxation behaviour under single and multiple loading as well as capillary pressure results are also included.

Chapter 5 provides and discusses the fundamental and phenomenological cracking behaviour of concrete. Thereafter initial curing results are presented and discussed. Furthermore possible links between the tensile properties obtained in Chapter 4 and the cracking behaviour results are considered.

Chapter 6 gives the final conclusions that can be drawn from this study as well as possible recommendations for future studies.

Chapter 2: Background study

This chapter provides a comprehensive background study on the various sections aspects to understand the cracking behaviour of plastic concrete. The first section of this chapter focusses on the use of concrete as a construction material followed by a discussion on the plastic state of concrete. Thereafter, the rheology of concrete is addressed in order to define the flow behaviour of plastic concrete. Lastly, the cracking behaviour of plastic concrete is discussed, followed by a final section on the tensile material properties of plastic concrete.

2.1 Concrete as a construction material

Concrete can be defined as a building material made from a mixture of stone, sand, cement, and water forming a stone-like mass once hardened (Owens, 2009). Through this definition, concrete can be recognised as a composite material consisting of cement, water, coarse aggregate (stone) and fine aggregate (sand). Modern day concrete, however, can be mixed to enhance certain fresh properties of concrete through the addition of admixtures, supplementary cementitious materials or a combination of both.

Admixtures are chemicals, normally supplied as an aqueous solution and added during the mixing process in order to change the fresh, early age or hardened properties of concrete (Domone & Illston, 2010). Furthermore, admixtures can also be used to provide an economic advantage to the concrete. Supplementary cementitious materials are defined by the BS EN 206 (2013) as finely grounded materials used in concrete, either to improve certain properties or to achieve special properties. These materials are added to replace part of the cement for property and/or economic and/or environmental benefits (Domone & Illston, 2010).

Throughout history, from the early forms of concrete used in the Egyptian Pyramids (3000 BC) and Roman architecture (300BC – 476 AD), concrete was used as a construction material to build many structures recognised throughout the world. However, the invention of

Portland cement in 1824 by Joseph Aspdin, was the first step towards the use of concrete on a large scale.

Today concrete has become one of the most widely used construction materials in the world. Its success is owed to its mouldability, compressive strength, permanence, durability and its resistance to fire, abrasion and especially water (Shetty, 2008). This contributes towards the continued use of concrete on a large scale for both established applications as well as new applications under varying environments. It is for this reason that there is continued research being carried out to better understand the properties and behaviour of this complex material throughout its service life.

The lifespan of concrete can be defined as the time period between time of casting and placing, up until the end of service life of the structure, which can range between 10 and 300 years. During this lifespan, there exist various aspects that affect the concrete, both positively and negatively. In terms of positive aspects, concrete may continue to improve in strength during the course of its life span. However, concrete, especially during the early phases, is more susceptible to certain volume changes and deformations which can hinder the performance of concrete as a construction material. These volume changes can be due to environmental conditions, hydration reactions and load induced stresses and strains. This therefore highlights the complexity of the material and explains the need for continued research on various stages of the concrete's lifespan.

Each stage during the lifespan of a concrete structure, determines its ability to resist the build-up of stress and resistance to strain in the following stage. For example, if cracks occur during the early ages of the concrete due to the stresses induced by environmental conditions, this can later affect the concrete structure during its load carrying stages, which can greatly decrease the serviceability of the structure. Previous research indicates that crack openings in concrete structures, accelerate the penetration of aggressive agents, which can deteriorate reinforcing steel, thus greatly decreasing the service life of the structure (Aldea et al., 1999). It can therefore be argued that the earlier cracks develop, the greater the effect on the later stages of the concrete element, in terms of durability and serviceability.

The earliest form of cracking occurs during the plastic state of the concrete. This plastic state can therefore be considered to give the largest potential for the reduction of the durability and serviceability of a structure (Combrinck, 2016). In light of this, the plastic period of concrete greatly influences and predicts the success of the concrete during its lifespan. The literature to follow in this chapter therefore focuses on concrete during the plastic state.

2.2 Concrete in its plastic state

Concrete in its plastic state refers to the phase that the concrete is in and is therefore referred to as plastic concrete throughout this document. The term "plastic" in plastic concrete, refers to the state of matter or phase of the concrete and can be further used to describe concrete that can be moulded to take on any shape (Powers, 1968). Plastic concrete can therefore be defined as freshly mixed concrete and the plastic period begins as soon as water is added to the dry constituents and placed shortly after. The end of the plastic period is however debatable (Neville, 1963; Sant et al., 2009). The main reason for this is due to the fact that the transition from a fluid to solid does not occur instantly and requires a certain amount of time to become fully rigid (Mehta & Monteiro, 2006). In order to gain a better understanding of the plastic to solid transition, the hydration phases along with points of setting and volume changes are discussed in the following sections.

2.2.1 Hydration of concrete

Anhydrous Portland cement contains a unique adhesive property which binds sand and stone together. This property however, is only activated when mixed with water, yielding products that possess both setting and hardening characteristics (Mehta & Monteiro, 2006). The speed of this reaction plays an important role in the placement of concrete. The initial reaction needs to be slow enough to allow for easy placement of the concrete, thereafter rapid hardening is desired (Brunauer & Copeland, 1964). For the purpose of this study, only the physical aspects of hydration are of interest and therefore the chemistry behind the hydration reactions fall out of the scope of this document and are not pursued further.

The hydration process of concrete can be divided into three stages, namely; the stiffening, setting and hardening phases (Powers, 1968; Mehta & Monteiro, 2006; Sant et al., 2009; Domone & Illston, 2010). Figure 2-1 shows the hydration stages corresponding to the concrete's state of matter, rate of heat generated due to hydration and the relative change in permeability, strength and porosity as the concrete hydrates.

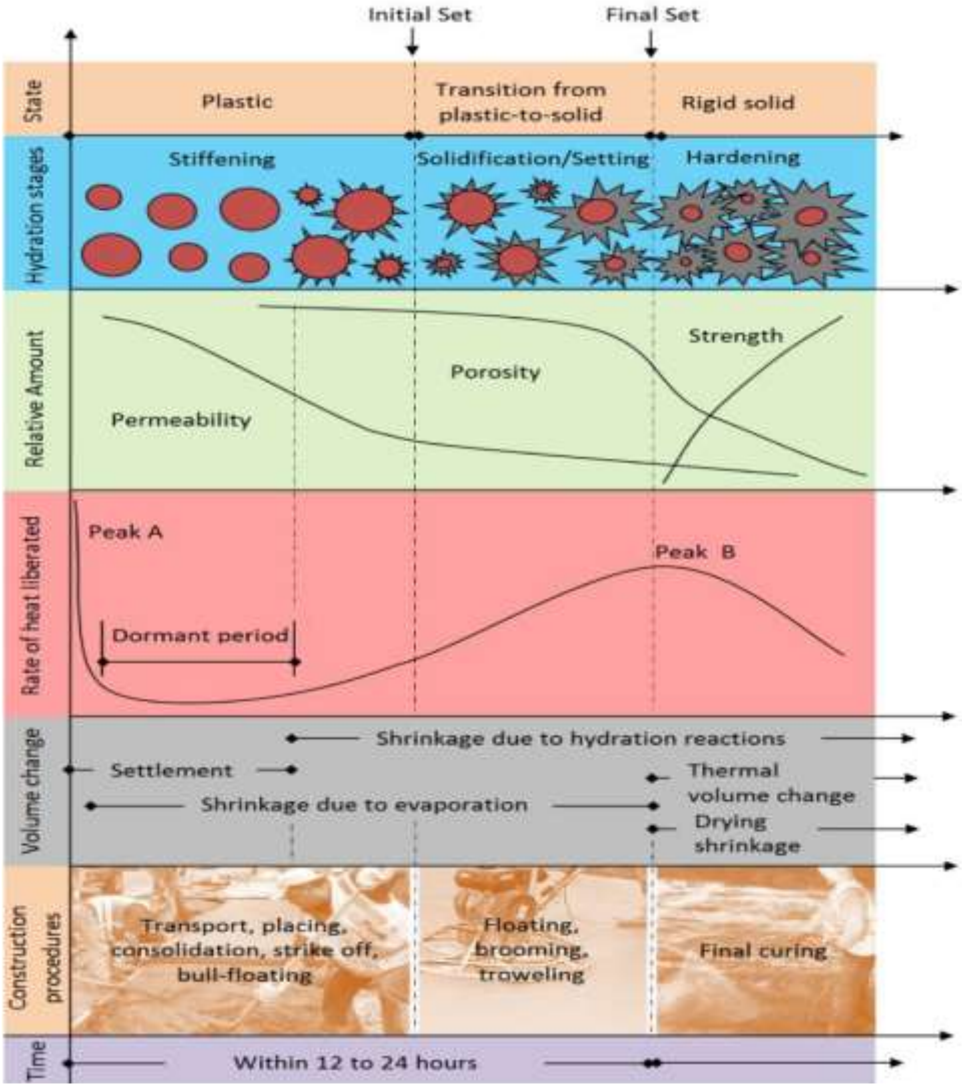

Figure 2-1: Stages of concrete hydration (Compiled by Combrinck 2016 as adapted from Powers, 1968; ACI 308R., 2001; Mehta & Monteiro, 2006; Sant et al., 2009; Domone & Illston, 2010)

The stiffening phase marks the first phase of cement hydration and starts as soon as water is added to the dry constituents. This phase can be defined as the loss of consistency of the plastic cement paste (Mehta & Monteiro, 2006). The consistency of concrete describes the flow behaviour of freshly mixed concrete. Measures of consistency include the standard slump and flow tests (Powers, 1968). Once initially mixed, the presence of free water is responsible for the plastic nature of the concrete. Once the concrete is placed, the loss of consistency commences. The main reason for the loss of consistency is mainly due to the consumption of free water resulting from the formation of hydration products, absorption by unsaturated aggregates, formwork, subgrade or poorly crystalline products as well as the loss of water due to evaporation (Mehta & Monteiro, 2006; Combrinck, 2016). The loss of free water during this stage explains why the consistency of the concrete changes as time progresses, also known as the slump loss phenomenon.

The rate of heat liberated during the stiffening phase is shown in Figure 1. The first contact between the cement and water particles marks the initial chemical reaction resulting in a rapid exothermic reaction at Peak A. The rate of heat liberated then drops suddenly to a low constant value before the rate starts to increase again after typically two to three hours, depending on the concrete's properties (Mehta & Monteiro, 2006). The period between the drop of Peak A and the point where the rate starts to increase again is referred to as the dormant period (Powers, 1968). During this period, little to no heat is liberated, implying that the reaction between cement and water is inactive during this period.

The initial Peak A is due to the reaction between the gypsum and aluminates in the cement forming a product known as ettringite. The addition of gypsum in cement prevents the more intense and violent reaction between the aluminates and water, which is the main mechanism behind the rapid stiffening or flash setting of the concrete (Domone & Illston, 2010; Mehta & Monteiro, 2006). The product ettringite, forms a protective layer on the aluminates, preventing any further rapid reactions between water and the aluminates (Domone & Illston, 2010). Without the addition of gypsum and the resulting dormant period, the concrete would not be workable long enough to enable ease of casting, placing and finishing (Combrinck, 2016).

The second stage is called the setting stage and refers to the solidification of the plastic cement paste. During this stage, the transition from a plastic material to a solid material occurs, which is graphically shown by the decrease in permeability of the concrete paste in Figure 2-1. The permeability of a material refers to the rate of viscous flow of fluid under pressure through the pore structure.

Most of the heat liberated at Point B is mainly due to the reaction between Alite (C_3S) and water which form calcium silicate hydrates or more popularly known as C-S-H crystals (Domone & Illston, 2010; Mehta & Monteiro, 2006). These crystals are responsible for the strength gain of concrete and acts as the main mechanism behind the solidification phase. The time taken for the cement paste to solidify completely marks the end of the setting stage and at this point the concrete is no longer plastic.

The final stage is called the hardening phase and is where the concrete starts to gain significant strength. Along with the reaction of Alite and water, the reaction between Belite (C_2S) and water starts at a much slower rate. This reaction contributes much less to the rate of heat development in the concrete but also produces C-S-H crystals which contribute to the long term strength of the hardened cement paste (Domone & Illston, 2010). At the beginning of this stage, it should be noted that the cement paste possesses nearly no strength since the hydration of Alite is still in the beginning stages, however, once this reaction starts, the reaction continues rapidly for weeks (Mehta & Monteiro, 2006). The continued hydration of Alite and Belite result in the progressive filling of void spaces with C-S-H crystals which decreases the porosity and increases the strength of the hardened cement paste (Mehta & Monteiro, 2006). The porosity is a measure of void spaces in the concrete and a decrease in porosity marks the filling of void spaces with C-S-H crystals.

2.2.2 Setting times and finishing operations

The setting stage marks the transition of a plastic concrete into a solid, hardened concrete. The initial and final setting times marking the start and end of the setting stage, are not consistently defined throughout literature. Some literature argue that the initial and final setting times do not indicate any physical or chemical change in the concrete and that initial set only suggests a time limit for handling and placing the concrete, while the final set indicates the start of strength gain (Mehta & Monteiro, 2006; Domone & Illston, 2010). Neville (1963) on the other hand, argues that the initial set corresponds to a rapid rise in temperature and that the final setting time, corresponds to the peak temperature marked as Point B in Figure 2-1.

Both of these definitions can be seen as correct, since the true definition of initial and final set depends on the testing method. Setting times can be determined in terms of rate of hydration or in terms of solidification by using standardised methods that involve measuring the depth of penetration of needles or plungers into the setting paste (Neville, 1963). Various methods of measuring the rate of hydration exist, however most of the methods are more suited to a laboratory environment. In practice however, using the rate of heat liberated to measure the setting points of concrete, is not an ideal method since results between setting time and rate of heat liberated show contrasting results when analysed in terms of w/c ratios (Bentz et al., 2009). The main reason for this is due to the fact the rate of heat build-up is related to the hydration reaction which accelerates before the time that the fluid to solid transition occurs (Sant et al., 2009). This then implies that from a fundamental point of view, solidification should not be related to the rate of the hydration reaction but rather the development of a solid structure (Bentz, 2007).

For the purpose of this study, the Vicat penetration device is used to determine the setting times. This is a commonly used test method and can be used in both a laboratory or construction environment. Although initial set and final set are arbitrarily chosen points, these points however, provide a good indication of the state of matter of the concrete and are regularly used in the construction industry to schedule placing and finishing operations.

The initial setting time marks the start of the setting phase and defines the limit for handling the fresh concrete. At this point, the concrete becomes unworkable and construction activities which include the transport, placing, consolidation, strike off and bull floating of concrete slabs should be completed before the initial set of the concrete is reached (ACI 308R, 2001).

The final setting time marks the beginning of the hardening stage, which is where the concrete starts to gain significant strength (Mehta & Monteiro, 2006). The period between the initial and final set is referred to as the window of finishability and all procedures relating to the finishing of the concrete mix such as floating, trowelling and brooming should be completed before the final setting time is reached.

2.2.3 Types of volume change in plastic concrete

During the early ages of concrete, directly after placement, several forms of volume changes occur. Figure 2-1 shows the occurring volume changes grouped according to the stages of hydration. These volume changes can be dependent on both time and state of matter of the concrete (Combrinck, 2016).

The first volume change that occurs is called settlement and occurs directly after the concrete has been placed. The main driving force behind the settlement volume change, is due to the vertical settlement of solid particles. The densities of these solid particles are much greater than water, resulting in a greater gravitational force that causes these particles to settle, leaving a concrete body with a reduced vertical dimension (Powers, 1968). This vertical settlement of solid particles displaces water to the surface of the concrete. This action is referred to as bleeding and ceases around the end of the dormant period during the stiffening phase (Powers, 1968).

The second volume change is called plastic shrinkage and this form of volume change occurs for as long as the concrete remains plastic. The main driving force behind this form of shrinkage is due to evaporation. Once all the bleed water has evaporated from the concrete's surface, ongoing evaporation draws out water from the pores of the concrete, causing a negative capillary pressure in the pores (Powers, 1968; Slowik et al., 2008). This build-up in stress, results in a concrete body with a reduced vertical and horizontal dimension. The end of this form of shrinkage coincides with the end of the setting stage, when the concrete is no longer considered plastic (Powers, 1968).

The third volume change occurs due to two forms of shrinkage, namely autogenous and chemical shrinkage. The main mechanism behind these volume changes are the ongoing hydration reactions that occurs once cement reacts with water. Chemical shrinkage can best be explained as an internal reduction in volume of the product (C-S-H) compared to the reactants (solids and liquids) associated with the hydration reactions (Hanson, 2011). Chemical shrinkage starts from the end of the dormant period and continues for as long as the hydration reaction continues (Sant et al., 2009).

Autogenous shrinkage is the visual dimensional change of a concrete element, due to the volume reduction of cement paste or concrete which is caused by self-desiccation (Hanson, 2011). Self-desiccation is explained as a phenomenon where water is drawn from the vapour-filled pores, creating internal capillary stresses that result in a visible dimensional change in the concrete (Sant et al., 2009).

In plastic concrete, chemical shrinkage is equal to autogenous shrinkage. The main reason for this is due to the plastic nature of the concrete paste. The concrete immediately fills the empty pores which form due to chemical shrinkage of the concrete. Once the concrete becomes rigid, the concrete is no longer able to close the empty pores, causing the formation of a porous structure which is susceptible to autogenous shrinkage (Sant et al., 2009).

Other volume changes include both thermal and drying shrinkage. These shrinkages however, only occur once the concrete has reached a hardened state and therefore fall outside the scope of plastic concrete (ACI 231R, 2010).

2.3 Rheology

Rheology can be defined as the branch of physics concerned with the deformation and flow of matter (Coussot, 2012). In the context of concrete, particularly fresh or plastic concrete, this relates to the science describing the consistency of concrete. Consistency however, is a fairly difficult term to define, as there is no quantifiable measure to accurately define consistency (Powers, 1968; Domone & Illston, 2010). As a result several definitions exist and can therefore create more confusion.

2.3.1 Defining Consistency

The lack of a true quantifiable measure of consistency often creates confusion when describing concrete. Concrete can be defined as having a wet, stiff or sticky consistency. This in turns means that the word can be used to describe different properties of the concrete. Powers (1968) explains that the consistency of concrete refers to the rheological properties that change as a result of a change in the water content, temperature, or the addition of a surfactant. Other definitions define consistency as the property of freshly mixed concrete or mortar which determines the ease and homogeneity, with which it can be mixed, placed, consolidated and finished (ACI 116R-90, 1990) or as the property which determines the effort required to manipulate a freshly mixed quantity of concrete with minimum loss of homogeneity (ASTM C125-93, 1993) or as a measure of the wetness of the concrete mixture (Mehta & Monteiro, 2006).

The three properties that describe the fresh state of concrete are generally, the fluidity, compactability and the cohesiveness (Domone & Illston, 2010). The fluidity relates to the ease at which the concrete can flow. It describes the ease at which the concrete can be placed for structural members. Compactability describes the ease at which the concrete can be consolidated to remove the entrapped air from the concrete. The cohesiveness is related to the ability of the concrete paste to keep all solid particles entrapped in the concrete paste. The two properties, namely the fluidity and compactability have been combined into the general property called consistency (Domone & Illston, 2010). Cohesiveness can also be related to compactability or more specifically, consolidation and segregation (Mehta & Monteiro, 2006). The cohesiveness is the property that governs segregation during consolidation. Therefore the consistency of fresh concrete can be broadened to include all three properties of fresh concrete.

Several definitions in literature either make reference to one, two or all three of the aforementioned properties when defining consistency. The key to understanding the term consistency is to understand the properties it describes. Therefore, rheology is the science that describes the factors relating to the fluidity, compactability and cohesiveness of the freshly mixed concrete.

2.3.2 Factors relating to consistency

Several factors relating to the rheological properties of fresh concrete can influence the consistency of the concrete to some degree. Important rheological terms are described as follows:

2.3.2.1 Shear stress

Visualises a liquid as having multiple layers stacked above each other with a horizontal force applied to the top layer, a shear force occurs between the two layers. The movement of the top layer relative to the lower layer induces a sliding action between the two layers (Coussot, 2012). This sliding action or sliding force between the two layers is referred to as shear. Shear stress can therefore be defined as a shearing force acting over a unit area as shown in Figure 2-2.

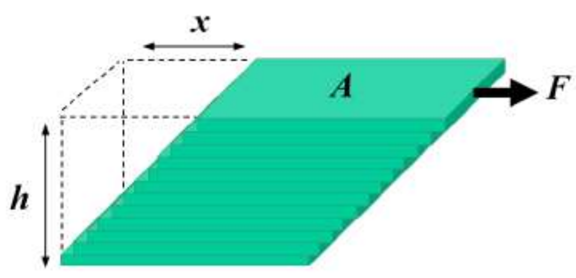

Figure 2-2: Schematic representation of shear flow

If no external force is applied, a positive component of shear acts on the bottom layer and an equal but negative component acts on the top layer, resulting in no movement. By applying an external force, equilibrium is lost between the two layers and hence the sliding motion occurs. The bottom layer however, still resists the movement of the top layer. The shear stress can therefore be further described as a measure of resistance to motion (Chhabra & Richardson, 2008).

2.3.2.2 Rate of shear strain

The shear strain rate refers to the change in displacement of the top layer relative to the bottom layer, after a shear force has been applied as seen in Figure 2-2. The strain (x/h) is defined as the ratio of the relative displacement of the top layer (x) to the thickness of the material (h) (Coussot, 2012). The rate of shear strain is therefore defined as the change in strain with time under a shear stress.

2.3.2.3 Viscosity

The viscosity of a material refers to the ability of a material to resist flow. It describes the velocity at which a given material flows once flow is initiated (Kovler & Roussel, 2011). A material with a high viscosity has a greater resistance of flow and therefore flows at a slower velocity compared to a material with a low viscosity.

2.3.2.4 Yield stress

The yield stress of a material can be defined as the stress required to initiate flow and refers to whether or not a material will start flowing under an applied stress (Kovler & Roussel, 2011). However, in concrete the flow behaviour is not as simple since a larger yield stress is required to initiate flow (initial yield stress),while a smaller yield stress is needed to maintain flow once it has begun (dynamic yield stress), as shown in Figure 2-3.

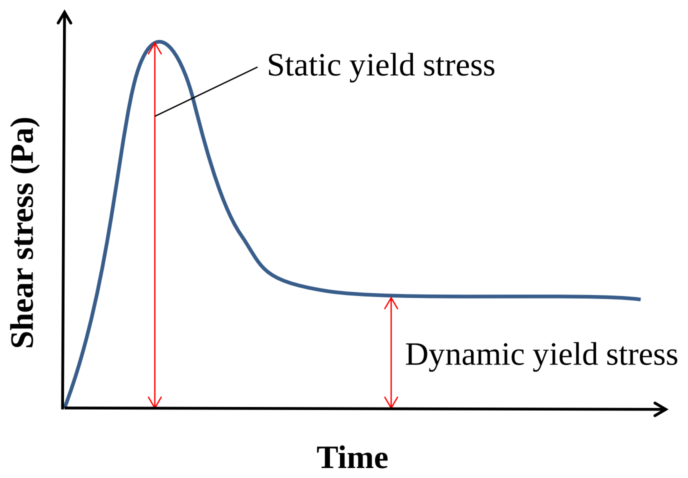

Figure 2-3: Concrete yield stress

The conventional single point slump test, commonly used to describe the consistency of fresh concrete, gives an indication of the yield stress in concrete. Domone et al. (1999) carried out a number of tests to investigate the relationship between yield stress and slump of fresh concrete as shown in Figure 2-4. Domone's results show that reasonable correlations can be obtained between slump and yield stress with minimal variability, provided the manner in which slump tests are conducted, are consistent. Furthermore, high yield stresses corresponds to a stiff concrete mix, while a low to near zero yield stress, corresponds to a high slump value.

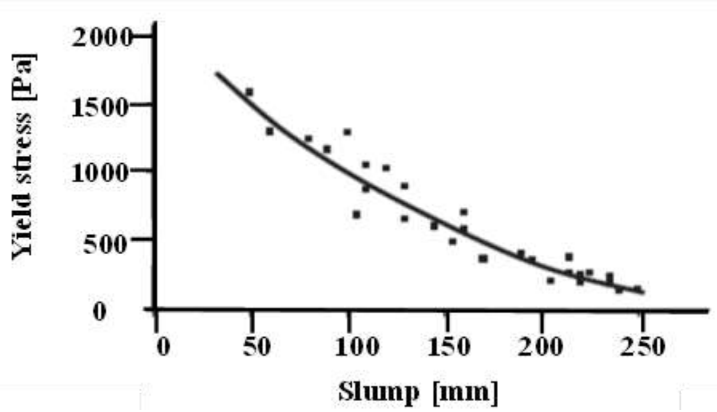

Figure 2-4: Relationship between yield stress and slump of fresh concrete (Domone et al., 1999)

2.3.3 Flow behaviour of Newtonian fluids

Two groups of fluids exist, the first being a Newtonian fluid and second being a non-Newtonian fluid. Consider a tall container of 1 litre capacity with 500 ml of water in the container. If the water filled container is placed on a level surface, the top layer of the water remains level and does not move. However, by gently tilting the container the water level inclines to an angle which is proportional to the tilting angle of the container. By tilting the container, a shear stress is induced in the liquid which causes the original shape of the water to deform. By increasing or decreasing the angle of tilt of the container, the water level either increases or decreases by a proportional amount. The speed or rate at which the water is able to change shape, depends on its ability to resist flow, namely, its viscosity. This describes the behaviour of a Newtonian fluid. Figure 2-5 shows the flow behaviour of a Newtonian fluid.

The flow represents a linear shape starting from the origin, which means that the shear stress is proportional to the shear strain rate with viscosity as the proportionality constant (Chhabra & Richardson, 2008). The viscosity of the Newtonian fluid is therefore equal to the gradient of the linear graph. Another property of such liquids, is that it contains no yield stress; meaning that no stress is needed to overcome the inter-particle forces to initiate flow and therefore the flow is only dependent on the viscosity of the fluid (Coussot, 2012; Domone & Illston, 2010).

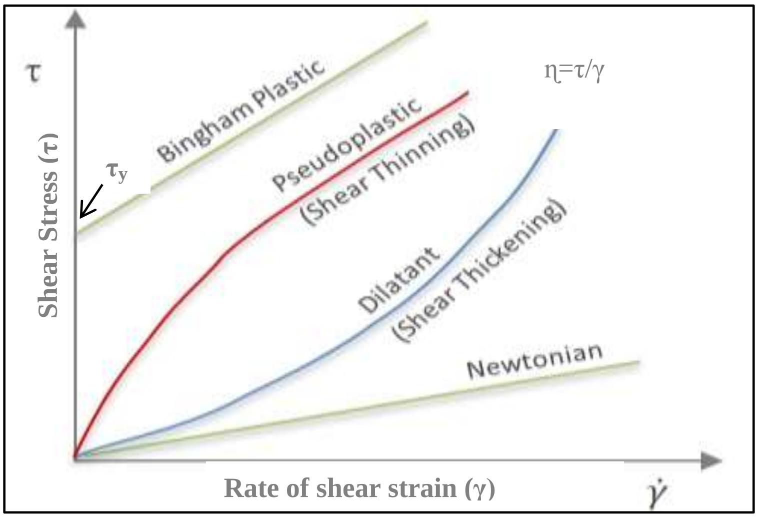

Figure 2-5: Flow behaviour of fluids

2.3.4 Flow behaviour of non-Newtonian fluids

Non-Newtonian fluids behave differently compared to Newtonian fluids and due to the complexity of such flow, the behaviour of such fluids can be further categorised into three different behaviours, namely: time independent fluids, time dependent fluids and visco-elastic fluids (Chhabra & Richardson, 2008).

2.3.4.1 Time independent fluids

The flow behaviour of time independent fluids remains constant with time. This means that at any point in time, the shear strain rate is dependent on the shear stress or vice versa. This category can be further divided into three groups, namely shear-thinning, shear thickening and Bingham fluids.

1) Shear-thinning fluids

Shear thinning fluids decrease in viscosity with increasing shear strain rate (Chhabra & Richardson, 2008). Figure 2-5 provides a visual representation of the behaviour of shear thinning fluids. The shear-strain plot starts at the origin indicating that it has no yield stress. The change in gradient of the curve decreases as the shear strain rate increases, indicating a decrease in viscosity and as the shear rate tends to zero, the viscosity tends to infinity. Furthermore, as the gradient changes, the shear strain curve becomes linear, indicating that the flow behaviour is identical to that of Newtonian fluids.

2) Shear-thickening fluids

Shear thickening systems increase in viscosity as the shear strain rate increases (Chhabra & Richardson, 2008). As shown in Figure 2-5, the flow behaviour of shear thickening fluids is similar up to a certain critical value of shear rate, thereafter, the viscosity increases rapidly.

3) Bingham fluids

Bingham fluids also referred to as yield stress fluids, contain a minimum yield stress that initiates flow. These fluids are unique in the sense that they behave as solids when a stress smaller than the yield stress is applied and as a liquid once a stress larger than the yield stress is applied (Coussot, 2012). The stress versus strain plot in Figure 2-5 shows that the curve does not pass through the origin but intersects the y-axis, indicating that a minimum stress is needed before flow is initiated. Once the yield stress is reached, the stress versus strain plot is largely linear and thus can be characterised by a constant viscosity (Coussot, 2012).

2.3.4.2 Time dependent fluids

The flow behaviour of certain materials change with time and therefore the viscosities of such materials vary with time and rate of shear. The time dependent fluid behaviour can be divided into two categories, namely thixotropic and rheopexy (Coussot, 2012). Figure 2-6 displays the flow behaviour of fluids falling within these two categories.

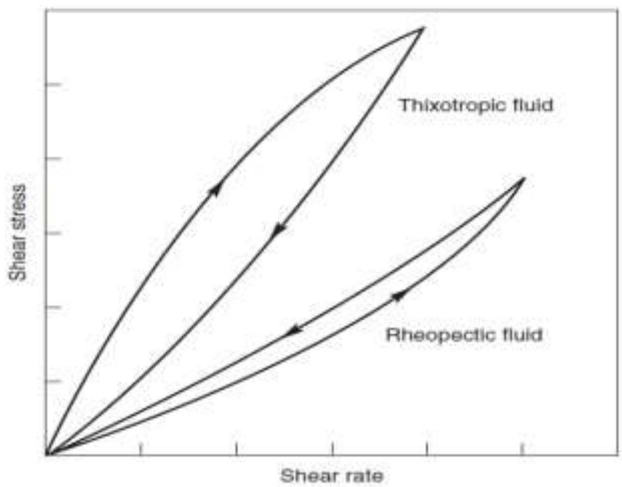

Figure 2-6: Flow behaviour of time dependent fluids

Materials are thixotropic when the viscosity of a fluid increases with an increase in time at rest and decreases with an increase in shear rate. Similarly, rheopexy refers to fluids with which the viscosity increases with rate of shearing.

2.3.4.3 Viscoelastic fluids

In some cases, materials can behave as part solid and part liquid. These materials are referred to as viscoelastic fluids. A viscous substance is one that has the ability to yield under a constant shearing stress (Coussot, 2012). An elastic material has the ability to recover its original size and shape after it has become deformed by external forces (Powers, 1968). Viscoelastic materials, therefore, contain elements of both viscous and elastic materials. This means that viscoelastic materials exhibit time dependent strain.

Figure 2-7 shows the viscoelastic creep behaviour of a material. When a load is applied to a pure elastic material, the strain experienced is directly proportional to the stress induced in the material. Once the load is removed, the elastic material recovers immediately and quickly returns to its original state. The viscoelastic material however, behaves differently. Once loaded, the material experiences an initial strain and once the load is removed, the strain immediately drops, followed by a gradually decrease in strain but does not reach its original position. This in turn means that the material undergoes some permanent deformation (Domone & Illston, 2010).

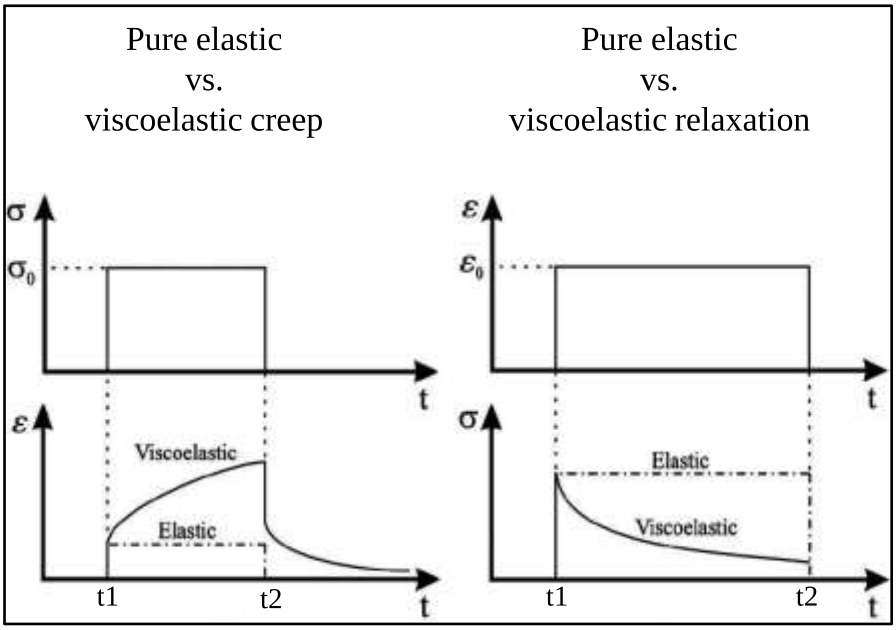

Figure 2-7: The creep and relaxation behaviour of viscoelastic fluids

Stress relaxation refers to the ability of a material to reduce the internal stress build-up under a constant strain (Mehta & Monteiro, 2006). Figure 2-7 displays the stress relaxation of a pure elastic solid compared to a viscoelastic material. Under constant strain, the elastic material is able to support the stress with no subsequent reduction between Times t1 and t2. The viscoelastic material however, is able to reduce the stress build-up between Times t1 and t2. A pure viscous material, although not shown in Figure 2-7, instantly reduces the stress build-up (Domone & Illston, 2010).

2.3.5 The flow behaviour of fresh concrete

The flow behaviour of fresh concrete is complex. Fresh concrete consists of solids in the form of cement particles, sand and stone, submerged in water. This combines the properties of solids with fluids and thus creates complex flow behaviour.

Fresh concrete displays the properties of yield stress fluids (Kovler & Roussel, 2011; Coussot, 2012). The Bingham model is a good representation of this flow behaviour (Domone & Illston, 2010). Figure 2-8 shows the flow behaviour of concrete in terms of the Bingham model.

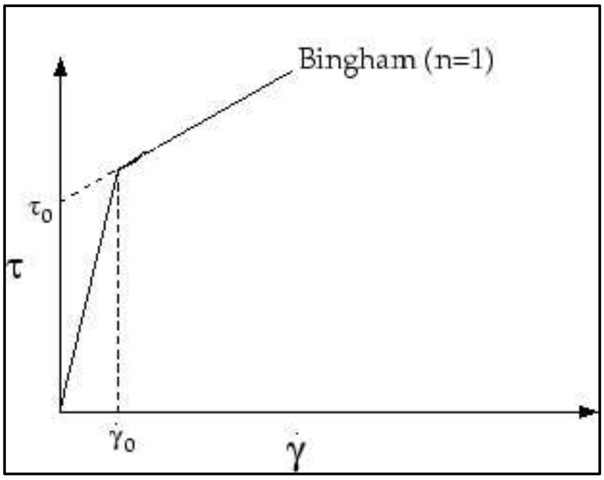

Figure 2-8: Bingham model representing the flow behaviour of fresh concrete (Coussot, 2012)

As the name suggests, yield stress fluids contain a yield stress, which is the minimum stress required to initiate flow. The concrete behaves as a solid, mainly elastic with possible viscoelastic effects before the yield stress is reached and once flow is initiated, the ratio of shear stress to shear strain rate is linear (Banfill, 2006; Coussot, 2012). This in turn means that the shear stress is directly proportional to the shear strain rate, with viscosity being the proportionality constant. Fresh concrete can also be categorised as thixotropic, since its viscosity increases the longer it is left at rest.

To conclude, fresh concrete can be defined as a non-Newtonian fluid with a combination of all three fluid behaviours. Fresh concrete behaves mainly as a yield stress fluid with time dependent and viscoelastic properties.

2.3.6 Viscosity modification agents

Through technological advancements in the concrete industry, modern day concrete can be designed to fulfil certain needs. Self-compacting concrete, high performance concrete and fast setting concrete are some of the examples depicting the advancement in the concrete industry. It should however be noted that in general, the more advanced the concrete, the more sensitive the concrete to material variation and quality, as well as incorrect or inconsistent production and placing. Through the incorporation of Viscosity Modification Admixtures (VMA), concrete with better robustness against the impact of variations in materials and on site conditions is possible (EFNARC, 2006).

When dealing with the rheology of fresh concrete, the two aspects of interest are mainly the yield stress and viscosity of the concrete. The key property of a VMA is to modify the rheological properties to further enhance the fresh properties of the concrete. VMAs are water-soluble polymers with a high molecular weight that increases the yield stress and or the plastic viscosity of fresh concrete (Khayat & Mikanovic, 2012). The increase in yield strength, although this increase is small, can affect the workability of the concrete by decreasing the slump measurement. Furthermore, the influence of VMAs on fresh concrete besides enhancing the rheological properties of concrete, has a minimum effect on the setting time and content of entrained air in the concrete is minimal (EFNARC, 2006).

The main mechanism behind the addition of a VMA is the build-up of three dimensional structures in fresh concrete, which enhances the rheological properties. The resulting concrete has an increase in the cohesion of the cement paste. This in turn improves the uniform distribution and suspension of the aggregates particles which in turn decrease the bleeding, settlement and segregation of the fresh concrete (EFNARC, 2006). In addition to the mentioned properties, the addition of a VMA can result in water and fines being more homogenously maintained throughout the mix. This creates a lubricating effect on rough aggregate surfaces, reducing frictional forces between particles which in turn improves the discharging and placement of fresh concrete (Jeknavorian, 2016).

Research conducted by Leemann and Winnefeld (2007) attempted to investigate the influence of different VMAs on the flow properties and rheology of self-compacting mortars. VMAs were categorised into either organic or inorganic categories depending on their chemical nature. At constant water-to-cement ratio, results show that the addition of a VMA (both organic and inorganic) increases both yield stress and plastic viscosity. Furthermore, organic VMAs showed almost no influence on hydration rate and compressive strength development. However, inorganic VMAs accelerated both rate of hydration and compressive strength development.

Al-Qassag et al. (2016) investigated the influence of a dry VMA on settlement cracking. Settlement cracking is defined as the cracks arising due to the restricted settlement volume change. Settlement cracking is discussed in greater detail in Section 2.4.1. Al-Qassag's findings show that settlement cracking increases with a corresponding increase in concrete slump. Results show that the addition of the dry VMA, increases both yield stress and plastic viscosity. The increased yield stress resulted in a stiffer concrete mix with a reduced slump. However, compared to mixes without VMA at similar slump values, lower crack intensity can be achieved through the addition of VMA. The addition of the dry VMA increased the cohesiveness of the plastic concrete and stability of the concrete matrix, leading to an improved plastic settlement cracking performance.

The reduction in bleeding, settlement, segregation and enhanced lubricating effect are all desirable properties that can be beneficial to certain applications in the concrete industry. The addition of a VMA is typically useful in self-compacting concrete due to its improved segregation property, underwater concrete by preventing cement paste washout and pumped concrete due to reduced wall friction and improved particle interlock (Jeknavorian, 2016).

2.4 Plastic cracking of concrete

As discussed in Section 2.2, the plastic state of concrete refers to the state of matter of concrete from time of placing up until the final setting time of concrete. During this time period, the concrete is likely to undergo three forms of volume change, namely settlement, plastic shrinkage and shrinkage due to the ongoing hydration of concrete. Literature however, indicates that shrinkage due to hydration is more apparent in concrete with low water-to-cement ratios of 0.4 or less and can therefore be ignored as a possible volume change, since this study does not focus on such low water-to-cement ratios (Sant et al., 2009).

In principal, cracks occur due to the build-up of tensile stresses if strains resulting from any one of the volume changes which are restrained. These restraints can be in the form of tensile steel reinforcing, formwork, change in geometry such as T-beams, etc. The ACI 201.1R (2008) defines a crack as “a complete or incomplete separation of either concrete or masonry into two or more parts produced by breaking or fracturing”. Cracking in concrete is one of the biggest problems experienced in the built environment and often lowers the aesthetics, durability and service life of the structure.

2.4.1 Plastic settlement cracking

Concrete consists of cement, water and aggregates. Once concrete is placed, the solid particles experience a downward force that causes the particles to settle and displace water to the surface of the concrete as explained in Section 2.2.3. This phenomenon is referred to as settlement and is one of the first volume changes experienced in plastic concrete. A concrete body that is allowed to settle without any form of hindrance or resistance to the volume change does not result in cracking. A crack only occurs if the volume change is restrained for example by reinforcing steel or a sudden change in cross-section (ACI 224R-80, 1984). Restraints create situations where differential settlement occurs; meaning that concrete settles at different rates and amounts in different parts of the concrete body (Kwak & Ha, 2006). Figure 2-9 shows the process of settlement as well as the resulting effects.

As the solid particles settle (top portion of Figure 2-9), water is displaced to the surface of the concrete. However, the settlement of particles situated above the reinforcing steel is prevented. This therefore results in a differential volume change in the concrete body between reinforcing bars. This results in the formation of tensile stresses directly above the reinforcing bars. The bottom portion of Figure 2-9 shows the portion of the concrete experiencing tensile stresses due to the resulting decrease in volume between reinforcing steel, which ultimately leads to the formation of a crack. Furthermore, the settlement of solid particles below the reinforcing steel, create voids which greatly reduce the bond between the concrete and reinforcing steel.

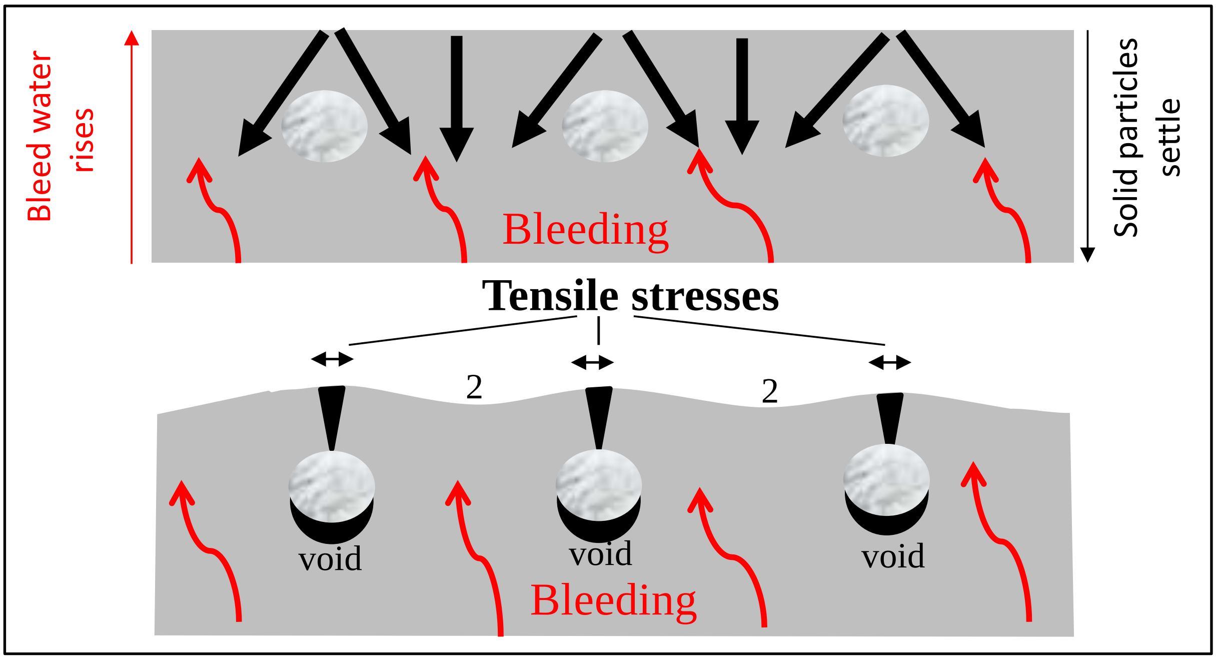

Figure 2-9: The mechanism behind settlement

The bleed water that displaces to the surface of the concrete can create two problems (Domone & Illston, 2010). The first problem is a phenomenon referred to as surface laitance. Surface laitance is the phenomenon whereby the cement paste at or just below the top layer becomes water rich and hydrates to a weak structure. The second problem is the formation of a weak interface zone between the cement paste and aggregates or reinforcing steel. As water displaces to the surface of the concrete, bleed water can get trapped under aggregate particles or reinforcing bars, resulting in water pockets forming below the hindrance. This then creates a weak interface zone between the cement paste and aggregate or reinforcing steel.

Settlement usually ceases at the end of the dormant period when hydration starts. The hydration products tend to form bridges or connections between inter-particle gaps which can prevent settlement from occurring. Settlement may also cease mechanically before the end of the dormant period. This occurs if particles come into contact with one another preventing further settlement (Powers, 1968).

2.4.2 Plastic shrinkage cracking

The settlement of solid particles as discussed in Section 2.2.3, displaces water to the surface of the concrete which is referred to as bleeding. If the surface of the concrete is exposed to an evaporation rich environment, the bleed water evaporates from the surface of the concrete.

Once all the bleed water has evaporated, ongoing evaporation draws out the free water from the concrete body. A visual representation of this phenomenon is shown in Figure 2-10. The removal of free water from the pores of the concrete (blue arrows) creates a capillary pressure (black arrows) within the capillary pores of the concrete body, which draws the solid particles closer together. As a result, a concrete body with a reduced horizontal and vertical dimension remains. This process is referred to as plastic shrinkage and is the second form of volume change that occurs after the concrete has been placed. The end of the setting stage and in the case of this study, the final setting time, marks the point when the concrete is no longer plastic and therefore marks the end of plastic shrinkage.

Plastic shrinkage itself does not cause cracking if the concrete is allowed to shrink freely. As discussed in Section 2.4.1, a crack only occurs if this volume change is restrained. As the free water is removed from the concrete body and if sufficient restraint is provided, the surface concrete contracts, resulting in tensile stresses that cause random cracking or cracking that follows the position of non-uniformities such as reinforcing steel or varying depth (ACI 224R-80, 1984; Combrinck, 2016). Cracking which occurs due to plastic shrinkage is referred to as plastic shrinkage cracking. This from of cracking and volume change is more prone to concrete elements with large exposed areas, such as bridge decks, pavements, slabs on grade and suspended slabs (Combrinck, 2016).

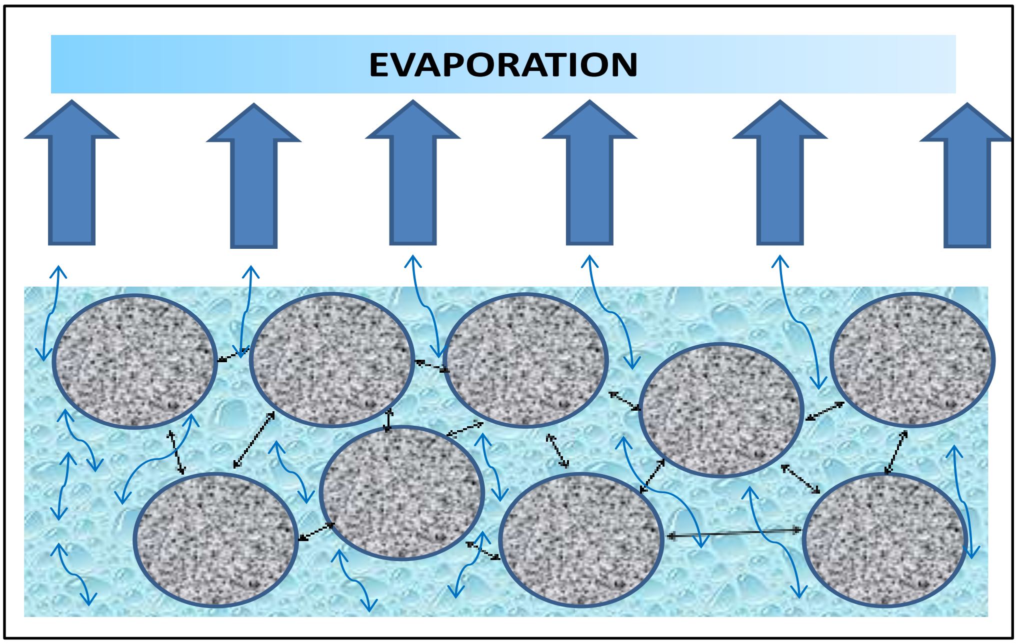

Figure 2-10: Mechanism behind plastic shrinkage

Evaporation is therefore seen as the driving force behind plastic shrinkage, while the main mechanism responsible for cracking under the influence of plastic shrinkage is the capillary pressure build-up within the pore system of the concrete (Wittmann, 1976; Slowik et al., 2008). Literature by Slowik (2008) explains the relationship between crack formation and capillary pressure and is visually represented in Figure 2-11.

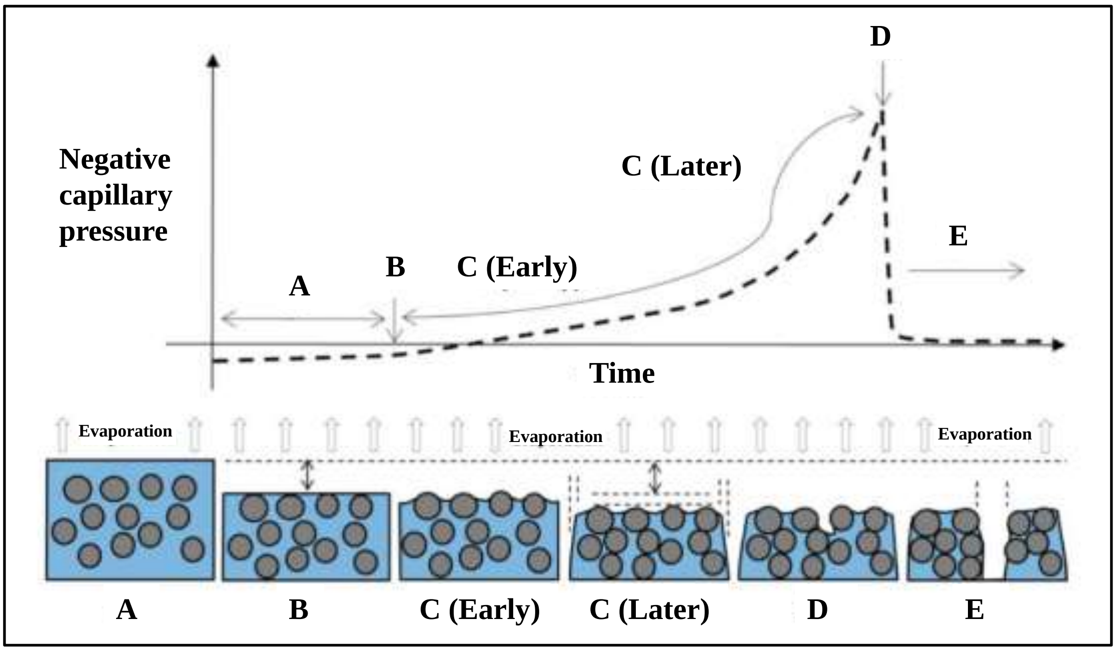

Figure 2-11: Important stages and points during the build-up in capillary pressure, within the pore system of plastic concrete (Compiled by Combrinck 2016 as adapted from Slowik et al., 2008)

Stage A represents a freshly placed concrete body and during this stage, the settlement of solid particles displaces water to the surface of the concrete, resulting in a thin film of water damming above the concrete's surface. As mentioned in Section 2.2.3, the displacement of water as a result of settlement is referred to as bleeding. At this point, the rate of bleeding is higher compared to the evaporation rate of the concrete and therefore no capillary pressure build-up occurs, since the surface of the concrete contains adequate moisture required for evaporation. As the rate of settlement decreases, the rate of bleeding slowly reduces until a point is reached where the rate of evaporation is higher compared to the rate of bleeding. Ongoing evaporation continues to draw water from the surface of the concrete until all the bleed water on the surface of the concrete has evaporated, as shown at Stage B. This is referred to as the drying time of concrete and represents the point where there is insufficient water available on the surface of the concrete for evaporation.

Due to insufficient moisture on the surface of the concrete, ongoing evaporation starts to draw water out from the capillary pores of the concrete body. This marks the start of capillary pressure build-up and due to the adhesive forces and surface tension of the pore water, water menisci are formed between the solid particles as represented by the early portion of Stage C. Water menisci can be explained as concave water surfaces formed between solid particles as shown in Figure 2-12. The curvature of the water menisci causes a negative pressure in the capillary water that tends to pull the particles together in both the vertical and horizontal directions as shown during the later portion of Stage C.

This negative capillary pressure experienced within pores can be explained using the Gauss-Laplace equation (Eq. 1) while Figure 2-12 provides a visual representation of this equation. The pressure build-up P is inversely proportional to the radius R as well as dependent on the surface tension σ_t of the pore water (Neville, 1963; Wittmann, 1976). This therefore reveals, that the more concave the water menisci become, the stronger the negative capillary pressure acting on the solid particles.

$$P = -\frac{2\times\sigma_t}{R} \qquad \text{(Eq. 1)}$$

With:

P = pressure build-up [N/m²];

σ_t = surface tension [Pa];

R = radius of water meniscus [m]

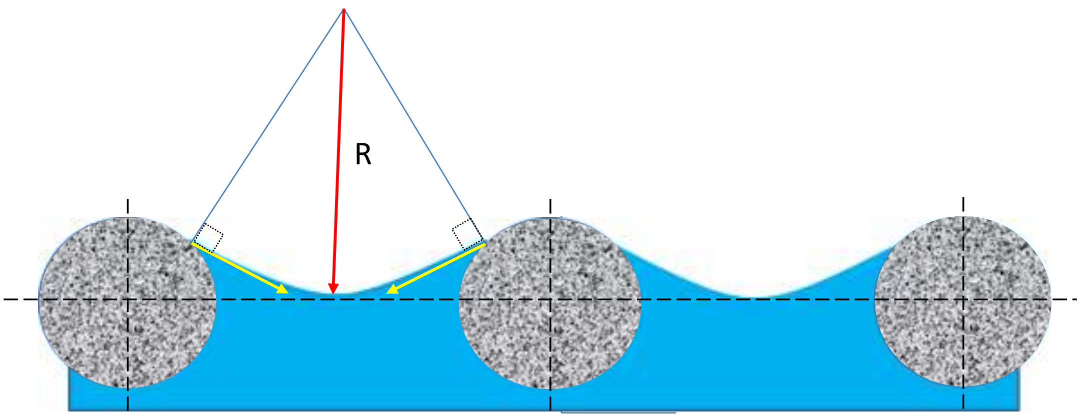

Figure 2-12: Pressure build-up due to the formation of water meniscus

Stage D marks the point of air entry and corresponds to Point D on the capillary pressure graph. As ongoing evaporation continues to draw water out from the capillary pores, the curvature of the water menisci become deeper until which point the water menisci become too small to bridge the gap between particles, resulting in the entrance of air into the pore system, which results in a break in pore pressure.

It should however be noted that the point of air entry is a local occurrence which forms weak spots throughout the concrete's body, which contribute towards future crack growth (Slowik et al., 2008; Boshoff & Combrinck, 2013). Furthermore, point of air entry should not be mistaken as the end of capillary pressure build-up, as it merely indicates that a break in pore pressure occurred at the sensors tip. This means that the capillary pressure sensors tip is no longer in contact with the pore water system of the concrete, which therefore results in a drop in pore pressure measurement. Capillary pressure continues to build-up at several different locations in the concrete body for as long as evaporation continues.

Stage E marks the cracking stage and due to ongoing evaporation, capillary pressure continues to build-up in areas adjacent to points of air entry. At this point the contracting forces between particles in the air penetrated regions are considerably smaller compared to the water filled pores experiencing negative capillary pressure build-up. This therefore results in a localisation of strains taking place within the concrete body and if these strains are restrained, possible crack formation occurs (Slowik et al., 2008; Combrinck, 2016). It should however, be emphasised that point of air entry does not necessarily result in the formation of a crack, however crack formation cannot form at a location where air entry has not occurred (Slowik et al., 2008).

2.4.3 Influencing factors

A wide range of influential factors affecting the cracking behaviour of plastic concrete exists. These factors can range from casting procedures, mix properties, environmental conditions, construction methods, material constituents, restraint conditions, etc. This highlights the diversity of the various factors affecting the cracking behaviour of plastic concrete. Discussing all factors in depth can result in cumbersome and circular discussions. The main reason for this is that all factors are interrelated and by changing one factor, could influence several other factors relating to the cracking behaviour of concrete. Furthermore, isolating factors in terms of volumetric changes is not possible since all factors are interrelated.

For example, the use of a viscosity modification agent, as discussed in Section 2.3.6, is expected to increase the cohesion properties, thereby reducing bleeding, which in turn reduces the risk of plastic settlement cracking. However, the reduced bleeding means that the concrete is more exposed to evaporation, which greatly increases the plastic shrinkage cracking risk. Therefore care needs to be taken when enhancing certain fresh properties in concrete, as this can influence other factors.

Table 1 displays various influential factors affecting the cracking behaviour of plastic concrete as well as the corresponding effect on each volumetric change in plastic concrete. It should however be noted that the factors outlined in Table 1, are summarised from various sources in literature and therefore other factors exist, which are not included in Table 1. However, the factors that are included in Table 1 provide valuable insight into the cracking behaviour of concrete needed to carry out this study. Table 1 comprises the following list of references: Powers (1968); Uno (1998); ACI 308R (2001); Mehta & Monteiro (2006); CCIP-048 (2010); Domone & Illston (2010) and Combrinck (2016).

Table 1: Factors influencing the cracking behaviour of plastic concrete

Influential factors affecting the cracking behaviour of plastic concrete		
Influencing Factor	**Influence on plastic shrinkage?**	**Influence on plastic settlement?**
Setting time	Yes - the longer the setting period, the greater the potential for plastic shrinkage cracking	Yes - The faster the cement hydrates, the shorter the setting period and therefore the shorter the settlement period
Evaporation	Yes - The higher the rate of water evaporation, the greater the risk of plastic shrinkage cracking	Yes - Factors that influence evaporation (wind speed, relative humidity, air temperature, concrete temperature, etc.) can affect the setting period of concrete
Capillary Pressure	Yes - Capillary pressure is the main mechanism behind plastic shrinkage cracking	Yes - Capillary pressure can affect the rate and amount of settlement as well as extend the settlement period
Bleeding	Yes - The more bleeding, the less potential for plastic shrinkage cracking as this delays the capillary pressure build-up	Yes - A reduction in bleeding, can reduce the risk of plastic settlement cracking by reducing the amount of settlement

Influential factors affecting the cracking behaviour of plastic concrete		
Influencing Factor	**Influence on plastic shrinkage?**	**Influence on plastic settlement?**
Admixtures	Yes - Admixtures can influence the setting time, capillary pressure build-up, bleeding, etc.	Yes, can influence concrete slump, settlement duration, bleeding, setting period, etc.
Material Constituents	Yes - Admixtures and cement type can influence setting times and therefore influences the setting and bleeding of the concrete. An increase in fine content, also increases potential for plastic shrinkage cracking	Yes - the larger the amount of fines and the smaller the fine particles, the lower the risk of plastic settlement cracking. The addition of admixtures can also influence plastic settlement cracking
Restraint	Yes - Restraint against plastic shrinkage can affect the cracking behaviour	Yes - Restraint, formwork geometry, concrete cover can affect the plastic cracking behaviour
Water content	Yes - A higher water-to-cement ratio can influence setting times	Yes - A higher water content can influence bleeding, aggregate dispersion, setting times, slump measurements, etc.
Plastic settlement cracking	Yes - Plastic shrinkage often increases the severity of crack width and area resulting from plastic settlement cracking	
Plastic shrinkage cracking		Yes - A longer settlement or bleeding period, may reduce the intensity of plastic shrinkage cracking

2.4.4 Preventative measures

The severity of plastic shrinkage and plastic settlement cracking can be reduced through the incorporation of several preventative measures. Section 2.4.1 identified the settlement of solid particles as the main mechanism behind plastic settlement cracking. Therefore in order to reduce the potential for settlement cracking, the rate and amount of settlement needs to be reduced, as well as the degree of differential settlement (Combrinck, 2016).

Section 2.4.2 identified evaporation as the main driving force behind plastic shrinkage. Ongoing evaporation continues to draw out water from the capillary pores, which in turn results in a negative capillary pressure build-up within the concrete body. This is believed to be the main mechanism behind plastic shrinkage cracking. Therefore in order to reduce the severity of plastic shrinkage cracking, the loss of water from the concrete's body needs to be either reduced or prevented.

Correct construction procedures can greatly reduce the severity or plastic shrinkage cracking potential of plastic concrete, however, negligence and lack of knowledge during the construction process ensures that plastic cracking remains a significant problem in the construction industry. Possible preventative measures for each volumetric change, are discussed separately in the following sections.

2.4.4.1 Plastic settlement cracking

The following preventative measures can be incorporated to reduce the severity of plastic settlement:

- Settlement cracks can be reduced through the re-vibration of concrete, provided that it is applied during the plastic period (Mehta & Monteiro, 2006). This in turn improves the bond between the concrete and the reinforcing steel by closing any form of cracks or voids formed during the initial settlement period.
- By increasing the ultra-fine content of the sand, the cohesion of the concrete mix is increased, which in turn reduces the amount of bleeding and therefore lowers the settlement cracking potential of the concrete. Furthermore, the amount of settlement can also be reduced by the addition of synthetic micro-fibres to the concrete (±0.9 kg/m^3) (Combrinck, 2012).
- The degree of differential settlement can be reduced by providing the maximum amount of cover to reinforcing steel. In general the provided cover to reinforcing steel should be at least twice the maximum aggregate size in the concrete element (CCIP-048, 2010).
- Lastly, the construction technique of sequential casting of concrete, can be used to reduce the degree of differential settlement (Powers, 1968). For example, the lower section of a T-beam can be placed and allowed to settle before placing the final layer of concrete. This will prevent the settlement of solid particles in the top layer of the T-beam from settling into the lower section of the T-beam, which in turn lowers the cracking potential caused by differential settlement.

2.4.4.2 Plastic shrinkage cracking

Preventative methods for reducing the severity of plastic shrinkage cracking can be further divided into internal and external methods. Internal preventative measures include:

- A reduction in the fine content of a concrete mix can decrease the plastic shrinkage cracking potential by increasing the amount of bleeding, which ultimately provides more water on the surface of the concrete for evaporation, which in turn lowers the capillary pressure build-up (Uno, 1998).
- The addition of a low volume of synthetic polymer fines (± 0.9 kg/m^3) can reduce the plastic shrinkage cracking potential of concrete (Combrinck, 2012).

External preventative measures aim at reducing the loss of water due to ongoing evaporation and are generally used during the construction process. External preventative measures include:

- Erecting temporary windbreaks to reduce the velocity of wind blowing over the surface of the freshly placed concrete element (Mehta & Monteiro, 2006).
- Erecting temporary sunshades to reduce the concrete surface temperature. Furthermore, casting during low temperatures, such as early morning, late afternoon or even sundown, can also reduce the amount of water lost due to evaporation (Mehta & Monteiro, 2006).
- Reducing the temperature of aggregates such as sand and stone by keeping these materials in cool shaded areas prior to mixing. A lower aggregate temperature reduces the concrete's temperature which in turn reduces the amount of evaporation (Mehta & Monteiro, 2006).
- Application of initial curing procedures once all bleed water has evaporated. Initial curing refers to procedures implemented anytime between placement and final finishing operations (final setting time), to reduce moisture loss from the surface of the concrete element (ACI 308R, 2001). Initial curing procedures include fogging, the use of evaporation reducers, sun shades, wind breaks and protecting the concrete's surface with temporary coverings such as polyethylene sheeting (ACI 308R, 2001; Mehta & Monteiro, 2006).

2.5 Tensile material properties of plastic concrete

The tensile properties of concrete play an important role in determining how the concrete performs under tensile induced stresses. Section 2.4 highlighted that a crack only forms if there is a restraint of some sort that prevents volume change. The restraint induces tensile stresses in the concrete which leads to the formation of a crack. There are two main principles that relate to the tensile strength and tensile strain capacity of the concrete which both dictate the likely hood of the formation of cracks in concrete (CCIP-048, 2010). The first principal states that a crack occurs if the tensile stress induced within the concrete is greater than the tensile strength of the concrete at that point in time. The second principal states that a crack occurs if the tensile strain that develops in the concrete is larger than the tensile strain capacity of the concrete at that point in time.

However, to understand why a concrete element may or may not crack, the viscoelastic effects of concrete also need to be considered. Section 2.3.4.3 explained that the viscoelastic effects can be identified by two phenomena, namely, the creep and relaxation behaviours. Creep can be defined as a gradual increase in strain under a constant stress, whereas relaxation can be thought of as the inverse of the creep behaviour. Relaxation is defined as a gradual decrease in stress with time under a given level of sustained strain. Figure 2-13 shows the cracking behaviour of concrete taking tensile strength, shrinkage and relaxation into account. Although Troxell (1956) originally presented this figure to explain the cracking behaviour of hardened concrete, the figure can also be applied to plastic concrete.

Curve (a) in Figure 2-13, shows the predicted elastic stress induced within the concrete. This stress (σ) is dependent on both the elastic modulus (E) of the concrete as well as the strain (ε) induced in the concrete ($\sigma = E\varepsilon$). Point (c) marks the point where the concrete is expected to crack when a combination of the elastic modulus and shrinkage induced strain induces a tensile stress level that exceeds the tensile strength of the concrete (Mehta & Monteiro, 2006). In reality however this elastic stress is not a direct indication of the behaviour of concrete. When a concrete element is restrained, the viscoelasticity of concrete relates to a decrease in stress with time which is shown by curve (b). Therefore under restraining conditions, the interplay between elastic tensile stresses, shrinkage strains and stress relaxation can be considered as important factors when investigating the cracking behaviour of structures (Troxell, 1956; Mehta & Monteiro, 2006).

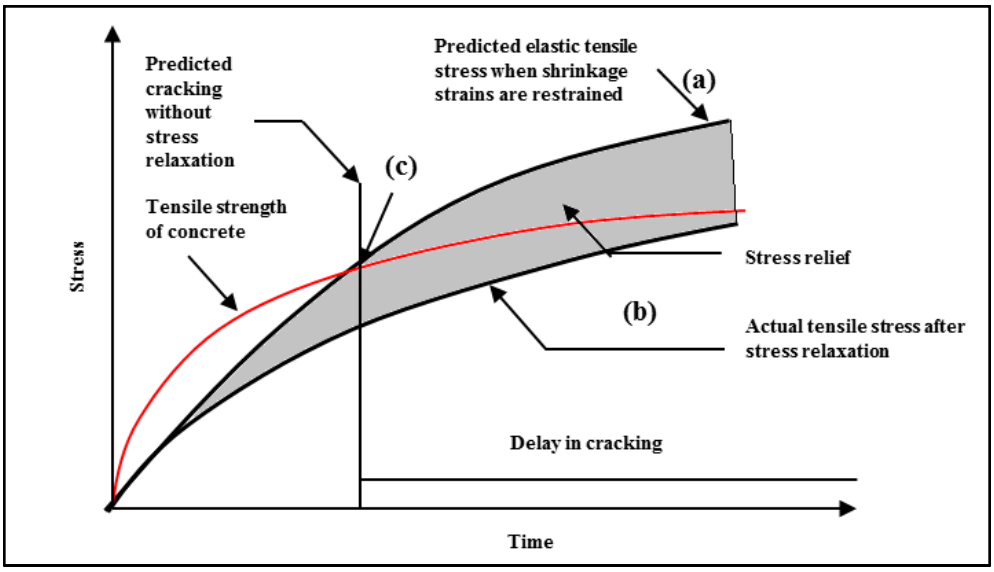

Figure 2-13: Influence of shrinkage and viscoelasticity on concrete cracking (Troxell, 1956)

2.5.1 Tensile Strength

The tensile strength (Ft) or peak stress of concrete is defined as the maximum strength that a concrete element can withstand before failure. Although literature on the tensile properties of fresh concrete remains limited the tensile strength of fresh concrete has been studied more compared to the other tensile properties. The most recent tensile strength results can be linked to that of Nguyen et al. (2017). Figure 2-14 shows the results of Nguyen et al. (2017) compared to literature by Kasai et al. (1972); Abel & Hover (1998); Hannant et al. (1999) and Dao et al. (2009). Results in Figure 2-14, show a similar trend of an exponential increase in tensile strength development with time across all studies. There is a general agreement between researchers that the development of strength for the first three hours is slow and once the dormant period has surpassed, the strength gain is more rapid (Hannant et al., 1999; Dao et al., 2009; Nguyen & Dao, 2015; Nguyen et al., 2017).

There are however, slight differences in the start and rate of strength development amongst the studies compared in Figure 2-14. Possible reasons for these differences could be due to the combined effects of the following (Nguyen et al., 2017):

- Difference in mix design and curing procedures and methods

- Effectiveness of measures taken to eliminate external forces such as friction
- Accuracy of data capturing methods and devices
- Assumed time of zero for measuring the age of concrete

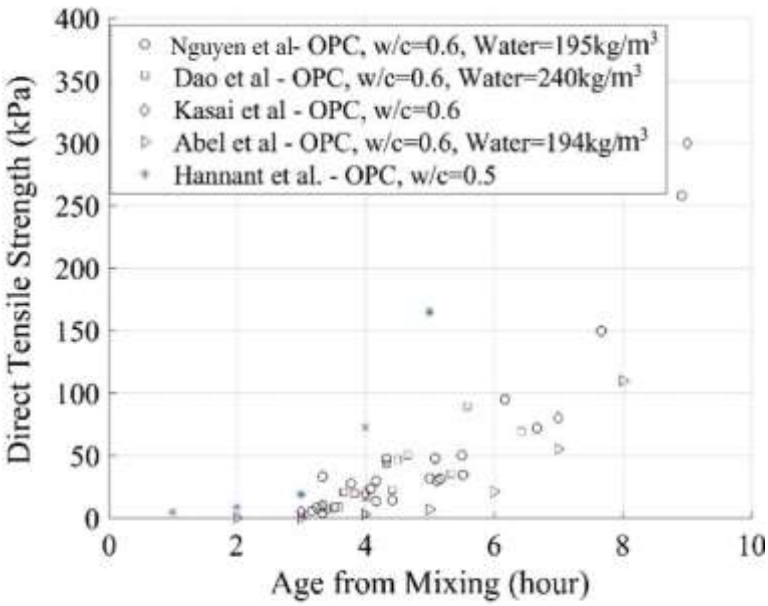

Figure 2-14: Comparison of tensile strength results by Nguyen et al. (2017).

Nguyen et al. (2017) also compared their results with current models used to predict the tensile strength of concrete, as seen in Figure 2-15.

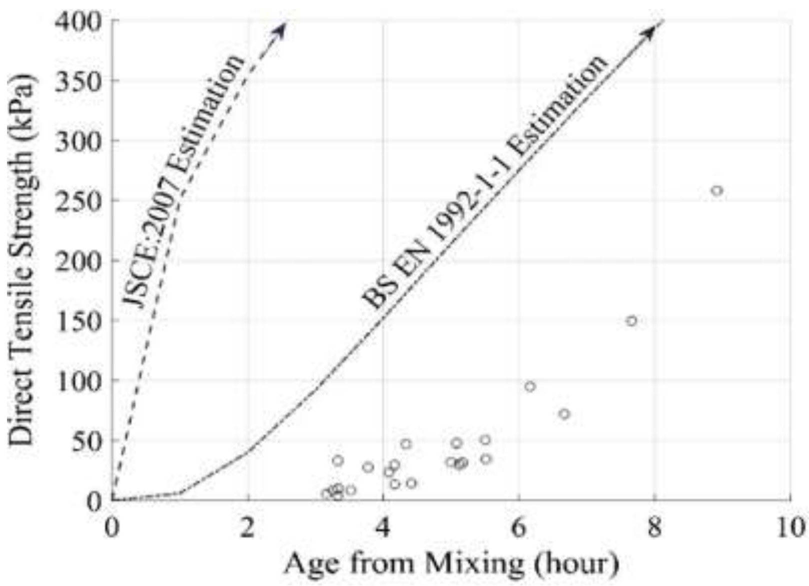

Figure 2-15: Effectiveness of tensile strength models compared to experimental results by Nguyen et al. (2017)

There is a significant difference in results obtained by the relevant models compared to experimental results. The main reason for this is that the models are more suited to hardened concrete which relies on the compressive strength of concrete with time in order to get the corresponding tensile strengths. Obtaining compressive strengths of plastic concrete at different times in the stiffening and setting stages, remains largely difficult since the concrete is still plastic to semi plastic during these hydration stages. This highlights the need of reliable data so that models which predict the tensile strength of fresh to early age concrete can be developed.

Furthermore, out of all the literature presented in Figure 2-14, only Hannant et al. (1999) and Abel & Hover (1998), appear to have investigated the tensile properties of plastic concrete before 3 hours after placement. There therefore remains a large void of knowledge on the tensile behaviour of plastic concrete younger than 3 hours after placement, especially considering that plastic shrinkage cracking often occurs before 3 hours after placement.

2.5.2 Strain capacity

The strain capacity (ε_{cap}) of concrete is the strain that occurs at maximum strength (Ft) or peak stress. The strain capacity can therefore be defined as the maximum deformation that the concrete element can undergo prior to failure. In other words, it is the maximum strain that occurs just before cracking occurs. The strain capacity of a material gives an indication of its ductility or brittleness. A ductile material is able to undergo large deformations before failure, whilst a brittle material's failure is more sudden with relatively small strains occurring before failure.

Figure 2-16 (a) shows results of tensile strain development with time by Roziere et al. (2015). Three concrete mixes, each with different aggregate types were compared to determine the influence on the strain capacity. Roziere et al. (2015) reported that whatever the aggregate type, all mixes showed a similar trend. The tensile strain decreased significantly between 3 and 7 hours after casting, reaching a minimum value between 7 and 10 hours which is around the final setting time. Thereafter the strain capacity increased during the hardening stage. Recent results by Nguyen et al. (2015) showed a similar trend of a decrease in strain capacity over time followed by a gradual increase to a relatively stable value, shown in Figure 2-16 (b).

Strain capacity results by both Roziere et al (2015) and Nguyen et al. (2015) are consistent with previous studies of Kasai et al. (1972); Hannant et al. (1999) and Dao et al. (2009) in that all studies showed a sharp decrease in strain capacity, recorded before the setting time of concrete. Furthermore, results in Figure 2-16 (b), show a high variability in strain capacity. This highlights the need to conduct multiple tests in order to obtain statistically valid results.

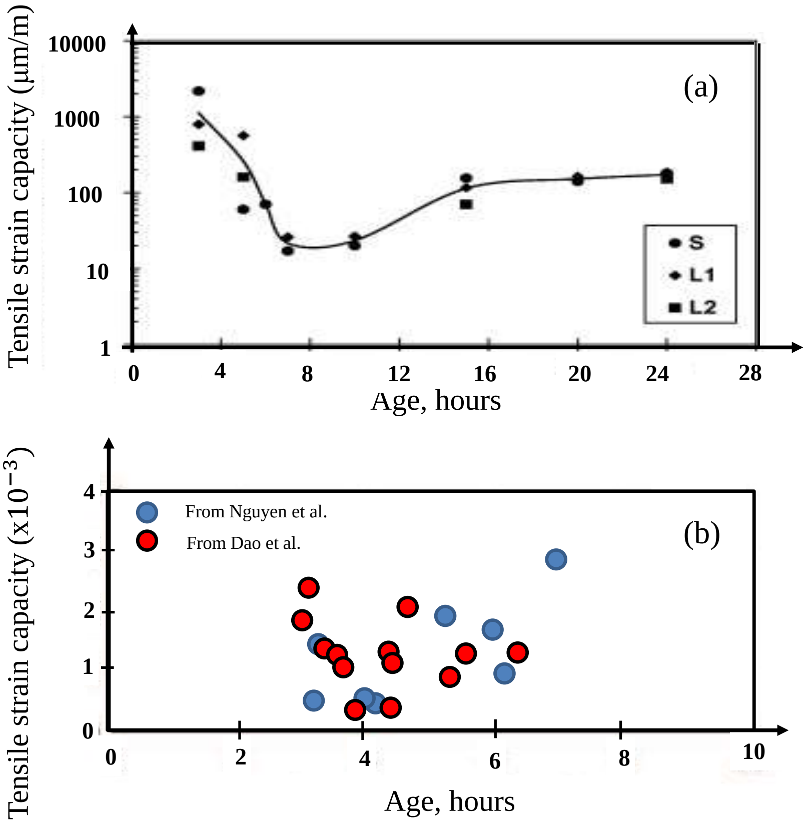

Figure 2-16: (a) Strain capacity by Roziere et al. (2015) (b) Strain capacity by Nguyen et al. (2015)

2.5.3 Elastic Modulus

The elastic modulus of concrete is defined as the ratio of uniaxial stress to the axial strain induced on the concrete element (Owens, 2009). Through this definition, one can recognise the elastic modulus of concrete as a representation of the concretes stiffness, to an imposed stress. Therefore the elastic modulus of a material describes the materials stiffness or as the name suggests the elasticity of the concrete.

The elastic modulus of plastic concrete remains largely scarce in literature. The only work that could be found, where the elastic modulus was determined by fitting a straight line to the initial ascending section of the stress versus strain graphs, was the work of Dao et al. (2009) and Nguyen et al. (2017). Figure 2-17 displays the elastic modulus results of Nguyen et al. (2017) compared to the results obtained by Dao et al. (2009) for early age concrete with a water-to-cement ratio of 0.6 and 80 mm slump.

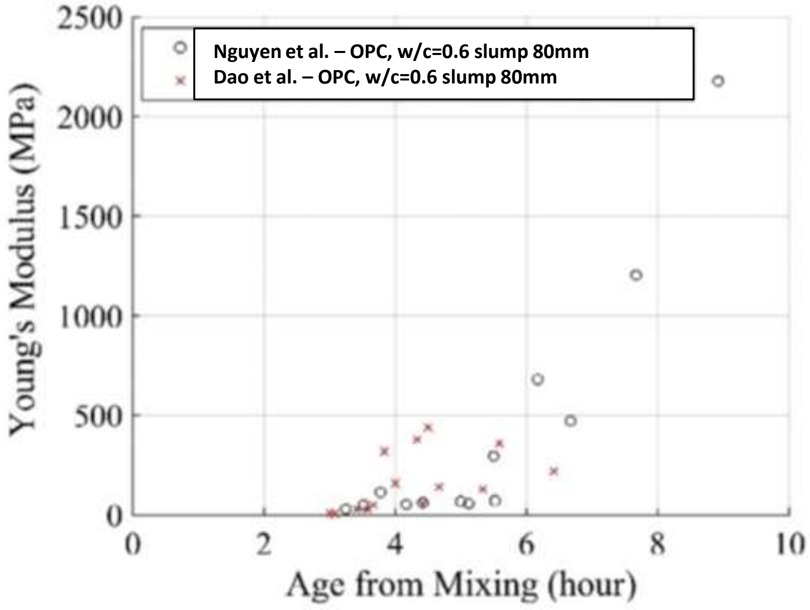

Figure 2-17: Development of Elastic modulus with time by Dao et al. (2009) and Nguyen et al. (2017)

Dao et al. (2009) identified the development of the elastic modulus with time similar to the development of tensile strength with time. Furthermore, Dao's results, display a larger amount of variation compared to the tensile strength and strain capacity results. This therefore means that in order to obtain usable results for comparison between mixes, more than one test needs to be conducted in order to obtain statistically valid results.

Nguyen et al. (2017) displayed similar results compared to Dao et al (2009) with a smaller amount of variation. This is mainly due to the difference in test procedure and apparatus used to determine the stress versus strain behaviour of the concrete. Both sets of results, however, are in agreement that the tensile strength and elastic modulus behaviour of early age concrete share a strong linear relationship. Nguyen et al. (2017) suggests that the linear relationship between the direct tensile strength and elastic modulus of early age concrete can be conveniently used to determine either property if either the elastic modulus or tensile strength is unknown.

Although both sets of results, successfully display the behaviour of early age concrete in terms of the elastic modulus, the behaviour of concrete younger than 3 hours remains largely unknown.

2.5.4 Relaxation

The relaxation behaviour of concrete, graphically shown in Figure 2-18, can be defined as a gradual decrease in stress with time, under a given level of sustained strain (Mehta & Monteiro, 2006). Figure 2-13, in Section 2.5 displays the influence of relaxation on the cracking behaviour of concrete. When a concrete element is restrained, the viscoelastic property of concrete results in a progressive decrease of stress with time (Mehta & Monteiro, 2006). This therefore means that the concrete element is exposed too much less stress than the elastic tensile stresses induced on the concrete element. Therefore the cracking behaviour of concrete is dependent on the following: the elastic tensile stresses induced by shrinkage restraints, the stress relief due to viscoelastic effects and the tensile properties of concrete. These three factors therefore greatly determine whether or not a concrete element will crack under restrained conditions.

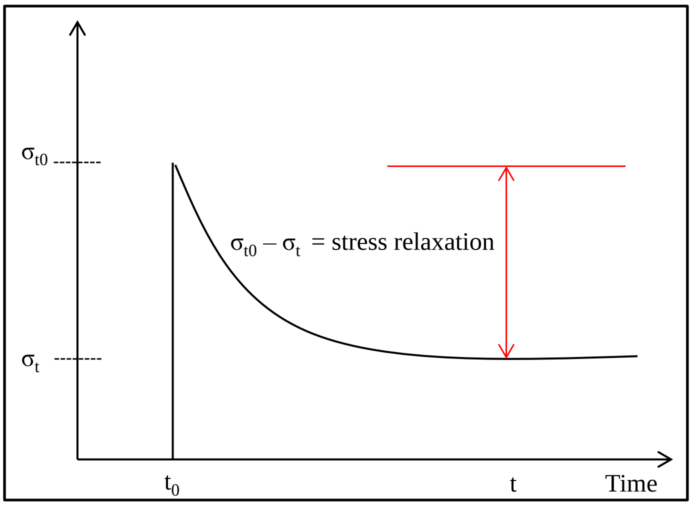

Figure 2-18: Relaxation phenomenon in concrete (Owens, 2009)

The relaxation behavior of plastic concrete remains largely unknown. Compared to the tensile strength, strain and elastic modulus, the relaxation behavior of concrete has not been given much attention in literature. The only work that could be found where relaxation was examined at early age was directly after the setting time, well past the plastic period of the concrete (Østergaard et al., 2001; Delsaute et al., 2016). Relaxation in plastic concrete was only recently explored; however this was on concrete at an age of 5 hours 5 minutes and 6 hours 40 minutes (D. H. Nguyen et al., 2017). At this age, concrete is nearing the end of its plastic state and therefore fails to explain the influence of relaxation on the plastic cracking behaviour of concrete.

Combrinck (2016) investigated the influence of multiple loading on concrete at an age of 3 and 6 hours after placement. These tests were carried out with an aim of imitating the drying (loading) and wetting (unloading) cycles of plastic concrete. Figure 2-19 shows the behaviour of the 3 hour sample under multiple loading. Combrinck's results show that as the sample is loaded to 50 % of the average maximum tensile strength, the stress drops rapidly into the compression zone. This occurrence is indicative of the relaxation behaviour of concrete.

The 3 hour sample was able to complete multiple loading cycles, however the 6 hour sample failed during the second loading cycle. Combrinck concluded based on the results obtained, that there is time-dependent relaxation of stresses in plastic concrete due to an applied strain.

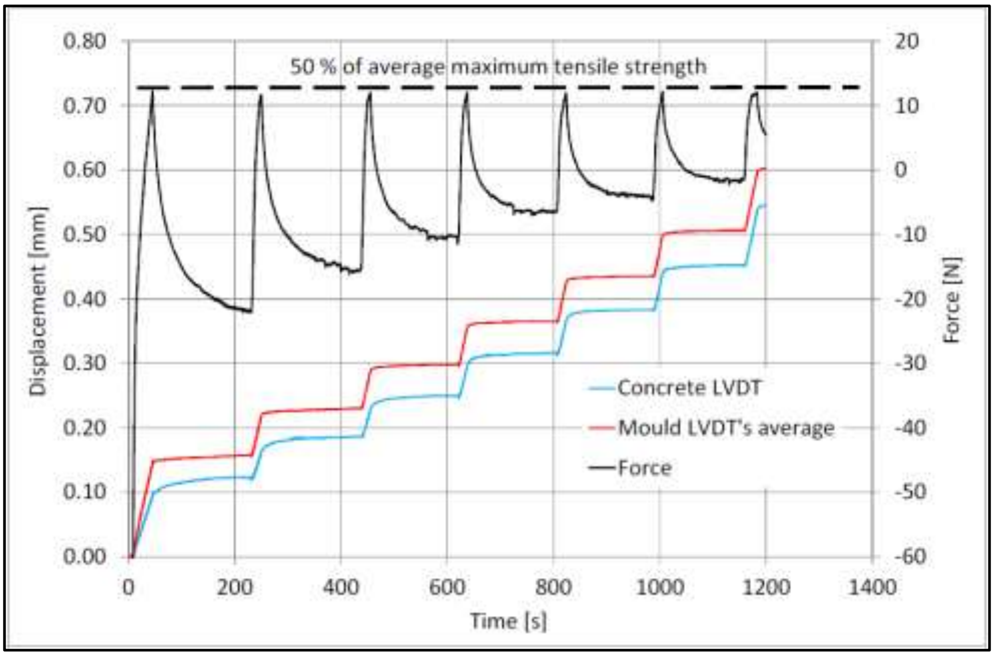

Figure 2-19: Influence of multiple loading on plastic concrete (Combrinck, 2016)

Although Combrinck (2016), successfully identified relaxation and the ability to complete multiple loading and unloading cycles, no further link between relaxation and curing was made.

Literature on the influence of curing on the cracking behaviour of concrete remains largely scarce. Apart from various literatures discussing the importance of curing during the initial plastic period of concrete, experimental research is not well documented. The only research that could be found is that of Slowik and Schmidt (2010) where a method of controlled concrete curing was applied to concrete during the first few hours after casting. Results indicate that by reducing the capillary pressure build-up within plastic concrete, the risk of cracking within the first few hours after casting may be reduced significantly. Slowik and Schmidt (2010) showed that by keeping the absolute value of capillary pressure below the value where the time of air entry occurs, crack initiation may be prevented.

Relaxation can therefore be assumed to be dependent on the viscoelastic effects of concrete. Furthermore, the relaxation behaviour is believed to hold a link to curing procedures in concrete. This therefore implies that rheology of plastic concrete can possibly affect the relaxation behaviour of plastic concrete as well as influence the response of plastic concrete to initial curing procedures. However, the lack of literature on these two topics remains largely scarce and this therefore highlights a need for further investigation into this topic.

2.6 Concluding summary

This chapter discussed the various topics needed to gain knowledge in order to conduct the current study. This included the phases of hydration, setting times and types of volume changes that occur with the plastic state of concrete. In addition to this, the various terminology and flow behaviour relating to the rheology of fresh concrete was addressed. Thereafter, the cracking of plastic concrete as well as the various influential factors and preventative measures of plastic cracking were discussed in detail. Lastly, the tensile material properties were investigated and discussed. The various experimental tests conducted to investigate the tensile and cracking behaviour of plastic concrete are discussed in the next chapter.

Chapter 3: Experimental framework

This chapter provides a detailed description of all the experimental tests conducted in this study. Experimental tests are grouped into two parts. The first part comprises of all tests relating to the tensile material properties of concrete. The second part comprises of tests relating to the plastic cracking behaviour of concrete. A detailed description of test apparatus, mould preparation and test procedures are provided for both parts. Furthermore, mix properties, mix constituents and lastly a suitable test program are also provided.

3.1 Environment simulation

All experimental tests were allowed to cure in a climate chamber to simulate extreme environmental conditions. Figure 3-1 shows the climate chamber used to simulate environmental conditions throughout the study. The climate chamber was designed to create extreme conditions that contribute to high evaporation rates, ideal for plastic shrinkage cracking. Temperature, wind speed and relative humidity can all be controlled through user-specified input values in order to reach the desired evaporation rate. The three main components that make up the climate chamber include: a heating element which is used to control air temperature, a dehumidifier unit to control the relative humidity in the climate chamber and two industrial axial fans are used to create a constant wind speed to circulate air via an internal wind tunnel, as shown in Figure 3-1. These components allow the climate chamber to simulate air temperatures as high as 50ºC, relative humidity conditions as low as 10% and wind speeds reaching up to 70 km/h. More information regarding the design aspects of the climate chamber can be found elsewhere (Combrinck, 2012).

The climate chamber was turned on at least 1 hour prior to testing. This provided sufficient time to reach the desired air, wind and humidity conditions. Furthermore, unless otherwise stated, time zero (t_0) was taken as the time the samples were placed in the climate chamber. This is further referred to as the time of environment exposure in this document.

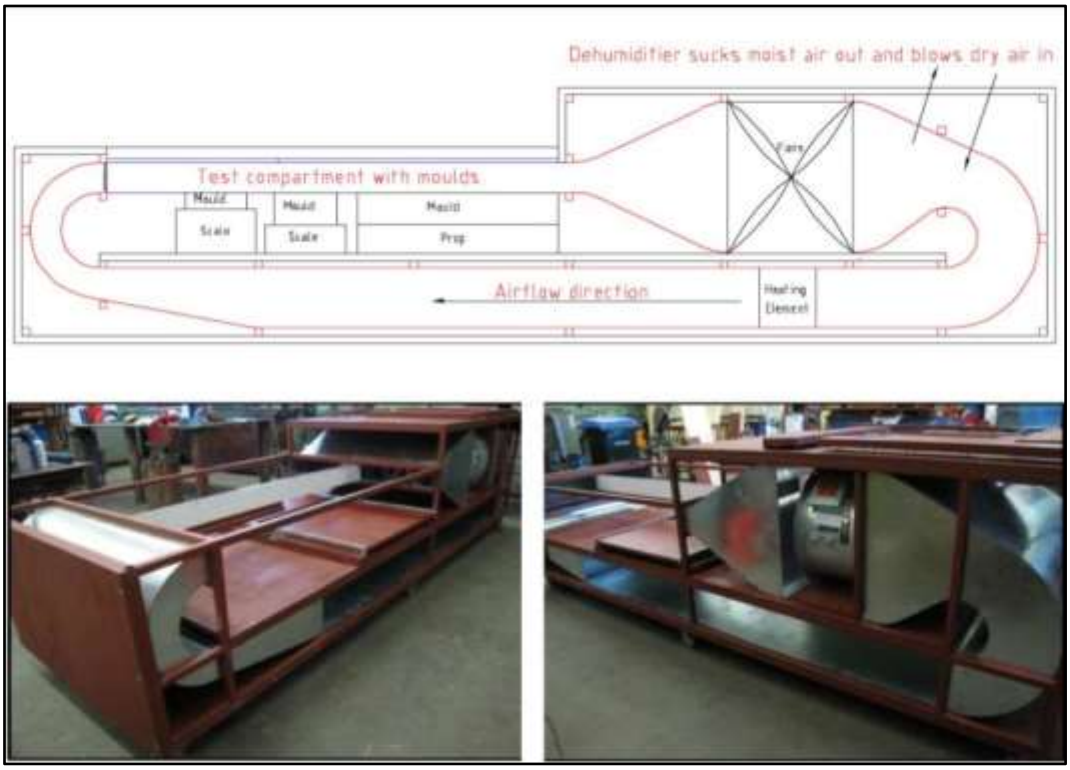

Figure 3-1: Climate chamber layout (Combrinck, 2012)

3.2 Tensile tests

Section 2.4 identified the tensile properties of plastic concrete as important factors that influence the early age cracking behaviour of concrete. Therefore to investigate the performance of plastic concrete under tensile induced loads, the cracking behaviour of concrete needs to be simulated and controlled through a mechanical induced tensile force. A state of the art tensile testing machine developed at Stellenbosch University was used throughout this study for capturing the tensile material properties of plastic concrete as shown in Figure 3-2. The sections to follow, firstly discuss the various test components that make up the tensile machine, as well as the calibration method followed and lastly the steps followed during testing. The testing procedures using this tensile set up is discussed later in Section 3.6.3.1.

3.2.1 The tensile testing machine

The tensile test machine is made up of a support beam, fixed and free loading platforms, a mechanical actuator and an air bearing as shown in Figure 3-2. Measurement sensors attached to the tensile machine are further connected to a data acquisition system for capturing all relevant information such as force, displacement and time. The tensile mould comprises of two halves and is used to conduct all tensile tests on the tensile testing machine. The sections to follow discuss each individual component, providing information on both function and design.

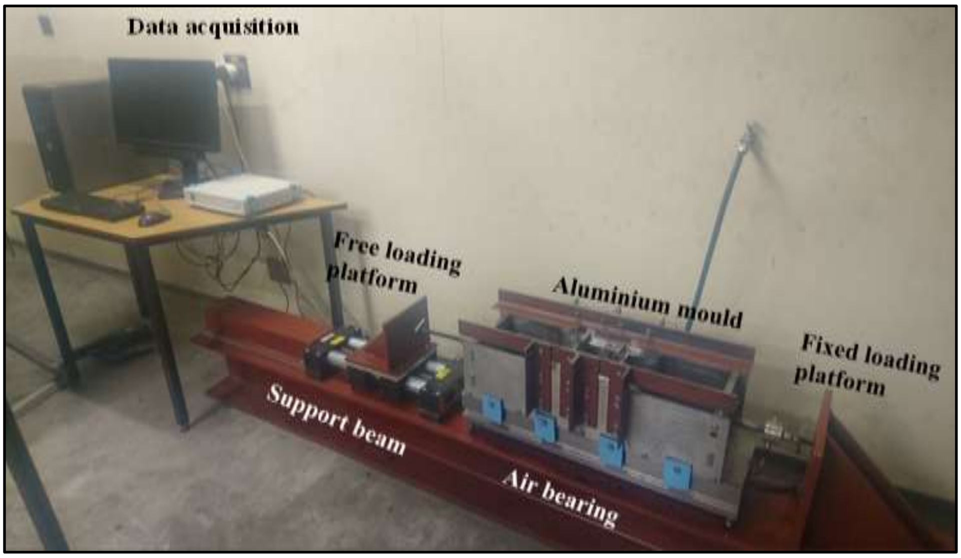

Figure 3-2: The tensile testing machine

3.2.1.1 The support beam

A steel H-beam with a 254 x 254 mm cross section is used as the supporting base structure of the test setup as seen in Figure 3-2. The 254 mm wide bottom flange is continuously supported along its entire length by the concrete floor and provides the tensile machine with adequate support and rigidity.

The beam weighs approximately 107 kg/m and provides the tensile machine with added fixity keeping the entire tensile machine in place ensuring that each test is performed under the exact same conditions as the previous test. Any movement of the support beam can greatly affect the accuracy of results as it may alter the levelling of the air bearing, which in turn affects the levelling of the mould on the air bearing, providing unwanted external forces on the concrete specimen.

The main purpose of the support beam is to provide adequate rigidity and support for the air bearing, mechanical actuator, loading platforms and the concrete filled mould. The 254 mm wide top flange provides adequate surface area to fix the mechanical actuator, air bearing and fixed loading platform on to the support beam.

3.2.1.2 Mechanical actuator

A mechanical actuator is directly bolted onto the support beam and provides the horizontal displacement required to induce a tensile force in the concrete filled mould as shown in Figure 3-3. The actuator is capable of applying a maximum tensile load of 1.7 kN and a minimum loading rate of 0.05 mm/min. This load is sufficient to induce cracking in conventional concrete during the plastic state. The variable loading rate allows the user to control the duration of the test as well as choose the optimum speed for capturing the pre- and post-cracking behaviour of the concrete.

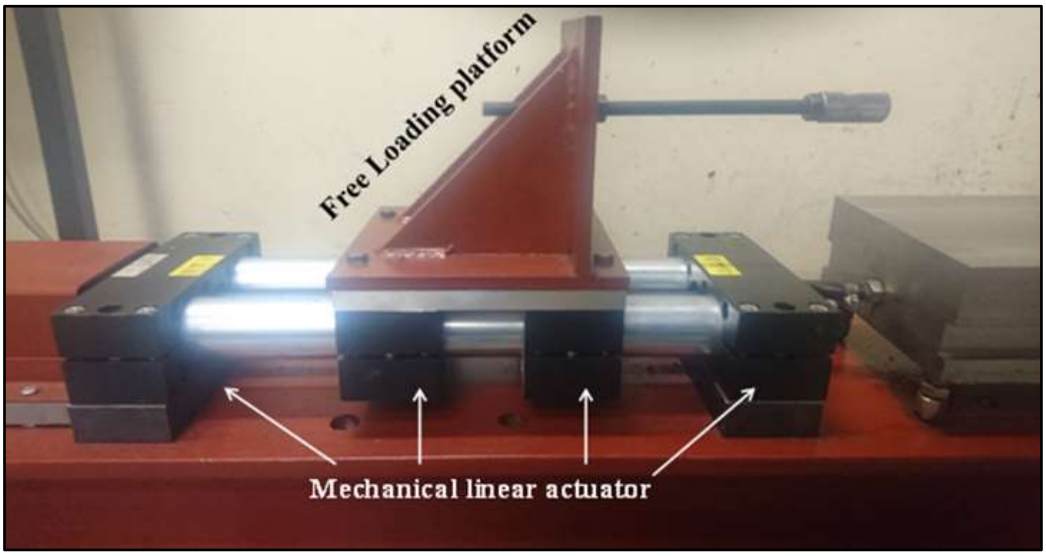

Figure 3-3: Free loading platform attached to the mechanical linear actuator

A loading rate of 0.25 mm/min is used as the loading rate for all tensile tests. At this rate a 1 mm displacement between the two mould halves takes 4 minutes. This rate is quicker than the 0.05 mm/min loading rate used by Dao et al. (2009) which resulted in undesirably long testing periods. At this loading rate, a displacement of 1 mm will take approximately 20 minutes. The tensile properties of early age concrete is believed to develop significantly during the early ages of concrete and therefore long testing periods do not reflect the tensile properties of the concrete specimen at a specific age of testing. However, a fast loading rate does provide quicker testing periods but may also affect the results obtained. Hannant et al. (1999) used a fast loading rate of 0.75 mm/min in their study which did not deliver adequate post-peak behaviour of the concrete specimens. Although this study mainly investigates the pre-peak tensile properties, it is believed that a fast loading rate would also affect the accuracy of the pre-peak tensile properties by inducing unwanted skewing between the two moulds. A loading rate of 0.25 mm/min used by Combrinck (2016) proved adequate in predicting both pre- and post-peak tensile properties.

3.2.1.3 Air bearing

The air bearing allows for frictionless movement while the moving loading platform attached to the actuator (Figure 3-4) pulls the two mould halves apart as shown in Figure 3-2 .The air bearing achieves this by using an ultra-thin film of highly pressurised air between the top surface of the air bearing and the bottom surface of aluminium mould. This ultra-thin layer of air supports the concrete filled mould by elevating the entire mould by a small distance, limiting contact between the air bearing and the mould which effectively reduces friction to a near zero magnitude. The air bearing is supported by four treaded levelling legs situated at each corner of the air bearing in order to perfectly level the air bearing and to account for uneven or unlevelled surfaces.

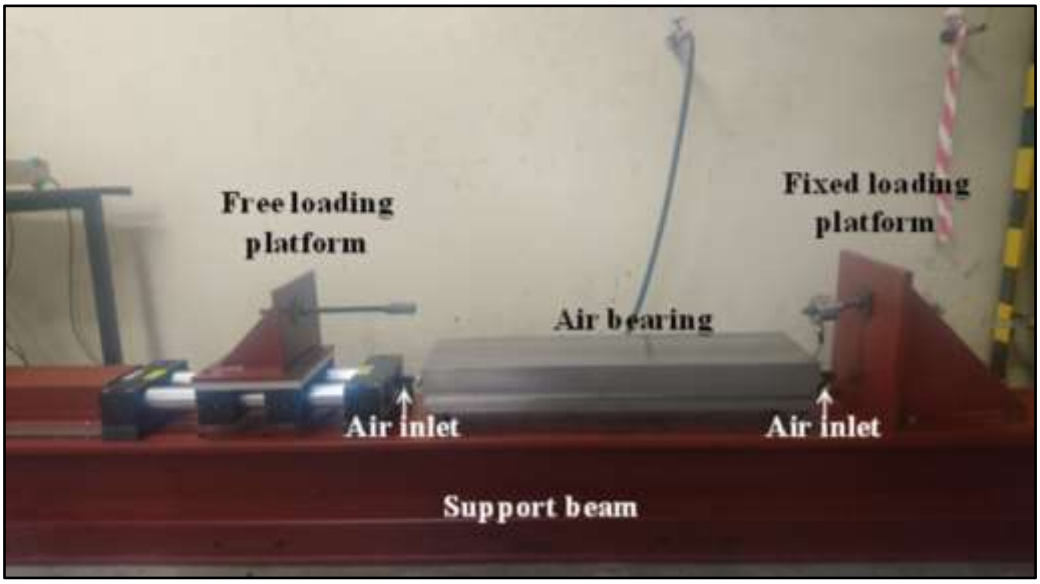

Figure 3-4: Layout of support beam, loading platforms, actuator and air bearing

The air bearing, machined from steel using computer numerical controlled (CNC) technology, contains two air inlet valves located on either side of the air bearing, an internal cavity and two rows of eight 1 mm diameter orifices spaced 100 mm apart. Air is supplied via an industrial sized air compressor with a functioning pressure of 750 kPa and reservoir size of 1.35 m^3. This air is fed into an air pressure regulator which is used to lower the air pressure supplied to the air bearing. The air regulator is manually set to allow 200 kPa of air into the two air inlet valves located on either side of the air bearing. The air travels through the air cavity and once this cavity becomes pressurised, air is forced out through the 1 mm sized orifices.

The concrete filled mould is able to float evenly at a minimum pressure of 120 kPa without any friction between the air bearing and concrete filled mould. As a precautionary, an air pressure of 200 kPa was chosen and kept constant for all tensile tests. At this pressure, the user is able to carry out long tests without depleting the air in the reservoir of the compressor.

3.2.1.4 Loading platforms

Two loading platforms, consisting of stiffened steel end plates (Figure 3-4), are used to bolt directly onto the aluminium mould as shown in Figure 3-2. The moving loading platform is directly bolted onto the mechanical actuator and moves simultaneously with the actuator as it displaces (Figure 3-3). A threaded rod, attached directly to a threaded coupling connector is used to screw onto the moving mould halve as seen in Figure 3-3. This platform is therefore responsible for inducing a tensile force in the concrete specimen as the actuator displaces away from the concrete filled mould.

The fixed loading platform is directly bolted onto the support beam and remains stationary for the entire duration of the tensile test. Attached to this platform is a 2 kN load cell which screws into a threaded coupling connector which is attached to the stationary mould halve. This loading platform together with the load cell is therefore responsible for capturing the magnitude of the tensile force induced by the moving loading platform.

The two loading platforms are also responsible for imposing certain boundary conditions onto the two mould halves. The fixed loading platform imposes a fixed boundary condition onto the stationary mould halve. This prevents any form of lateral and rotational degrees of freedom from acting on the stationary mould halve at the connection. The moving loading platform imposes a semi-fixed boundary condition on the moving mould halve. The threaded rod used to attach the moving mould halve onto the moving loading platform is longer compared to the threaded connector found on the completely fixed stationary end. This allows a certain amount of lateral movement which is needed for two reasons. The first reason is to ensure that the tensile force induced by the moving platform is perfectly aligned with the fixed loading platform. This ensures that a pure tensile force without any rotational moments is induced on the concrete specimen. The second reason is to allow the threaded rod attached to the moving platform to adjust itself as the tensile load pulls the two mould halves apart. This is important to prevent and rectify any form of skewing that may result as the two mould halves move away from each other.

3.2.1.5 Tensile mould

The mould used to conduct tensile tests on concrete specimens, is shown in Figure 3-5. The mould comprises of a dog bone shape, machined from aluminium using CNC technology. Aluminium was chosen as the preferred material to keep the weight of the mould as low as possible to ease in transportation, as well as to allow for easy floatation of the mould above the air bearing. Once filled with concrete, the mould weighs approximately 80 kg, which is owed due to the large capacity of the mould in order to test concrete mixes containing larger aggregates.

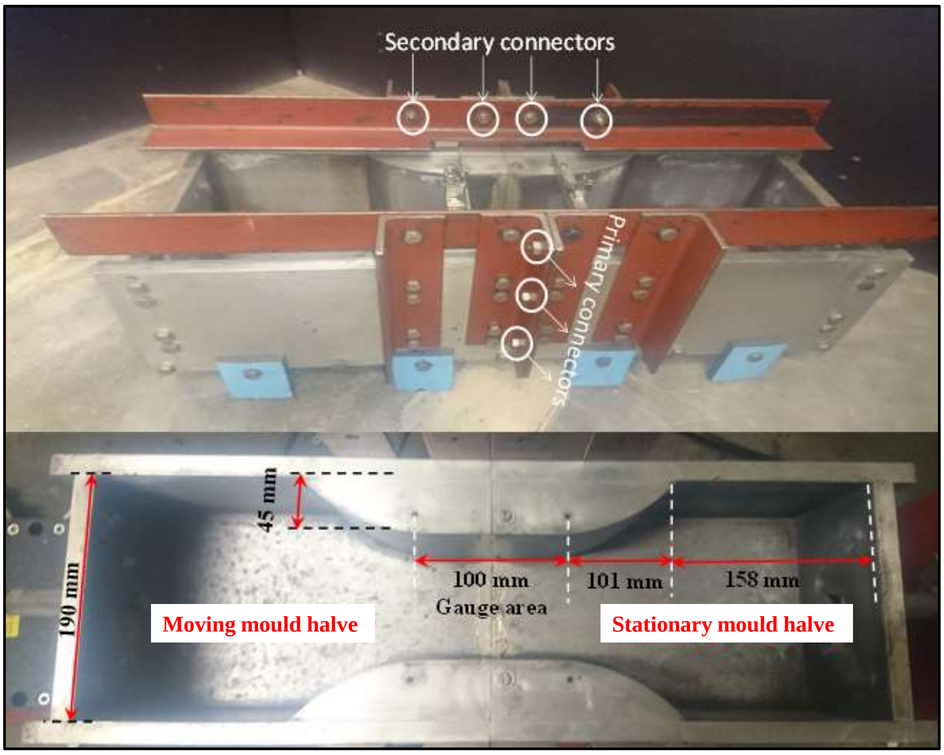

Figure 3-5: Aluminium tensile testing moulds

The dog bone shape of each tensile mould contains two curved transitions on each side as seen in Figure 3-5 that reduce the surface area of concrete within the gauge area. These curved transitions have two important functions that help improve the tensile testing of plastic concrete. The first function is to help grip the concrete and effectively transmit the induced tensile load to the concrete as the two mould halves move apart. The second function is to minimise any stress concentrations occurring outside of the gauge area. This effectively limits cracking to the gauge area of the concrete filled mould.

Each concrete mould comprises of two mould halves, namely the moving and stationary mould halve, which are connected together using a series of bolts, nuts and angle profiles as shown in Figure 3-5. The assembly of the two mould halves are first assembled by using the primary connectors which are responsible for marrying the two mould halves into a single dog bone shape mould. Each mould halve contains a set of angle profiles, one on each side of the mould (first set of primary connectors) which sits flush with the face of the mould as shown in Figure 3-6. By bolting the two angle profiles (one on each side of the mould) to the corresponding angle sections of the second mould halve (second set of primary connectors), the end result is a single mould where the face of each mould halve sits flush with one another.

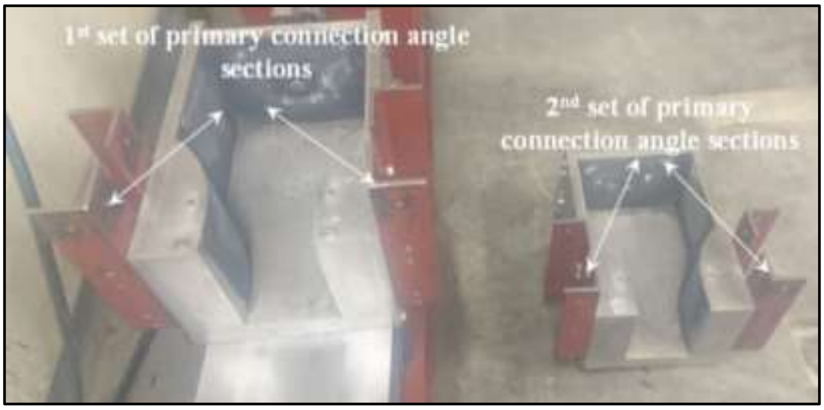

Figure 3-6: 1st and 2nd set of primary connectors

The secondary connection as shown in Figure 3-5 is done as soon as the primary connection is complete. The secondary connection comprises of two angle sections which bolt horizontally onto the primary connection angle sections and serve as transportation handles to assist during the transportation of the concrete filled moulds. The following procedure in conjunction with Figure 3-7 outlines the step by step process followed to prepare the moulds for testing:

Step one

The bottom surface and face of each mould halve is first wiped clean with a damp cloth in order to remove any dirt or dust particles that may cause friction between the mould and air bearing. Once wiped thoroughly, an oil lubricant is lightly sprayed over each mould surface and lightly wiped to ensure that a small film of oil exists over the entire mould's bottom surface. Oil lubricant is also sprayed over the air bearing before the main tap is opened to allow air to flow into the air bearing. Both mould halves are placed gently on to the air bearing and allowed to float freely (Figure 3-7 a).

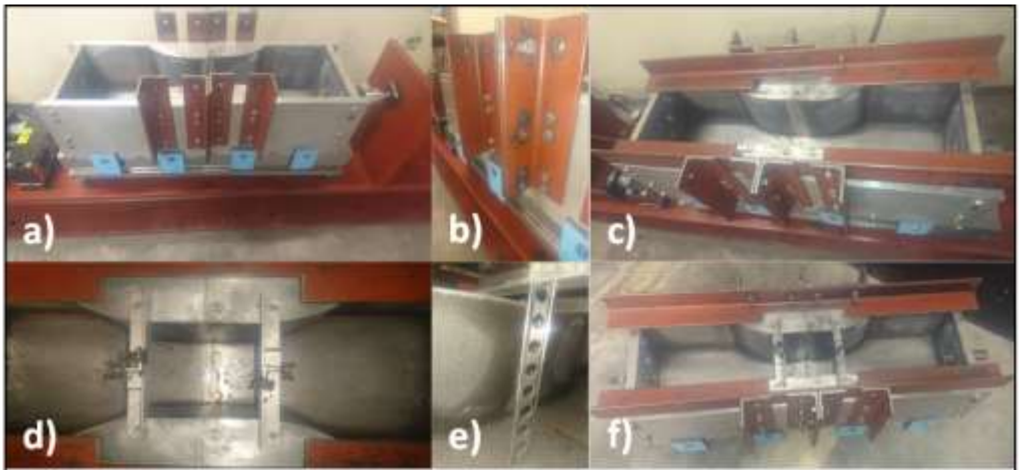

a) Align mould on air bearing
b) Fasten primary connectors
c) Fasten secondary connectors
d) Fitment of brackets and greasing
e) Insert Aluminium strips
f) Oiling concrete exposed areas

Figure 3-7: Mould assembly

Step two

The primary connection can now be bolted to marry the two mould halves together. The two mould halves are joined together by bolting each angle profile on each mould, starting from the lowest level on each side before bolting up the next level. It is important to first bolt the bottom level of connectors on each side before attempting to bolt the next level. This ensures that each mould halve is aligned accurately with one another in order to ensure that the married mould floats freely without any hindrance or friction (Figure 3-7 b).

Step three

The secondary connectors are now bolted onto the primary connection angle sections. Both transportation handles are bolted simultaneously to ensure perfect alignment (Figure 3-7 c).

Step four

The aluminium insert brackets are first screwed onto each mould halve (Figure 3-7d) after which the aluminium inserts are inserted and pegged in place (Figure 3-7 e). A light layer of grease is then traced around the connection junction between the mould halves. This is necessary to minimise any concrete from seeping through, which may hinder the free flotation of the concrete filled mould during testing. A light layer of mould oil is then applied to all concrete exposed areas within the mould in order to minimise friction and ease the de-moulding process. The complete assembled mould is shown in Figure 3-7 f.

3.2.1.6 Measurement devices

In order to investigate and capture the tensile properties of plastic concrete, three important measuring devices are needed to capture information during testing. The first device needs to capture the tensile force induced within the concrete while the second measuring device needs to record the deformation of concrete under a tensile induced force. The third measuring device needs to capture the capillary pressure build-up within the concrete under a tensile induced load. The first two measurements namely, force and displacement, are used to obtain the tensile properties relating to the stress, strain and elastic modulus of the concrete. The third measurement, namely capillary pressure, allows the user to observe and gain a better understanding of the internal capillary pressures experienced within the concrete under a tensile induced force. Figure 3-8 shows all three measuring devices attached to the concrete filled mould.

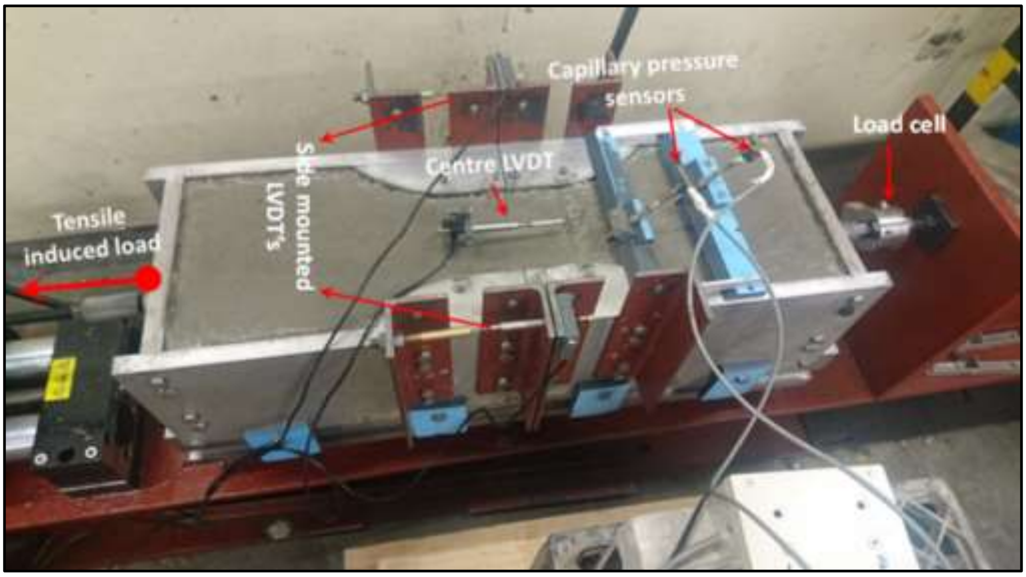

Figure 3-8: Measuring apparatus

A 2 kN load cell located on the fixed loading platform measures the corresponding force induced within the concrete as the moving platform induces a tensile load on the concrete specimen. Two linear variable differential transducers (LVDT) situated on either side of the concrete filled mould and a single LVDT fixed to the centre of the mould captures the displacement. The two side LVDT's capture mould displacement, while the centre LVDT captures concrete displacement. Two internal capillary measuring sensors inserted into the gauge and out of gauge zones within the concrete filled mould, capture the internal capillary pore pressure in corresponding zones, under tensile induced loads. Displacement and capillary pressure measurement are discussed in more detail in the following sections.

1) Displacement

The two side mounted LVDT's are attached to each side mounted angle section, situated on either side of the moving mould halve using custom made brackets, to hold the LVDT's in place. Two threaded connectors are attached directly onto the side mounted angle sections situated on either side of the stationary mould halve and held in place using threaded nuts on either side of the angle section. The LVDT's are then screwed onto the threaded connectors as shown in Figure 3-9. As the moving mould halve moves away from the stationary mould halve, the threaded connectors pull onto the LVDT's piston, which then measures the corresponding mould displacement. Capturing the mould displacement allows the user to access whether any severe skewing took place, which may alter the accuracy of the results.

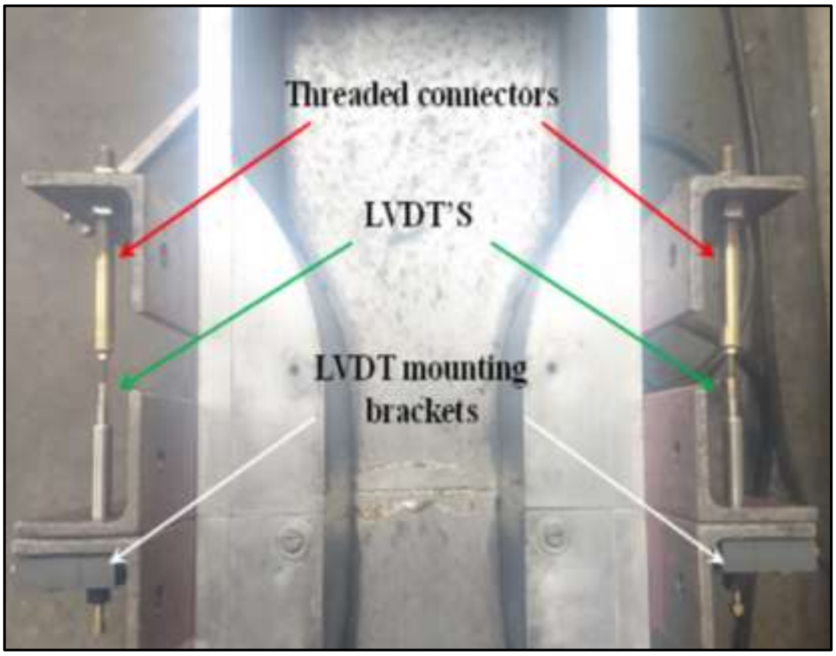

Figure 3-9: Side LVDT setup

The single centre LVDT is fixed onto the aluminium strips embedded in the concrete, within the gauge area of the mould. Aluminium inserts are placed in the mould before concrete is added and held in place by aluminium brackets as discussed in Step 5 of Section 3.2.1.5. Once the mould is filled with concrete and transported to the desired environment, the aluminium brackets are slowly removed leaving only the top section of the inserts extruding above the surface of the concrete as seen in Figure 3-10.

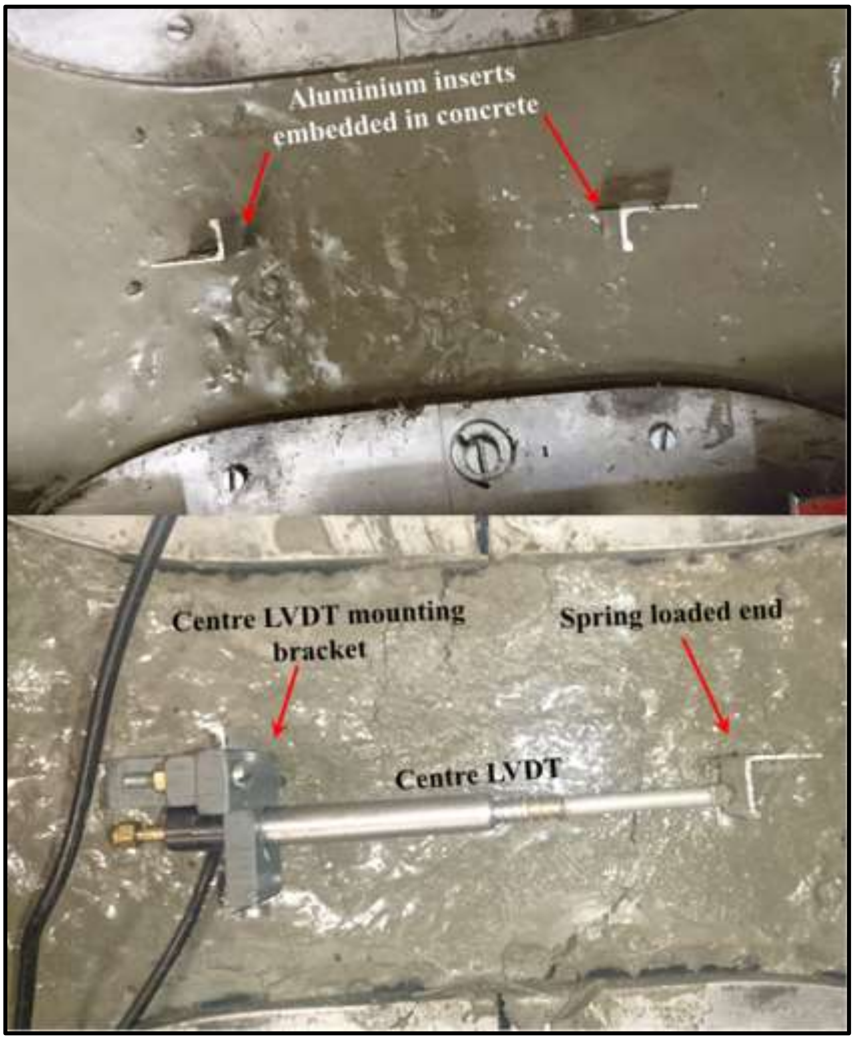

Figure 3-10: Centre LVDT setup

The aluminium inserts are left in the concrete while the concrete cures under the desired environment before being transported to the tensile machine for testing. At this point, the inserts are bonded within the concrete in the gauge area. These inserts contain a number of large holes along its length, in order to improve the bond between the inserts and the concrete. The LVDT is then fixed onto a centre bracket before being fixed onto one of the aluminium inserts situated within the stationary mould while the spring loaded point of the LVDT, rests on the second aluminium insert situated within the moving mould halve, as shown in Figure 3-10. Once the two mould halves move apart, the concrete deforms, before reaching its maximum strength or strain capacity at which point a crack occurs within the gauge area, between the two aluminium inserts, which is thus captured by the centre LVDT.

2) Capillary pressure

Figure 3-8, shows two capillary pressure measuring devices inserted into the gauge and out of gauge zones in the concrete filled mould. The development of the capillary pressure measurement sensors followed a similar method to that used by Slowik et al. (2008). Each capillary pressure measurement device comprises of a small electronic pressure sensor connected to a long hollow metal tube via a threaded connection at the tip of the pressure sensor. The electronic sensor is connected to a 3.5 mm male jack which provides power and transmits the measured capillary pressure signal to the data acquisition system for measurement.

The first step of the procedure followed to setup the sensor for capillary pressure measurement, begins by wrapping a small piece of plumbers tape around the threaded connector attached to the tip of the sensor. The hollow threaded connecter is then filled with distilled water using a syringe and hypodermic needle. The long metal tube is then screwed onto the threaded connecter before being filled with distilled water using the syringe and hypodermic needle. During filling the pressure sensor is tapped various times to remove any air bubbles trapped within the metal tube. The plumbers tape prevents any form of leakage occurring around and between the metal tube and threaded connector. Once the metal tube is filled to the brim, a small piece of sponge is lightly soaked into distilled water before being inserted into the tip of the metal tube. This small piece of sponge used, contains two functions. The first function is to prevent any solid particles from entering the metal tube once concrete is added to the mould. The second function is to prevent excessive drainage of the distilled water once inserted into the mould. The sponge therefore acts as a barrier between the concrete and distilled water within the metal tube while maintaining contact between the pore water in the concrete and the distilled water located within the metal tube.

A special bracket made to hold the capillary pressure sensors in place is fixed between the two angle sections as shown in Figure 3-11. The mould is then filled with concrete to the bottom quarter mark before the sensors are inserted and attached to the mounting bracket. The sensors rest at 45° angles on the mounting bracket and are fixed in place by tightening the secondary brackets holding the sensors in place. The moulds are then filled to capacity and vibrated. The sensors are screwed in place preventing the sensors from settling excessively during the vibration period. Once vibration is complete, the moulds are transported to the desired climate at which point the secondary brackets holding the sensors tightly in place are loosened to allow the sensors to settle freely with the solid particles. At time of testing, before transporting the moulds to the tensile machine, the secondary brackets are tightened once again to prevent the capillary pressure sensors from moving or shaking out of place which may break the pore water contact resulting in invalid results. The capillary pressure layout, mounting bracket and secondary brackets are shown in Figure 3-11.

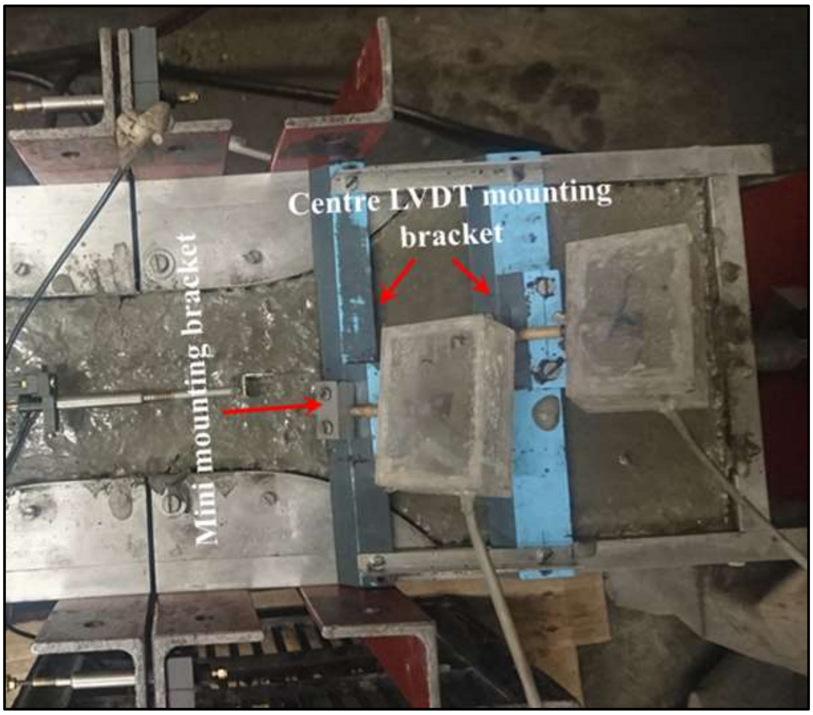

Figure 3-11: Capillary pressure sensor layout

Inserting the sensors in a horizontal position may prevent the free settlement of solid particles directly above the metal tip, creating weak spots in the concrete element. This can present a problem, especially when inserting the sensor in the gauge area as it may influence the accuracy of the tensile results and result in the formation of a crack along the length of the sensors tube. Pure vertical placement (90° angle) of the sensor may result in excessive drainage of the distilled water and by placing the tip in a vertical position in the gauge area, may also produce weak spots resulting in the formation of a crack across the metal tube. Therefore the sensors are placed in a certain orientation which allows the sensor to settle freely with the concrete particles without resulting in weak spots in the gauge area which may influence the tensile results. By inserting the sensors at 45° angles both in and out of the gauge areas the sensors are free to settle with the solid particles and found to have a minimum to negligible effect on the crack position and tensile properties of the concrete.

3.2.1.7 Data acquisition

An HBM Spider 8 data acquisition hardware device is used to capture all relevant data during the tensile test. Information from the load cell, LVDT's and capillary pressure sensors are transmitted directly to the Spider, which captures voltage differences transmitted by the measuring devices and converts this information to either force, pressure or displacement.

The load cell and LVDT's were connected directly to the Spider, while the capillary pressure sensors were first plugged into a separate power controller to power the pressure sensors and transmitted voltage readings to the Spider. This information is then transmitted to the connected computer, running a software package that continuously stores information. The software package allows the user to choose the number of data points being captured before saving this information for analysis. Data acquisition was set to 50 Hz which amounts to 50 data points being captured per second. This provides sufficient data points to capture the pre-peak behaviour of concrete under an induced tensile load.

3.2.2 Calibration

Calibrating the tensile machine involves simulating a typical tensile test without concrete. This is performed to ensure that the tensile machine induces a pure tensile force at near zero eccentricity, to ensure that measuring devices are working accurately and finally to ensure that the air bearing, mould and loading platforms are perfectly aligned to ensure minimal skewing and friction between mould faces. During this process both force and mould displacement are monitored to ensure that no rotation occurs and to ensure that zero friction occurs between the mould and air bearing.

3.2.2.1 Calibration process

The following step by step procedure in conjunction with Figure 3-12 was followed to set up the mould for both calibration and concrete testing:

Step one

The tensile mould is assembled following the four steps outlined in Section 3.2.1.5.

Step two

An oil lubricant is sprayed over the air bearing before air is allowed to flow into the air bearing. The mould is then placed onto the air bearing and allowed to float freely. During this step, the height of the air bearing is adjusted on each corner using the threaded adjustable legs to ensure that the mould floats freely without lateral movement. This step ensures that the load cell does not record any external forces such as weight due to the movement of the mould on the air beating.

Step three

The stationary mould end is now connected to the load cell and locked in place using the locking bolt (Figure 3-12 a). The moving mould end is then connected to the moving loading platform by screwing on the threaded connector onto the mould (Figure 3-12 b). If the threaded rod floats within the connecting hole without touching either end (Figure 3-12 c), the threaded rod can then be tightened using the bolts and washers as shown (Figure 3-12 d). The bolts and washers are tightened to induce a compressive force on the mould to ensure that the two mould halves do not separate during the remaining steps. If the threaded rod does not float freely and touches either end of the hole, the stationary mould halve needs to be loosened and adjusted until the free moving mould end settles within the centre of the connecting hole on the moving loading platform. This step ensures that the tensile force has near zero eccentricity. During this step, the air bearing is constantly adjusted to allow for proper mould alignment.

Step four

This step involves loosening and hand tightening the primary connectors for easy removal during the final step. Bolts located on level one are loosened and hand tightened on both sides before moving onto the bolts located on level two, following the same procedure. The bolts located on level three are completely removed to allow for easy access to the secondary connectors (Figure 3-12 e). During this step, the secondary connectors are responsible for holding the two mould halves in place.

Step five

The secondary connectors are now removed, starting from row one working up to row four. Each bolt is removed on both sides of the mould before approaching the next row of bolts (Figure 3-12 f). At this point the mould is held together by the hand tightened primary connector bolts and care needs to be taken to prevent any excessive shock or movement of the mould. Once the connectors are removed, weights are placed on the mould to mimic the weight of concrete (Figure 3-12 i).

Step six

The two side LVDT's are fixed onto the vertical angle sections on the moving mould halve while threaded connectors are bolted onto the vertical angle sections situated on the stationary mould halve. The LVDT's are then screwed onto the threaded connectors as shown in (Figure 3-12 g). Care needs to be taken to ensure that the threaded connectors and LVDT'S are perfectly aligned before being connected to each other. If not correctly aligned, additional frictional forces may be recorded by the load cell.

For tensile tests where the mould contains concrete, the centre LVDT is fixed onto the aluminium insert situated on the moving mould halve, while the spring loaded end rests against the aluminium insert situated on the stationary mould halve.

Step seven

The end connectors are slowly loosened and the mould is left to float freely once again. At this point no force is exerted on the load cell and therefore any force reading at this point on the load cell is zeroed. The mould is now fixed into place by repeating step three.

Step eight

The primary connectors are now gently removed on both sides of the mould, starting from level one, working up to level two (Figure 3-12 h). At this point the mould should be in compression, ranging anywhere between 1 and 30 N. If the compressive force is too high, the end connector on the moving platform can be lightly loosened until the desired compressive force is reached. Care however needs to be taken and it is recommended that the compressive force is adjusted in step six before removing the primary connectors.

Step nine

LVDT's are now set to a zero position using the computer aided software before turning on the actuator.

Figure 3-12: Setting up procedure

3.2.2.2 Calibration results

Figure 3-13 shows a typical force (measured by the load cell) and displacement (measured by the two LVDT'S) graph plotted against time after carrying out the calibration procedure in Section 3.2.2.1. The tensile mould was initially loaded to a compressive force between 4.5 and 5 N. Once the actuator is started, the force gradually increases towards the tensile regime before reaching a constant tensile force of 0.72 N as shown in the graph. After approximately 320 seconds the LVDT's are unscrewed from their respective threaded connectors at which point the force decreases to 0.24 N. This therefore means that the measured tensile force was mainly due to the friction caused by the plunger within the LVDT. The plunger is screwed onto the threaded connectors and as the moving mould halve, with which the LVDT's are connected, displaces away from the stationary mould halve, the plunger slides against the LVDT'S metal encasing. This sliding action between the two metal parts results in friction which is captured by the load cell attached to the fixed loading platform.

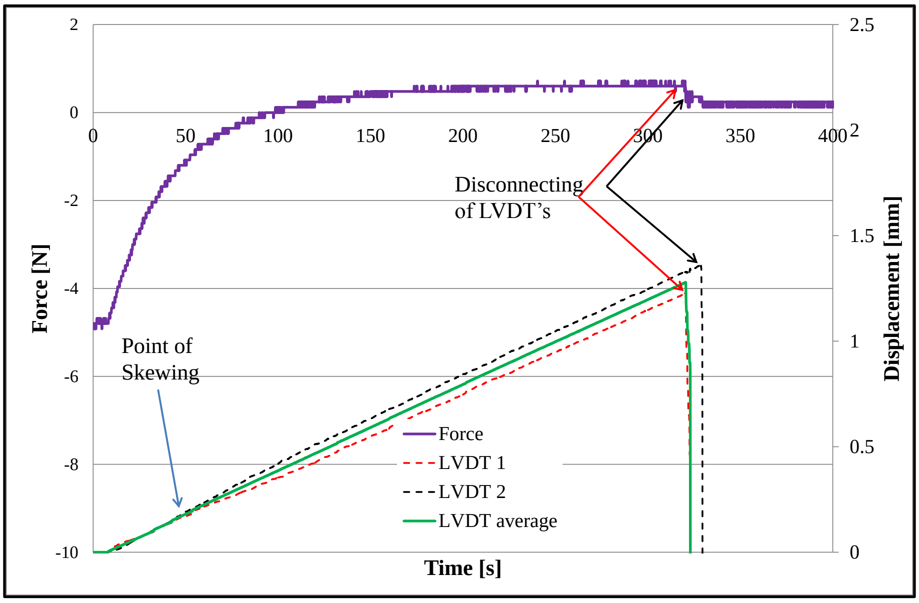

Figure 3-13: Dry run tensile test result

Initially the LVDT's displace at similar values before slight skewing occurs as the force approaches the tensile regime. Skewing or rotation of the two mould halves can be explained as the rotation of one mould halve relative to the other. Severe skewing or rotation can cause contact between the two mould faces on the side with the smaller displacement. This can cause an increase in the measured compressive force as well as cease displacement of one of the LVDT's while the LVDT with the higher displacement continues to increase. The constant decrease in force and continued displacement of both LVDT's indicate that the skewing in Figure 3-13 is acceptable and not severe enough to influence the results. Possible reasons for skewing may include: incorrect alignment of mould halves before connecting the primary connectors and/or slight eccentricity of the induced tensile force onto the mould. This eccentricity may occur if either the air bearing, mould or threaded connectors are not perfectly aligned during the setting up of the mould on the air bearing. Incorrect levelling of the tensile mould on the air bearing may also cause skewing.

In order to rectify the skewing problem, the diameter of the alignment holes located on the fixed and moving loading platforms were increased in size. This gives the mould more freedom to align itself. As the threaded connector is screwed onto the mould, by readjusting the stationary end of the mould allows the moving end to perfectly align within the respective alignment hole, without making contact on either end of the hole. If contact is made with either end, a rotational force can be induced on the mould as the two mould halves are pulled apart. Another important step is to ensure that the air bearing is perfectly centred under the mould. This will also assist in reducing the eccentricity of the applied force by ensuring an even distribution of air under the mould. Incorrect levelling of the mould on the air bearing may also result in excessive skewing between the two mould halves.

3.3 Plastic cracking tests

To gain a better insight into the cracking behaviour of plastic concrete, experimental tests were conducted on the cracking potential of plastic concrete as well as several influential factors. These influential factors include evaporation, bleeding, rheology tests, settlement, shrinkage, setting times, surface tension and capillary pressure build-up. Plastic cracking tests can therefore be divided into two groups, namely, tests pertaining to the various influential factors of plastic cracking followed by cracking measurement tests. A description of the different moulds used are discussed in the following sections, while the test procedures followed using each of these moulds are discussed later in Section 3.6.3.2.

3.3.1 Influential factor tests

The measurements of various influential factors pertaining to the cracking behaviour of concrete were carried out in order to gain a better understanding as to how the process of cracking occurs. These factors include plastic shrinkage, plastic settlement, capillary pressure build-up, evaporation, bleeding and setting times. Experimental tests on plastic settlement, shrinkage and capillary pressure build-up were carried out simultaneously using one type of mould while evaporation, bleeding and setting times were carried out separately using different mould types.

3.3.1.1 Plastic settlement, shrinkage and capillary pressure build-up moulds

Figure 3-14 shows the mould layout used to carry out plastic settlement, shrinkage and capillary pressure tests simultaneously. A 300 x 300 x 100 mm mould was used to capture the vertical settlement, lateral shrinkage and capillary pressure build-up of plastic concrete simultaneously by fitting the required measuring apparatus to four similar moulds. Previous research studies measured the capillary pressure build-up using a separate 300 x 300 x 100 mm mould, however; a simple mounting bracket was used to incorporate the capillary pressure measuring devices into the plastic shrinkage and settlement moulds. This therefore gives a good indication of how the capillary pressure build-up occurs during plastic shrinkage and plastic settlement.

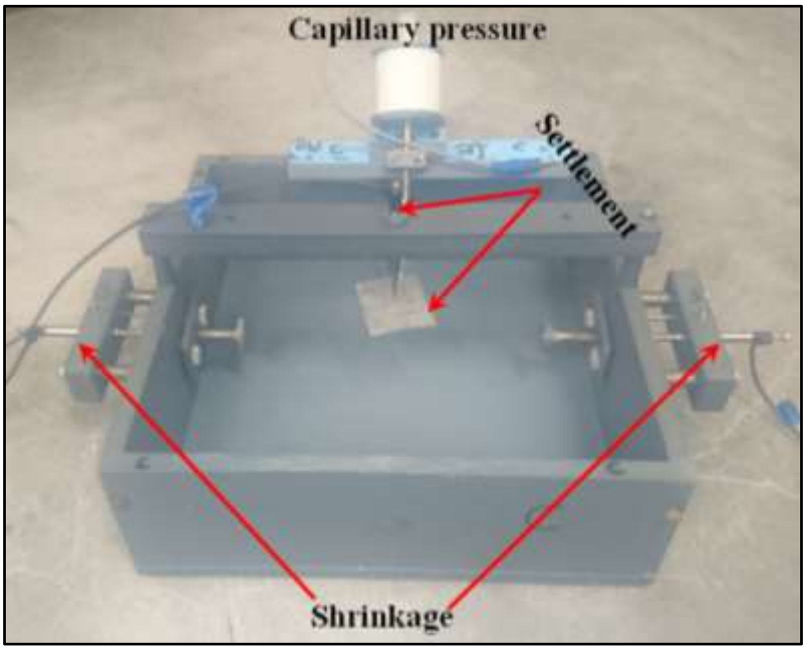

Figure 3-14: Capillary pressure, plastic shrinkage and plastic settlement test layout

3) Plastic settlement

For the purpose of the current study, the total vertical dimensional change between the start and end of the testing period is classified as plastic settlement. This therefore includes the vertical dimensional change due to bleeding of the concrete as well as the vertical dimensional change caused by the evaporation of pore water.

Figure 3-15 shows the 300 x 300 x 100 mm mould used to capture the vertical settlement of concrete. A top mounted LVDT is used to capture the unhindered vertical displacement of the concrete specimen which is held in place by the top mounting bracket. A 50 x 50 mm piece of wire lattice mesh is connected to the top mounted LVDT. This latticed mesh bonds with the concrete while allowing bleed water to pass through without affecting the wire-to-concrete bond. As the concrete settles, the mesh displaces vertically while the LVDT captures the corresponding displacement.

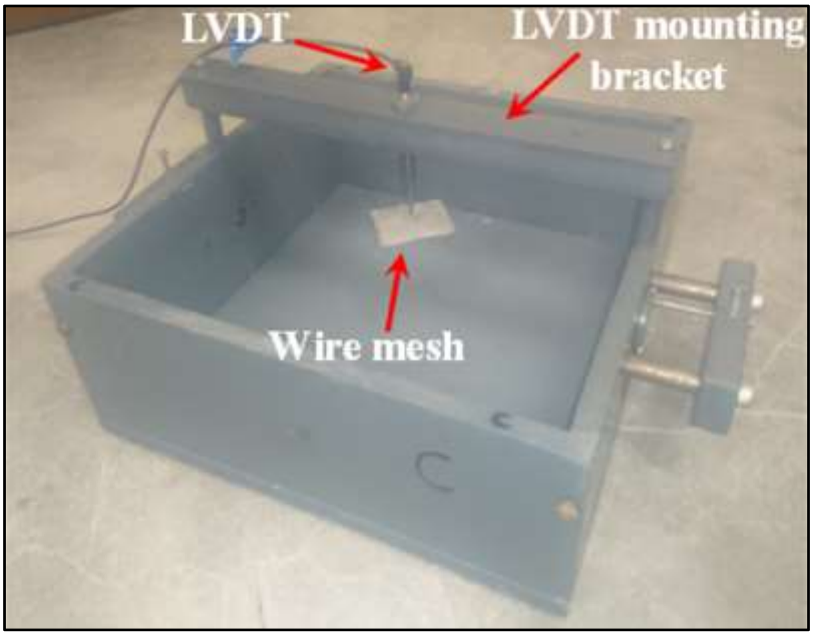

Figure 3-15: Plastic settlement mould layout

4) Plastic shrinkage

For the purpose of the current study, shrinkage is defined as the lateral contraction of a concrete body due to the evaporation of pore water. Figure 3-16 shows the 300 x 300 x 100 mm mould used to investigate the behaviour of concrete under free shrinkage. The two LVDT's connected to each mounting bracket were used to capture and measure the unrestrained shrinkage within the concrete mould over time.

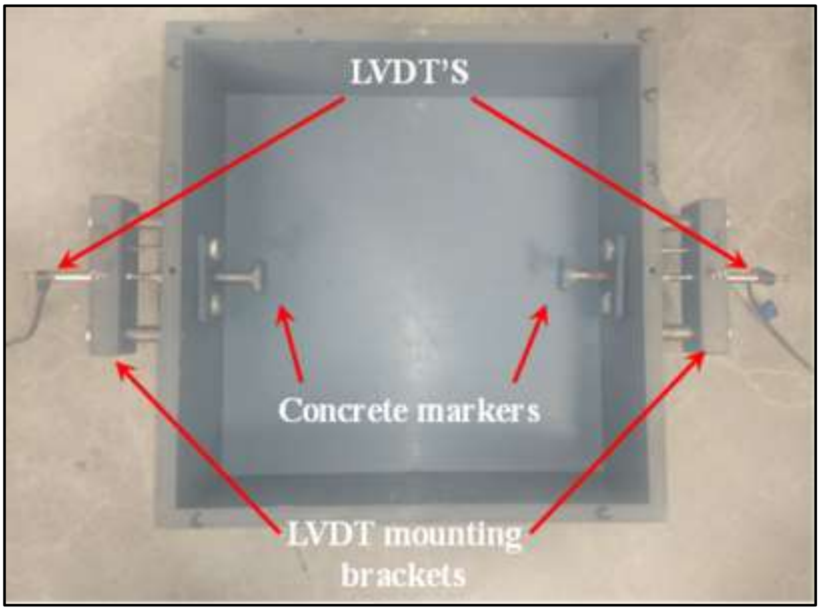

Figure 3-16: Shrinkage mould layout

The mould makes use of two markers connected to shafts, which are able to move freely through each mould end with near zero friction. The shaft slides through a hole drilled out on each side of the mould. Embedded on each side, in each hole, is a bearing which allows for frictionless movement of the shaft in and out of the hole. This provides for frictionless movement as the markers embedded within the concrete displace, allowing the shaft to displace through the bearing as the concrete shrinks as shown in Figure 3-17.

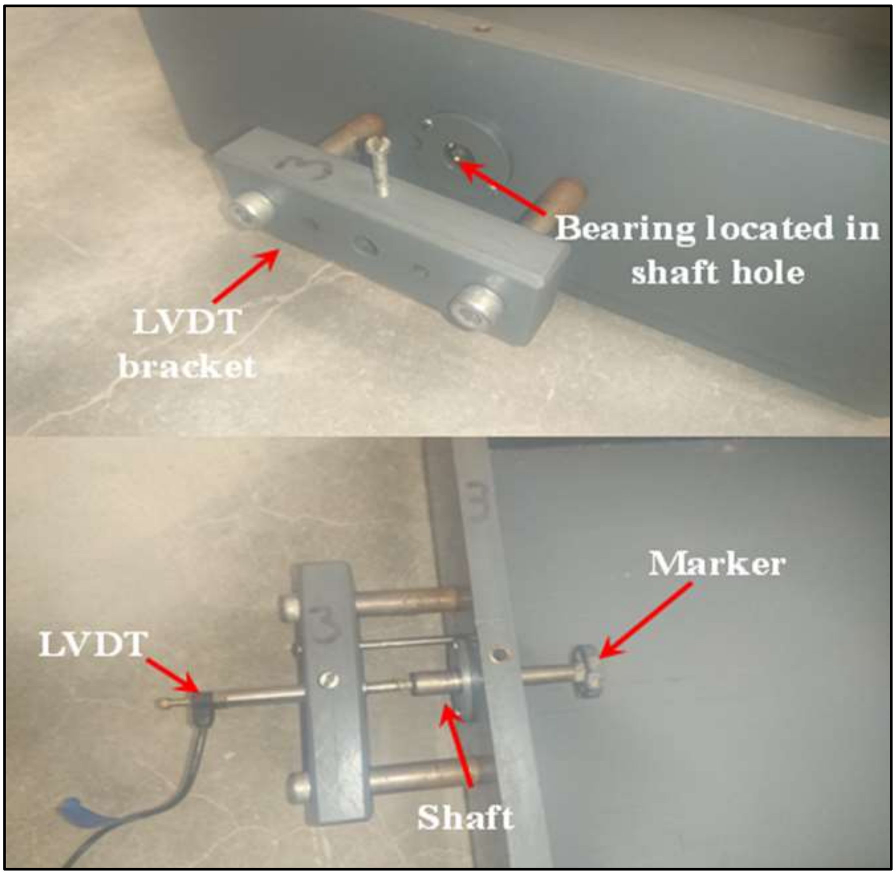

Figure 3-17: LVDT layout on shrinkage mould

The two LVDT's are held in place by the screw situated on top of the mounting bracket, while the spring loaded end is in contact with the shaft, connected to the marker embedded in the concrete. As the concrete shrinks, the markers embedded in the concrete together with the connected shafts, displaces with the concrete while each LVDT captures the corresponding displacement.

5) Capillary pressure

Figure 3-18 shows the layout of the 300 x 300 x 100 mm shrinkage and settlement mould used to capture the capillary pressure build-up of concrete during lateral shrinkage. Similar capillary pressure sensors as used during the tensile tests were used to capture the capillary pressure build-up in these moulds. A more detailed description of the sensors and setting up procedures can be found in Section 3.2.1.6.

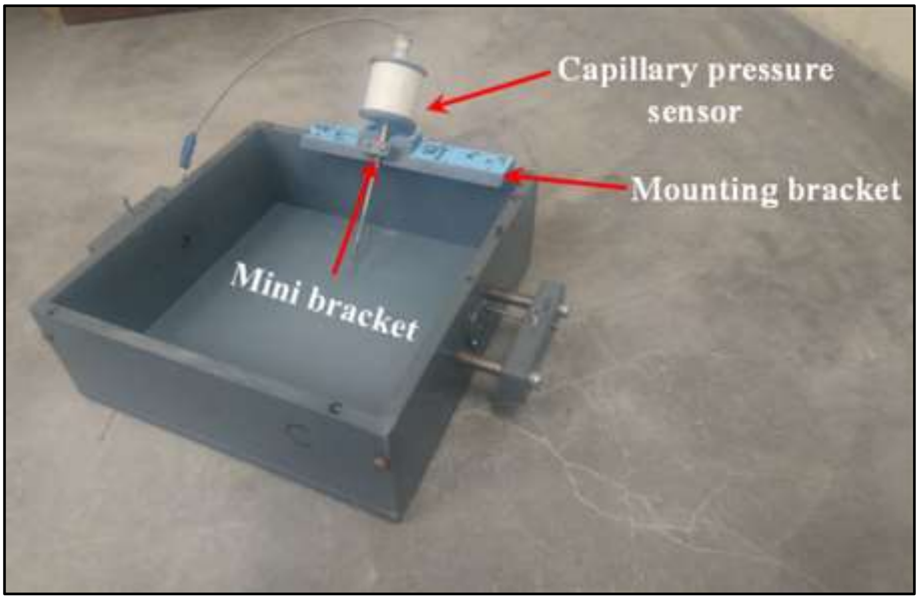

Figure 3-18: Capillary pressure mould layout

Capillary pressure sensors were held in place using mounting brackets which allow the sensors to rest at 45° angles. The mounting brackets contain secondary brackets which are used to hold the capillary pressure sensors in place during consolidation and transportation. Once left undisturbed under the desired climate, these brackets can be loosened to allow the sensors to settle with the concrete.

3.3.1.2 Evaporation

The rate of evaporation was captured using a 200 x 200 x 100 mm mould. A scale with a 0.001 kg resolution and maximum weight reading of 30 kg was used to measure the weight difference of the mould in order to capture the amount of water evaporated.

3.3.1.3 Surface tension

Surface tension tests were carried out on the mixing water used in the concrete mixes, in order to obtain surface tension results of the internal pore water in concrete. Surface tension tests were carried out in accordance with specifications prescribed by ASTM D971 (2004), using the Attension Sigma 702ET tensiometer as seen in Figure 3-19.

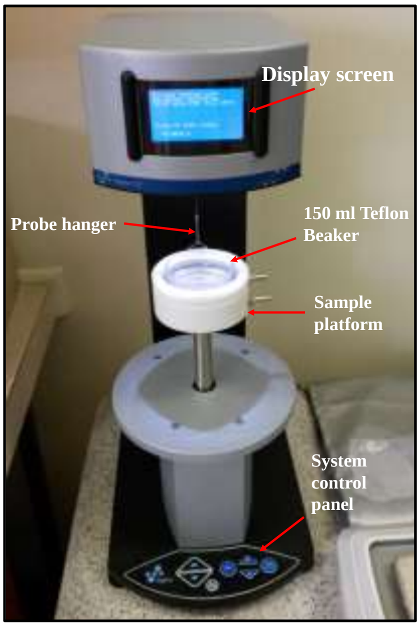

Figure 3-19: Surface tension apparatus

3.3.1.4 Bleeding

All bleeding tests were carried out in accordance with ASTM C232 (2004). Figure 3-20 shows the 120 mm deep bleeding mould and apparatus used to capture the bleeding of concrete. The same scale used during evaporation tests, was used to capture the amount of bleed water rising to the surface of the concrete.

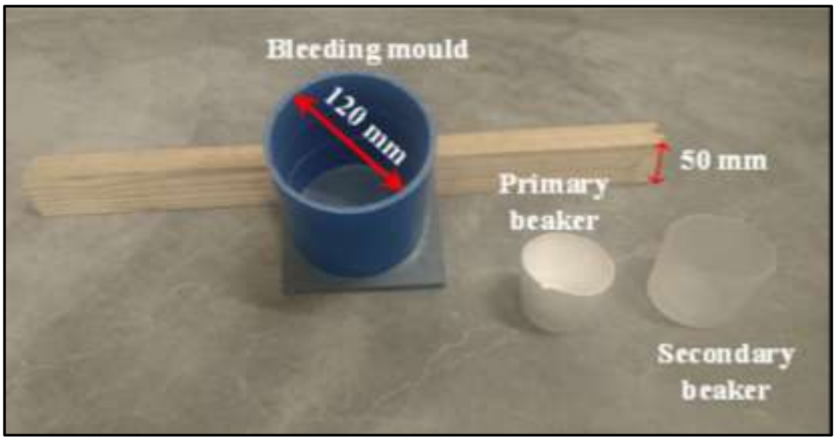

Figure 3-20: Bleeding apparatus

3.3.1.5 Setting time

The method used to determine the setting time of concrete is based on the EN 196-3 (2005) standard and determined using the Vicat penetration apparatus as shown in Figure 3-21.

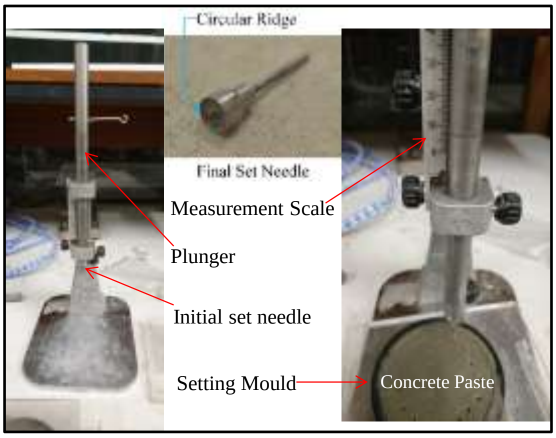

Figure 3-21: Vicat needle apparatus

3.3.1.6 Rheology

The rheological properties, namely the viscosity and static yield stress of the concrete mixes used in the current study, were determined using the ICAR Rheometer as seen in Figure 3-22. More information regarding the design aspects of the ICAR rheometer can be found elsewhere (Koehler & Fowler, 2004).

Figure 3-22: ICAR Rheometer

3.3.2 Cracking tests

Figure 3-23 shows the mould used to investigate the cracking behaviour of plastic concrete. Initially the moulds were based on the proposed mould design by ASTM C1579 (2006) to investigate plastic shrinkage cracking, however, these moulds were later modified to add an additional steel bar at each end of the mould, with the main aim of assisting the two smaller triangles in laterally restraining the concrete to induce cracking.

Combrinck (2016) investigated the cracking behaviour of concrete using the same mould design as that in Figure 3-23. Results showed that the mould does not result in pure plastic shrinkage cracking but can rather be termed as "plastic shrinkage cracking induced by differential settlement". This means that plastic settlement cracks were present well before plastic shrinkage commenced. Therefore plastic settlement is believed to influence the crack location; however plastic shrinkage is believed to be the controlling factor in crack widening after the crack formed. For the purpose of the current study, this is actually beneficial since it incorporates both plastic shrinkage and plastic settlement cracking.

The mould in Figure 3-23 has a rectangular shape with two steel bars, two small triangles and a centre larger triangle. The two steel bars along with the two small triangles situated on each end of the mould, provide lateral restraint to help induce plastic shrinkage cracking. The single centre triangle acts as a stress raiser and along with the lateral restraints, cracking is forced directly above the central region of the mould. The large centre triangle is believed to induce a small amount of plastic settlement cracking which is partly responsible for determining the main crack location. The crack is then driven by plastic shrinkage as the concrete body contracts while being restrained by the two end steel bars and triangles.

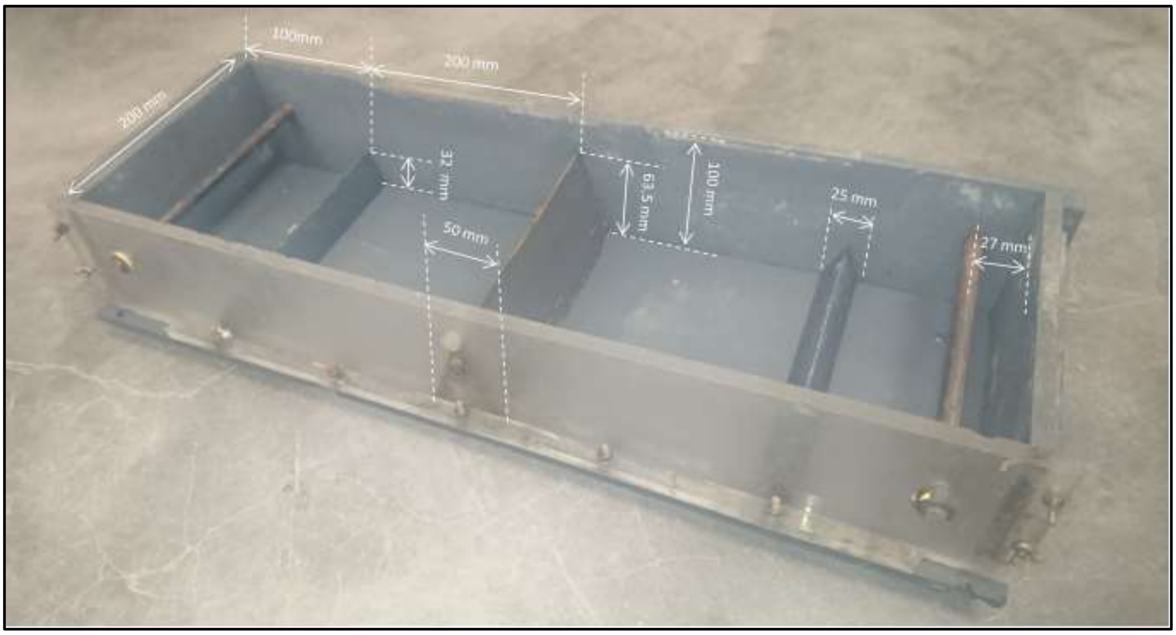

Figure 3-23: Cracking mould layout

3.4 Mix specification

Section 2.1 defined concrete as a composite material consisting of water, cement, fine aggregate (sand) and coarse aggregate (stone). Modern day concretes tend to incorporate admixtures in order to enhance certain fresh properties. A total number of three different concrete mixes were used to carry out the experimental tests discussed in the aforementioned sections. A standard conventional concrete mix, designed with a 0.55 water cement ratio and a slump value of 70 mm, was used as the reference concrete mix throughout the study. The mentioned concrete mix is referred to as Mix Ref in this study.

A viscosity modification agent was then used to modify the viscosity of Mix Ref. This mix, referred to as Mix VMA, was used in conjunction with Mix Ref to conduct and compare all experimental tests in order to evaluate the influence of viscosity on the tensile properties and cracking behaviour of plastic concrete. The addition of a 0.8 % dosage of VMA, double the prescribed recommended dosage, resulted in a slight increase in slump value to 85 mm.

Table 2: Material constituents, proportions and mix properties

Mix abbreviation	Mix REF	Mix VMA
Material constituents [kg/m³]		
Water	205	205
Cement	373	373
6 mm Greywacke stone	1037	1037
Natural quarry sand	795	795
Viscosity modification admixture (% of binder content)	-	0.80%
Fibres	-	-
Mix properties		
Slump [mm]	70	85
Average 28 day strength [MPa]	48.3	47.4
w/c ratio	0.55	0.55

3.5 Material specifications

This section focusses on the specification of the constituent materials used in all three mixes. Material source, supplier and batch numbers were kept consistent throughout the study.

3.5.1 Viscosity modification agent

An organic polysaccharide viscosity modification agent, with commercial name Quad 20, supplied by Chryso SA (Pty) Ltd was used throughout the study for all experimental tests conducted using Mix VMA. A dosage of 0.8 % by mass of cement content was used in Mix VMA. According to the manufacturer (Chryso SA, 2007), this VMA increases the viscosity of the cement paste, with little impact on concrete slump, while preventing segregation, bleeding and honeycombing (Chryso SA, 2007).

3.5.2 Water

Potable municipal tap water from the same source was used throughout the experimental framework. This includes mixing water used in all concrete mixes as well as water used during curing procedures. Distilled water however was used to prepare capillary pressure sensors for testing as described in Section 3.2.1.6.

3.5.3 Cement

All mixes contained CEM II/A-L 52.5N Portland cement with a strength rating of 52.5 N. The main constituent material of the cement includes both clinker and between 6-20% limestone by mass. All cement used was supplied by Pretoria Portland Cement Company Limited and therefore cement from the same batch was used throughout the study in order to eliminate variation due to inconsistent cement composition.

3.5.4 Coarse aggregate

The South African National Standard code defines coarse aggregate as that which 90% of particles does not pass the 4.75 mm sieve (SANS 201, 2008). In order to investigate and compare the tensile properties and plastic cracking behaviours, a Greywacke stone with an angular particle shape and nominal size of 6 mm was used as coarse aggregate in all concrete mixes. A small stone size was preferred over larger aggregate since a smaller stone is believed to have a smaller influence on the tensile properties, shrinkage, settlement and cracking results. Therefore, said results are more dependent on the cement paste, rather than aggregate.

3.5.5 Fine aggregate

The South African National Standard code defines fine aggregate as that which 90% of particles pass the 4.75 mm sieve (SANS 201, 2008). Siliceous pit sand known as Malmesburry sand and found locally in the Western Cape region in South Africa was used as fine aggregate in all concrete mixes. Malmesburry sand is formed through the natural disintegration of rock and contains a round particle shape. Sands from different batches of the same origin have shown to vary in FM and dust content. Therefore to ensure consistent results, sand from the same batch with a FM of 1.39 was consistently used throughout the study. The grading analysis of sand, determined in accordance with SANS 201 (2008) is shown in Figure 3-24

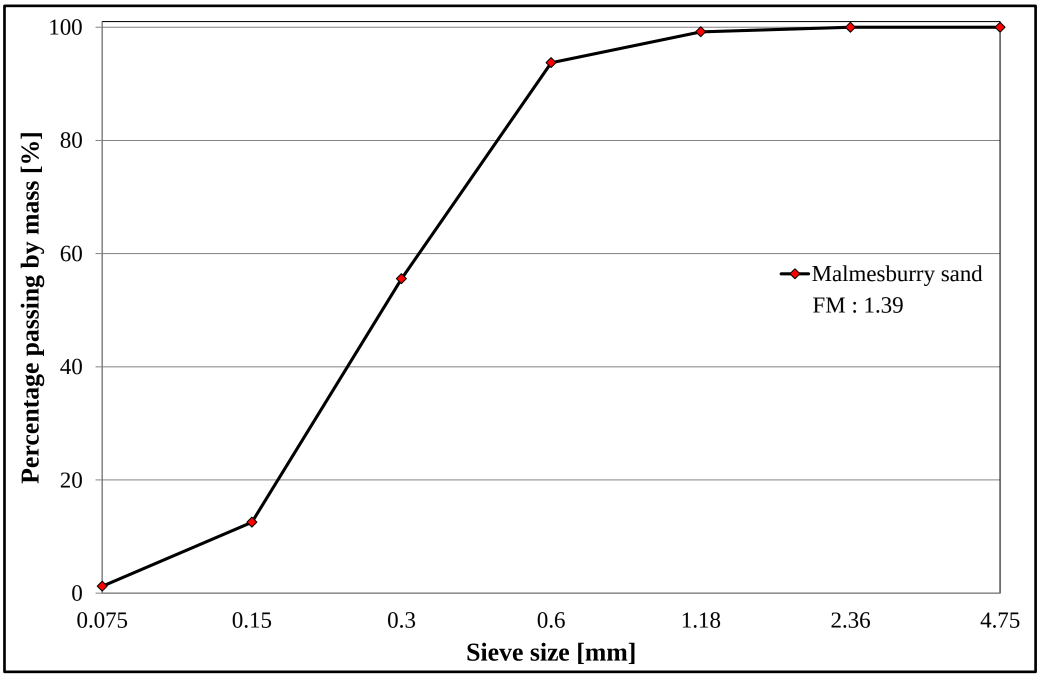

Figure 3-24: Sand grading

3.6 Experimental procedures

Consistent mixing and casting procedures were followed throughout the study to reduce any variation in results pertaining to casting and mixing methods. Therefore unless otherwise stated in subsequent sections, the following mixing procedures and test procedures were used throughout. Section 3.6.1 first describes the climate conditions used to carry out the tensile and plastic cracking tests. Thereafter Sections 3.6.2 and 3.6.3 discuss the mixing and testing procedures respectively.

3.6.1 Climate conditions

Prior to testing, tensile tests were allowed to cure under an ambient temperature of 40ºC and wind speed of 4 km/h. These climate conditions were chosen to ensure that the tensile tests were allowed to cure under high temperature with relatively low plastic shrinkage potential. Furthermore, test samples were continuously wet with water to ensure that sufficient water remained on the surface of the samples for evaporation. This ensured that plastic shrinkage was not a concern.

Plastic shrinkage tests, similar to the tensile tests, were exposed to an ambient temperature of 40ºC, wind speed of 4 km/h and relative humidity of 10%. These conditions amount to an evaporation rate of 0.4 kg/m²/h as calculated using Eq. 2 developed by Uno (1998).

Uno suggests that an evaporation rate greater than 1 kg/m²/h is ideal for plastic shrinkage cracking. However, a lower evaporation rate was used in order to identify the point where settlement ceases and plastic shrinkage starts. High evaporation rates increase the difficulty in observing the end of settlement and start of plastic shrinkage. Furthermore, environmental conditions were kept similar to the environmental conditions used to conduct tensile tests in order to draw links between tensile and plastic cracking tests in Chapter 5. However, the low evaporation rate of 0.4 kg/m²/h, proved sufficient in causing plastic shrinkage to occur within test samples.

$$\mathrm{ER} = 5 \times 10^{-6}\,(\mathrm{V}+4)[(\mathrm{Tc}+18)^{2.5} - \mathrm{r}(\mathrm{Ta}+18)^{2.5}] \qquad \text{(Eq. 2)}$$

With:

ER = evaporation rate [kg/m²/h]

V= wind velocity [km/h]

Tc= concrete temperature [ºC]

r= relative humidity [%]

Ta = air temperature [ºC]

3.6.2 Mixing procedures

All mix constituents were first weighed off in kilograms according to the mix proportions required for each test. The constituents were then placed in a climate controlled room at least 14 hours prior to mixing. This was done to ensure a constant and consistent temperature between all mix constituents which therefore resulted in a constant concrete temperature once mixing was completed. The climate controlled room contained a regulated temperature of 23ºC with a relative humidity rating of 65%. A single rotary pan mixer with a capacity rating of 50 litres was used for all concrete mixes. The rotary pan was consistently wet and towel dried prior to mixing for all tests.

Dry mix constituents, were added in the order of sand, cement and stone. The dry constituents were mixed for a period of 1 minute before water was added. Within 30 seconds after adding water any predefined dosages of admixtures or fibres were added to the concrete. The entire concrete mix was then further mixed for a period of 3 minutes. This amounted to a total mixing time of 4 minutes and 30 seconds.

3.6.3 Testing procedures

Moulds were prepped prior to mixing to ensure a quick casting process without any concrete pouring delays. Once mixing was completed, concrete was poured into the respective moulds to half capacity before consolidating the concrete on a vibrating table. Once the concrete levelled to an acceptable degree in the respective moulds, the vibrating table was turned off, after which the moulds were further filled to at least 5 mm below the top surface of the mould. After this the vibrating table was turned on again to fully consolidate the concrete filled moulds. Full compaction was achieved once the majority of entrapped air bubbles have been removed from the concrete. Due to the different mould dimensions, a consistent vibrating time could not be followed for different test types, since each test required a certain amount of time before the majority of entrapped air bubbles were expelled. A constant vibrating time between tests involving the same mould, was however adhered too.

After vibration, with the exception of bleeding and setting time samples, surface finishing was applied to all concrete filled moulds using trowels to smooth out the surface of the concrete. For tensile and cracking tests, this improved the visibility of cracks. For shrinkage and settlement tests, this improved the bonding between the wire mesh and concrete surface.

Care was taken in applying consistent levels of surface finishing on all moulds. A more detailed description on mould prepping and casting procedures of different tests are discussed in subsequent sections.

3.6.3.1 Tensile tests

The tensile testing machine was used to carry out three different tests, namely, tensile property tests, relaxation tests under single loading and relaxation tests under multiple loading cycles. The first test includes measuring the pre-peak tensile properties while relaxation tests measure and observe the stress relaxation of concrete under single and multiple loading cycles.

As mentioned in Section 3.1, time zero (t_0) was taken as the time of environment exposure (40ºC) and fifteen minutes prior to testing, moulds were removed and transported to the tensile machine situated in a climate controlled room. Once fixed onto the tensile machine, the actuator applied a constant displacement rate of 0.25 mm/minute. Test duration for all tensile tests was at least ten minutes long and tensile force, concrete displacement and mould displacement were recorded for the entire test duration.

Tensile property tests

Prior to mixing, the two tensile moulds were assembled, greased and oiled as per the step by step procedure outlined in Section 3.2.1.5. Capillary pressure sensors were then prepped before mixing procedures commenced. Moulds were filled to half capacity and vibrated for approximately 1 minute before inserting and fixing the capillary pressure sensors to the mounting brackets. The capillary pressure sensors were screwed in place using the secondary brackets in order to prevent the sensors from moving around excessively during vibration. For tensile tests where the capillary pressure was not monitored or measured, the fitment of capillary pressure sensors and corresponding brackets were omitted. Moulds were then filled to 5 mm below the top surface of the mould after which the mould was vibrated for a further 4 minutes. Moulds were therefore vibrated for a total time of 5 minutes before ceasing vibration. This was found to be the optimal time required to remove the majority of entrapped air bubbles from the concrete without causing excessive settlement of solid particles. Surface finishing was then carried out on both moulds before being transported to the climate chamber.

Moulds were then placed in the climate chamber after which the aluminium angle-profiles and mounting clips holding the aluminium inserts in place where carefully removed. For tests where the capillary pressure was monitored and measured, the secondary mounting brackets holding the capillary pressure sensors in place were loosened to allow the sensors to settle with the concrete. The moulds were then left undisturbed at the appropriate temperature and were only removed 15 minutes prior to testing. While the moulds were allowed to cure inside the climate chamber, care was taken to ensure that no capillary pressure and therefore no plastic shrinkage could occur by ensuring a thin dammed layer of water continuously covered the concrete's surface. Water was applied using a fog spray to lightly add water to the surface concrete.

Moulds were then removed 15 minutes prior to testing and transported to the tensile testing machine situated in a climate controlled room with a temperature of 23ºC and 65% relative humidity. Moulds were then placed onto the air bearing and set up using the step by step procedure outline in Section 3.2.2.1. The actuator was then used to pull the two concrete filled mould halves apart from each other until failure, resulting in a well-defined crack in the gauge area.

Relaxation tests under single loading

The procedure followed for tensile property tests were repeated from mixing to setting up of the mould on the air bearing. Once the mould was set up on the air bearing and ready for testing, the concrete was loaded to 50% of the average maximum tensile strength for each corresponding hourly test followed by an abrupt stop of loading by ceasing the displacement of the actuator. Relaxation of the tensile induced force was then captured for a period of at least 10 minutes.

Relaxation tests under multiple loading cycles

Relaxation tests were repeated and allowed to relax for a time period of 5 minutes before loading the concrete again to 50 % of the average maximum tensile strength in the tensile regime. This process was repeated until cracking occurred.

3.6.3.2 Plastic cracking tests

All tests, namely influential factor tests and cracking tests were carried out within the climate chamber and therefore exposed to constant environmental conditions throughout the test duration. The various procedures followed during each plastic cracking test are described in the following sections.

Plastic settlement, plastic shrinkage and capillary pressure

Figure 3-14 shows the complete 300 x 300 x 100 mm mould used to measure all three influential factors, namely: plastic settlement, shrinkage and capillary pressure. Four sets of moulds were cast, consolidated and transported simultaneously during the testing procedure. The following procedure was followed consistently.

The first step involves prepping the mould for testing. Side LVDT mounting brackets were removed to gain access to the shaft holes. Bearings were removed and the two holes located on either side of each mould were cleaned to ensure no concrete residue remained from previous tests. Bearings were then greased and placed back in the shaft holes. The shafts were greased next and pushed through the shaft holes on each side of the mould. The side LVDT mounting brackets were then screwed back onto the mould and the shaft fixing screw was tightened to ensure that the markers do not move during casting and transportation. Greasing of bearings and shafts ensure that no resistance occurs between the bearings and shafts as the markers displace with the contracting concrete specimen. Once the shafts were fixed in place, surfaces exposed to concrete were lightly coated with demoulding oil to ease in demoulding after test completion. Finally, capillary pressure sensors were prepped and mounting brackets were fitted to each mould. This concluded mould preparation.

Once mixing and casting procedures were complete, concrete was poured into each mould to half capacity. Moulds were then vibrated for 30 seconds before ceasing vibration. Capillary pressure sensors were then inserted into each mould and screwed in place to prevent any excessive movement during further consolidation and transportation. Moulds were then further vibrated for 2 minutes and 30 seconds before surface finishing was applied to all three moulds.

Moulds were then placed in the climate chamber and after which the two side LVDT’s and top mounted LVDT were fitted to all four moulds. Latticed wire meshes, used to measure settlement were screwed onto each top mounted LVDT and gently placed in contact with the top surface of the concrete. Capillary pressure sensors were then plugged into the data acquisition system used to capture capillary pressure. The secondary brackets holding the capillary pressure sensors in place were then loosened and allowed to settle freely. The screws holding the shafts in place were then unscrewed and removed to allow shrinkage capturing. The entire process from adding water to the start of data capturing, consistently took 15 minutes. Moulds were then left undisturbed for a period of 6 hours before removing and demoulding.

Surface tension

Water mixed with several varying dosages of VMA was prepared in 250 ml samples and poured into plastic containers which were rinsed thoroughly with water. Prior to testing, the tensiometer was levelled by placing a bubble levelling device on the sample platform and adjusting the supports accordingly, to ensure accurate levelling of the sample platform. Thereafter the tensiometer was calibrated in accordance with prescribed procedures specified by the manufacturer.

During testing, approximately 150 ml of each test sample was poured into a clean Teflon beaker, rinsed thoroughly with acetone and water. The sample platform was then raised to a distance of 10 mm clear from the platinum ring attached to the probe hanger. The tensiometer then automatically raised the sample platform until the ring was completely immersed in the sample, at a depth of 6 mm from the surface of the liquid. The platform was the gradually lowered by the tensiometer, while recording the force exerted by the liquid on the platinum ring as the ring detaches from the surface of the liquid. A total of 3 samples per VMA dosage were used to obtain the surface tension results.

Evaporation

Upon completion of mixing and casting procedures, concrete filled moulds were first weighed to get the reference mass of each mould before being placed in the climate chamber. Thereafter, moulds were weighed in 20 minute intervals for a period of 6 hours. The amount of water evaporated during each 20 minute period was calculated as the difference in weight of the concrete filled mould before and after each 20 minute period.

Bleeding

Three samples of concrete filled bleeding moulds were used to measure the bleeding rate simultaneously. Moulds were first wiped clean using a damp cloth and allowed sufficient time to dry. No further preparations such as oil application were applied to the bleeding moulds. If mould oil is applied in excess, this accumulates on the top surface of the concrete. This alters the accuracy of results since extracted bleed water may be contaminated with oil, which would result in a higher measured bleed rate compared to the actual bleeding of the concrete.

Upon completion of mixing procedures, all three concrete filled moulds were then transported to the climate chamber and weighed to get the reference mass of each concrete filled mould before placing the moulds into the climate chamber.

All bleeding tests were carried out within the climate chamber. Moulds were first tilted using a 50 mm wooden block prior to extraction, to facilitate in the accumulation of bleed water on the lower part of the tilted mould. Moulds were left in this position for 2 minutes before extraction of bleeding water. The evaporation covers were then removed and bleed water was extracted using a syringe to extract out all accumulated water. The mould evaporation cover was then placed back on and the mould was placed back in its un-tilted position. Extracted bleed water was then transferred to the primary measurement beaker which allowed any extracted solid particles to settle to the bottom. The remaining contents were then transferred to the secondary beaker and weighed to obtain the amount of bleed water during each specific measurement.

Evaporation of bleed water was accounted for by measuring the concrete filled mould before tilting, for each measurement. The difference in weight of the concrete filled mould between measurement periods minus the extracted bleed water, results in the amount of water that evaporated during measurement periods.

Setting times

Two samples were tested simultaneously during each test. After the completion of mixing procedures, the concrete was sieved through a 4.75 mm sieve leaving a cement paste free of solid particles. The paste was then filled into each mould and covered with evaporation covers to prevent any loss of moisture. The moulds were then transported to the climate chamber.

Upon testing, the sample was placed directly under the plunger and the initial set needle was lowered until in contact with the top surface of the concrete paste. Thereafter the plunger was released allowing the initial setting needle to penetrate the concrete paste. Penetration depth readings were then recorded 30 seconds after releasing the plunger. The initial setting time was reached when penetration depth was measured to be 6 ± 3 mm from the bottom of the mould.

Once initial set was reached, the setting mould was inverted and the final setting needle was fitted to the plunger. A similar procedure as that used to measure the initial setting time was used to measure the final setting time. Final set was reached when the circular ridge of the final set needle no longer left an imprint on the surface of the specimens.

Rheology tests

Upon completion of mixing and casting procedures, the container of the rheometer was filled to capacity immediately after mixing. No vibration of the concrete prior to testing was necessary as per the manufacturer's guidelines. The torque meter unit was then inserted into the concrete filled container and fixed in place, after which the computer aided software was used to conduct the flow curve test to obtain the Bingham properties of the respective concrete mix. One rheology test per VMA dosage was conducted. The total time taken from completion of mixing to the start of the flow curve test, consistently amounted to 7 minutes. More information regarding the testing procedure and flow curve test can be found within the manufacturer's guideline catalogue (Germann Instruments, 2010).

Cracking Tests

Upon completion of mixing and casting procedures, a total number of 4 cracking moulds were placed in the climate chamber, crack onset was expected to occur somewhere between the initial and final setting times. Therefore high resolution photographs were taken every 20 minutes from the occurrence of the first crack to 6 hours after environmental exposure (time zero). The method used to observe and measure crack development with time is explained as follows:

Step one

Captured photographs for each test specimen were uploaded to CAD software and scaled to a known reference length that was captured in each photograph. A metal ruler, as shown in Figure 3-25 with a total length of 128 mm was used to scale pictures accordingly.

Step two

The photograph captured at 6 hours was used to measure the corresponding well defined crack that occurred over the larger centre triangle as shown in Figure 3-25. The 25 mm lines on each side of the mould as shown in Figure 3-25 were used as reference positions to mark the beginning and end of crack measurements. This was done to eliminate the influence of boundaries as prescribed by ASTM C1579 (2006). The crack was then divided into 10 mm segments along the entire crack profile (red lines in Figure 3-25). Centrelines were then drawn perpendicular to each 10 mm line segment (blue lines in Figure 3-25). These lines intersect the crack area and therefore were used to measure to corresponding crack width.

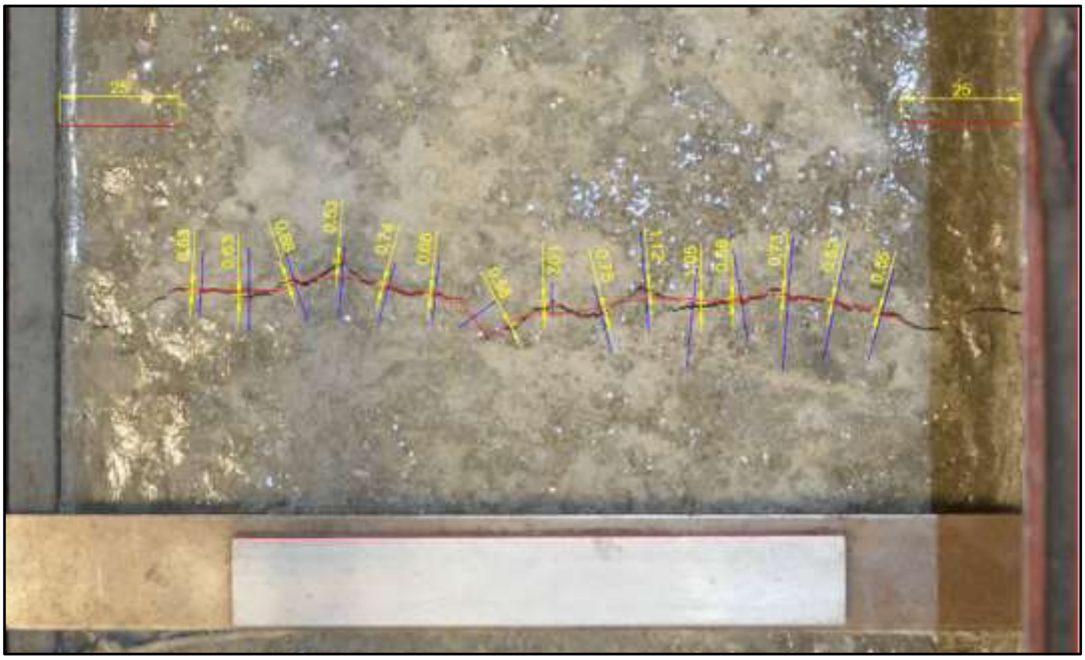

Figure 3-25: Example of a cracked specimen analysed on CAD software

Step three

Crack patterns and crack measurement locations were then copied and fitted to earlier images of the corresponding crack pattern. This therefore allowed the capturing of crack measurements at approximately the same positon for each crack image of the respective mould.

Step four

The development of average crack area over time for each mould was then documented. A choice of either average crack area or average crack width could be used to compare crack development over time. Crack width is ideal for comparing crack development over time in moulds with different widths. Crack area combines the crack length and crack width and therefore gives a better indication of crack severity over the entire concrete element. This is ideal for comparing different cracking results obtained from the same mould. Average crack area was therefore chosen as the indicator of choice when describing crack growth. The equation used to calculate average crack area is as follows:

$$Average\ crack\ area\ [mm^2] =$$

$$Average\ crack\ width\ [mm] \times number\ of\ line\ segments\ \times 10\ mm \qquad \text{(Eq. 3.)}$$

3.7 Test program

All experimental tests conducted throughout the current study can be grouped into one of seven different tests. The plastic nature of concrete varies extensively and therefore in order to obtain accurate results for comparison purposes, more than one test per group was needed in order to average and ensure repeatability of results. Groups 1 to 7 are explained in greater detail in subsequent sections.

Group 1 – Influence of a viscosity modifying agent on the fresh mix properties of plastic concrete

These tests aimed to investigate the influence of an admixture based viscosity modifying agent on the fresh properties of plastic concrete. A viscosity modification agent (VMA) was used to modify the rheological properties of a reference mix (Mix VMA) which formed the basis of subsequent tests. In addition to rheological properties, the surface tension of water was compared to different dosages of VMA. This gave an indication of the attractive forces between adjacent molecules within concrete. One rheology test per mix was carried out on different VMA dosages while at least three samples of varying VMA dosages were used to obtain average surface tension results.

Group 2 - Tensile Properties

The objectives of these tests were to investigate the pre-peak tensile properties of concrete for Mix Ref and Mix VMA. This was carried out to investigate the influence of a VMA on the tensile properties of plastic concrete. The pre-peak tensile properties include: tensile strength, Young's modulus and strain capacity. The tensile testing machine was used to carry out all tensile tests in 60 minute intervals to a final testing time of 240 minutes. In addition to this, capillary pressure was measured during tensile tests to observe the behaviour of internal capillary bonds under tensile induced loads.

Group 3 - Relaxation behaviour under single loading

The objectives of these tests were to identify and observe the stress relaxation behaviour of both Mix Ref and Mix VMA under a constant applied strain. The tensile strength results obtained during the tensile tests were used to load test samples to 50 % of the corresponding average tensile strength on the tensile testing machine. Tests were carried out on at least two test specimens for each time period in order to observe repeatability of results. In addition, the capillary pressure results were also used to observe the behaviour of capillary pressure during stress relaxation.

Group 4 - Relaxation behaviour under multiple loading

These tests aimed to investigate the relaxation response of plastic concrete under multiple loading periods for both Mix Ref and Mix VMA. Relaxation tests were repeated by loading test specimens to 50 % of the corresponding average tensile strength for each test period. Loads were then immediately ceased and resumed 5 minutes later by further increasing the applied load in the tensile regime to 50 % of the average tensile strength. Combined with capillary pressure measurements, these tests aimed to mimic curing procedures by mechanically controlling tensile induced loads by ceasing the displacement of the mechanical actuator. At least two results per test were obtained.

Group 5 - Initial Curing Procedures

Initial curing procedures were carried out on Mix Ref to investigate the influence of plastic shrinkage; plastic settlement and capillary pressure build-up on final crack areas. The objectives of these tests were to investigate the appropriate time to apply initial curing. At least four results per curing test were obtained.

Group 6 - Influence of curing on the cracking behaviour of plastic concrete

The objectives of these tests were to investigate the influence of applying curing procedures during capillary pressure build-up on both Mix Ref and Mix VMA. During these tests, plastic shrinkage, plastic settlement and capillary pressure build-up under curing were used to compare final crack areas. As opposed to tests carried out in Group 3 and 4 to mechanically control tensile induced loads, the application of curing procedures by using a fog spray for example, can be thought of a way of controlling tensile induced forces driven by environmental conditions. At least four results per test were obtained.

Group 7 - Plastic cracking

These tests aimed to investigate the cracking response of a conventional concrete mix, namely Mix Ref compared to Mix VMA. Plastic cracking tests were also carried out to investigate the cracking behaviour of concrete under different initial curing times. Bleeding, evaporation, plastic settlement, plastic shrinkage and capillary pressure results were used to explain the cracking behaviour of both Mix Ref and Mix VMA. At least four results per test were obtained.

3.8 Concluding summary

This chapter provides a detailed description of the experimental tests conducted to obtain the tensile properties and cracking behaviour of plastic concrete. This includes the tensile properties and relaxation tests as well as tests relating to plastic shrinkage cracking. Furthermore, the mix properties and constituents were discussed, revealing the two main mixes used throughout the study, namely Mix Ref (the control mix) and Mix VMA (the viscosity modified mix). Chapter 4 includes the test results and discussions of test pertaining to Group 1 to Group 4, namely the tensile material properties and relaxation behaviour of plastic concrete.

Chapter 4: Tensile material properties - Test results and discussion

Mix Ref and Mix VMA are the two main concrete mixes used to conduct experimental tests on the tensile properties and cracking behaviour of plastic concrete. Mix Ref, a conventional concrete mix with a 0.55 water cement ratio and an initial slump of 70 mm is used as a reference concrete mix to compare with Mix VMA throughout the study. Mix VMA, a viscosity enhanced version of Mix Ref, incorporating a 0.8 % dosage of a viscosity modification agent, to investigate the influence of an admixture based viscosity modifying agent on the tensile and cracking behaviour of plastic concrete. However, before conducting experimental tests on the tensile properties and cracking behaviour of plastic concrete (Chapter 5); several preliminary tests were carried out in order to investigate the influence of a viscosity modification agent (VMA) on the fresh mix properties of plastic concrete.

This chapter firstly focusses on the influence of VMA on the surface tension and rheological properties of plastic concrete, followed by an in depth analysis on the pre-peak tensile properties and relaxation behaviour of both Mix Ref and Mix VMA. Results are presented in subsequent sections.

4.1 Influence of VMA on the mix properties of plastic concrete

Surface tension tests were carried out on water mixed with increasing dosages of VMA. Three samples per dosage of VMA were carried out to minimise variability between results. In addition to the surface tension tests, rheology tests were carried out using a rheometer to obtain the Bingham parameters of Mix Ref, with varying dosages of VMA. One test per dosage with fewer varying dosages were carried out, since the rheometer is believed to be less sensitive to human testing error and more sensitive to concrete consistency compared to the tension meter used to conduct surface tension tests. Mixing and casting procedures were therefore kept constant for all three tests involving the rheometer to minimise variability. Furthermore, the main aim of carrying out rheology tests, was to gain an understanding of the influence of varying dosages of VMA on Mix Ref, and therefore the accuracy or repeatability of rheology results fall outside the scope of this study and therefore further investigation needs to be carried out to investigate the accuracy and repeatability of the rheometer used.

4.1.1 Surface tension

The average surface tension results of water mixed with several dosages of VMA are presented in Figure 4-1. Results indicate a general decrease in surface tension, with increasing dosages of VMA. The surface tension rating of water with a 0 % VMA dosage was recorded at 65.7 mN/m. Thereafter, surface tension decreases to 61.9, 60.9, 60.7, 59.7 and 59.6 mN/m for dosages at 0.2, 0.4, 0.6, 0.8 and 1.6 % respectively. This amounts to an initial drop of 5.8 % in surface tension between water and water containing a 0.2 % VMA dosage. Further drops include 7.3, 7.6, 9.1 and 9.3% for dosages at 0.4, 0.6, 0.8 and 1.6 % respectively compared to pure water.

The manufacturer of the VMA (Chryso SA, 2007), recommends a prescribed dosage of 0.4 % of VMA per kg of cement in concrete. Results indicate that an initial dose of 0.2 % marks the largest drop in surface tension while the largest 1.6 % dosage, shows similar surface tension strengths compared to smaller dosages. This therefore implies that the addition of VMA, more specifically, a minimum dosage, affects the surface tension greatly, however higher dosages have a minimal effect on further decreasing the surface tension.

The Gauss-Laplace equation (Eq.1) presented in Section 2.4.2 explains the relationship between capillary pressure, surface tension and the radius of water meniscus. Capillary pressure is directly proportional to the surface tension of the pore fluid and inversely proportional to the radii of water meniscus. The addition of VMA therefore seems to weaken the bonds between water molecules and correspondingly decreases the capillary pressure within pores.

The surface tension results therefore give an indication of the capillary pressure experienced in fresh concrete. Mix Ref with a 0% VMA dosage can be expected to experience high negative capillary pressures and as the dosage of VMA increases, the negative capillary pressure decreases.

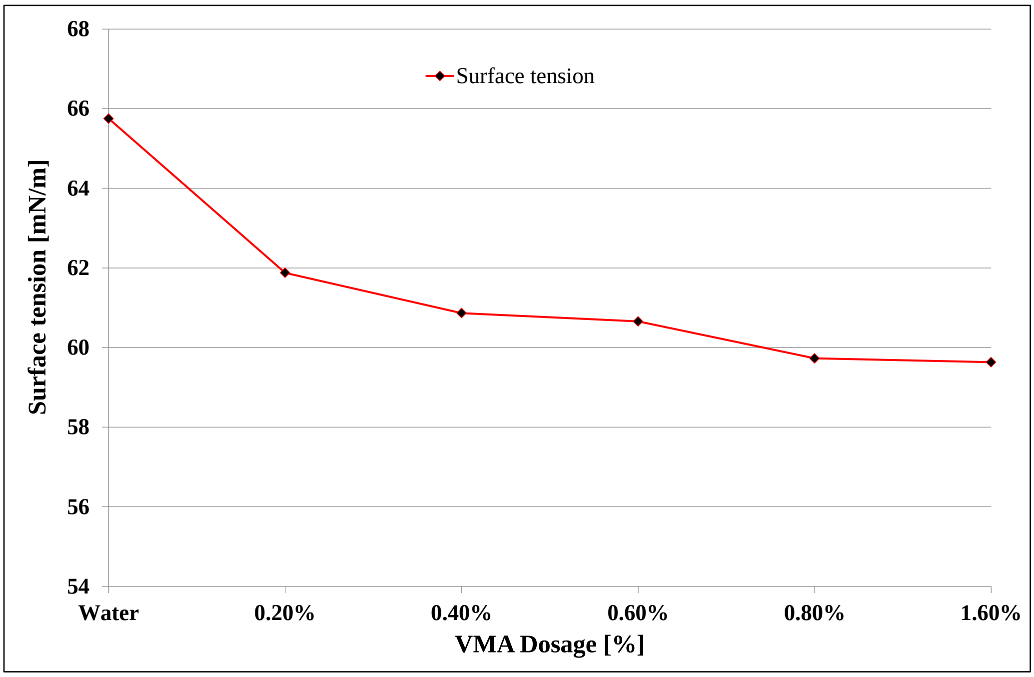

Figure 4-1: Effect of VMA concentration on surface tension

4.1.2 Rheology

Rheology tests were conducted to investigate the Bingham parameters of fresh concrete with varying dosages of VMA. The two Bingham parameters, namely dynamic yield stress and plastic viscosity, describe the flow properties of fresh concrete. The concrete's yield stress refers to the minimum amount of stress needed to initiate or maintain flow, while plastic viscosity describes the resistance to flow once initiated. Figure 4-2 shows the Bingham properties of concrete with varying dosages of VMA, namely 0, 0.4 and 0.8 % respectively.

The dynamic yield stress results indicate a decrease in yield stress with increasing dosages of VMA. The yield stress decreases from 1342 Pa for concrete containing no VMA to 1236 and 1103 Pa for 0.4 and 0.8 % VMA dosage respectively. This is slightly contradictory to literature discussed in Section 2.3.6, where the addition of a VMA has a tendency of increasing the yield stress by a small margin, which may alter the workability of the concrete. The conventional one point slump test, gives an indication of the yield stress in concrete. A slump measurement of 70 mm was recorded for Mix Ref (0 % VMA) while the addition of a 0.8 % dose of VMA (Mix VMA), increased the slump measurement reading to 85 mm.

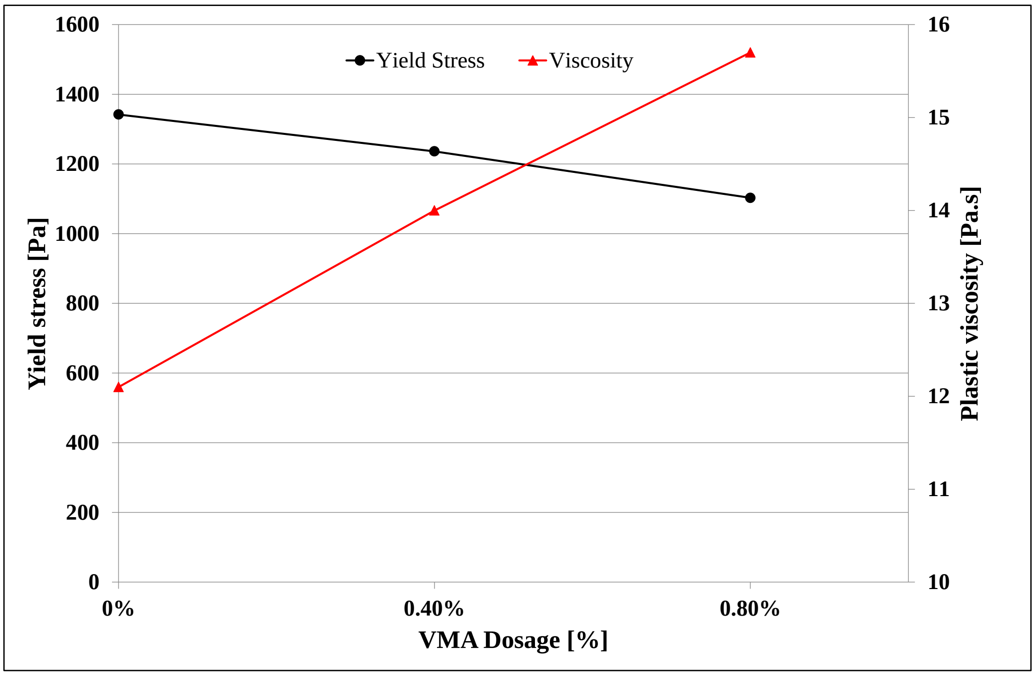

Figure 4-2: Bingham properties of plastic concrete with increasing dosages of VMA

As discussed in Section 2.3.2.4, Domone et al. (1999) carried out a number of tests to investigate the relationship between yield stress and slump of fresh concrete. Slump values obtained for Mix Ref and Mix VMA are plotted against Domone's results in Figure 4-3.

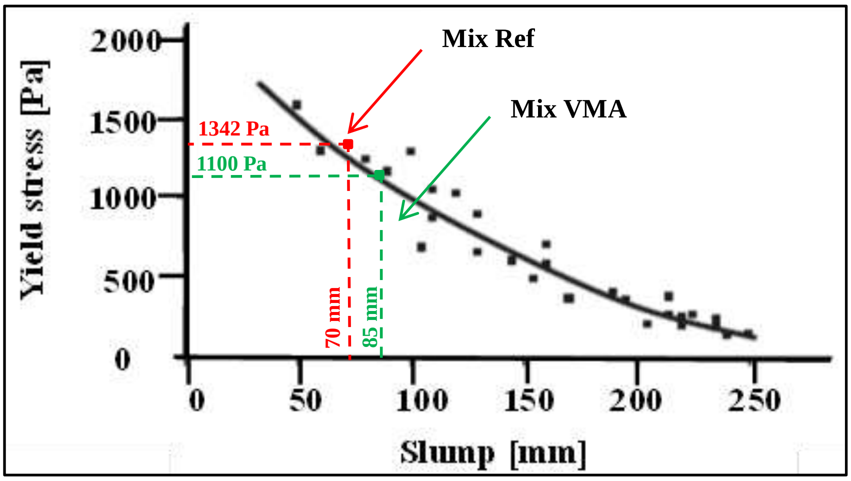

Figure 4-3: The relationship between yield stress and slump of fresh concrete (Domone et al., 1999)

The findings of Domone et al. (1999) and yield stress results in Figure 4-2, correspond well with the slump values obtained for mixes containing 0 % (Mix Ref) and 0.8 % (Mix VMA) VMA. A yield stress difference of 242 Pa corresponds to a slump difference of 15 mm. This indicates that the reduction in yield stress, due to the addition of VMA, corresponds with the measured slump increase. The reason for this increase in slump is believed to be due to the high dosage of VMA used. A 0.8 % VMA dosage amounts to 3 litres of VMA added per cubic metre of concrete. The 3 litres of VMA also contains a certain amount of water which increases the water-to-cement ratio of Mix VMA. This additional water is believed to have increased the slump and lowered the yield stress.

The plastic viscosity results obtained in Figure 4-2, increase in magnitude with increasing dosages of VMA. Results show that the plastic viscosity increases from 12.1 Pa.s to 14 and 15.7 Pa.s for VMA dosages amounting to 0, 0.4 and 0.8 % respectively. The addition of a VMA in a conventional concrete mix, therefore, has a significant effect on the viscosity of the concrete.

Viscosity is a measure of the internal resistance to change shape under the influence of shear or tensile stresses during motion. Surface tension however, describes the attractive forces in a liquid whilst remaining stationary. Therefore correlating a link between viscosity and surface tension is not easy (Rame'-hart, 2014). Mercury for example contains a higher viscosity and surface tension compared to water (Cracolice & Peters, 2006). Once flow is initiated in mercury, the liquid breaks into smaller droplets and flows independently. Honey on the other hand, contains a higher level of viscosity with a lower surface tension compared to water (Cracolice & Peters, 2006). Once flow is initiated, the lower internal frictional forces allow honey to flow smoothly as a uniform body, without breaking into small droplets compared to mercury. The addition of a VMA to conventional concrete is therefore argued to lower the internal frictional forces (lower surface tension) in the pore fluid, to allow better flow properties without segregating. However, this requires further investigation which does not form part of this study.

4.1.3 Setting time

In order to investigate the influence of VMA on the setting times of fresh concrete, two sets of tests, with each set containing two setting time samples, were carried out on both Mix Ref and Mix VMA. This amounts to a total of four samples for each mix. Figure 4-4 shows the setting time results of Mix Ref compared to a 0.8% VMA dosage. Consistent with literature, setting time values were similar, with Mix Ref obtaining initial and final setting times of 135 and 195 minutes respectively. Mix VMA showed slightly higher but still similar results for initial and final setting times with values of 140 and 205 minutes respectively. The increase in water content through the addition of the VMA is believed to be responsible for the slightly retarded setting time of Mix VMA compared to Mix Ref.

A 0.8 % VMA dosage was therefore used to obtain Mix VMA. Similar setting times, 28 day compression strengths and slump values, provide for perfect comparison between the two mixes when investigating the influence of VMA on various plastic concrete properties.

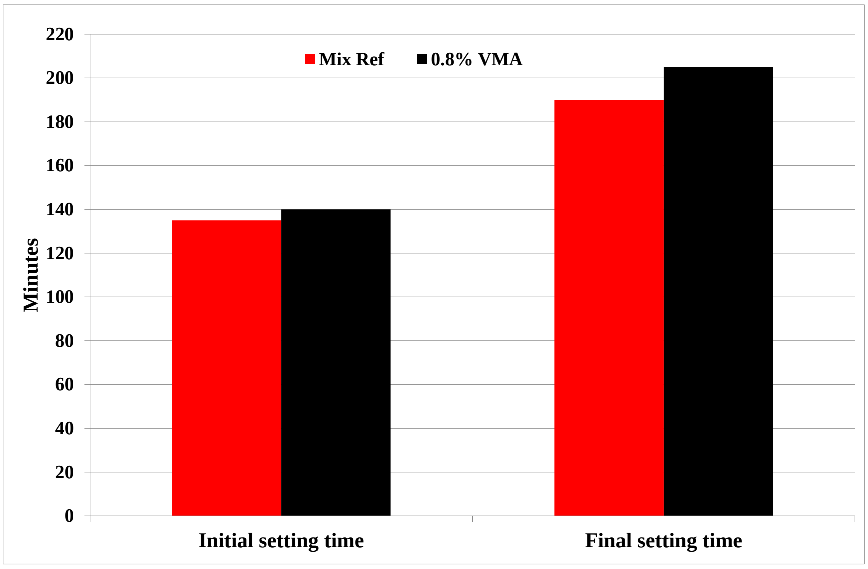

Figure 4-4: Setting times

4.2 Tensile properties

This section aims to investigate the pre-peak tensile properties of two concrete mixes, namely the reference mix (Mix Ref) and the viscosity modified concrete mix (Mix VMA). As discussed in Chapter 3, at least four tensile tests were carried out at 60, 120, 180 and 240 minutes after casting. The tensile properties, namely, stress versus strain, tensile strength, strain capacity and elastic modulus are discussed in subsequent sections.

4.2.1 Stress versus strain

The stress versus strain results for 60, 120,180 and 240 minutes after environment exposure, is displayed for both Mix Ref and Mix VMA in Figures 4-6 and 4-7 respectively. These are single results of individual samples, while the average values for tensile strength etc. are discussed in Sections 4.2.2 to 4.2.4. The stress values were calculated as the tensile force recorded divided by the cross sectional area of the concrete in the gauge area of the mould.

The corresponding strain values were calculated as the deformation of concrete in the gauge area, divided by the total gauge length.

Results show that the initial ascending part of the curves and point of crack are suitably captured for the determination of the pre-peak tensile properties. Point of crack is identified by the rapid decrease in stress after a peak stress (F_t) is reached. The pre-peak tensile properties include the tensile strength (F_t), strain capacity (ε_{cap}) and the Young's modulus (E) as shown on the ascending portion of the stress versus strain curve in Figure 4-5. The stress versus strain results for Mix Ref are first analysed and discussed in Section 4.2.1.1. Thereafter results for Mix VMA are analysed and compared to Mix Ref in Section 4.2.1.2.

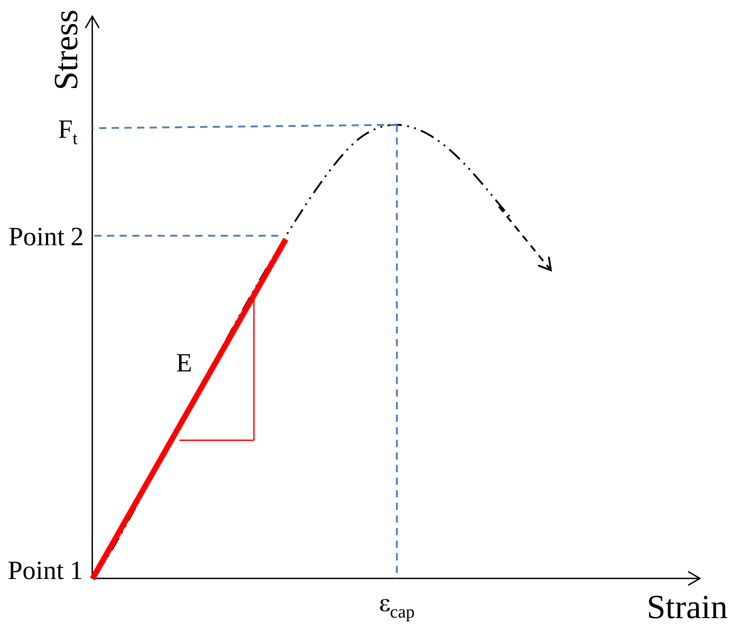

Figure 4-5: Ascending part of stress versus strain curve, showing the definitions of the Young's modulus, tensile strength and strain capacity

4.2.1.1 Stress versus Strain – Mix Ref

Figure 4-6 shows the stress versus strain results from 60 to 240 minutes after environment exposure in 60 minute intervals. The stress versus strain results, give a good indication of the ductility and brittleness of the concrete before, during, and after the setting stage of concrete. Initial setting time for the Mix Ref was recorded at 135 min whilst final setting time was recorded at 195 min. Results for the 60 and 120 minute time period fall well below the initial setting time. During this period the concrete is still plastic with a relative low tensile strength capacity, however results show that a greater amount of strain can occur before complete failure. This implies that concrete before the initial setting time is able to incur a greater amount of deformation before failure. This displays the ductile behaviour of concrete before the initial setting time.

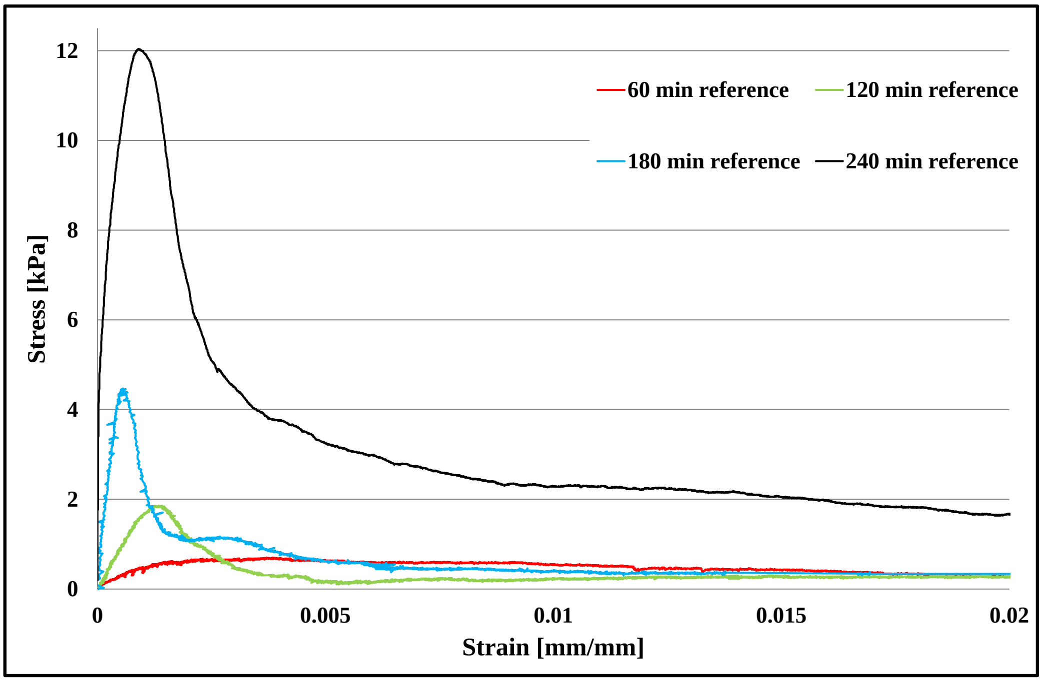

Figure 4-6: Stress vs strain results for Mix Ref

The stress versus strain result of the 180 minute time period falls just before the final setting time while the 240 minute time period result, falls after the final setting time. The period between the initial and final setting time, marks the transition from a plastic to semi plastic material, as the hydration products fill up the empty pores of the concrete. Results show that the specimens undergo a smaller amount of strain during the setting and hardening phase, resulting in a sudden failure once the peak stress is reached. This indicates that as the concrete begins to harden, the failure mode of the specimens change from ductile to brittle.

Figure 4-6 also shows a difference between peak stresses captured for the 180 and 240 minute time periods. The transition from a plastic to solid material can clearly be seen by the significant increase in stress between these two sets of results.

4.2.1.2 Stress versus Strain – Mix VMA

Figure 4-7 shows the corresponding stress versus strain results for Mix VMA. Mix VMA shows similar stress versus strain trends compared to Mix Ref, however, one distinguishing property is the decrease in peak stress compared to Mix Ref. Both mixes show a significant increase in peak stress between the 180 and 240 minute time periods, which marks the change in phase from the setting to the hardening phase. Mix Ref however, showed peak stresses for the 180 and 240 minute results equating to almost double that of the corresponding peak stresses for the same time periods of Mix VMA. The build-up in tensile strength for the reference mix therefore seems to increase at a higher rate compared to the VMA mix. A better comparison between the rates of strength gain is presented in Section 4.2.2.2.

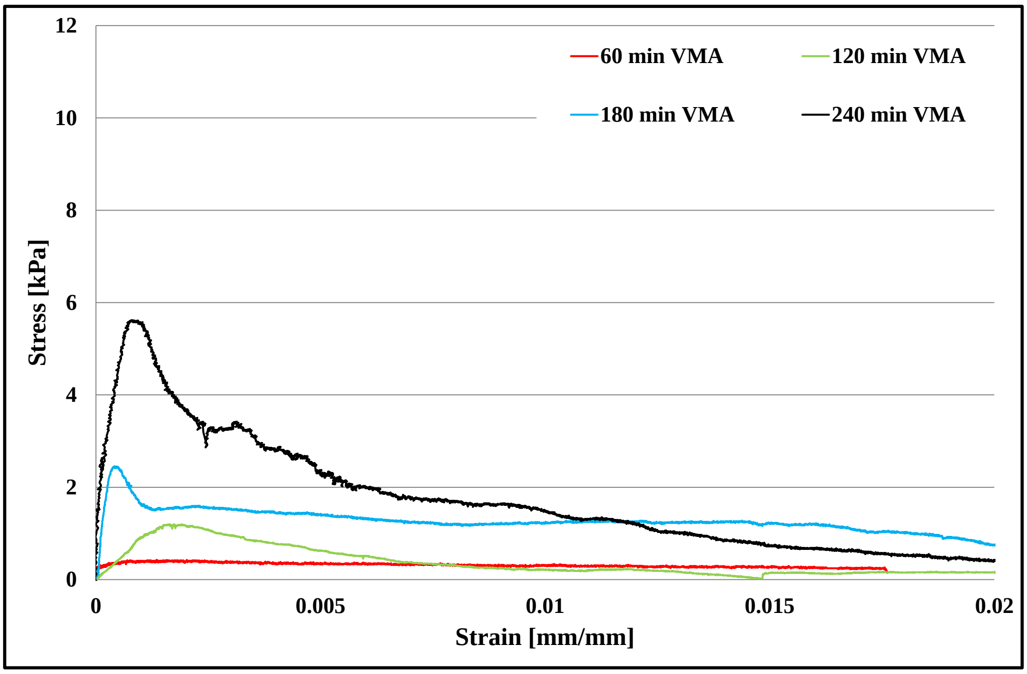

Figure 4-7: Stress vs strain results for Mix VMA

4.2.2 Tensile strength (Ft)

Upon closer inspection and evaluating the stress versus strain results in terms of strength development with time, allows a clearer observation of the tensile strength development during each phase of concrete, namely the stiffening, setting and hardening phases as shown in Figure 4-8.

The stiffening phase occurs soon after water is added to the dry constituents up until the initial setting time. Thereafter the setting phase commences and ends at the final setting time. The hardening phase then continues for as long as the concrete is able to hydrate. The strength development with time graphs in Figures 4-8 and 4-9 are plotted using the peak stress at point of cracking for all test periods, namely, 60,120,180 and 240 minute time periods. Peak stress values were averaged and plotted with the corresponding error bars representing plus and minus one standard deviation. Section 4.2.2.1 first considers the strength development with time in terms of hydration phases for Mix Ref, while Section 4.2.2.2 considers Mix VMA's results as well as a comparison between the two mix results.

4.2.2.1 Tensile strength (Ft) – Mix Ref

The strength development with time for Mix Ref is plotted against the three hydration phases in Figure 4-8. The stiffening phase takes place soon after water reacts with cement particles. During this phase, there is a dormant period within which little to no hydration occurs. This is important to allow for easy casting, consolidating and placing of the material. The 60 minute test samples showed very little strength development from time of placing to testing. Concrete in this hydration phase is still in a plastic state and due to the low strength, is ideal for transport, placing and consolidating. Towards the end of the stiffening phase at the 120 minute test samples, the hydration reactions start taking effect as can be seen from the strength development between the 60 and 120 minute test samples. The exact time that the dormant period ends is unknown, however, the strength increase from the 60 to 120 minute sample indicates that the dormant period ends somewhere between these time periods.

Towards the end of the stiffening phase marks the initial setting time which further marks the end of the window for placing and consolidating the concrete. Once initial set is reached, the setting phase starts. During this phase, the cement paste becomes stiff and unworkable due to the ongoing hydration reactions. The results show that between the initial and final setting times, the tensile strength develops rapidly which resembles the stiffening of the concrete paste. This trend in strength gain is consistent with results discussed in Section 2.5.1 from previous research. During this phase bleeding typically has ceased since the stiffening of the cement particles prevents settlement. This therefore means that surface finishing which includes floating, brooming and trowelling should commence and end by the final setting time.

During the setting stage, shrinkage due to evaporation poses great risk for cracks to develop if proper care is not taken in keeping the concrete surface moist. The low tensile strength of the 180 minute test samples demonstrates clearly why concrete is so vulnerable at this age.

The final setting time marks the beginning of the hardening phase and is where concrete starts to gain most of its strength. Figure 4-8 clearly shows an increase in gradient from the 180 to the 240 minute test samples. This can also be seen with the dramatic increase in stress between the 180 and 240 minute test samples from Figure 4-6. This phase marks the end of power floating and trowelling as the concrete soon starts to become a rigid solid. Final curing measures usually take place and end soon after this phase begins. At this age, the concrete has gained significant strength in both tension and compression and is therefore less prone to plastic cracking.

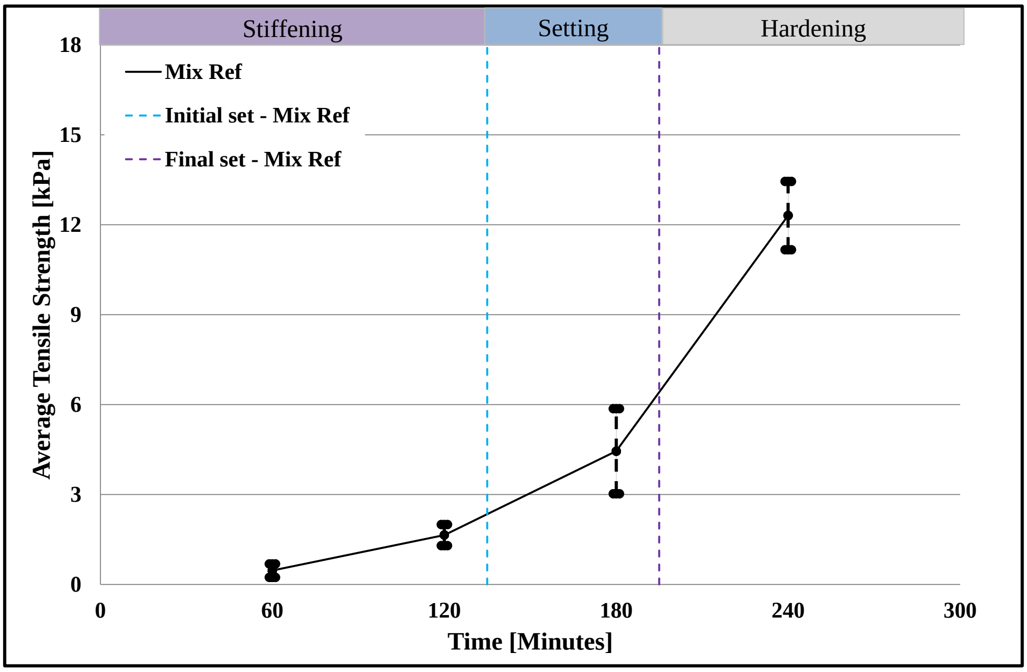

Figure 4-8: Mix Ref Strength development with time

4.2.2.2 Tensile strength (Ft) – Mix VMA

Figure 4-9 shows the strength development with time for Mix VMA plotted against the results obtained in Figure 4-8 for Mix Ref. Consistent with results obtained for Mix Ref, Mix VMA shows an increase in strength during the setting period, followed by another increase in strength during the hardening phase. Comparing the results between the reference and viscosity enhanced mix in Figure 4-9, highlights significant differences. The 60 minute results between the two mixes are similar, however, the rate of strength gain from the 120, 180 and 240 minute results for Mix VMA show a lower rate of strength gain compared to Mix Ref. The 180 and 240 minute results of Mix VMA showed much lower peak stresses, almost half that compared to Mix Ref, indicating a much slower rate of strength gain.

Setting times for Mix VMA were recorded at 140 and 205 minutes for the initial and final setting times respectfully. Similar setting times between the two mixes indicate that the rate of solidification due to hydration is similar but still slightly retarded. Furthermore, results indicate that the addition of the VMA influences both the rate and amount of strength gain.

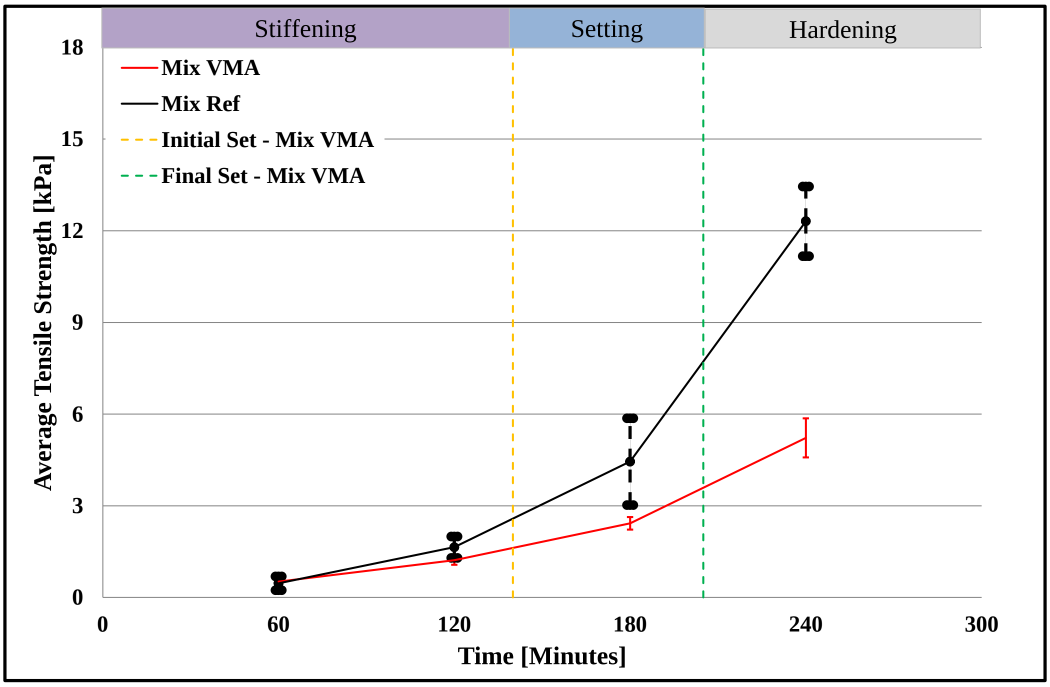

Figure 4-9: Strength development with time of Mix VMA vs Mix Ref

The main reason behind the slower rate of strength gain for Mix VMA is unclear; however several possible reasons could contribute to the observed tensile behaviour. Firstly, the slightly increased water-to-cement ratio of Mix VMA, as discussed in Sections 4.1.2 and 4.1.3, could possibly explain the slightly retarded setting period and hence slower rate of strength gain. A slower rate of setting, although minimal compared to Mix Ref, could contribute towards slower rates of strength gain. Secondly, the addition of VMA was found to lower the surface tension of the pore water in the fresh concrete. This could also contribute towards lower tensile strengths during the stiffening and setting periods. This however is discussed in greater detail in Section 4.2.5.

Therefore, the increased water-to-cement ratio, higher slump readings, slower setting times and lower surface tension of pore water is believed to contribute towards the observed tensile strength behaviour of Mix VMA, acting either in isolation or as a combination.

4.2.3 Strain capacity (ε_{cap})

Evaluating the stress versus strain results in terms of the evolution of strain capacity with time, allows the observation of the brittle and ductile behaviour of fresh concrete. Similar to Section 4.2.2, the strain capacity development during each phase of concrete, namely, the stiffening, setting and hardening phases is plotted in Figures 4-10 and 4-11. The strain capacity is calculated as the displacement of the concrete in the gauge area at failure or maximum strength divided by the length of the gauge area. Section 4.2.3.1 first considers the results obtained for Mix Ref. Thereafter the results for Mix VMA are discussed and compared to Mix Ref in Section 4.2.3.2.

4.2.3.1 Strain capacity (ε_{cap}) – Mix Ref

The results of strain capacity as it develops with time for Mix Ref are shown in Figure 4-10. From 60 minutes to just before the initial setting time at 120 minutes, the strain capacity of Mix Ref is high at 0.139 % to 0.182 % in elongation between 60 and 120 minutes. After 120 minutes, the strain capacity decreases rapidly as it enters the setting stage reaching a minimum value of 0.054 % elongation at 180 minutes. After this rapid decrease, the strain capacity increases slightly to an elongation value of 0.088 %.

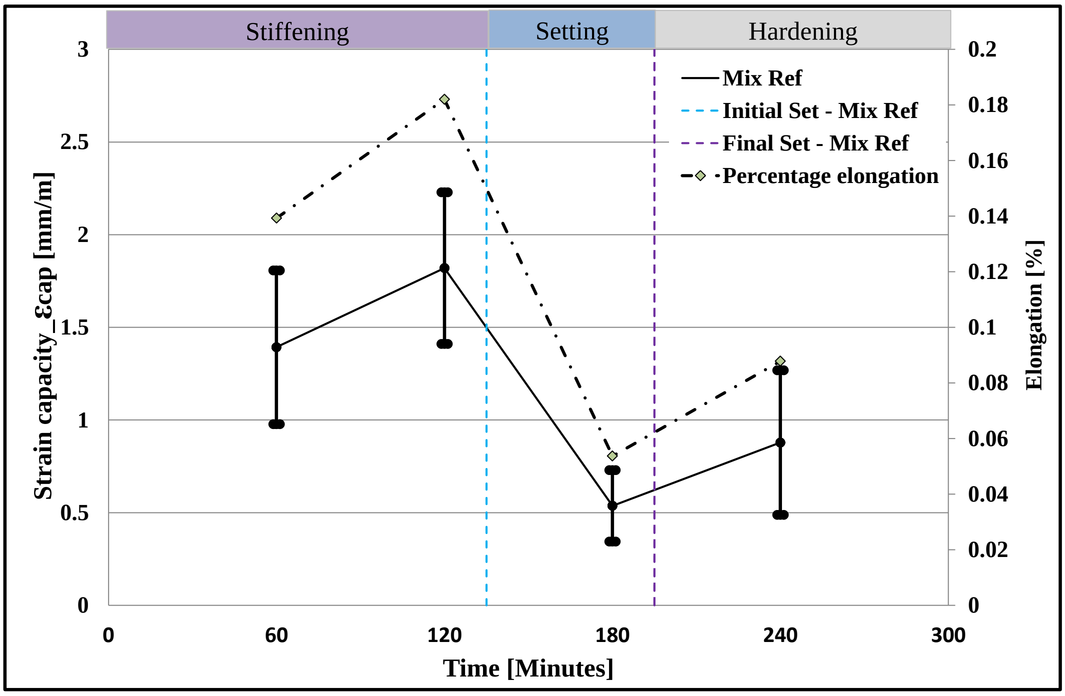

Figure 4-10: Strain capacity at different ages for Mix Ref

The rapid decrease in strain capacity between the 120 and 180 min results marks the transition from a plastic to a solid material and therefore gives a clear indication of the ductile to brittle behaviour. The smaller capacity of deformation together with the low tensile strengths discussed in Section 4.2.2.1, further confirms why plastic concrete is prone to plastic cracking during the setting period of concrete.

4.2.3.2 Strain capacity (ε_{cap}) – Mix VMA

Similar to Section 4.2.3.1, Mix VMA shows an elongation difference of 0.169 % to 0.190 % in elongation between 60 and 120 minutes. As the concrete enters the setting stage, the strain capacity decreases suddenly to a minimum value of 0.049 % in elongation at 180 minutes. As the concrete enters the hardening phase the strain capacity decreases slightly to a value of 0.047 % in elongation.

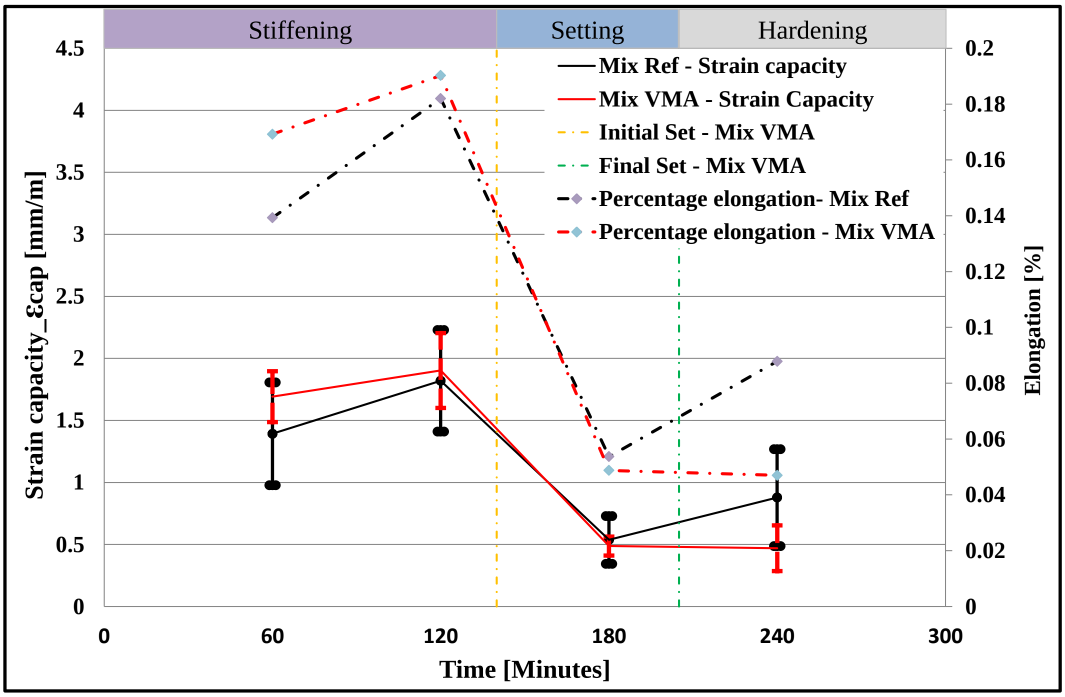

Figure 4-11: Strain capacity at different ages for Mix Ref vs Mix VMA

Results for both mixes are consistent with previous literature discussed in Section 2.5.2 showing that there is a rapid decrease in strain capacity as the concrete enters the setting stage. Results for both mixes show similar values for strain capacity between 60 and 180 minutes. While Mix Ref showed an increase in strain capacity, Mix VMA showed a slight decrease in strain capacity between 180 and 240 minutes. As discussed in Section 4.2.2 the rate and amount of strength development in Mix VMA was noticeably lower from 120 minutes onwards. The low rate of strength development is further evident between 180 and 240 minute strain capacities for Mix VMA. Where the strain capacity of Mix Ref increased between 180 to 240 minutes, Mix VMA showed a near constant strain capacity between these two time periods. The slightly retarded setting time of Mix VMA could possibly be reason as to why this occurs.

It should however be emphasised, that although the two mixes displayed different strain behaviours after the setting period, both mixes show similar behaviour trends during the plastic period. The differences are minimal and it can therefore be concluded that the addition of VMA has a minimal effect on the strain capacity of the concrete apart from a slightly slower strain capacity development during the hardening phase.

4.2.4 Young's modulus (E)

The Young's modulus of a material refers to the tensile elasticity or stiffness of the material. It describes the tendency of the material to deform under tensile or compressive induced loads. For linear elastic materials, where stress is directly proportional to strain (Hooke's law), the Young's modulus is taken as the slope of the stress versus strain curve. However, for plastic concrete, the initial stress versus strain behaviour is believed to be linear, meaning that the material follows Hooke's law before it starts deforming excessively as the strain capacity nears, at which point the stress versus strain capacity is believed to be non-linear.

Traditional methods used to determine the Young's modulus of hardened concrete under compressive forces, include either using the tangent or secant modulus. The tangent modulus involves fitting a straight line, tangent to the elastic portion of the ascending curve while the secant modulus, involves fitting a straight line between any two points of the ascending portion of the stress versus strain curve. The current study adopts the secant modulus method by fitting a straight line between two sets of points on the pre-peak stress versus strain curve as shown in Figure 4-5.

In light of the initial linear and non-linear behaviour as the concrete nears the strain capacity, two secant lines were used to investigate the Young's modulus as shown in Figure 4-12. The first method involves fitting a straight line between the origin and peak stress of the ascending portion of the stress versus strain curve. This method captures both the initial linear portion of the curve as well as the non-linear portion before failure. The second method involves fitting a straight line between the origin and 70 % of the maximum peak stress. This captures the Young's modulus based on the initial near elastic behaviour of the concrete.

These two methods therefore allow for comparison of Young's modulus between the initial ascending linear portion and non-linear portion of the stress versus strain curve. Section 4.2.4.1 first considers the results obtained for Mix Ref, incorporating both sets of secant points, while Section 4.2.4.2 discusses and compares the corresponding results of Mix VMA to Mix Ref.

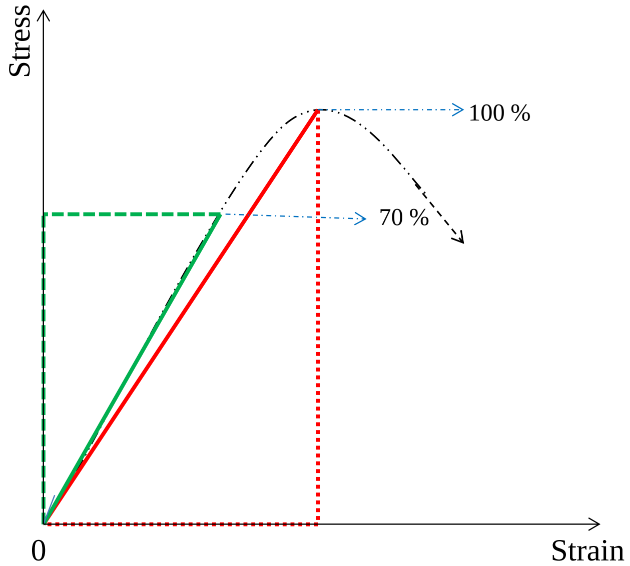

Figure 4-12: Method followed for the determination of the Young's modulus in plastic concrete

4.2.4.1 Young's modulus (E) – Mix Ref

The development of Young's modulus with time, obtained by fitting a secant line between 0 and 70 % (Graph (a)) and between 0 and 100 % (Graph (b)), are shown in Figure 4-13 for Mix Ref. The average Young's modulus values obtained in Graph (a), shows slightly higher magnitudes compared to the results displayed in Graph (b).

Graph (b) in Figure 4-13, corresponds to the strain capacity of fresh concrete and as a result includes the nonlinear portion of the stress versus strain graph. The start of the nonlinear portion of the ascending peak marks the end of the elastic period of the concrete and captures the excessive strain measured in the gauge area as the concrete nears its peak strength. This nonlinear portion, therefore, reduces the Young's modulus experienced during the initial elastic portion of the ascending peak.

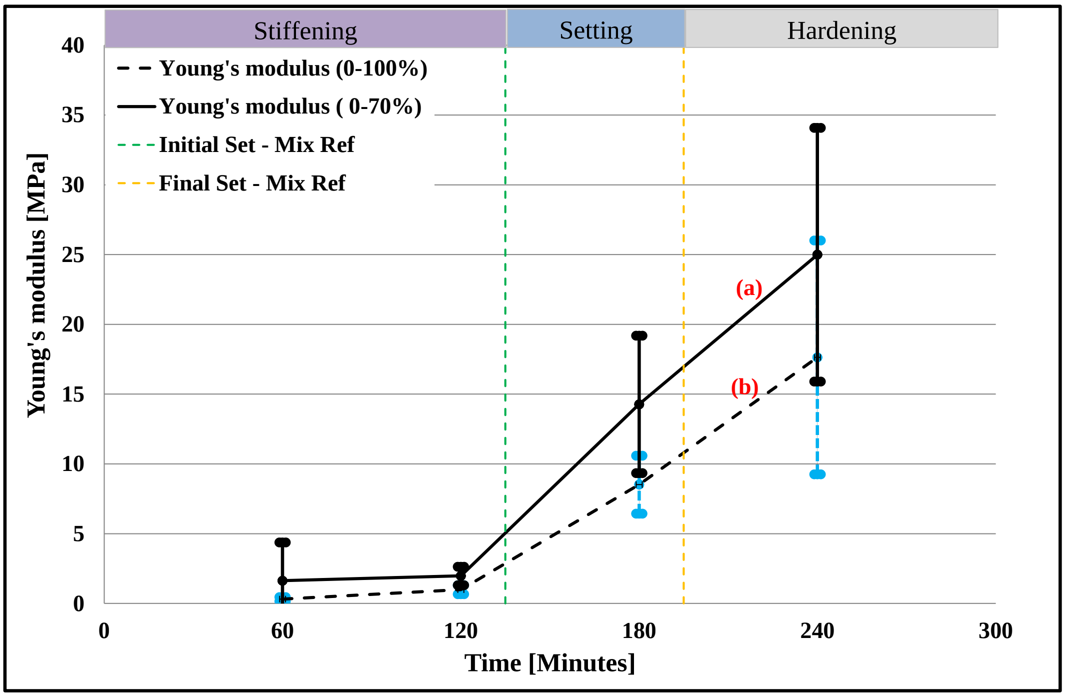

Figure 4-13: Young’s modulus at different ages for Mix Ref

Graph (a) in Figure 4-13, however, captures the elastic portion of the ascending curve by fitting a secant line between 0 and 70 % of the peak tensile strength. This method, therefore, excludes the excessive strain experienced by the concrete as it nears its peak strength. Therefore Graph (a) gives a better indication of the elastic behaviour of plastic concrete, whereas Graph (b), incorporates the corresponding strain capacity and gives an indication of how the Young’s modulus develops with time by incorporating both linear and nonlinear behaviour of the concrete.

Between 60 and 120 minutes for both graphs, the Young’s modulus develops very slightly during the initial stiffening phase. As the concrete approaches the setting and hardening phase, the Young’s modulus develops rapidly, giving an indication of the plastic to solid transition.

4.2.4.2 Young’s modulus – Mix VMA

Figure 4-14 displays the Young’s modulus results for Mix VMA, determined between 0 and 70 % (Graph (a)) and 0 and 100 % (Graph (b)) plotted against the corresponding results of Mix Ref as discussed in Section 4.2.4.1. Graph (a) contains higher magnitudes and develops slightly faster compared to Graph (b), similar to the results discussed in Section 4.2.4.1. This therefore confirms that the low Young’s modulus results obtain in Graph (b), between 0 and

100 % of the peak tensile strength, is mainly due to the excessive strain that the concrete experiences as the concrete nears the peak strength before cracking. However, comparing the Young's modulus results of Mix VMA, to Mix Ref, magnitudes are significantly lower. The higher tensile strengths observed for Mix Ref compared Mix VMA, is the main reason why Mix Ref displays higher Young's modulus results compared to Mix VMA.

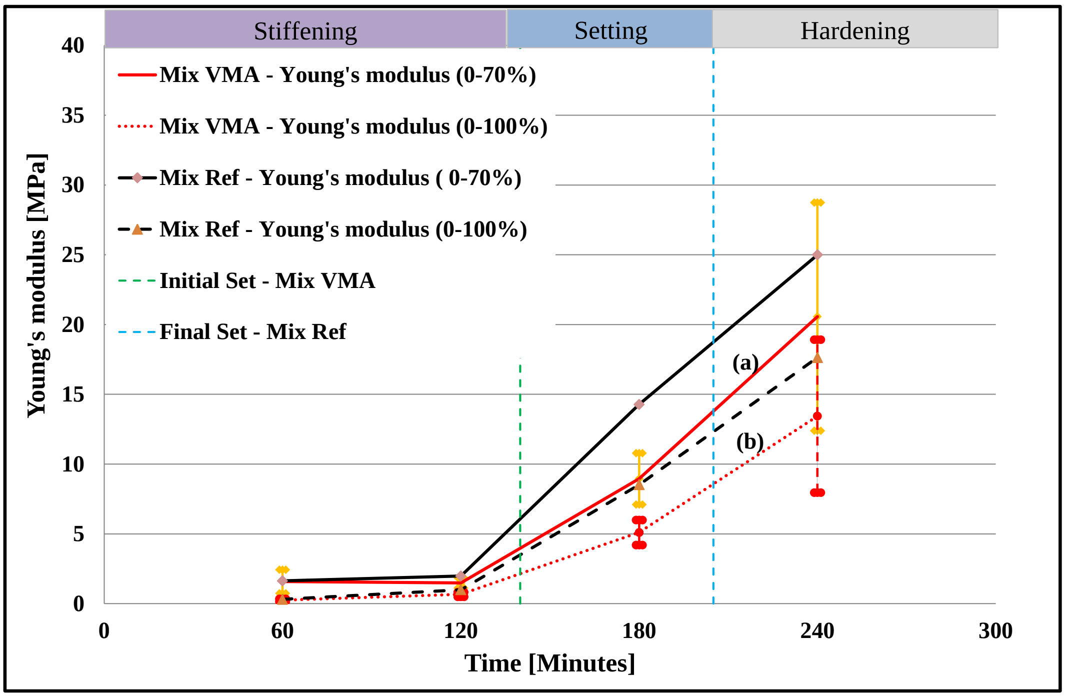

Figure 4-14: Young's modulus development with time for Mix VMA vs Mix Ref

As the concrete enters the setting phase, between the 120 and 180 minute test samples, the Young's modulus develops at a slower rate compared to Mix Ref. During these two time periods, the two concrete mixes share similar strain capacities (Figure 4-9), however, the strength development for Mix VMA is slightly slower compared to Mix Ref during the 120 and 180 minute test results. This is the main reason why the development of elasticity for Mix VMA is slightly lower between these two time periods.

As the concrete enters the hardening phase, Mix VMA shows a slightly faster development in Young's Modulus between 0 and 70 % of the peak stress (elastic region) compared to Mix Ref, however, the Young's modulus results for both mixes, incorporating the nonlinear portion of the ascending curve, show similar development rates. This therefore indicates that the two mixes develop at similar rates during the plastic to solid transition; however, the linear elastic results indicate that Mix VMA gains elasticity at a slightly faster rate.

4.2.5 Influence of capillary pressure on tensile behaviour

As discussed in Chapter 3, capillary pressure sensors were inserted at two locations in the concrete filled moulds. The first sensor was inserted into the gauge area were cracking is likely to occur, while the second sensor was inserted at a distance away from the gauge area, where no cracking is expected to occur. The main purpose of these experiments, were to investigate the build-up of stress in water filled pores when a tensile load is applied. Currently, no literature could be found on this topic which can help explain the development of strength in plastic concrete.

Section 4.2.5.1, first discusses the build-up of capillary pressure under tensile loads for Mix Ref. Thereafter Section 4.2.5.2, discusses the corresponding results for Mix VMA which also includes a comparison between the two mixes. Section 4.2.5.3 then aims to further explain the general behaviour of capillary pore pressure development with time.

4.2.5.1 Influence of capillary pressure on tensile behaviour – Mix Ref

Figure 4-15 shows the capillary pressure readings for both gauge and out of gauge pressure zones plotted against the stress versus strain results for time periods 60, 120, 180 and 240 minutes for Mix Ref. The gauge pressure of the 60 minute result increases at a similar rate and shows a similar shape compared to the stress versus strain result of the concrete. The out of gauge pressure however, increases at a much slower rate. At 60 minutes, the concrete is still in plastic form with very little strength gain from time of placing. The results indicate that much of the strength gain observed for the 60 minute results is due to the capillary force in the pores of the fresh concrete which keeps the particles together. This indicates that the presence of free water in plastic concrete is responsible for much of the tensile strength experienced for the 60 minute test result.

The gauge pressure for the 120 minute result, increases at a much slower rate and is of a slightly lower value compared to the corresponding stress versus strain result. This shows that the concrete has already started gaining some tensile strength from the hydration products; however, much of the strength measured is still due to the pressure of free water holding the solid particles intact. The out of gauge pressure results showed very little pressure build-up compared to the gauge area results. At this age the concrete is nearing the start of the setting stage and the concrete is already starting to gain tensile strength due to the commencement of the hydration reactions.

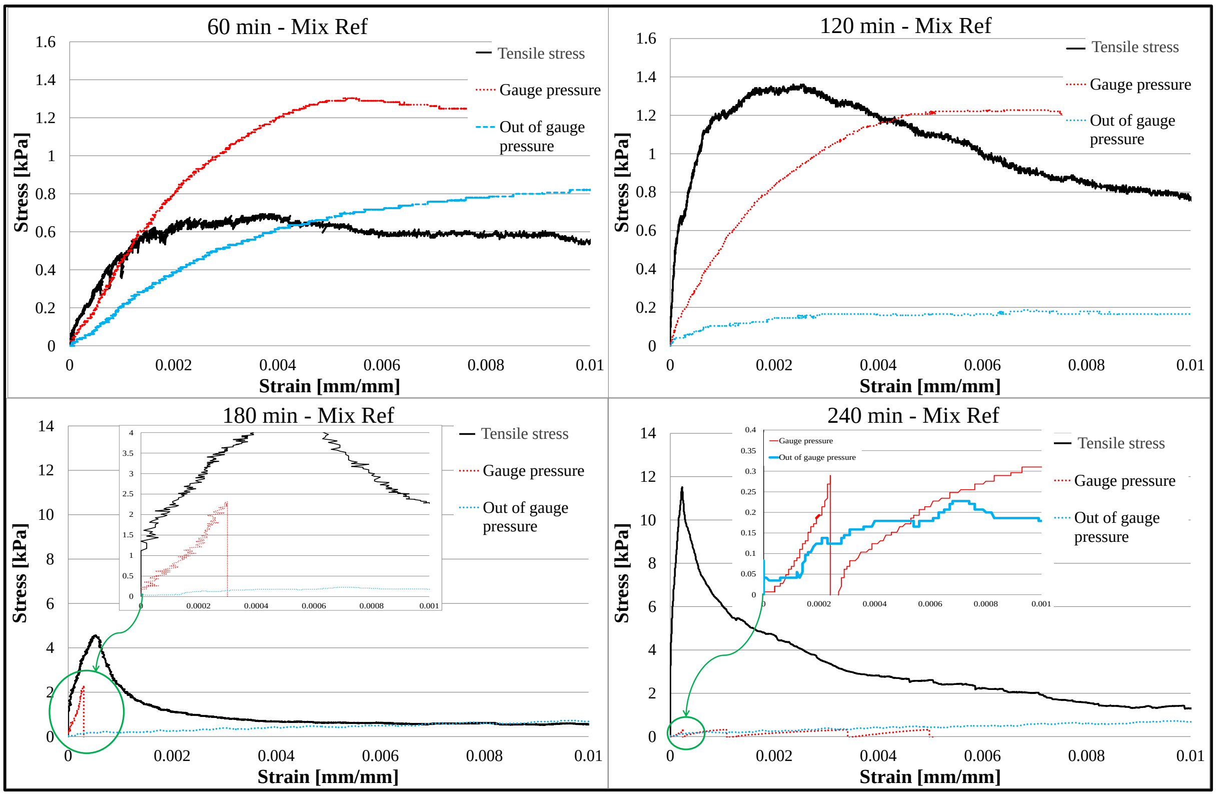

Figure 4-15: Capillary pressure measurements for Mix Ref at 60, 120, 180 and 240 minute time periods

The hydration reactions are expected to start at the end of the dormant period and falls somewhere between 60 and 120 minutes as discussed in Section 4.2.2.1. This indicates that the deformation of concrete in the gauge area has a very small influence on the rest of the concrete out of the gauge area. The larger area of concrete in the out of gauge area, experiences a smaller stress compared to the smaller area of concrete in the gauge area which ultimately experiences a larger stress. The small stress build-up in the out of gauge area seems to have a greater effect on the 60 minute results compared to the 120 minute results. A possible reason for this occurrence could be due the strength gain of the 120 minute test sample. The interconnectivity of the pores at 60 minutes, is more pronounced (clearer path) than for the 120 minute test sample. As the strength develops, the hydration products bridge the gaps between surrounding molecules, reducing the interconnectivity of the pore and therefore preventing free movement of water.

The 180 minute results in Figure 4-15, shows that the pressure build-up in the gauge area fails at 2.3 kPa which marks the point of air entry at the pressure sensor, indicating that air has locally entered the pore system. At this point, the concrete's stress continues to build-up until cracking or failure. The presence of free water is still believed to provide the concrete with some form of strength, however, after air entry; the tensile capacity is believed to mainly come from the hydration products. The out of gauge pressure showed no corresponding peak, similar to that of the 120 minute results.

The 240 minute results showed a very low increase in gauge pressure as the tensile load was applied. This gives an indication of the low amount of free water in the concrete and the density of the hydration products around the pressure sensors tip. The low localised pore water pressure in the gauge area therefore indicates that the pores around the sensors tip are now much more rigid, preventing the pores and pore water from moving and in turn causing an increase in gauge pressure. The out of gauge pressure readings continued to increase at a constant rate, however it is believed that this is due to the ongoing evaporation. This behaviour is further explained in Section 4.2.5.3.

4.2.5.2 Influence of capillary pressure on tensile behaviour – Mix VMA

Figure 4-16 shows the capillary pressure readings for both gauge and out of gauge pressure zones plotted against the stress versus strain results for time periods 60, 120, 180 and 240 minutes for Mix VMA. The results show similar trends compared to that of Mix Ref in terms of the general behaviour of capillary pressure under a tensile induced load. The 60, 120 and 180 minute results all show a visible increase in gauge pressure under a tensile induced load. This therefore implies that similar to Mix Ref, the capillary pore pressure is responsible for part of the strength gain during these time intervals. The 120 and 180 minute results show greater values in strength compared to the measured gauge pressure values. This greater strength difference is believed to be due to the hydration products bridging the gaps in and around the pores.

Section 4.2.2.2 identified the strength development of Mix VMA with time being significantly lower compared to Mix Ref. Figures 4-15 and 4-16 identified the capillary pore pressure as being responsible for part of the measured strength gain observed for both mixes between 60, 120 and 180 minutes. The capillary pore pressure readings for both mixes at 240 minutes, give an indication of the rate of hydration. At 240 minutes, during the hardening phase, the hydration products bridge the gaps between particles, preventing a capillary pressure measurement at a localised area in the gauge area zone. However, the presence of pore water between particles where the crack is likely to form still exists and possibly provides a portion of the strength measured for the 240 minute test samples. The capillary pressure results, therefore, give an indication of two phenomena. The first describes the rate of hydration affecting the interconnectivity of pores while the second describes the contribution of capillary pressure to the measured strength gain.

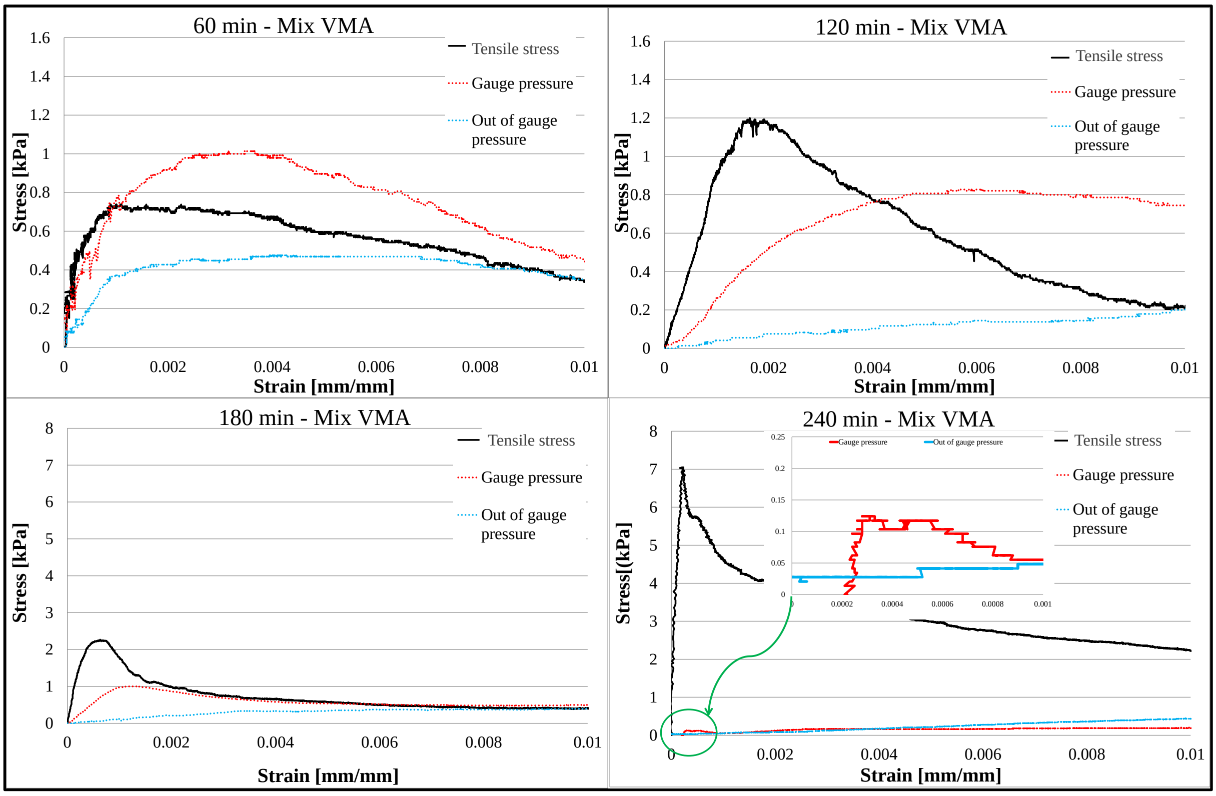

Figure 4-16: Capillary pressure measurements for Mix VMA at 60, 120, 180 and 240 minute time periods

The Gauss Laplace equation (Eq.1) presented in Section 2.4.2 can be used to explain the varying strength difference between Mix Ref and Mix VMA. The capillary pressure within pores is directly proportional to surface tension of the pore fluid and inversely proportional to the radius of the water menisci. As a tensile load is induced within the concrete, the tensile load pulls the concrete's solid particles apart, decreasing the radius of water menisci; this creates a corresponding increase in the measured capillary pressure reading. The surface tension of the pore fluid controls the amount of pressure experienced within pores. The surface tension results presented in Section 4.1.1, indicate that the surface tension of pore fluid decreases with increasing dosages of VMA. Therefore the surface tension of pore fluid in Mix Ref is significantly higher compared to Mix VMA. This therefore indicates that Mix Ref contains higher negative capillary pore pressures under tensile induced forces compared to Mix VMA. This, together with the presence of pore water between particles at the crack location, controls the measured strength observed for both concrete mixes. This partly explains why Mix Ref showed higher tensile strengths compared to Mix VMA.

4.2.5.3 Development of capillary pressure with time

Figure 4-17 can be used to explain the influence of stress experienced in the gauge area on the out of gauge particles. The diagram is further divided into four sections with each section representing a specific time period, namely the 60, 120, 180 and 240 time intervals. Each section contains a block of three particles surrounded by pore water. This block of particles represents a simple representation of the more complex capillary pore system in plastic concrete. Each section aims to explain the negative capillary pressure experienced between particles in the gauge and out of gauge zones when a tensile force is applied to the pore system.

The 60 minute diagram falls within the stiffening phase and is believed to be somewhere within the dormant period or directly after the dormant period. Its exact location with regards to the dormant period is unknown; however, it is known that the 60 minute results showed very little strength gain from time of placement to testing. The pore water diagram shows three particles surrounded by pore water with little to no hydration products between pores. There is a slight water meniscus between particles indicating that the pore water bonds are in tension as they hold the particles together.

As the actuator induces a mechanical tensile force between Particles 1 and 2 in the gauge area for the 60 minute test sample, Particle 1 moves away from Particle 2 and as the pore pressure tries to keep these two particles in place, an increase in pore pressure is measured in the gauge area. The displacement of Particle 1 in the positive U direction causes Particle 2 to move by a smaller distance of U_2, which in turn induces a smaller build-up in pore pressure between Particles 2 and 3. This process continues to occur until a crack forms between Particles 1 and Particle 2. The formation of a crack results in a drop in pressure between Particles 1 and 2, which is seen in the gauge pressure graph in Figure 4-17. This drop in pressure represents a break between the pore water bonds. In the case of a still liquid concrete without any significant strength gain, except for the pore water forces holding the particles together, the pressure build-up between Particles 2 and 3, remains largely constant after a crack occurs and decreases with time as Particle 2 displaces close to its original position.

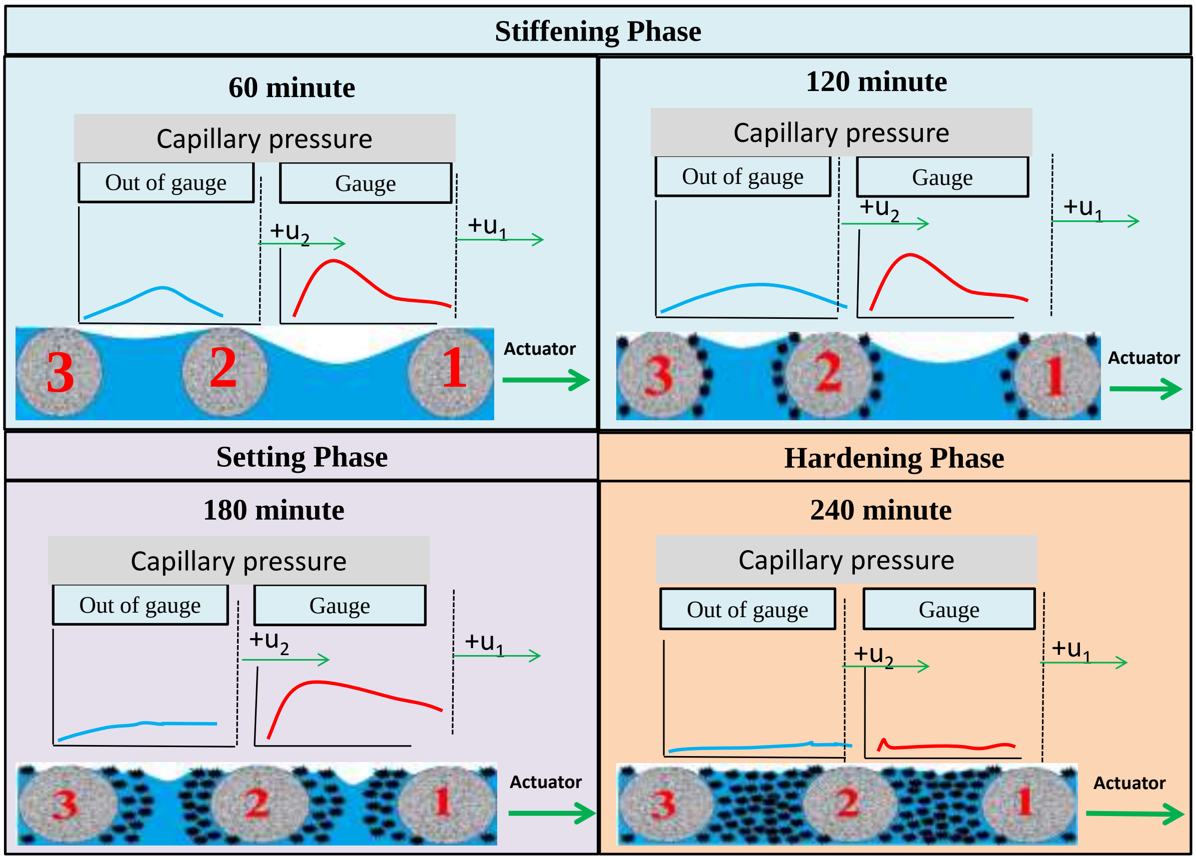

Figure 4-17: influence of capillary pressure on internal concrete particles

In the case of a plastic concrete that is already undergoing hydration, such as concrete specimens at 120 minutes, ongoing evaporation results in a greater pore pressure experienced between particles and is represented by the deeper concave meniscus formed between hydration products. At this age, hydration reactions are constantly filling the pores with hydration products. As a mechanical tensile load is applied to the pore system, the gauge pressure continues to build-up until a drop in pore pressure occurs, at which point the measured tensile strength of the concrete is believed to be due to the hydration products. Before the pore pressure drops, the pore pressure is believed to provide the concrete with most of its strength. The pressure build-up in the out of gauge area remains largely constant after the initial peak. This constant measurement is believed to be due the hydration products which fill up the empty pores in the concrete, which in turn adds rigidity to the concrete and prevents Particle 2 from displacing back to its near original position.

The 180 minute results fall within the setting phase and the concrete is believed to be nearing the end of setting. At this age, there is an increased pore pressure experienced between pores as ongoing hydration continues to fill up the empty pores with hydration products, in turn reducing the size of pores, resulting in smaller menisci forming between hydration products as seen in the 180 minute section in Figure 4-17. The smaller concaved meniscus is believed to result in a larger pore pressure experienced within pores and provides a good indication of the difference in pore pressure between the 120 and 180 minute results. The hydration products continue to bridge the gaps in and between the empty pores and provide the concrete with most of its tensile strength. As a mechanical tensile load is applied to the concrete, Particles 1 and 2 move further away from each other. This distance however, is much smaller compared to the 60 and 120 minute particle displacements. The difference in displacement is further confirmed by the strain capacity results, where the strain capacity reduces significantly as the concrete enters the setting phase. The smaller amount of free water between pores and smaller meniscus means that more tensile force is needed to break the pore water bonds. The gauge pressure measures an increase in pore pressure at this point. The increase in tensile load however, has no effect on the out of gauge pressure since the hydration products have already bridged the gaps between pores, meaning that the out of gauge pores are held in place by the hydration products.

The out of gauge pressure continues to build-up at a slow rate for as long as the test duration continues. Ongoing evaporation is believed to be the driving force behind this negative capillary pressure build-up. After the pressure drop, the stress in the concrete continues to build as the hydration products hold the particles in place. Once the tensile load exceeds the tensile capacity of the concrete, a crack initiates and the gauge pressure drops slightly and remains constant, unless the pore breakage occurs at the tip of the sensor, at which point a sharp drop in pore pressure occurs. If the pore pressure breaks away from the sensors tip, the pore pressure surrounding the sensor’s tip drops slightly and remain largely constant, since the particles are not able to rearrange to reduce the pore pressure build-up compared to the 60 and 120 minute results.

The 240 minute results fall within the hardening phase and most of the concretes strength is believed to be due to the hydration products. The 240 minute illustration in Figure 4-17 shows a smaller meniscus formed between hydration products, indicating that the amount of free water in the concrete is significantly less compared to the 180 minute results. This is mainly due to the filling of pores with hydration products. At this age the hydration products continue to bridge the gaps in and around the empty pores.

The small amount of free water between pores should ideally mean that more force is needed to break the pore water bond; however, as a mechanical tensile load is applied to the concrete, no gauge pressure is recorded. A possible reason for this is due to the bridged pores around the capillary sensors tip. The dense hydration products prevent the pores surrounding the sensors tip from moving and recording a change in gauge pressure. It is believed that the gauge pressure at the point of crack would increase and provide a certain amount of tensile strength to the concrete, however measuring the gauge pressure at the exact point of crack presents a great amount of difficulty. Nevertheless, the localised gauge pressure readings showed very little pressure build-up and therefore gives a good indication of the amount of hydration that has occurred within this hardening phase.

4.3 Relaxation behaviour under single loading

This section aims to investigate the relaxation behaviour of Mix Ref and Mix VMA under single loading. As discussed in Chapter 3, at least 2 relaxation tests were carried out at 60, 120, 180 and 240 minutes after casting. Tests were performed by loading the actuator to 50 % of the average maximum tensile load for each corresponding time period, followed by an abrupt stop by ceasing the displacement of the actuator. Test duration for all relaxation tests were at least ten minutes long. Section 4.3.1 first considers the relaxation behaviour of Mix Ref under single loading. Thereafter the results for Mix VMA are discussed and compared to Mix Ref in Section 4.3.2.

4.3.1 Relaxation – Mix Ref

Relaxation tests were carried out on Mix Ref in order to identify and capture the plastic relaxation behaviour of concrete. Relaxation results for the 60 and 120 minute time periods are displayed in Figure 4-18, while results for the 180 and 240 minute time periods are displayed in Figure 4-19.

For the purpose of the current study, the term “relaxation potential”, will be used to quantify the relaxation results. The relaxation potential refers to the initial drop in stress from point of constant strain to the lowest stress value resulting due the relaxation behaviour of the concrete specimen. The relaxation potential is therefore represented as a percentage of the total decrease in stress occurring within 5 minutes after the displacement of the actuator is ceased divided by 50 % of the average tensile stress capacity for each respective time period.

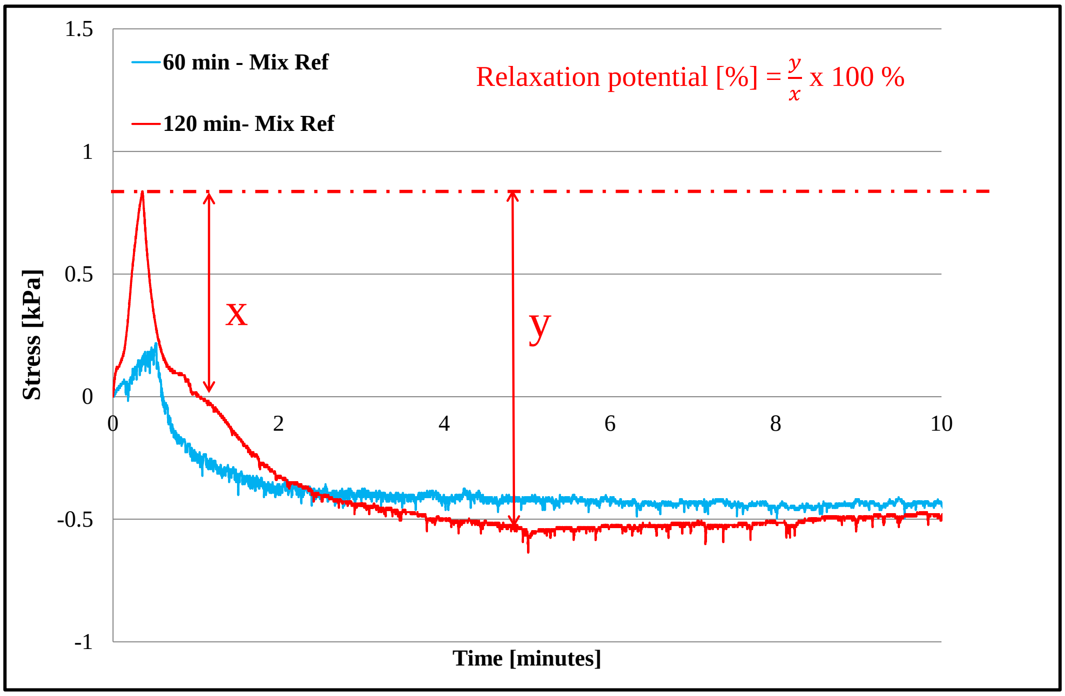

Figure 4-18: Relaxation for test samples at 60 and 120 minute time periods

Both the 60 and 120 minute time period specimens in Figure 4-18, drop into the compression zone once the displacement of the actuator is ceased. By ceasing the displacement of the actuator, a constant strain is applied throughout the test period. The corresponding drop in stress as a result of the constant strain represents the relaxation behaviour of the concrete specimen. The 60 minute time period specimens displayed an average relaxation potential of 307 %, while the corresponding 120 minute time period specimens displayed a much lower 175 % relaxation potential. After the initial drop of stress in the 60 minute test specimen, the force remains constant throughout the test period; however, the 120 minute test result displays a slight increase in gradient after 5 minutes.

Figure 4-19 shows the relaxation behaviour of the 180 and 240 minute test samples. The 180 minute test samples displayed an average relaxation potential of 55 %. During this time period, the concrete is nearing the end of the setting period and as a result, the concrete is much more rigid compared to the younger specimens. The 240 minute test sample showed nearly no relaxation with an average relaxation potential of 6.5 % between all 240 minute test samples. Both the 180 and 240 minute test samples, display an increase in gradient after the initial relaxation drop.

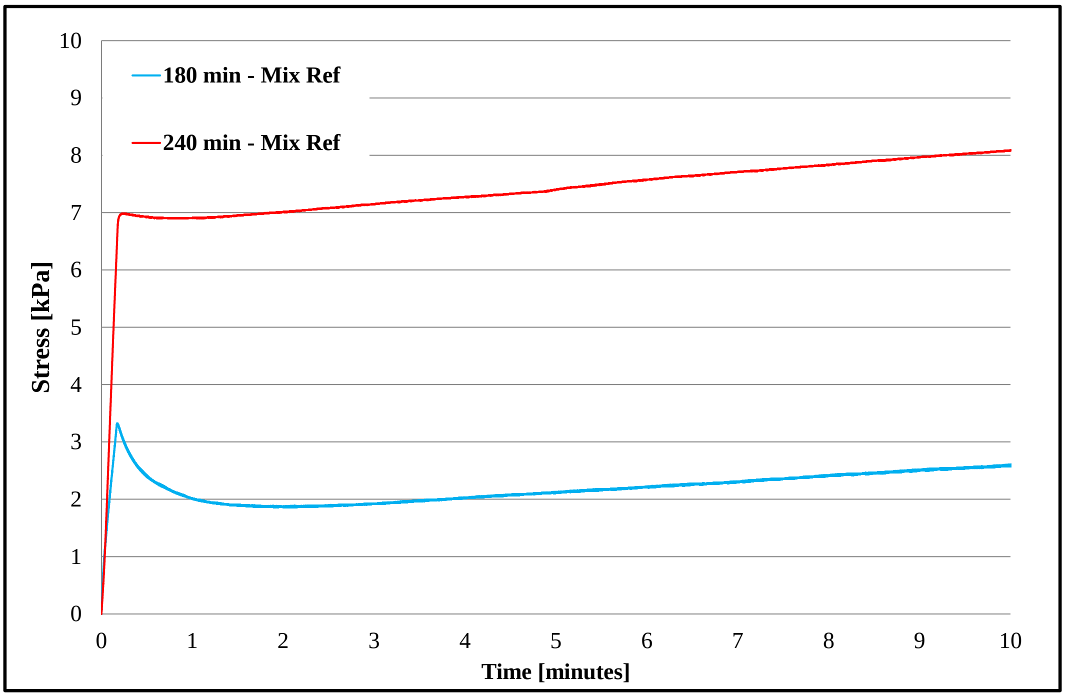

Figure 4-19: Relaxation for test samples at 180 and 360 minute time periods

The increase in gradient for the 120, 180 and 240 minute test samples is believed to be due to the ongoing shrinkage of the concrete. Once the actuator is ceased, the load cell reads a tensile force since both mould halves are pulled apart. Any additional shrinkage in the concrete samples pulls the two mould halves towards each other. The mechanism behind the measured shrinkage is uncertain; however, two possible reasons may be the cause:

The first reason is due to the ongoing evaporation that continues to draw out water from the concrete's capillary pores. This in turn pulls the concrete's particles towards each other as the radii of the surrounding water menisci decreases, resulting in a corresponding increase in pore pressure. This is confirmed with the out of gauge pressure readings discussed in Section 4.2.5. This in turn causes the concrete in the mould to shrink, while the load cell captures the amount of shrinkage stress induced. However, due to the relatively high water-to-cement ratio of 0.55, the contribution of self-desiccation is believed to be minimal.

The second possible cause could be due to self-desiccation. Self-desiccation is defined as the suction of water from water filled pores due to ongoing hydration. This in turn causes the particles to move towards each other, resulting in the measured shrinkage in a similar manner as discussed for ongoing evaporation.

4.3.2 Relaxation – Mix VMA

Relaxation tests were carried out on Mix VMA in order to determine the influence of viscosity on the relaxation behaviour of concrete. Mix VMA showed a slower rate of strength development compared to Mix Ref in Section 4.2.2.2. This therefore means that Mix VMA's test samples were loaded at a much lower stress compared to Mix Ref's test samples; however, loading was performed on both mixes as a percentage of the corresponding tensile capacity of the concrete at each time zone for both mixes. This therefore allows for comparison between the two mixes.

Figure 4-20 displays the relaxation results of the 60 and 120 minute time periods for Mix VMA. Both times zones relax into the compression zone displaying similar behaviour compared to Mix Ref's results. The 60 minute time period specimens displayed an average relaxation potential of 299 % while the corresponding 120 minute time period specimens displayed a slightly lower 236 % relaxation potential. Mix VMA therefore showed a much higher relaxation potential for the 120 minute test samples compared to Mix Ref's corresponding result.

Figure 4-21 displays the relaxation results of Mix VMA's 180 and 240 minute test samples. The 180 minute test sample relaxes into the compression zone with an average relaxation potential of 134 %. The 240 minute test samples, displayed a relaxation potential of 29 %. Both of these results display a much higher relaxation potential compared to the 55 % and 6.5 % relaxation potential obtained to Mix Ref for the 180 and 240 minute time periods respectively. Mix VMA therefore has a greater relaxation potential compared to Mix Ref.

The Relaxation potential of both Mix Ref and Mix VMA, suggests that the relaxation of plastic concrete is dependent of the rate of hydration since the relaxation potential decreases as the concrete begins stiffen and harden. Mix VMA however, showed greater relaxation across all time periods compared to Mix Ref. As discussed in Section 4.2.2, the 0.8 % dosage of Mix VMA is believed to increase the water-to-cement ratio of Mix VMA, thus slightly retarding the setting time and increasing the slump measurement. This possibly explains why Mix VMA showed greater relaxation potential compared to Mix Ref.

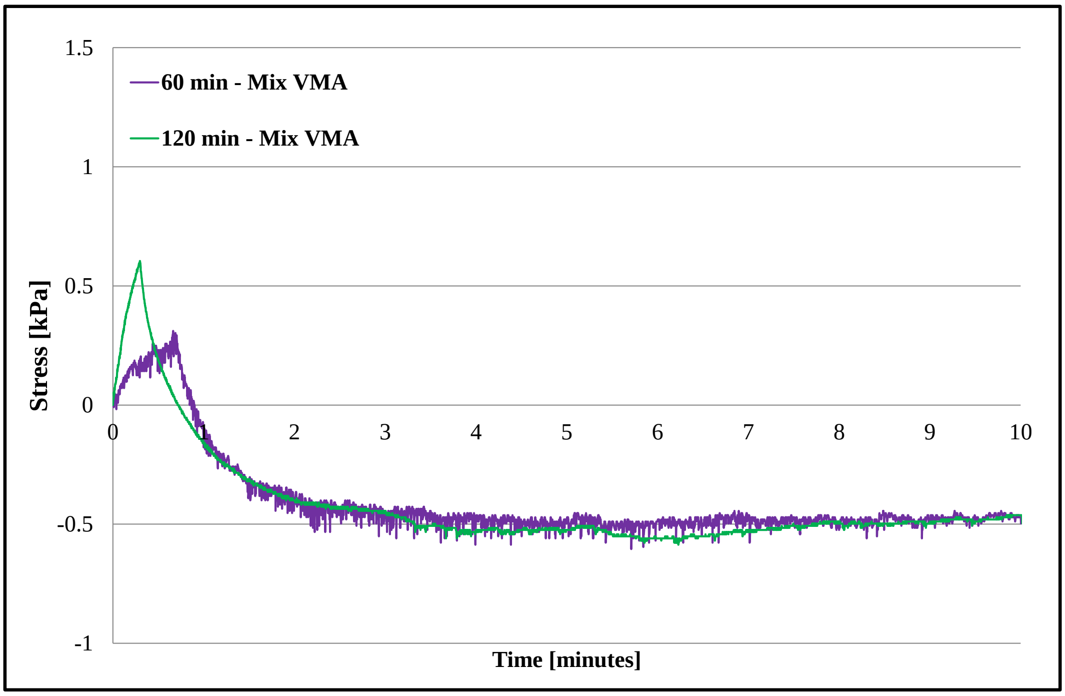

Figure 4-20: Relaxation for test samples at 60 and 120 minute time periods (Mix VMA)

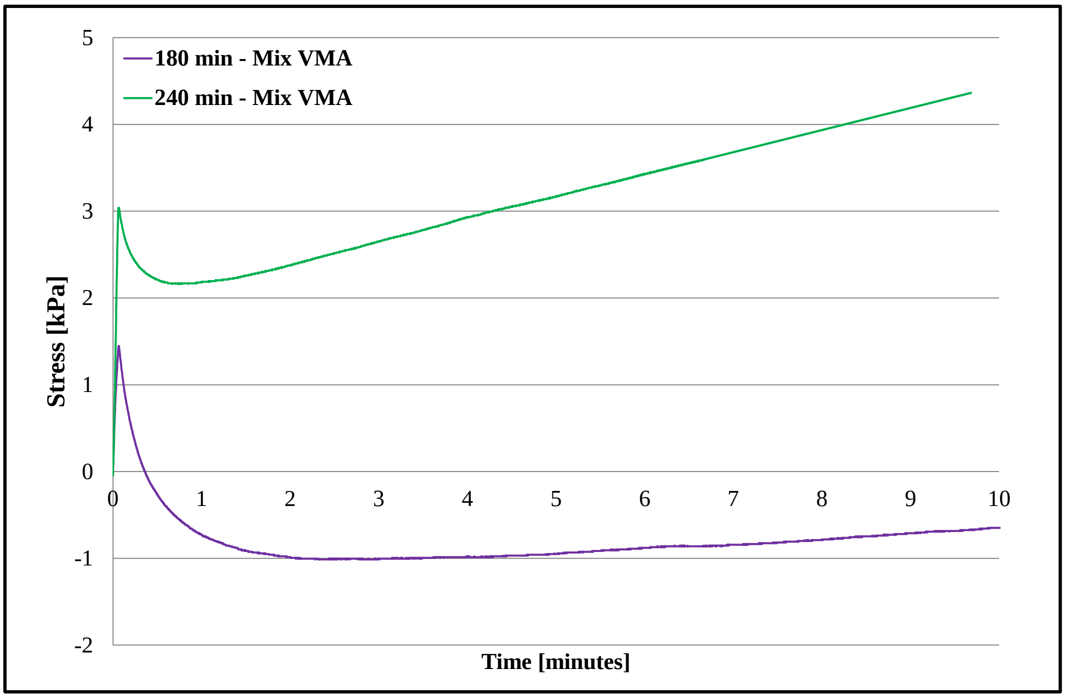

Figure 4-21: Relaxation for test samples at 180 and 240 minute time periods (Mix VMA)

4.4 Relaxation behaviour under multiple loading

During the early of ages of concrete, typically during the stiffening and setting phases, the concrete is likely to undergo multiple loading and unloading cycles. One form of loading and unloading may occur during the initial curing period of concrete, typically between the stiffening and hardening phases. In evaporation rich environments, the concrete element experiences a stress build-up and by lightly wetting the atmosphere above the concrete's surface, for example with a fog spray, reduces this stress build-up.

To simulate this behaviour, relaxation tests were repeated by loading the actuator up to 50 % of the average maximum tensile capacity followed by an abrupt stop by ceasing the displacement of the actuator. The concrete was then left to relax for a period of 5 minutes before further increasing the stress to 50 % of the average maximum tensile capacity in the tensile regime. This process was either repeated for at least three cycles or until the concrete test samples failed. Section 4.4.1 discusses the results obtained for Mix Ref while Section 4.4.2 discusses the results obtained for Mix VMA followed by a comparison between the two concrete mixes.

4.4.1 Multiple loading – Mix Ref

Figure 4-22 displays the relaxation behaviour of Mix Ref under multiple loading cycles at 60 and 120 minute time periods. At least two sets of multiple loading tests were carried out for all time zones. Consistent with results in Section 4.3, both test periods relax into the compression zone, relieving the mechanically induced tensile stress. The 60 minute test sample is able to complete multiple loading cycles without failure. As each cycle progresses, the concrete sample is able to relax all of the induced mechanical stress, however a slight decrease in relaxation potential is observed as each cycle is completed. The 120 minute test sample displays similar behaviour compared to the 60 minute test result in that all cycles relax the induced mechanical stress; however, the decrease in relaxation potential after each cycle is more defined.

The last loading cycle marks the point at which the actuator is loaded until the specimen failed. From Figure 4-22, it is seen that the peak stress of the 120 minute test sample at point of crack, is very similar compared to the loading applied to each cycle. The main reason for the low stress needed to crack the concrete specimen, is possibly due to the cumulative amounts of strain induced during multiple loadings. The 60 minute test sample is cracked during the seventh cycle, however, the high tensile load needed to induce cracking, indicates that the concrete still contains sufficient loading capacity to perform more loading cycles.

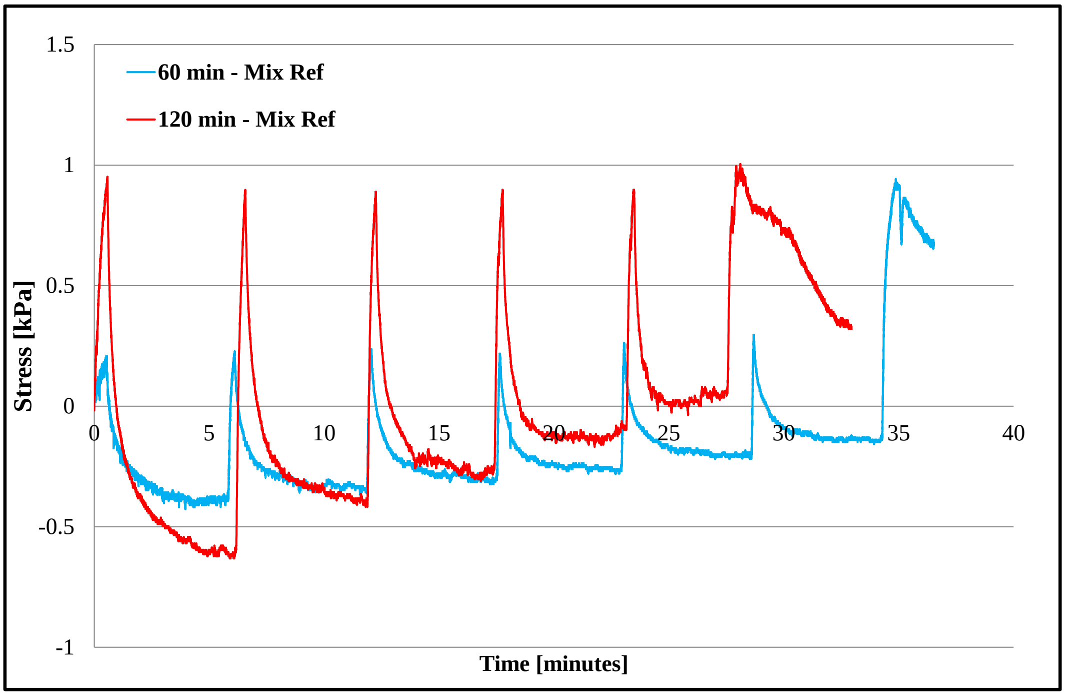

Figure 4-22: Multiple loading results for test samples at 60 and 120 minute time periods (Mix Ref)

Figure 4-23 displays the relaxation behaviour under multiple loading for the 180 and 240 minute test samples. The 180 minute test sample is able to complete three cycles before failure during the fourth cycle. At this age, the concrete is nearing the end of the setting phase and the results show that the concrete is not able to relax all the induced mechanical stress. As a result, the remaining tensile stress after the initial relaxation during the first cycle is carried over to the next cycle, where the total load induced within the concrete sample, is equivalent to 50 % of the average maximum tensile strength, plus the remaining stress of the previous cycle. This method is repeated until the fourth cycle where failure occurs, resulting in a crack.

The 240 minute test sample is only able to complete one cycle before failure. The main reason for this occurrence is believed to be due the brittle nature of the concrete, which lacks the ability to relax stress build-up compared to the 60 and 120 minute test samples. The small amount of stress relaxed during the first cycle, is not sufficient in allowing for a second successful loading cycle.

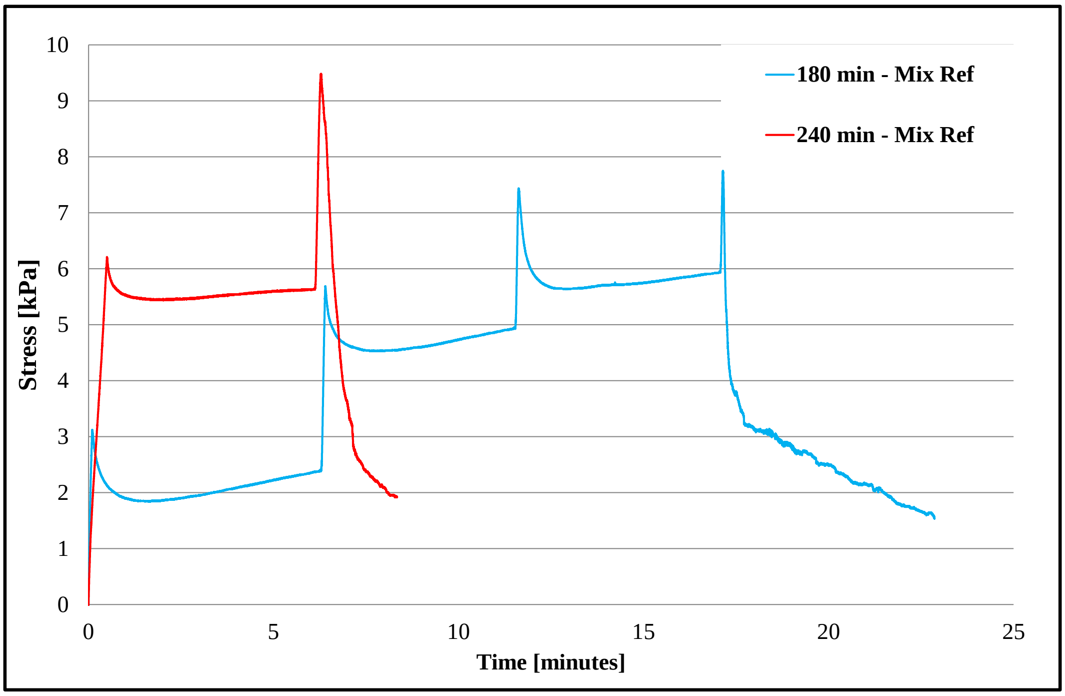

Figure 4-23: Multiple loading results for test samples at 180 and 240 minute time periods

The ability to complete multiple cycles such as for the 60 and 120 minute test periods, gives an indication of the ductility and forgiving nature of the concrete under stress build-up and deformation. At these ages, the concrete is still plastic nearing the start of the setting phase and results show that the concrete is able to withstand multiple loading cycles before failure.

The 180 and 240 minute test samples fall within the setting and hardening phases of the concrete. Concrete at this age is semi plastic, beginning to solidify and the low amount of completed cycles displays the brittle nature of the concrete. The low amount of relaxation during each cycle as well as the low amount of completed cycles, gives an indication as to why plastic shrinkage cracking is more severe during the setting period of the concrete. Furthermore, the 180 and 240 minute test samples, have lower strain capacities compared to the 60 and 120 minute test samples as discussed in Section 4.2.3.1. This possibly explains why samples at 180 and 240 minutes lack the ability to withstand or resist multiple cycles compared to the 60 and 120 minute test specimens.

4.4.2 Multiple loading – Mix VMA

Figure 4-24 displays the relaxation behaviour of Mix VMA under multiple loading for test periods 60 and 120 minutes. Similar to Mix Ref, both test samples were able to complete multiple cycles without failure. The 60 minute test sample completed six cycles before the actuator was loaded to initiate cracking. The high tensile stress required to initiate cracking, approximately the average maximum tensile stress for the 60 minute test result, indicates that the concrete still contained sufficient loading capacity to complete a few more cycles before failure.

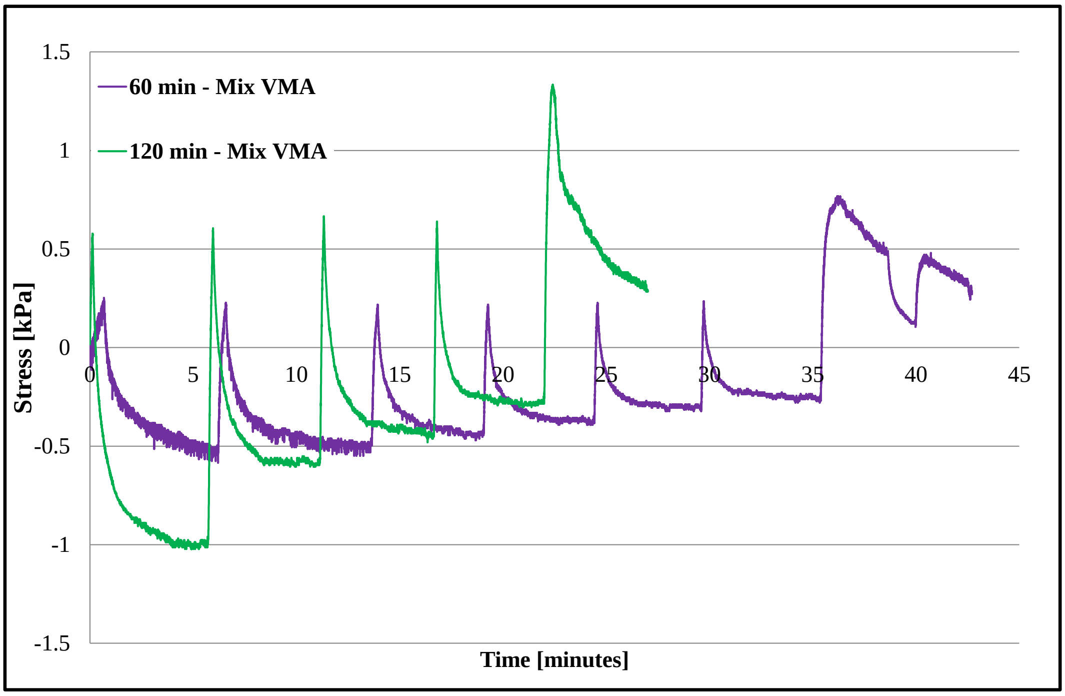

Figure 4-24: Multiple loading results for test samples at 60 and 120 minute time periods (Mix VMA)

The 120 minute test sample completed four cycles before loading the actuator to initiate cracking. Similar to the 60 minute test sample, results show that the sample still contained sufficient loading capacity, since the amount of stress required to initiate cracking is similar to the average maximum tensile strength of the 120 minute test samples. Similar to Mix Ref, the relaxation potential for the 60 and 120 minute test samples, decrease as each cycle progresses.

Figure 4-25 displays the relaxation behaviour of Mix VMA under multiple loading cycles at 180 and 240 minute test periods. The 180 minute test sample successfully completes a minimum of three cycles before failing during the fourth cycle. Two sets of multiple loading tests were carried out on the 180 minute time period and the second result showed the concrete was able to complete five cycles before failure. Mix Ref however, consistently completed between two and three cycles before failure. Results for Mix VMA show that the concrete relaxes into the compression zone; however the range of relaxation decreases after each cycle progresses. Furthermore, the larger relaxation potential of Mix VMA at 180 minutes, possibly explains why a greater amount of successful cycles was achieved compared to Mix Ref.

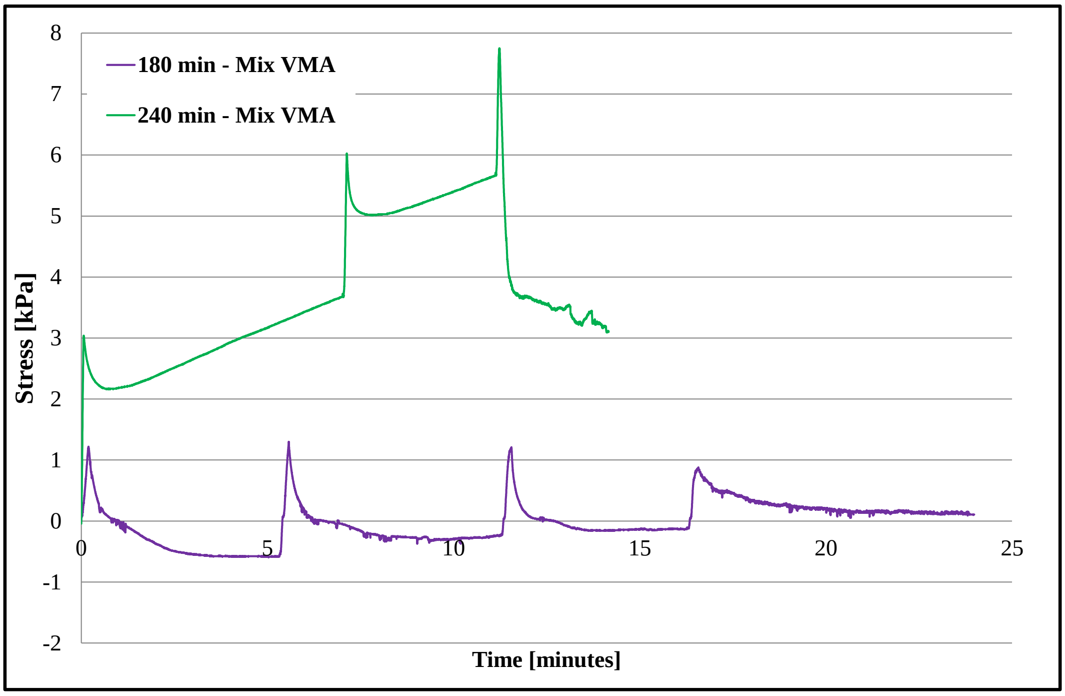

Figure 4-25: Multiple loading results for test samples at 180 and 240 minute (Mix VMA)

The 240 minute test sample successfully completed two cycles before failing on the third cycle at a tensile stress of 7.7 KPa. This is slightly higher than the corresponding average strength at 240 minutes. The ongoing hydration as well as the ability to relax part of the stress build-up, similar to the 180 minute test sample for Mix Ref and Mix VMA, could be possible reasons for this occurrence. Similar to the 180 and 240 minute test samples for Mix Ref, the low relaxation potential prevents the sample from completing multiple loading cycles.

Mix VMA therefore showed similar behaviour during the 60 and 120 minute test periods compared to Mix Ref. However the 180 and 240 minute test samples completed a greater amount of successful cycles compared to Mix Ref.

Figure 4-26 displays multiple loading and peak stress results in terms of stress versus strain for both Mix Ref and Mix VMA at 180 minutes. Mix Ref is able to complete three cycles before a load of 8 kPa initiates cracking. This load is much higher compared to the average peak stress results as shown in Figure 4-8. This could be due one or both of the following reasons. The first reason is possibly due to ongoing hydration. Peak stress tests were carried out at 180 minutes, whereas multiple loading tests were carried out at 180 minutes in 5 minute intervals. This means that the concrete cracked 20 minutes later compared to the peak stress results. During these 20 minutes, ongoing hydration provides the concrete with additional tensile capacity to complete the third cycle. The second possible reason could be due to the relaxation behaviour of Mix Ref. After the first loading cycle, the concrete is able to relax at an average relaxation potential of 55 %. Although the relaxation potential decreases as cycles progressed, it is believed that the concrete is able to reach higher amounts of stress before failure as a result of this relaxation.

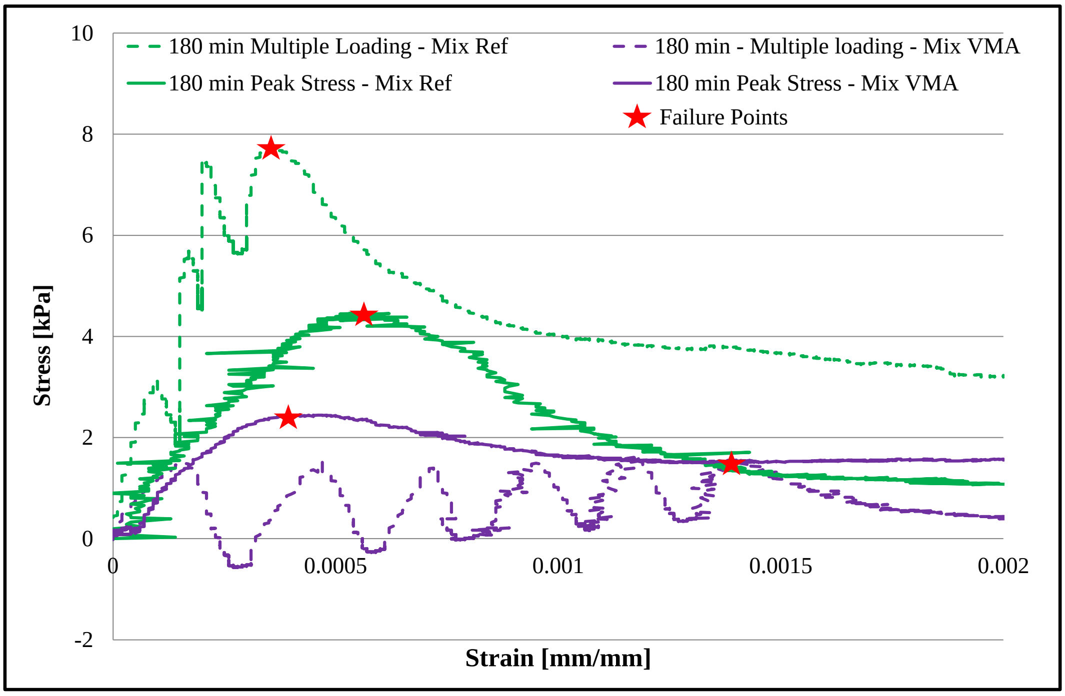

Figure 4-26: Multiple loading vs peak loads for Mix Ref and Mix VMA at 180 minutes

Mix VMA managed to complete between three and five cycles of loading before failure. Figure 4-26 displays the 5 cycle result plotted against a typical 180 minute stress versus strain graph. Results show that the concrete is able to complete a number of loading cycles before failing on the sixth cycle. The cumulative strain induced during multiple loading cycles, is much larger than the average strain capacity of the concrete. This therefore indicates that if the concrete is able to relax most of the stress induced during points of loading, the amount of strain that the concrete is able to withstand is significantly greater than the average maximum strain capacity. This is why the 60 and 120 minute test samples for both mixes are able to complete multiple loading cycles before reaching the strain threshold which induces failure.

Mix VMA therefore successfully manages to increase the amount of relaxation during the setting period of the concrete. This in turn provides the concrete with slightly more strain capacity during points of loading and unloading as well as the ability to relax stress build-up during loading and unloading cycles.

4.5 Influence of capillary pressure on the relaxation behaviour of concrete

In previous sections, the relaxation behaviour of concrete is successfully identified and its development with time is discussed in detail. Given this knowledge, the mechanism behind relaxation is still uncertain. However, the behaviour of free water within capillary pores under tensile loading and its relation to relaxation provides valuable information on the relaxation phenomenon.

Capillary pressure build-up was monitored using pressure sensors for both single and multiple loading tests in two separate areas within the concrete specimens. One sensor was inserted into the gauge area of the mould to better understand the behaviour of pore water subjected to loading and unloading in areas experiencing extreme stress. The second sensor was inserted at a distance away from the gauge area in order to investigate the influence of tensile loading on capillary pores situated out of the gauge area. The sections to follow discuss the influence of capillary pressure at each time period, namely 60, 120, 180 and 240 minutes after environment exposure.

4.5.1 At 60 minutes

Figure 4-27 displays the typical relaxation behaviour of plastic concrete and capillary pressure measured in the gauge and out of gauge zones at a time period of 60 minutes under single loading. Results in Sections 4.3 and 4.4 displayed similar behaviour during relaxation periods at 60 minutes with no significant difference between Mix Ref and Mix VMA. Results show that as the actuator is loaded to the desired force, the capillary pressure in the gauge area increases at a similar rate to a peak value, similar to the concrete's mechanically induced stress. The out of gauge pressure increases at a slightly slower rate compared to the build-up in gauge pressure and concrete stress before reaching a peak. Once the actuator is ceased, both the capillary pressure in the gauge zone and stress in the concrete, decrease in magnitude from the tension zone into the compression zone. The out of gauge pressure relaxes very slightly during points of no loading.

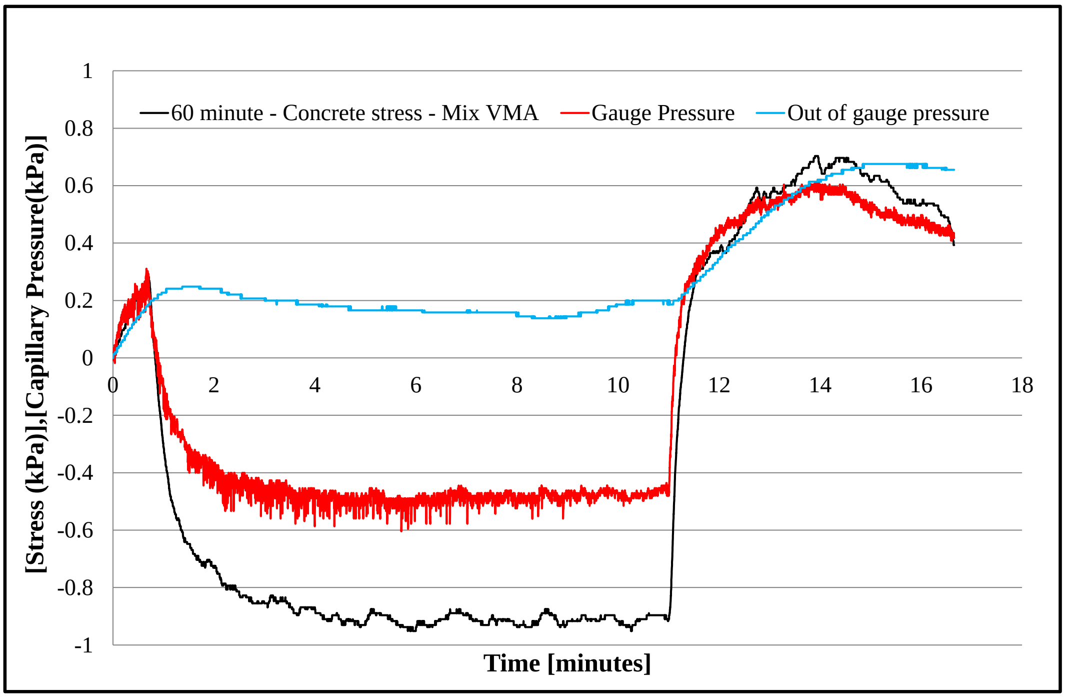

Figure 4-27: Relaxation behaviour of concrete and capillary pressure at 60 minutes

The similarity between the gauge pressure and stress in the concrete indicates that the drop in stress recorded during periods of no loading, is mainly due to the relaxation in capillary pores. Figure 4-28 shows a system of particles surrounded by water in three stages. Particles 1 and 2 are situated in the stationary mould halve, while Particles 3 and 4 are situated in the moving mould halve. The first stage marks the point of no loading, followed by the point in which the actuator is loaded and finally the unloading part which marks the start of relaxation.

As discussed in Section 4.2.5, much of the tensile strength observed in concrete at 60 minutes, is believed to be due to capillary pressure holding the particles in place. Therefore, before the actuator is loaded, the particles within the concrete are at rest with mainly gravitational forces acting on the particles. Once the actuator is loaded and Particles 2 and 3 move apart, the water meniscus between Particles 2 and 3 decreases in radius, creating a negative capillary pressure within surrounding capillary pores. This is represented by the steep increase in stress in both the concrete and gauge pressure readings. In order to resist the movement of Particles 2 and 3, tensile forces are experienced between Particles 1 and 2 as well as Particles 3 and 4. Since the main function of these tensile forces are to resist and balance the large amount of stress experienced between Particles 2 and 3, these forces only build-up once Particles 2 and 3 move away from each other. This force is represented by the increase in pore pressure in the out of gauge pressure zone and explains why the rate of increase of this pressure is much slower compared to the gauge pressure reading.

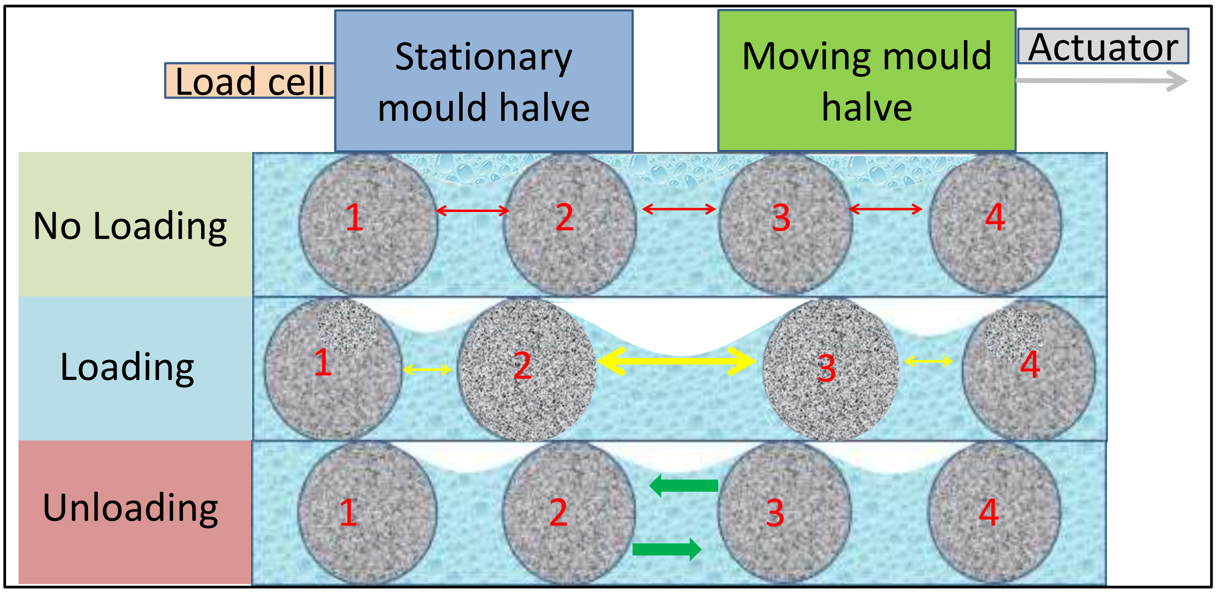

Figure 4-28: Relaxation behaviour during points of loading and unloading

Once the displacement of the actuator is ceased (unloading), the high tensile force experienced during points of loading, starts to reduce as the particles rearrange in a way that decreases the tensile force measured in the gauge area. This is seen in Figure 4-28 by the sudden drop in stress and capillary pressure as the two centre particles move towards each other. This is followed by an increase in the radius of the water meniscus between Particles 2 and 3. Therefore the drop in stress experienced in both the gauge pressure and concrete stress, marks the rearrangement of internal particles in order to relieve the load induced during loading. The relaxation behaviour of concrete before the setting phase is therefore due to the rearrangement of particles surrounded by capillary pores in order to relieve the stress build-up induced during loading.

4.5.2 At 120 minutes

As discussed in Section 4.3, Mix VMA showed a slightly higher relaxation potential compared to Mix Ref. This trend continued throughout the 180 and 240 minute test times. Figure 4-29 displays the relaxation behaviour of concrete as well as the capillary pore pressure within the gauge and out of gauge areas for Mix Ref at 120 minutes. Results show that as the actuator is loaded for the first cycle, the gauge pressure increases at a similar rate compared to the stress in the concrete. The out of gauge pressure increases at a much lower rate and to a much smaller value compared to the gauge pressure. A reason for this is explained in Section 4.5.1. Once displacement is ceased, the stress of the concrete and gauge pressure relaxes into the compression zone, while the out of gauge pressure decreases at a much slower rate.

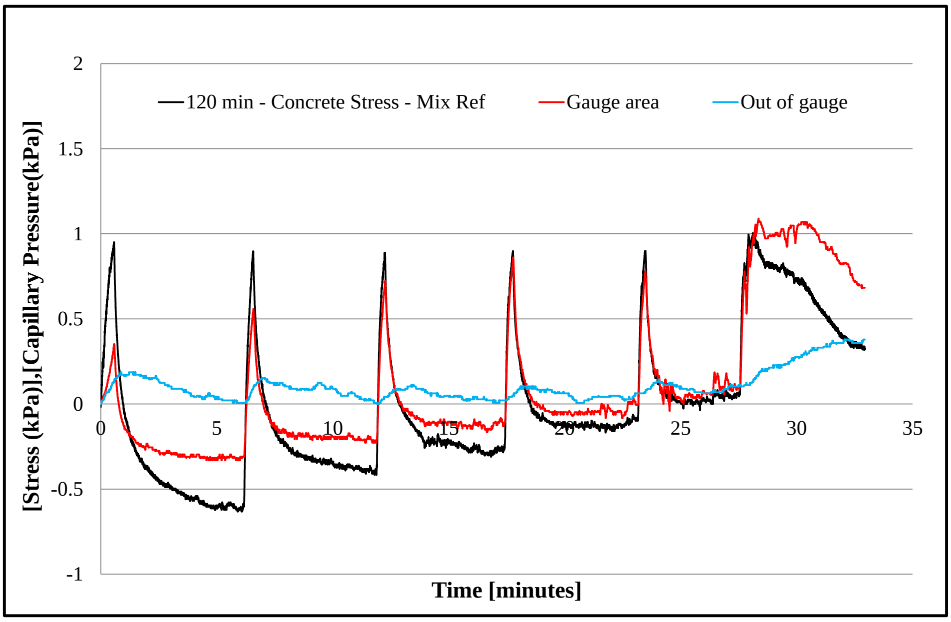

Figure 4-29: The relaxation behaviour of concrete and capillary pressure at 120 minutes for Mix Ref

The change in relaxation potential of the stress in the concrete decreases after each cycle to such an extent, that the range of relaxation during the last successful cycle, falls within the tensile regime. This change in relaxation potential is also apparent in the gauge pressure readings and is believed to be the cause of the decrease in relaxation potential observed by the stress in the concrete. Therefore results indicate that the potential for relaxation in concrete corresponds to the potential for relaxation of the capillary pressure experienced within pores.

Figure 4-30 displays the relaxation results for Mix VMA. During the first cycle, the gauge pressure increases steadily with the concrete before dropping rapidly into the compression zone. Relaxation for the out of gauge pressure relaxes in a similar manner but slightly more well-defined compared to Mix Ref.

Similar to Mix Ref, the concrete and gauge pressure readings both displays a smaller relaxation potential during each successful cycle, although, this behaviour in terms of capillary pressure is much more severe in Mix Ref compared to Mix VMA. This therefore confirms that the range of relaxation is dependent on the ability of the capillary pores to rearrange themselves during points of no loading. The bottom peak of the gauge pressure in Mix VMA displays a more consistent value compared to the bottom peak of the gauge pressure in Mix Ref after each loading cycle.

Referring to Figure 4-28 during the loading stage, a force develops between the gauge area particles during loading. Once the loading is ceased, these particles rearrange themselves to reduce this stress build-up. By applying this same principal to the current results, shows that Mix VMA is able to rearrange the particles to a greater extent or with greater ease, to reduce the stress build-up between capillary pores. The bottom peak of each successful cycle compared to Mix Ref, displays this behaviour.

The first possible reason for this occurrence could be due to the higher water-to-cement ratio in Mix VMA compared to Mix Ref. The addition of VMA, as stated previously is believed to increase the water-to-cement ratio of the concrete. Furthermore, previous literature indicates that the addition of VMA reduces the amount of bleeding due to the added cohesion of the concrete mix. In light of this, together with the slightly retarded setting time, Mix VMA is believed to contain a greater amount of free water compared to Mix REF. This therefore indicates that Mix VMA contains a clearer path of inter-particle movement, allowing the particles to rearrange with greater ease compared to Mix Ref. This possibly explains why Mix VMA showed near constant relaxation potential in terms of capillary pressure as loading cycles progressed.

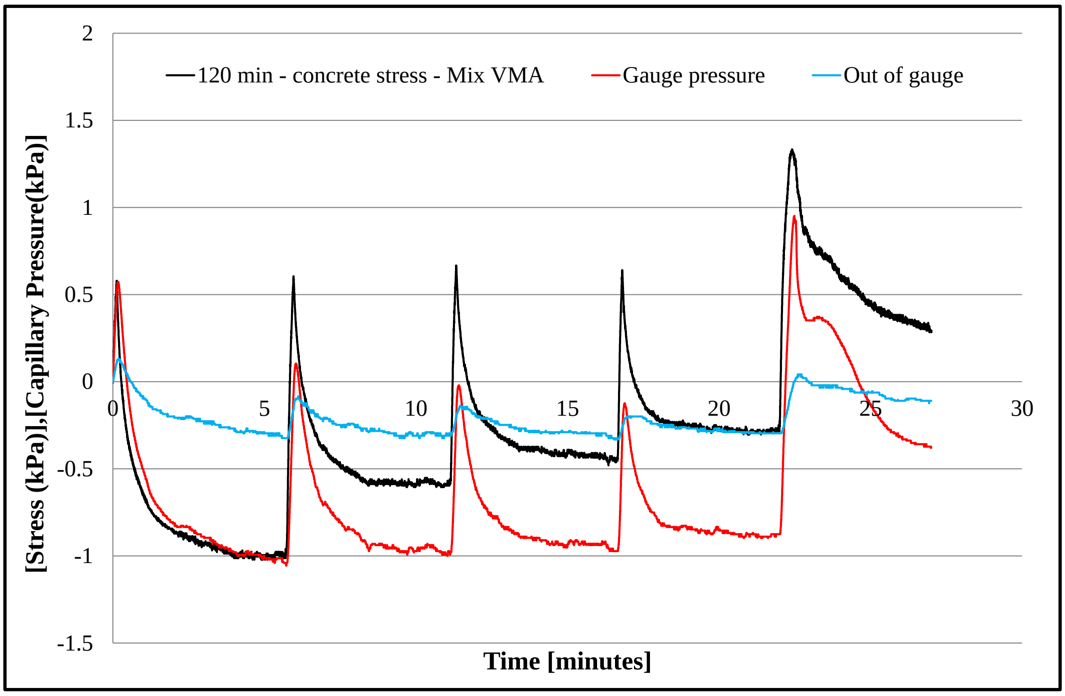

Figure 4-30: The relaxation behaviour of concrete and capillary pressure at 120 minutes for Mix VMA

The second possible reason could be due to the lower surface tension of the pore fluid in Mix VMA. The lower surface tension of pore fluid in Mix VMA compared to Mix Ref, results in a smaller capillary pressure between particles. After each cycle, the particles relax to a position slightly further apart than their original position before loading. Therefore each successful cycle, leaves Particles 2 and 3 further apart, compared to their original starting position before loading. The high surface tension in Mix Ref, allows the particles to relax to a closer position to each other compared to Mix VMA. This therefore means that the particles in Mix VMA have a greater tendency of rearrangement, due to the lower capillary forces holding the particles in place, compared to Mix Ref. This also explains why particles relax to a smaller magnitude after each loading cycle, since the capillary pressure increases after each cycle, indicating that a larger capillary pressure exists after each successful loading. However, this theory requires further investigation.

4.5.3 At 180 minutes

Figure 4-31 displays the relaxation behaviour of Mix Ref under single loading at 180 minutes. As the concrete is loaded to 50 % of its average tensile strength, the gauge pressure increases at a similar rate but to a much lower magnitude, while the out of gauge pressure displays no corresponding effect. Concrete at this age, displays a reduced amount of relaxation compared to concrete at ages of 60 and 120 minutes as discussed in Section 4.3.1. This is also seen in Figure 4-31 by the reduced amount in relaxation of capillary pressure in the gauge area compared to concrete at 60 and 120 minutes. This is believed to be the reason behind the reduced relaxation in concrete at these ages.

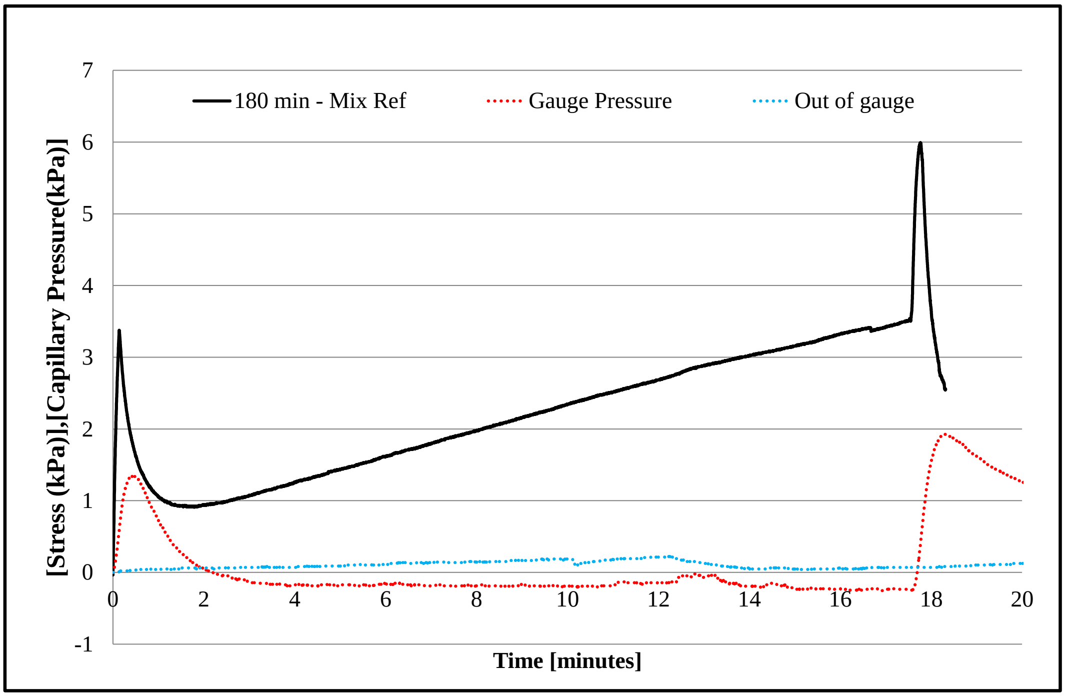

Figure 4-31: The relaxation behaviour of concrete and capillary pressure at 180 minutes for Mix Ref

At this age, ongoing hydration, bridges the gaps between concrete particles, which in turn reduces the amount of free water between concrete particles. The presence of hydration products and reduced amount of free water hinders the rearrangement of particles and therefore results in a lower amount of relaxation during points of no loading.

As the actuator is loaded for the second time to initiate cracking, the gauge capillary pressure increases at a similar rate compared to the concrete's stress. This, together with the initial capillary pressure peak, gives a better indication of the build-up in capillary pressure as a tensile load is induced in the concrete, compared to Figure 4-15 in Section 4.2.5.1. This confirms that part of the strength experienced under tensile failure is due to the capillary pressure within pores.

Figure 4-32 displays the relaxation behaviour of concrete stress and capillary pressure for Mix VMA under single loading. Compared to Mix Ref, the capillary pressure drops well into the compression zone once loading is ceased. This further confirms that Mix VMA contains a greater rearrangement ability compared to Mix Ref. The out of gauge pressure measures a corresponding increase in pressure as the concrete is loaded and relaxes slightly during periods of no loading. This therefore means that Mix VMA has a clearer path of interconnectivity compared to Mix Ref.

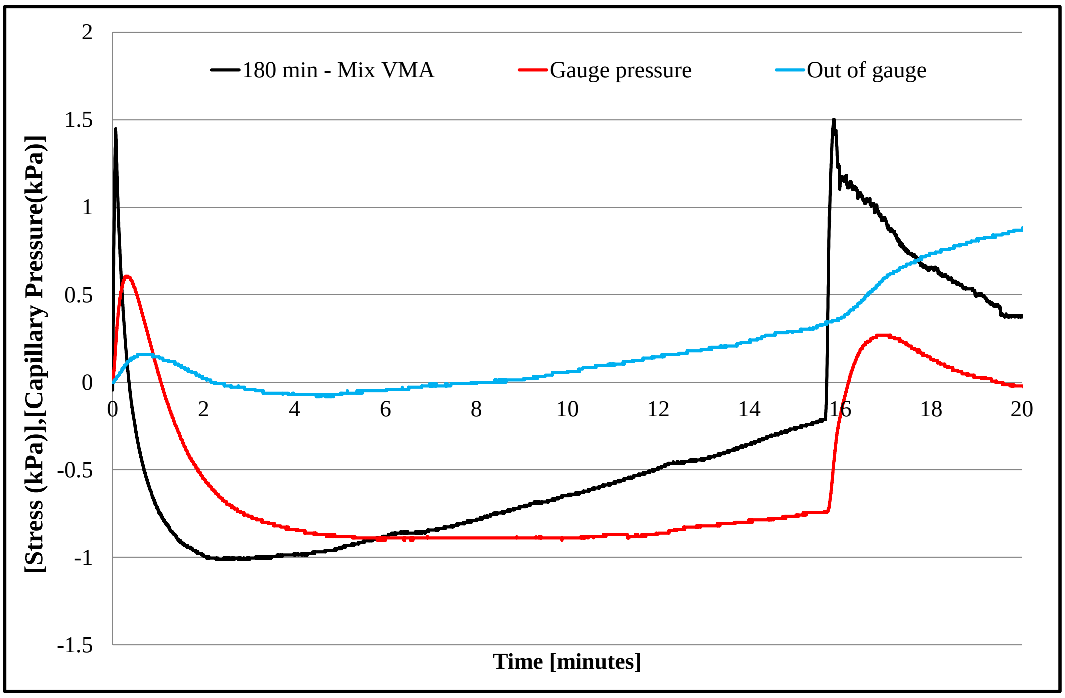

Figure 4-32: Relaxation behaviour of concrete and capillary pressure at 180 minutes for Mix VMA

This leads to the assumption that the rate of hydration between the two mixes differs slightly compared to Mix Ref. This is further confirmed by the slight difference in setting times between both mixes, discussed in Section 4.1.3. However, both mixes showed similar initial setting times with only a 10 minute difference in final setting time between the two mixes. It should however be noted that the Vicat setting time method measures the solidification of the concrete paste and therefore gives no indication of the internal structure of the concrete during hydration. The amount of free water between concrete particles can influence the interconnectivity path and with the lower surface tension in pore fluid of Mix VMA affecting the way the tensile force is transferred between particles provides a better explanation for this occurrence. Therefore at this age, the internal formation of hydration products, the amount of free water and surface tension of pore fluid can all be possible reasons as to why the out of gauge pressure sensor measures a corresponding pressure under loading.

4.5.4 At 240 minutes

Obtaining capillary pressure readings at 240 minutes proved extremely difficult due to the low amount of free water available within capillary pores. At 240 minutes, Mix Ref displayed a low relaxation potential compared to Mix VMA and it is reasonable to assume, that at this age, hydration products have and continues to bridge any gaps between particles leaving little room for particle rearrangement. As the actuator is loaded, an instant break in pore pressure is observed, similar to the 240 minute result in Figure 4-15, which gives a further indication of how dense the internal particles are arranged at 240 minutes. Mix VMA however proved a little easier in obtaining capillary measurement readings. This describes the internal arrangement of particles and free water in Mix VMA compared to Mix Ref.

Figure 4-33 displays the relaxation behaviour of concrete stress and capillary pressure for Mix VMA at 240 minutes. As the actuator is loaded, the capillary pressure builds up slightly and relaxes soon after the actuator is ceased. This trend is consistent for the second loading cycle and during the third loading where cracking occurs, a slight peak in pressure is observed, after which the pressure continues to increase at a constant rate.

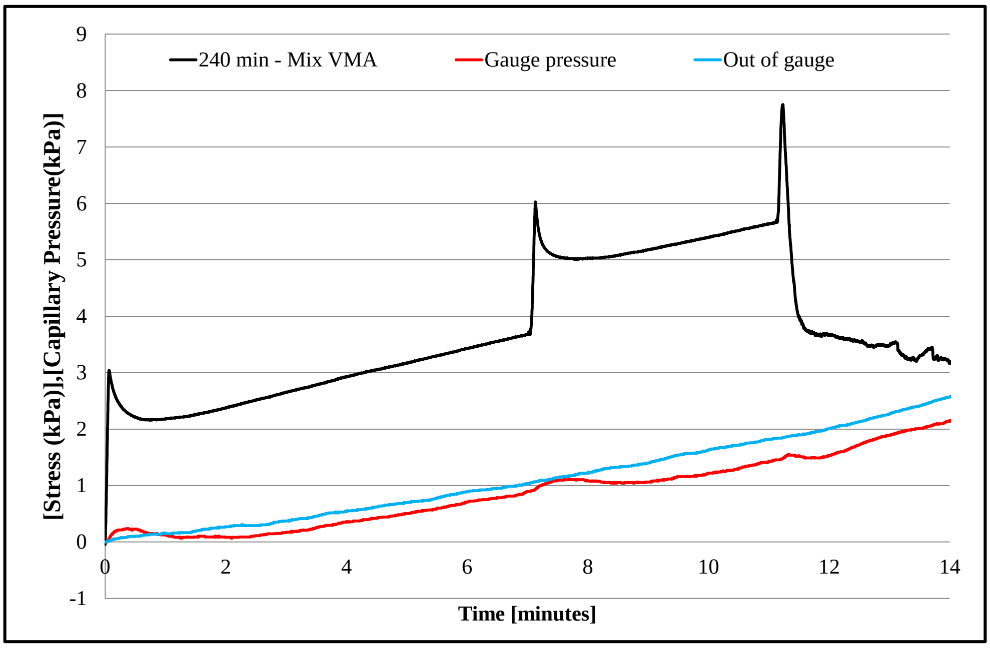

Figure 4-33: The relaxation behaviour of concrete and capillary pressure at 240 minutes for Mix VMA

The out of gauge reading showed no corresponding effect during loading and unloading cycles, however, the rate of increase of concrete stress, gauge and out of gauge pressures seem to increase at similar rates during points of no loading, indicating that the shrinkage captured by the load cell shares a close relation to the measured capillary pressures. This therefore confirms that the increase in stress observed for 120, 180 and 240 minutes during periods of no loading is due to the removal of pore water from the concrete due to evaporation. Furthermore, the ability to record and capture capillary pressure readings in Mix VMA, suggests that Mix VMA contains slightly more pore water and a clearer path of interconnectivity compared to Mix Ref. This behaviour is observed in 120, 180 and 240 minute test samples. The presence of pore water between pores further confirms why Mix VMA contains a lower force compared to Mix Ref under tensile induced loads.

To conclude, the mechanism behind the relaxation phenomenon of fresh concrete is believed to be due to the negative capillary pressure build-up induced by the mechanical applied tensile strain. Furthermore, Mix VMA displayed a slightly higher relaxation potential compared to Mix Ref. The increased amount of pore water and slower rate of setting, as well as the lower surface tension is believed to be the resulting cause of this observation.

4.6 Concluding summary

This chapter outlined and discussed the tensile material properties of plastic concrete during the three phases of hydration. Furthermore, relaxation under single and multiple loading cycles were addressed and interpreted in terms of the capillary pressure results obtained from relaxation tests. The results of actual plastic cracks and their influencing factors are discussed in the next chapter.

Chapter 5: Cracking behaviour – Test results and discussion

This chapter contains the results and discussions of the plastic cracking tests outlined in Section 3.3. These tests were conducted in a climate chamber, set to a temperature of 40ºC, wind speed of 5 km/h and relative humidity of 10 %, in order to simulate extreme environment conditions, ideal for plastic shrinkage cracking. These tests were carried out to investigate the influence of viscosity, on the phenomenological and fundamental cracking behaviour of plastic concrete. Furthermore, the influence of initial curing conditions on the cracking behaviour of plastic concrete, are also addressed. Finally, possible links between the results obtained on the cracking behaviour of concrete in this chapter, with the results of the tensile tests in the previous chapter are discussed.

5.1 Plastic shrinkage cracking behaviour

This section aims to investigate the influence of viscosity on the cracking behaviour of fresh concrete using two concrete mixes, namely Mix Ref and Mix VMA. Plastic cracking tests, as discussed in Chapter 3, were used to obtain results relating to bleeding, evaporation, shrinkage, settlement, capillary pressure and crack area, to investigate the cracking behaviour of concrete from time of placing, up to 6 hours after environment exposure. The cracking behaviour of Mix Ref is first analysed and discussed in Section 5.1.1. Thereafter results for Mix VMA are analysed and compared to Mix Ref in Section 5.1.2.

5.1.1 Plastic cracking behaviour of Mix Ref

Figure 5-1 displays the plastic cracking behaviour of Mix Ref, exposed to evaporation rich conditions, with the aim of promoting plastic shrinkage cracking. The stiffening phase starts directly after casting and continues until the initial setting time. During this period, solid particles in a freshly mixed concrete body begin to settle, displacing water to the surface of the concrete body. This is called bleeding and commences directly after placement of concrete, as shown in Figure 5-1.

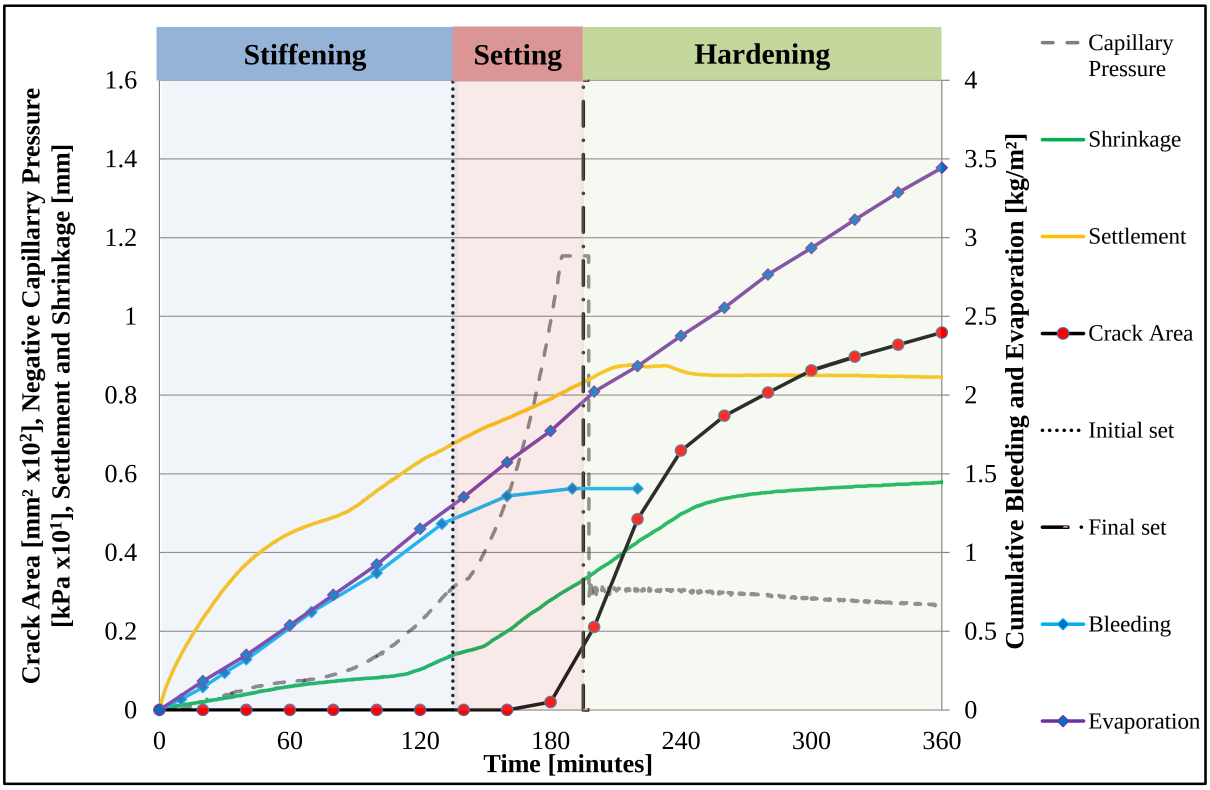

Figure 5-1: Plastic cracking behaviour for Mix Ref

Initially, both bleeding and evaporation graphs display similar rates for the initial portion of the stiffening phase, however, the rate of bleeding slowly decreases towards the end of the stiffening phase into the initial portion of the setting phase, before ceasing at approximately 190 minutes with a total cumulative bleeding of 1.41 kg/m³. The cumulative bleeding of the concrete gives an indication of the amount of water displaced to the surface of the concrete, due to the settlement of solid particles. The deviation of the bleed and evaporation rates, indicate that the amount of water surfacing the concrete's surface, does not meet the demand of water required for evaporation. Therefore the point of deviation is believed to be the drying time of the concrete which results in a corresponding build-up in capillary pressure. The drying time occurs at around 85 minutes, which falls during the later stage of the stiffening phase as seen in Figure 5-1.

The initial portion of the settlement graph captures the vertical dimensional change of the concrete's body as solid particles settle in the freshly placed concrete body. The initial settlement rate increases sharply, before decreasing to a final value of around 0.5 mm at 85 minutes. This indicates that the end of settlement is nearing and corresponds well with the decreased rate of bleeding during the stiffening phase.

It should however be noted that comparing the bleed rate directly with the rate of settlement, is ill advised and should only be used to display the initial behaviour of the concrete. Combrinck (2016) showed that the measurement of bleed water at 20 minute intervals differs from the settlement of the concrete's surface. Combrinck's findings show that the variability between bleed and settlement is dependent on the reabsorption of bleed water back into the concrete, different extraction methods and intervals used as well different mould types used to conduct bleeding and settlement tests.

Once the drying time of the concrete is reached, ongoing evaporation starts to draw water out from capillary pores in order to meet the evaporation demand. This results in concrete particles being drawn towards each other, as the free water located between particles, is continuously drawn out through evaporation. This then results in a capillary pressure build-up within capillary pores and marks the start of plastic shrinkage, as seen by the sharp increase in gradient of the shrinkage, settlement and capillary pressure graphs in Figure 5-1. Shrinkage, settlement and capillary pressure measurements, were carried out simultaneously and therefore all three graphs correlate well with each other. As the rate of settlement decreases at approximately 85 minutes, this indicates that the end of settlement is nearing, however the sharp increase after 85 minutes, indicates that the rate of bleeding is slower compared to the evaporation rate and therefore gives an indication of the drying time in the concrete. The increase in settlement thereafter is believed to be driven by ongoing evaporation. Plastic shrinkage is a volumetric dimensional change and therefore occurs in both the horizontal and vertical dimensions. The rapid increase in capillary pressure creates a corresponding increase in both settlement and shrinkage graphs and gives a good indication of the end of settlement and start of plastic shrinkage which occurs towards the end of the stiffening phase and continues into the setting phase.

The initial setting time marks the start of the setting phase, where the transition from a plastic to a solid concrete body is believed to occur. The capillary pressure continues to build-up to a maximum point before dropping rapidly, symbolising a break in pore pressure. This break, also known as the time of air entry, occurs at localised points in the concrete body, forming weak spots for future crack growth (Slowik et al., 2008; Boshoff & Combrinck, 2013). The continued increase in shrinkage, both horizontally and vertically, after the time of air entry during the setting phase, eventually results in the formation of a crack, if sufficient restraint is present. Crack formation in Figure 5-1, starts at around 180 minutes, well before the final setting time of concrete at 195 minutes is reached. Towards the end of the setting phase, the constant increase in shrinkage and settlement driven by ongoing evaporation, contributes to further crack growth.

The hardening phase starts soon after final set is reached and is where the concrete starts to gain significant strength as discussed in Section 4.2.2. During this phase, the concrete is believed to be a solid material and therefore plastic shrinkage is expected to cease somewhere during the initial stages of the hardening phase. The end of vertical settlement and horizontal displacement due to plastic shrinkage occurs at approximately 210 and 245 minutes respectively. This amounts to a 50 minute difference between the final setting time and end of plastic shrinkage. The final setting time in theory, marks the end of plastic shrinkage, since the concrete is no longer a plastic material. The 50 minute time difference, amounts to 14 % difference in time over a period of 360 minutes. This percentage difference is minimal and provides adequate correlation between setting times obtained using the Vicat penetration method and setting time observed through plastic shrinkage graphs.

Final settlement and shrinkage values of 0.85 and 0.58 mm respectively, were measured at 360 minutes, marking the end of the test duration. This results in a final crack area of 96 mm^2, recorded at 360 minutes for Mix Ref as shown in Figure 5-1. Cracking tests were carried out in a different mould type compared to the mould type used to measure the shrinkage, settlement and capillary pressure behaviour of concrete. Cracking results, however, correspond well with the plastic shrinkage graphs as the crack area rate decreases once plastic shrinkage is ceased.

5.1.2 Plastic cracking behaviour of Mix VMA

The cracking behaviour of Mix VMA as shown in Figure 5-2, follow similar trends compared to Mix Ref. The initial rate of settlement increases rapidly before reaching its lowest rate during the first 75 minutes of the stiffening phase. Thereafter, an increase in capillary pressure is observed, which creates a corresponding increase in both settlement and shrinkage rates. Crack formation occurs at approximately 180 minutes during the setting stage and continues to increase in area as evaporation drives vertical and horizontal shrinkage into the hardening phase. This increase occurs during the early ages of the hardening phase, at which point a break in capillary pore pressure occurs, followed by a decrease in both shrinkage and settlement rates. This creates a corresponding decrease in crack area rate as the rate of shrinkage slowly decreases to zero as the concrete starts to gain rapid strength during the hardening phase.

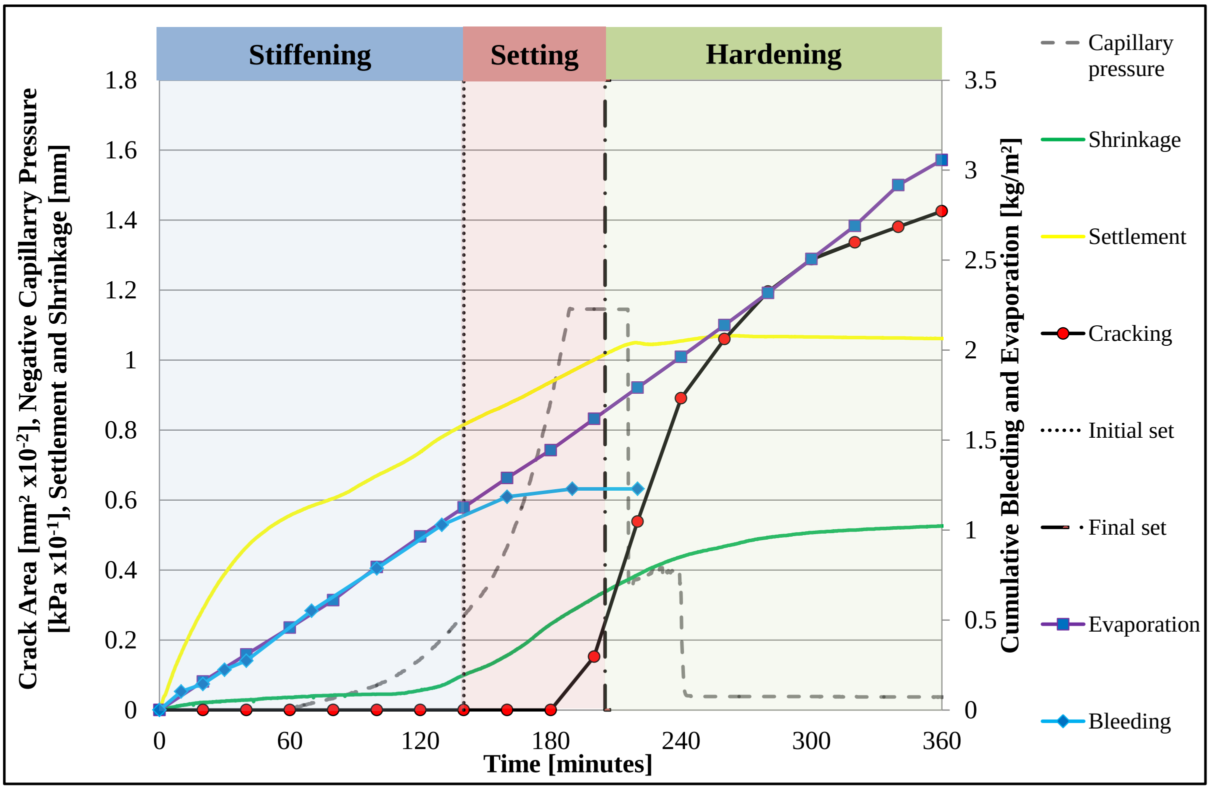

Figure 5-2: Phenomenological plastic shrinkage cracking behaviour for Mix VMA

Comparing Figures 4-1 and 4-2 highlights a number of differences in the cracking behaviour between Mix Ref and Mix VMA. These differences are discussed further in subsequent paragraphs:

1) Bleeding and evaporation

Figure 5-3 displays the cumulative bleeding and evaporation for both Mix Ref and VMA plotted against time. Initially, both Mix Ref and Mix VMA, bleed at similar rates during the first 40 minutes. Thereafter Mix Ref bleeds at a higher rate compared to Mix VMA, before both mixes cease bleeding at 190 minutes. Mix Ref, results in a total cumulative bleed of 1.41 kg/m^2 of concrete while Mix VMA displayed a slightly lower cumulative bleed of 1.23 kg/m^2. This amounts to a 14 % reduction in bleed between the two mixes.

Consistent with literature discussed in Section 2.3.6, the addition of a VMA in concrete decreases the amount of bleeding. The main property behind the incorporation of a VMA in concrete is to improve the flow properties of the freshly mixed concrete. This is achieved through added cohesion in the cement paste, reducing the amount of segregation, which in turn decreases the amount of settlement of solid particles. The reduction in bleeding therefore displays the increased cohesion properties of Mix VMA compared to Mix Ref.

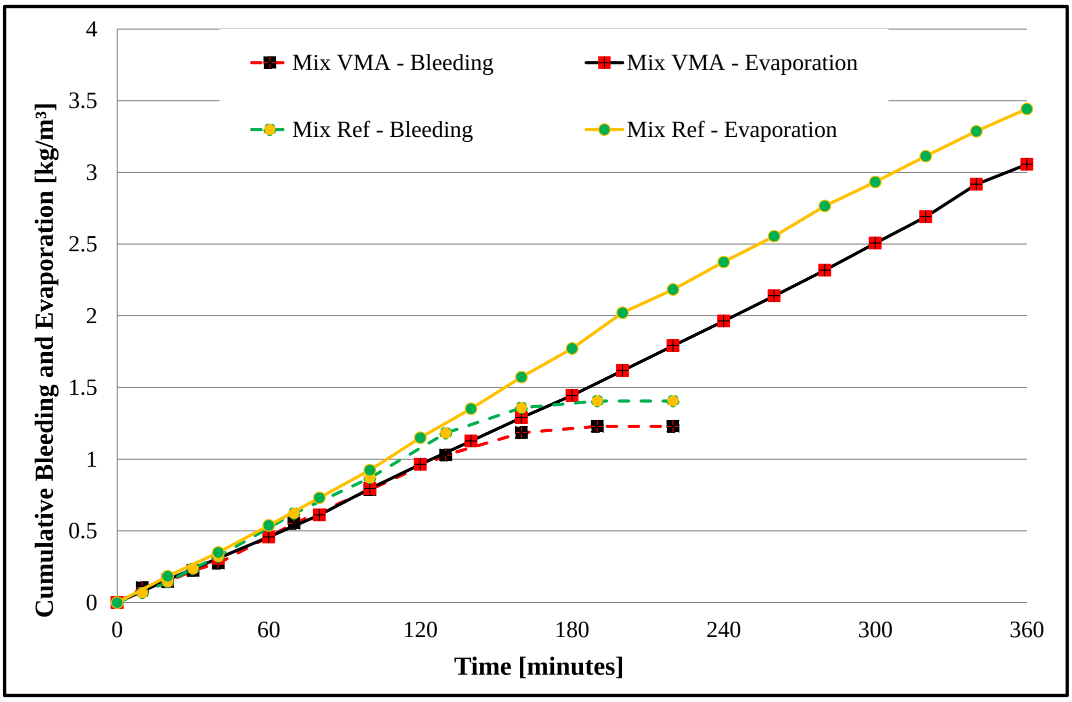

Figure 5-3: Comparison between Mix Ref and Mix VMA in terms of cumulative bleeding and evaporation

The cumulative evaporation graphs, as shown in Figure 5-3, gives an indication of the ability of a concrete body to retain water under constant evaporation. Mix Ref displayed a final cumulative evaporation of 3.44 kg/m^3. This is slightly higher compared to Mix VMA with a total cumulative evaporation of 3.06 kg/m^3. This amounts to a decrease of 11 % in loss of water under constant evaporation, through the addition of a VMA.

The improved cohesion through the addition of VMA reduced the amount of bleeding and therefore the lower evaporation rate of Mix VMA is possibly due to the lower amount of bleeding water available. Furthermore, VMA's are commonly used in under water concrete due to their increased capability in minimising the movement of water and fines away from the concrete, while maintaining a homogenous composition (Jeknavorian, 2016). This is achieved through increased cohesion in the cement paste. This also explains why Mix VMA, displayed lower rates of bleeding and evaporation compared to Mix Ref.

2) Settlement, shrinkage and capillary pressure build-up

Figure 5-4 displays the horizontal shrinkage, vertical settlement and capillary pressure build-up of both Mix Ref and Mix VMA plotted against time. The initial slope of the settlement graph, as discussed in Section 5.1.1, is believed to be driven by the settlement of solid particles, which in turn displaces water to the surface of the concrete. The decrease in settlement rate during the settlement portion of Figure 5-4 indicates that the end of settlement is nearing and therefore a reduction in bleeding can be expected. This therefore means that the corresponding decrease in bleed rate, results in a lower amount of water available at the surface of the concrete for evaporation. In order to meet the water demand required by evaporation, water is drawn out of the capillary pores and therefore results in a capillary pressure build-up within the concrete. After the initial settlement slope, the build-up in capillary pressure, results in an increase in vertical settlement. This settlement is driven by the increase in capillary pressure as well as a slight settlement of solid particles due to bleeding. However, judging by the decrease in rate of settlement before capillary pressure build-up, the amount of settlement occurring due to the settlement of solid particles, is believed to be minimal during the second portion of the settlement graph. For this reason, any further increase in settlement, is believed to be due to ongoing evaporation and can therefore be referred to as plastic shrinkage.

Mix Ref and Mix VMA, both displays similar initial settlement durations of 85 and 87 minutes respectively. During this period, Mix Ref displays a total settlement of 0.5 mm compared to a slightly higher settlement of 0.6 mm in Mix VMA. The VMA used in the current study, decreased the yield stress as discussed in Section 4.1.2 and therefore resulted in an 85 mm slump compared to a 70 mm slump obtained for Mix Ref. This increase in slump, although minimal, is believed to be the cause of the increase in amount of settlement occurring during the initial stages of the stiffening phase.

Al-Qassag et al. (2016) recently investigated the influence of slump and viscosity on plastic settlement cracking. Results show that the crack intensity increases with an increase in concrete slump. The addition of VMA to the control mixture in Al-Qassag et al. (2016) study, increased the yield stress, and therefore resulted in a lower slump with an overall reduction in settlement crack intensity.

As discussed in Section 2.3.6, the reduction in bleeding through the addition of a VMA, decreases the amount of settlement in the concrete. The increased cohesion of the cement paste prevents the tendency of solid particles from displacing to the bottom of the concrete body. However, this decrease in settlement is possibly based on the ability of the VMA to increase the yield stress of the concrete. An increase in yield stress, results in a lower slump value due to a stiffer concrete mix.

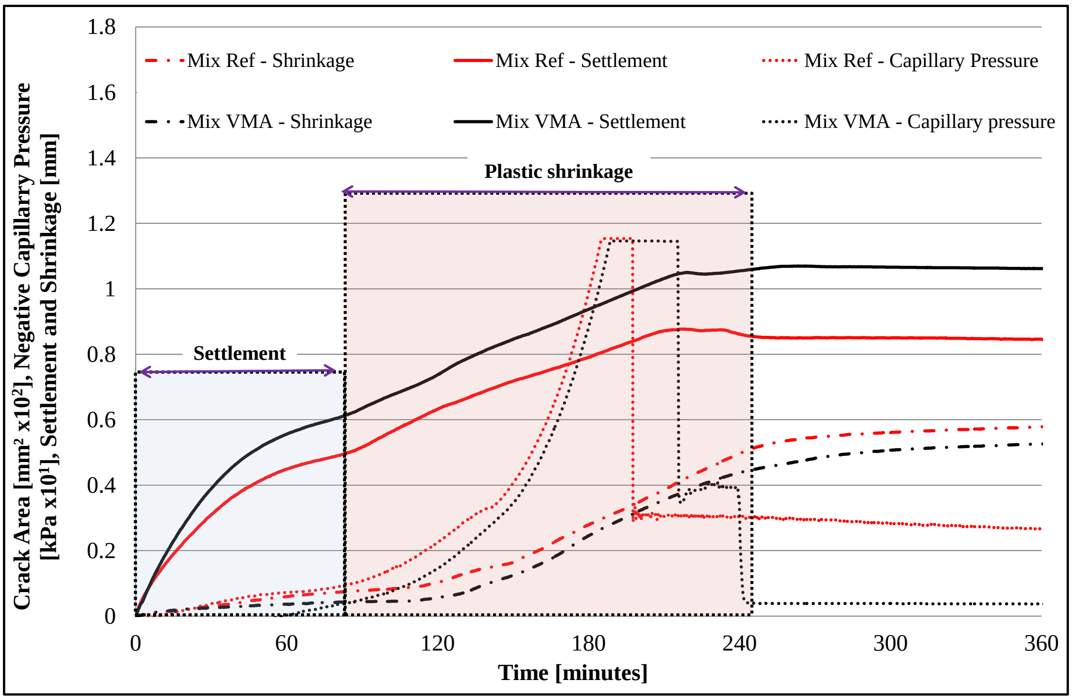

Figure 5-4: Settlement, shrinkage and capillary pressure build-up for Mix Ref and Mix VMA

As discussed earlier, the change in gradient of the settlement graph indicates that water is now being drawn out of the concrete's body by ongoing evaporation. This is further confirmed by the build-up in capillary pressure as the settlement graph changes gradient. The increase in capillary pressure marks the start of the plastic shrinkage period and therefore any corresponding increase in settlement after the initial settlement slope, is believed to be due to plastic shrinkage. Therefore the change in gradient and build-up in capillary pressure represents the start of plastic shrinkage.

Figure 5-4, however, does not provide a comparable representation of the vertical displacement of the concrete body due to ongoing evaporation. In order to investigate the vertical displacement after the initial settlement period, the total amount of settlement occurring during the settlement period can be subtracted from the amount of settlement occurring during the test period. This gives a better indication of the plastic shrinkage occurring during the plastic shrinkage period in the vertical direction. Figure 5-5, displays the plastic shrinkage and capillary pressure build-up for both Mix Ref and Mix VMA during the plastic shrinkage period. Horizontal and vertical shrinkage in Figure 5-5, display similar rates of build-up, indicating that the method used to determine the vertical shrinkage is adequate.

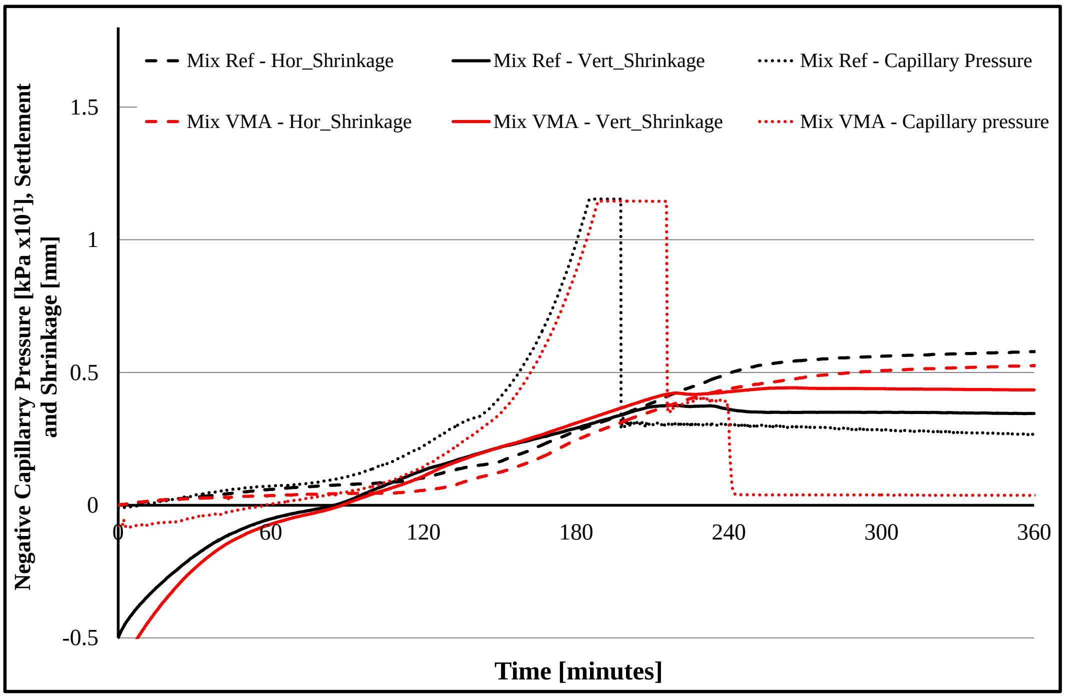

Figure 5-5: Plastic shrinkage and capillary pressure build-up in both Mix Ref and Mix VMA

Both concrete mixes display similar rates of capillary pressure build-up after the drying time of concrete is reached. Point of air entry for Mix Ref occurs between 197 and 206 minutes, while point of air entry for Mix VMA occurs between 215 and 225 minutes. This amounts to a 5 % difference in air entry times over a period of 360 minutes. The build-up in capillary pressure results in a corresponding increase in both horizontal and vertical shrinkage for both mixes. Both mixes build-up in vertical shrinkage at similar times with final vertical measurement readings of 0.346 mm and 0.435 mm for Mix Ref and Mix VMA respectively. This amounts to a 20 % difference in vertical shrinkage measurements between Mix VMA and Mix Ref. The higher slump and settlement of solid particles, occurring in Mix VMA, could be a possible reason for the slightly higher vertical shrinkage compared to Mix Ref. Horizontal shrinkage measurements of 0.58 and 0.53 mm were recorded at 360 minutes for Mix Ref and Mix VMA respectively. This amounts to a 9 % difference in horizontal shrinkage values. Both Mix Ref and Mix VMA, display similar horizontal shrinkage values and therefore the addition of the VMA seems to have a minimal effect on the horizontal shrinkage of concrete.

The surface tension results discussed in Section 4.1.1 shows that Mix Ref has a higher surface tension in pore fluid compared to Mix VMA. A higher surface tension in pore fluid should result in a slightly higher capillary pressure build-up when compared to a lower surface tension pore fluid. By comparing the capillary pressure graphs in Figure 5-5, the difference in surface tension between the two mixes is not instantly apparent. However, differences in point of air entry and horizontal shrinkages, although minimal between the two mixes, could be a result of the difference in surface tension between the two mixes.

3) Crack Area

Figure 5-6 displays the measured crack areas for both Mix Ref and Mix VMA plotted against time. Initial crack formation for Mix Ref starts at approximately 203 minutes after environment exposure. Thereafter, the rate of crack growth develops rapidly before reducing to a final crack area of 96 mm². Mix VMA however, develops visible hairline cracks at approximately 214 minutes after environment exposure. After crack formation, the rate of crack growth develops at a faster rate compared to Mix Ref, before reaching a final crack area of 143 mm². Results show that visible hairline cracks, between the two mixes, occur within 11 minutes of each other. However, the difference in crack formation times between the two mixes are minimal and can be considered as insignificant when comparing the cracking behaviour between the two mixes.

The difference in crack areas between the two mixes amounts to 32 %. However, the differences in horizontal shrinkage values do not correlate with the large difference in crack areas. As discussed in Section 3.3.2, the cracking moulds used to investigate the cracking behaviour of Mix Ref and Mix VMA, are based on the proposed mould design by ASTM

C1579 (2006) to investigate plastic shrinkage cracking. However, Combrinck (2016) identified the formation of settlement cracks well before plastic shrinkage induces cracking in the concrete specimen. This therefore implies that settlement cracks, although not visible, may be responsible for initial crack formation, as solid particles settle over the large centre triangle in Figure 3-23. Once the crack is formed, plastic shrinkage is responsible for further crack growth.

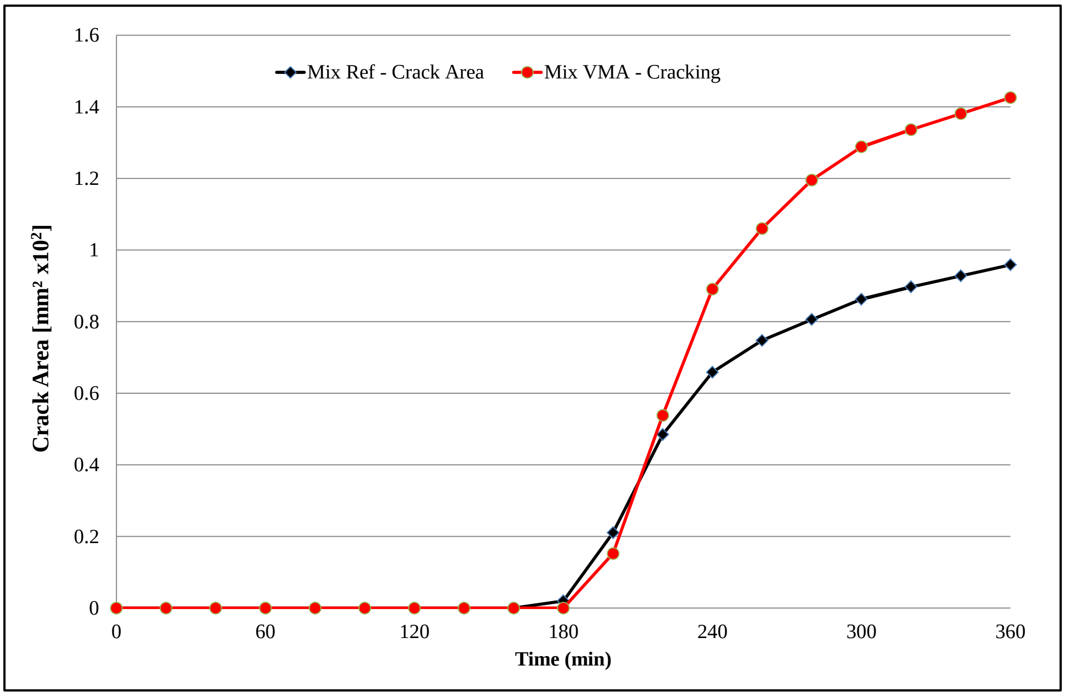

Figure 5-6: Measured crack areas for Mix Ref and Mix VMA

Mix VMA, as shown in Figure 5-4, displayed higher settlement during the stiffening phase, compared to Mix Ref. Therefore, it is possible that settlement cracks occurred during the stiffening phase and only became visible once plastic shrinkage contributed towards further crack growth. This would explain why Mix VMA, results in a larger crack area compared to Mix Ref in Figure 5-6. Furthermore, the low tensile strength of Mix VMA compared to Mix Ref, in Figure 4-9, could also contribute to the larger crack area observed in Figure 5-6. The low tensile strength of Mix VMA could increase crack growth and result in a larger crack area compared to Mix Ref at the end of the 360 minute test duration.

5.2 Initial curing procedures

This section aims to investigate the influence of initial curing on the cracking behaviour of plastic concrete. Initial curing refers to curing procedures applied before the final setting time of concrete is reached. This is necessary for concretes with low to near zero bleeding rates or in cases where excessive evaporation rates result in premature surface drying well before the initial setting time of concrete is reached. ACI 308R (2001) suggests that initial curing methods be applied immediately after placing, as well as before and during the finishing process under hot weather conditions, to avoid plastic shrinkage cracking. This however, is often neglected, leaving concrete structures prone to cracking during the plastic period of concrete.

Literature on the effectiveness of initial curing during the plastic period is scarce and therefore leaves a significant knowledge gap on the influence of curing on the cracking behaviour of plastic concrete. In an attempt to investigate the behaviour of concrete structures exposed to initial curing methods; tests were conducted using two predetermined curing times during the plastic period. Figure 5-7 displays a typical capillary pressure build-up graph for Mix Ref, identifying two critical points during plastic shrinkage.

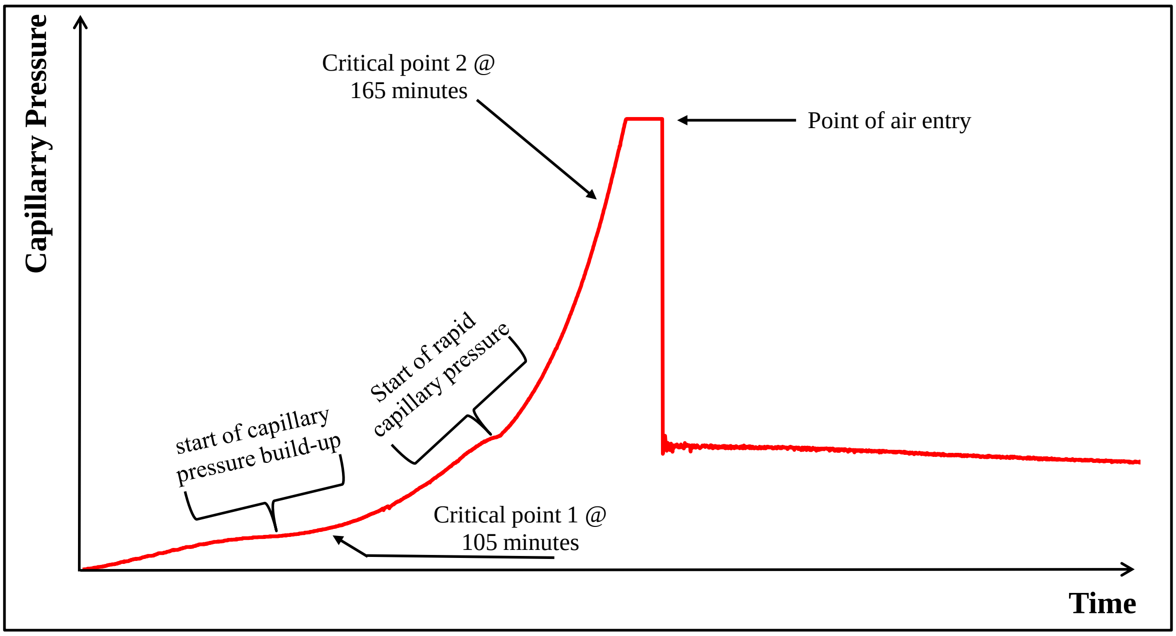

Figure 5-7: Identified critical points during capillary pressure build-up

The first critical point is identified as the start of capillary pressure build-up, which further marks the start of plastic shrinkage build-up in plastic concrete. The second important critical time is identified as the point where the rate of capillary pressure is at its peak. This corresponds to the point where the rate of displacement occurring due to plastic shrinkage is at its peak. These two critical points therefore represent two points where curing can be applied to prevent plastic shrinkage cracking.

Once the critical curing times were identified, plastic shrinkage, settlement, capillary pressure and cracking tests were carried out in the climate chamber for a period of 6 hours. Curing was then applied at the aforementioned critical times, using a fog spray to apply a thin layer of water over the surface of the concrete. Curing procedures were applied consistently to all moulds during the test period. The influence of curing on Mix Ref in terms of capillary pressure, shrinkage and crack area at each critical time is analysed and discussed in the following sections.

5.2.1 Influence of initial curing on the build-up of capillary pressure

Figure 5-8 displays typical capillary pressure results of Mix Ref, plotted against the capillary pressure results of curing applied at 105 minutes and 165 minutes on separate specimens. When no curing is applied, Mix Ref shows a build-up in capillary pressure at approximately 95 minutes after placement, followed by a significant increase in pressure build-up between 140 and 195 minutes. Thereafter, the pore pressure breaks indicating that air entry has occurred.

The second capillary pressure reading displays curing applied at approximately 105 minutes after placement. This was identified as the point where capillary pressure starts building up, indicating that the rate of bleeding is lower compared to the evaporation rate and therefore marks the start of plastic shrinkage. Results show that curing applied at 105 minutes, delays the build-up in capillary pressure by approximately 55 minutes after curing is applied. The capillary pressure then starts building up before reaching air entry at approximately 215 minutes. This therefore delayed air entry by approximately 25 minutes, compared to Mix Ref where no curing methods were applied.

The third capillary pressure reading displays curing applied at approximately 165 minutes after placement. This critical curing time marks a point approximately 30 minutes before point of air entry occurs. Results show that as curing is applied, the capillary pressure is immediately relieved, before building up again at approximately 200 minutes, reaching air entry at 240 minutes.

Results therefore show that curing applied just before the time of air entry, has a greater effect on delaying the point of air entry. Furthermore, by applying curing at 105 minutes, the build-up in capillary pressure is delayed, however at 165 minutes, curing relieves the accumulated capillary pressure, which could be a reason as to why the point of air entry is delayed by a greater amount compared to curing at 105 minutes.

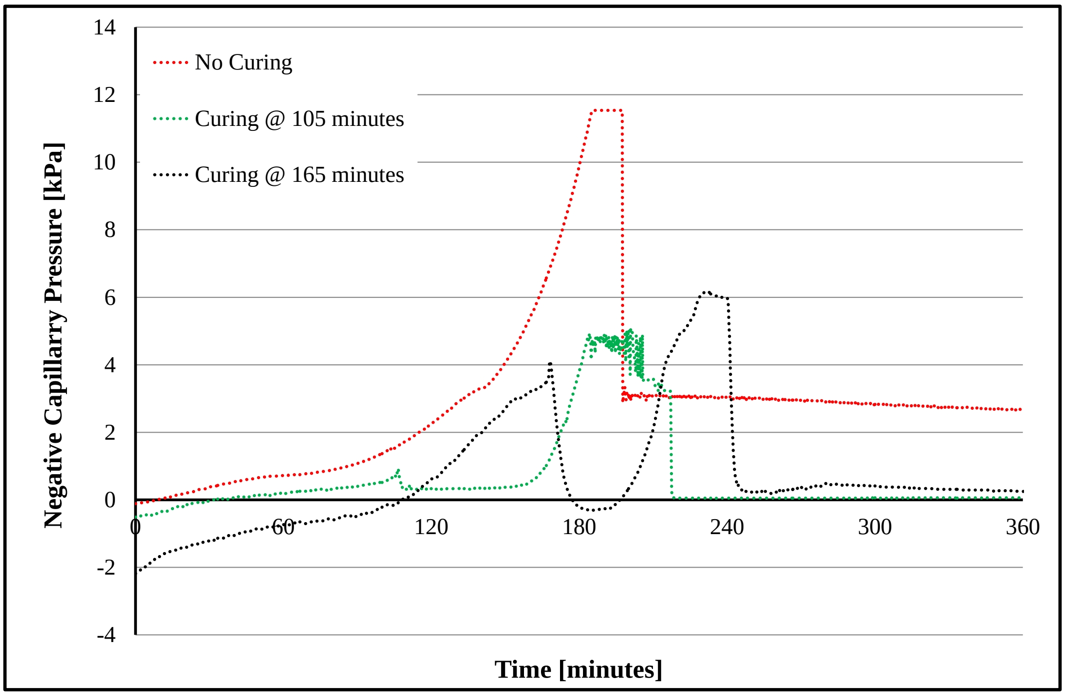

Figure 5-8: Capillary pressure results at different initial curing critical points

5.2.2 Influence of initial curing on plastic shrinkage

Figure 5-9 displays the average vertical shrinkage of Mix Ref plotted against the vertical shrinkages of specimens cured at 105 and 165 minutes after placement. All three results start building up in shrinkage at similar times before curing is applied at 105 minutes. This ceases shrinkage for approximately 50 minutes before the build-up in capillary pressure starts increasing vertical shrinkage to a final value of 0.245 mm. Similar to curing applied at 105 minutes, curing at 165 minutes ceases vertical shrinkage for approximately 45 minutes before increasing to a final vertical shrinkage value of 0.36 mm. This is similar to the final vertical shrinkage value of Mix Ref when no curing is applied. A possible explanation for this behaviour could be due the 0.24 mm of vertical shrinkage already present before curing is applied. Therefore any further capillary pressure build-up adds to the existing vertical shrinkage. This therefore possibly results in similar vertical shrinkage values compared to Mix Ref when no curing is applied.

Results indicate that delaying or relieving capillary pressure build-up, temporarily ceases vertical shrinkage until capillary pressure starts building up once more. Furthermore, by delaying the start of shrinkage through curing at 105 minutes, a larger reduction in vertical shrinkage is obtained, amounting to a 32 % difference in final vertical shrinkage values for curing applied at 165 minutes.

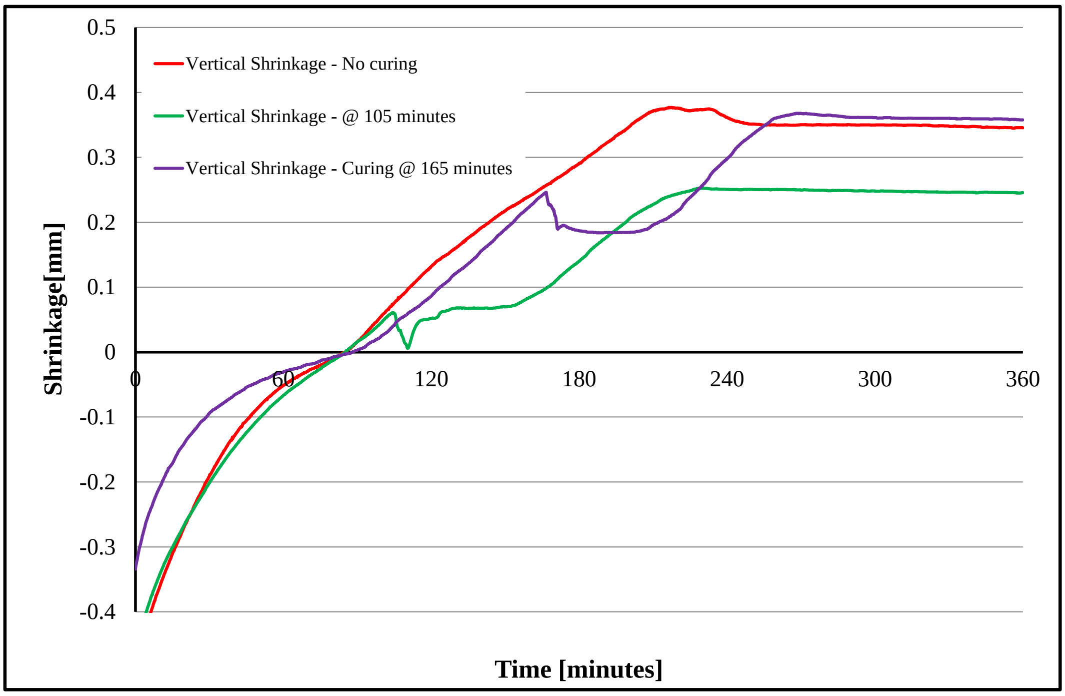

Figure 5-9: Influence of initial curing on vertical shrinkage

Figure 5-10 displays the average horizontal shrinkage of Mix Ref plotted against the horizontal shrinkages of specimens cured at 105 and 165 minutes after placement. Initially all three horizontal shrinkages are similar up to 105 minutes. At 105 minutes, curing is applied to certain samples which delays the build-up in horizontal shrinkage for approximately 60 minutes before building up to a final shrinkage value of 0.4 mm. Similar to curing applied at 105 minutes, curing at 165 minutes ceases shrinkage build-up for approximately 57 minutes before building up to a final value of 0.44 mm. This amounts to a 9 % difference and therefore it can be concluded that both curing times result in similar horizontal shrinkages, however curing at 105 minutes, seems to have a greater effect in reducing shrinkage build-up compared to the latter.

Comparing the results obtained for vertical and horizontal shrinkages, it is immediately apparent that initial curing seems to have a greater effect in reducing horizontal shrinkage build-up compared to vertical shrinkage. Furthermore, both horizontal and vertical shrinkage rates seem to decrease and cease at an earlier time when curing is applied at 105 minutes, compared to curing at 165 minutes. A possible reason for this occurrence could be due to the capillary pressure build-up that has already formed at the 165 minute curing time compared to the near zero values at 105 minute curing time. This therefore explains why shrinkage is slightly higher in the 165 minute curing results compared to the 105 minute curing results.

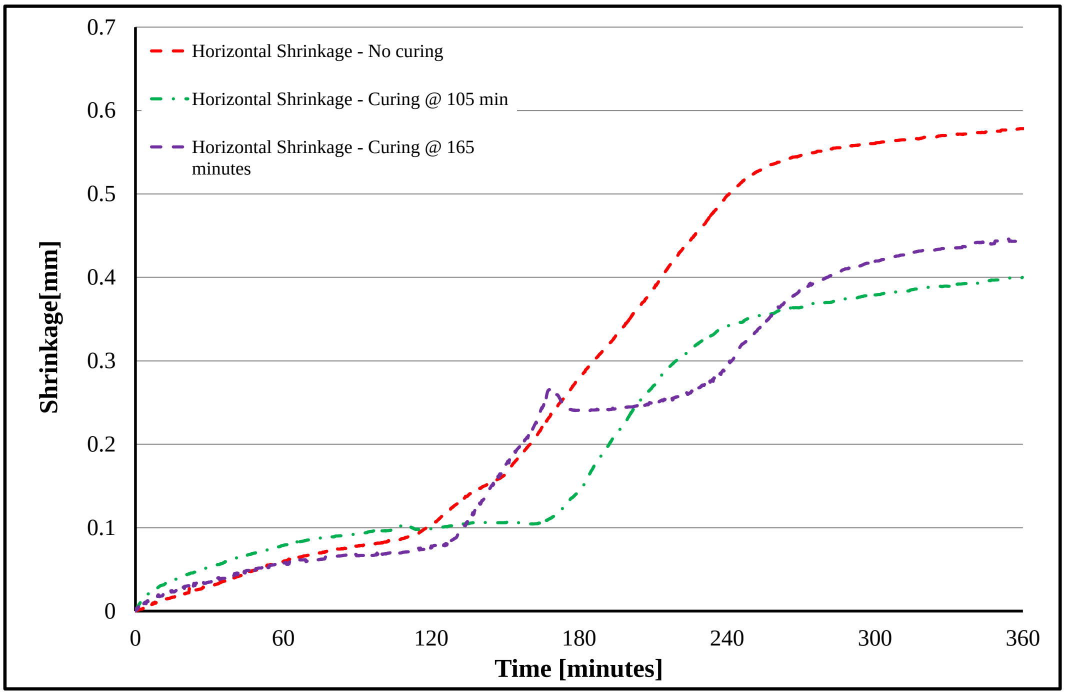

Figure 5-10: Influence of initial curing on horizontal shrinkage

5.2.3 Influence of initial curing on crack area

Figure 5-11 displays the cracking result of Mix Ref plotted against the cracking results of specimens cured at 105 and 165 minutes after placement. Mix Ref displayed a final crack area of 96 mm², followed by 85 mm² and 47 mm² for curing applied at 105 and 165 minutes respectively. Results show that curing applied at 165 minutes after placement, results in a larger crack area reduction, compared to specimens cured at 105 minutes. This however, contradicts the results discussed in Section 5.2.2, where curing applied at 105 minutes results in a lower vertical shrinkage and similar horizontal shrinkage compared to curing applied at 165 minutes after placement. However, Section 5.2.1, showed that point of air entry occurs 25 minutes earlier compared to specimens cured at 165 minutes. This therefore results in hairline cracks appearing at approximately 200 minutes after placement, compared to 260 minutes for specimens cured at 165 minutes. This possibly indicates that specimens cured at 105 minutes were exposed to plastic shrinkage for a longer period of time compared to specimens cured at 165 minutes after crack formation. The extended plastic shrinkage exposure, possibly results in a longer crack growth period, allowing the crack to increase in area for a longer period of time. This suggests that samples cured at 105 minutes contained a greater amount of stress build-up compared to specimens cured at 165 minutes.

Relaxation results discussed in Section 4.5 suggest that capillary pressure relaxes upon ceasing the actuator. Therefore it can be assumed that if curing relieves the capillary pressure, it also relieves any stresses due to shrinkage and settlement. Therefore Mix Ref cured at 165 minutes had a smaller crack area since after curing it showed much less shrinkage than when cured at 105 minutes. This is discussed further in Section 5.5.

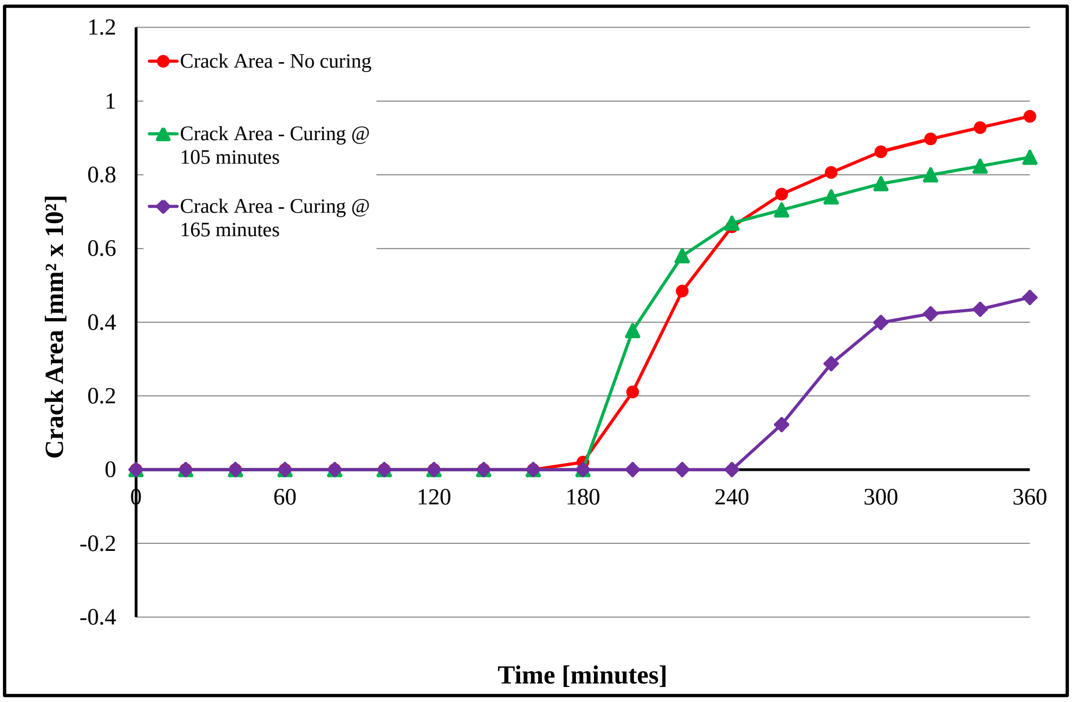

Figure 5-11: Influence of initial curing on crack area

Furthermore, by delaying point of air entry or more specifically crack formation, gives the plastic concrete sufficient time to develop strength, which possibly results in a lower crack area. Cracking for specimens exposed to no curing as well as specimens exposed to curing at 105 minutes, occurs during the setting phase. Whereas specimens cured at 165 minutes, cracked during the hardening phase, where the tensile strength is believed to develop significantly. This added tensile capacity possibly added towards a lower crack area for specimens cured at 165 minutes.

Results therefore show that curing applied at certain points during the build-up in capillary pressure, reduces cracking in plastic concrete; however, it does not prevent cracking. This therefore suggests that curing applied only once is not sufficient. However, if this is the only option, then curing applied just before the time of air entry, gives greater potential towards reducing crack areas.

5.3 Influence of viscosity and curing procedures on the cracking behaviour of concrete

Section 5.2 identified curing applied at 165 minutes as being more effective in reducing final crack area compared to curing applied at 105 minutes. Therefore this section aims to investigate the effect of Mix VMA, exposed to curing at 165 minutes, on the cracking behaviour of fresh concrete. Section 5.1 showed that Mix Ref and Mix VMA, share similar capillary pressure behaviours, in terms of capillary pressure build-up and points of air entry. This therefore means that both mixes share similar critical points, where plastic shrinkage is at its peak. A critical time period at approximately 165 minutes, was identified as the point where capillary pressure builds up rapidly just before air entry.

A more detailed analysis on the effect of curing at 165 minutes on Mix Ref is first discussed and analysed in Section 5.3.1. Thereafter Mix VMA is analysed and compared to Mix Ref in Section 5.3.2

5.3.1 Influence of curing procedures on Mix Ref

The effect of curing on capillary pressure, shrinkage and crack area on Mix Ref versus the results obtained in Section 5.1.1 for Mix Ref under no curing conditions, is shown in Figure 5-12. Initially, the capillary pressure starts building up at approximately 88 minutes after placing; reaching a final value of 4 kPa before dropping instantly once curing is applied. At this point, almost all of the induced capillary pressure is relieved after building up for a period of 80 minutes. The capillary pressure then starts building up 25 minutes after curing is applied, before reaching air entry at 240 minutes.

Similar to Figure 5-5, the vertical and horizontal shrinkage starts increasing rapidly after the initial settlement period. This rapid rate of increase in plastic shrinkage ceases immediately as the capillary pressure is relieved. Once the capillary pressure starts building up for the second time, the vertical and horizontal shrinkages increase to a final value of 0.358 and 0.443 mm respectively. This amounts to a 3.5 % increase in vertical shrinkage and a 24 % decrease in horizontal shrinkage compared to the results obtained for Mix Ref without any curing procedures applied. Crack formation, occurs at 260 minutes with a final crack area of 47 mm², amounting to a 51 % decrease in crack area compared to Mix Ref without any applied curing methods.

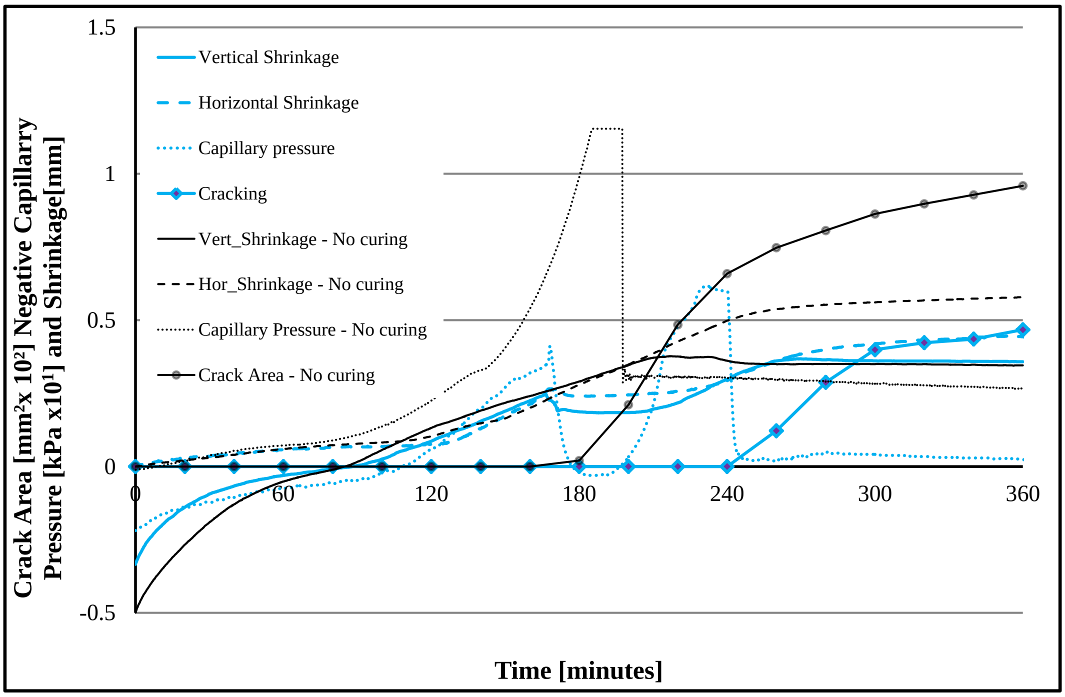

Figure 5-12: Curing applied on Mix Ref at 165 minutes

Section 5.1.2 identified the settlement of solid particles occurring during the beginning stages of the stiffening phase, as one of the main contributors to crack formation. Thereafter, plastic shrinkage is believed to drive crack growth as evaporation removes water from the capillary pores. Results show that curing significantly reduces the horizontal plastic shrinkage and corresponding crack area. Vertical shrinkage is slightly increased, however, this difference of 3.5 %, can be considered negligible and therefore relieving the capillary pressure build-up during the setting stage, shows no real influence on the vertical shrinkage of the specimens. However, the reduction in horizontal shrinkage significantly reduced the amount of cracking occurring after the point of air entry.

5.3.2 Influence of curing procedures on Mix VMA

Figure 5-13 displays the capillary pressure, shrinkage and crack area results for curing applied between 165 and 170 minutes for Mix VMA. Similar to Mix Ref, the capillary pressure starts building up at approximately 85 minutes, reaching a maximum value of 7.7 kPa before curing is applied. Directly after curing is applied, the capillary pressure drops rapidly, relieving the entire pressure built-up over a period of 90 minutes. Thereafter the capillary pressure starts building up at approximately 25 minutes after curing is applied, before reaching air entry at 240 minutes, similar to Mix Ref.

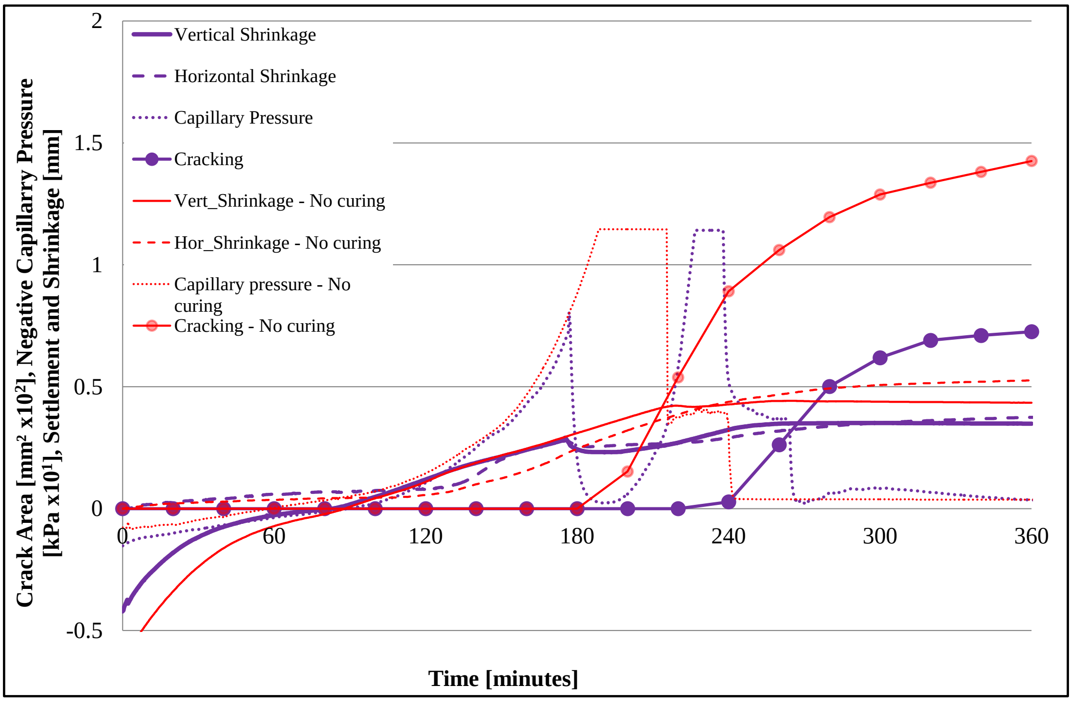

Figure 5-13: Curing applied on Mix VMA at 165 minutes

The initial build-up in capillary pressure creates a corresponding increase in both vertical and horizontal shrinkage. Once curing is applied, both shrinkages remain largely constant before increasing in rate as the capillary pressure builds up. This increase, results in a final vertical and horizontal shrinkage of 0.35 and 0.37 mm respectively. This amounts to a 14 % and 33 % decrease in vertical and horizontal shrinkage respectively. Crack formation occurs at a similar time compared to Mix Ref, reaching a final crack area of 73 mm². This amounts to a 49 % decrease in crack area for Mix VMA.

Both Mix Ref and Mix VMA share similar behaviour trends after curing is applied, with no significant difference between results. Both mixes relieve capillary pressure build-up after curing is applied which ceases plastic shrinkage, until capillary pressure starts building up for the second cycle, at which point both horizontal and vertical shrinkages start increasing in rate. Furthermore, both mixes display similar crack area reductions of 51 % and 49 % for Mix Ref and VMA respectively. Mix VMA, however, displayed a greater reduction in horizontal and vertical shrinkages (-14 % and -33 % respectively), compared to Mix Ref (+3.5 % and 24 % respectively). This possibly implies that Mix VMA contains a greater amount of stress reduction ability compared to Mix Ref. However, given that Mix VMA reduces a greater amount of stress build-up compared to Mix Ref, the crack area difference between the two mixes remains largely the same at 36 %, compared to the crack area difference of 32 % when no curing is applied.

The larger relaxation potential of Mix VMA in Section 4.3.2, possibly explains why Mix VMA results in a larger plastic shrinkage reduction. However as discussed in Section 5.1.2, the lower tensile strength capacity, explains why Mix VMA results in a larger crack area.

5.4 Link between the tensile properties and cracking behaviour of plastic concrete

Section 4.2 highlights a number of interesting behaviour trends of plastic concrete. The tensile strength develops slowly during the stiffening phase, where most of the tensile strength capacity is believed to be a result of the capillary pressure holding the concretes particles together. The strength thereafter, develops significantly during the setting phase, as the concrete changes from a plastic to a solid material; however the hardening phase is where the tensile strength is believed to develop at a significantly faster rate compared to the setting phase. In addition to the tensile strength, the strain capacity decrease by almost 70 % (Mix Ref) as the concrete enters the setting phase.

Combrinck and Boshoff (2009), identified plastic shrinkage cracking as most likely to occur during the setting phase of the concrete. The current cracking results, in agreement with

Combrinck and Boshoff (2009), showed that visible crack formation and growth both occur during the setting phase. This is largely due to the high amount of shrinkage occurring as ongoing evaporation continues to draw out pore water from the concrete. This creates a capillary pressure build-up, at which point the break in capillary pressure symbolises the point of air entry. Soon after air entry occurs, visible hairline cracks appear on the surface of the concrete. Continued shrinkage, is believed to contribute towards further crack growth in the concrete. In addition to this, the low tensile strength and strain capacity of the concrete during the setting phase, gives an indication as to why plastic concrete is vulnerable during this stage and possibly explains why cracking occurs during the setting phase.

Mix VMA presented similar plastic shrinkage values compared to Mix Ref; however crack areas between the two mixes varied greatly. The difference in setting time, yield stress and surface tension could all be possible reasons as to why Mix VMA resulted in a larger crack area. Mix VMA, showed similar strain capacities compared to Mix Ref, however the tensile strength of Mix VMA, varies greatly compared to Mix Ref. The addition of VMA at such a high dosage to the concrete is believed to increase the water-to-cement ratio of the mix, which could possibly explain the lower and slower tensile strength development of Mix VMA compared to Mix Ref. This low tensile strength is believed to be reason as to why Mix VMA showed greater crack areas compared to Mix Ref.

Furthermore, initial curing results indicate that curing applied just before air entry, results in a larger crack area reduction compared to curing applied before the capillary pressure starts building up. By applying curing at 165 minutes, point of air entry is delayed to a greater extent compared to curing applied at 105 minutes. This possibly allows the concrete to gain a larger amount of strength before crack formation occurs. Tensile strength results show that the measured tensile strength of Mix Ref, during the hardening phase of concrete, is much greater compared to the strengths obtained during the setting phase. Therefore it is possible that the larger tensile strength capacity, contributes to a lower crack area.

5.5 Link between the relaxation behaviour and curing behaviour of plastic concrete

In practice, concrete elements with large open surfaces are at great risk to plastic shrinkage cracking. Under evaporation rich conditions, the stress build-up in concrete occurs at a slower rate compared to the mechanically induced stress used in Chapter 4. At this slow rate, the concrete is believed to be able to continually relax part of the stress as it builds up. Under curing conditions, by lightly wetting the atmosphere above the surface of the concrete, the relaxation behaviour also decreases the stress build-up in the concrete by reducing the capillary pressure build-up due to ongoing evaporation. Concrete with a greater relaxation potential, is therefore expected to experience less stress build-up and greater benefits from curing.

The initial curing results discussed in Section 5.2 showed that curing applied before the build-up in capillary pressure, results in a lower amount of vertical and horizontal shrinkage compared to curing applied before the point of air entry. However, specimens cured before the build-up in capillary pressure, results in a larger crack area compared to specimens cured before point of air entry. This displays slightly contradictory results. However, the relaxation results discussed in Section 4.3, suggests that the capillary pressure relaxes when the actuator ceases. Therefore since capillary pressure was identified as the mechanism behind relaxation, it can be assumed that if curing relieves the capillary pressure build-up, it also relieves any stress build-up due to shrinkage and settlement. Therefore Mix Ref cured at 165 minutes had less cracks, since after curing it showed much less shrinkage than when cured at 105 minutes. This is visually displayed in Figure 5-9 for the vertical shrinkage and Figure 5-10 for the horizontal shrinkage.

Mix Ref showed a much smaller relaxation potential during the setting stage, while Mix VMA was able to relax more of the mechanically induced stress during the stiffening and setting phases, at a cost of a lower tensile capacity. This implies that in practice, Mix VMA is able to relax a larger amount of stress build-up; however the lower tensile capacity may affect the cracking behaviour of the concrete. Section 5.3 aimed to investigate the influence of curing procedures on Mix VMA. By applying the same aforementioned principal of stress and capillary pressure relaxation, Mix VMA showed much less shrinkage build-up after applying curing at 165 minutes compared to Mix Ref. Furthermore, the total reduction in shrinkage for Mix VMA was slightly larger than Mix Ref. Therefore, consistent with relaxation results in Section 4.3, Mix VMA displayed a greater relaxation potential compared to Mix Ref. However, the larger crack area of Mix VMA is due to the lower tensile capacity of the concrete. This ultimately results in a large crack area, even though a greater amount of stress relaxation occurred.

5.6 Concluding summary

This section discussed the fundamental and phenomenological cracking behaviour of Mix Ref compared to Mix VMA. Furthermore, the influence of initial curing on the cracking behaviour of plastic concrete was addressed and compared to Mix VMA. Lastly links between the tensile properties and cracking behaviour as well as links between initial curing and the relaxation behaviour of plastic concrete were presented. Conclusions based on Chapter's 4 and 5 as well as recommendations for potential future studies are discussed in the next chapter.

Chapter 6: Conclusions and recommendations

This study investigated the tensile and relaxation behaviour of plastic concrete as well as its resistance to multiple loading. Furthermore the cracking behaviour of plastic concrete was investigated as well as the influence of initial curing on the cracking behaviour of plastic concrete. In addition to these tests, a viscosity modified concrete mix was used to investigate the influence of an admixture based viscosity modifying agent on the tensile, relaxation and cracking behaviour of plastic concrete. The significant conclusions that can be drawn from this study are discussed in Sections 6.1 to 6.8, while possible potential recommendations for future research are discussed in Section 6.9

6.1 Influence of VMA on the rheological properties

- The addition of a 0.8 % VMA dosage to a conventional concrete mix, displayed a decrease in yield stress and an increase in the viscosity of the concrete. In addition to this, the surface tension of the mixing water was significantly reduced after the addition of the VMA. Furthermore, the addition of the VMA resulted in a slightly retarded setting time compared to the reference concrete mix.

- The high 0.8 % dosage of VMA is believed to increase the water-to-cement ratio of the concrete mix, which further explains the decrease in yield stress, slump measurement and slightly retarded setting times.

6.2 The tensile material properties of plastic concrete

- The initial ascending portion of the stress versus strain results, proved adequate in determining the pre-peak tensile properties of plastic concrete.

- The tensile strength of plastic concrete showed very little strength gain during the stiffening phase of the concrete. However, the strength increased exponentially during the setting and hardening phases.

- The strain capacity decreases significantly during the setting period of the concrete. This together with the low tensile strength during the setting phase possibly explains why plastic shrinkage cracking often occurs during the setting phase of the concrete.

- The Young's modulus results, increased rapidly during the setting phase of the concrete. Furthermore, the Young's modulus results incorporating the final non-linear portion of the concrete, displayed a significantly lower elasticity compared to the Young modulus results obtained from the linear portion of the ascending curve. This is mainly due to the excessive strain occurring as the concrete nears the non-linear portion of the ascending stress versus strain graph.

- Capillary pressure results show that most of the measured strength gain during the stiffening phase of the concrete is due to the capillary pressure in pores of the fresh concrete which keeps the particles together. This therefore indicates that the presence of free water in plastic concrete is responsible for much of the tensile strength experienced for the 60 and 120 minute test results. The 120 minute test results showed a slight strength gain, indicating that part of the measured strength is due to the commencement of the hydration reactions, providing the concrete with added tensile strength. The 180 minute test results displayed much higher tensile strength magnitudes compared to the 60 and 120 minute test results. Although much of the strength measured is believed to be due to the hydration products bridging the gaps between molecules, however, the presence of free water in the gauge area indicates that part of the measured strength is also due to the capillary pressure holding the particles in place. At 240 minutes, most of the strength gain is believed to be due to the hydration products since a very low pore pressure was measured, indicating that the hydration products prevent the pores and pore water from moving, giving an indication of the low amount of pore water present in the concrete.

- The capillary pressure results, therefore, give an indication of two phenomena. The first describes the rate of hydration affecting the interconnectivity of pores while the second describes the contribution of capillary pressure to the measured strength gain.

6.3 The influence of VMA on the tensile material properties

- Mix VMA displayed similar behaviour in terms of tensile strength compared to Mix Ref, however the addition of VMA, significantly reduced the tensile strength of the concrete during the setting and hardening phases. This is believed to be due to the higher water-to-cement ratio of the concrete after the addition of the VMA. This, together with the higher slump measurement and slightly retarded setting time, explains why Mix VMA displayed a reduced tensile strength capacity.

- Mix VMA displayed similar strain capacity behaviour as that of Mix Ref, in that the strain capacity decreased significantly during the setting phase of the concrete.

- Mix VMA displayed a lower elasticity magnitude compared to Mix Ref. The tensile strength of Mix VMA compared to Mix Ref, is believed to be the reason for this occurrence.

- Similar to Mix Ref, capillary pressure results indicate that much of the strength gain experienced for the 60 and 120 minute test samples is believed to be due to the capillary pressure within pores holding the particles together. Results also indicate that part of the 180 minute test samples measured strength is partly due to the capillary pressure within capillary pores.

- Using the Gauss Laplace equation, the lower surface tension of pore water in Mix VMA, results in a lower capillary pressure within pores compared to Mix Ref. Therefore this indicates that if the pore pressure is believed to be responsible for part of the measured strength, the lower capillary pressure in Mix VMA could be a reason as to why Mix VMA displayed lower tensile strengths compared to Mix Ref.

6.4 The relaxation behaviour of plastic concrete

- The relaxation behaviour of plastic concrete was successfully measured using the direct tensile test setup. Results indicate that the 60 and 120 minute test samples are able to reduce a larger amount of stress build-up compared to the 180 and 240 minute test samples. This therefore indicates that the relaxation behaviour of plastic concrete is dependent on the rate of hydration.

- Multiple loading results indicate that concrete at 60 and 120 minutes are able to complete multiple loading cycles compared to the 180 and 240 minute test samples. The ability to complete multiple loading cycles gives an indication of the resilient nature of concrete during the stiffening phase.

- Results indicate that the mechanism behind the relaxation behaviour of plastic concrete is due to the negative capillary pressure build-up induced by the mechanical applied tensile strain.

6.5 The influence of VMA on the relaxation behaviour of plastic concrete

- Mix VMA displayed a higher relaxation potential during all four time periods compared to Mix Ref. The relaxation behaviour of Mix VMA under multiple loading cycles, show that Mix VMA is able to complete a few more cycles during the 180 and 240 minute time periods compared to Mix Ref.

- Capillary pressure results indicate that Mix VMA contains a larger amount of free water and therefore results in a larger relaxation potential compared to Mix Ref. Furthermore, the slightly slower rate of hydration indicates that Mix VMA contains a clearer path of interconnectivity between pores compared to Mix Ref. This also explains why a larger amount of relaxation potential occurs in Mix VMA.

6.6 Influence of VMA on the plastic cracking behaviour

- Mix VMA displayed a lower bleed and evaporation rate compared to Mix Ref. Therefore consistent with literature, the added cohesion through the addition of VMA reduces the amount of bleeding.

- Settlement in Mix VMA was significantly higher compared to Mix Ref. This is believed to be due to the increased high dosage of Mix VMA, which possibly increased the water-to-cement ratio of the concrete, resulting in a higher slump measurement. The higher slump measurement is believed to result in a higher settlement of solid particles compared to Mix Ref.

- The method used to investigate the portion of plastic shrinkage after settlement ceased, proved adequate since both vertical and horizontal shrinkages shared similar start times and rates of build-up in both horizontal and vertical shrinkage.

- Vertical shrinkage showed slightly higher cumulative shrinkage values compared to Mix Ref. However this difference was fairly minimal. Furthermore, horizontal shrinkages for both mixes, shared similar values and it can therefore be concluded that the influence of VMA on the plastic shrinkage of concrete is minimal.

- Mix VMA resulted in a much larger crack area compared to Mix Ref. A possible reason for this occurrence could be due to the high initial settlement rate, which possibly resulted in settlement cracks during the stiffening phase of the concrete. This therefore indicates that crack formation occurred much earlier compared to Mix Ref and only became visible once plastic shrinkage contributed towards further crack growth. Another possible reason could be due to the low tensile strength observed for Mix VMA compared to Mix Ref. The low tensile strength of Mix VMA could increase crack growth and result in a larger crack area compared to Mix Ref at the end of the 360 minute test duration.

6.7 Influence of initial curing on the plastic cracking behaviour

- Curing results indicate that curing applied just before the time of air entry, has a greater effect on delaying the point of air entry compared to curing applied before the build-up in capillary pressure.

- Curing applied before the build-up in capillary pressure, results in lower horizontal and vertical shrinkage compared to curing applied before the point of air entry occurs.

- Curing applied just before point of air entry, results in a smaller crack area compared to curing applied before the build-up in capillary pressure. Relaxation results suggest that capillary pressure relaxes upon ceasing the actuator. Therefore it can be assumed that if curing relieves the capillary pressure build-up, it also relieves any stresses due to shrinkage and settlement. Therefore, although samples cured at 165 minutes displayed larger amounts of plastic shrinkage, it is assumed that a smaller amount stress exist within these samples compared to samples cured at 105 minutes. Mix Ref cured at 165 minutes showed a smaller crack area since after curing it showed much less shrinkage than when cured at 105 minutes.

- Results therefore indicate that applying curing only once, is not sufficient in prevent plastic cracking. However if this is the only option, curing applied just before the point of air entry, contains greater benefits in terms of crack area reduction compared to curing applied before the build-up in capillary pressure.

6.8 Influence of VMA on curing procedures

- Both Mix Ref and Mix VMA, share similar vertical and horizontal shrinkages after curing procedures are applied. However, Mix VMA displayed a slightly larger stress reduction compared to Mix Ref. The larger relaxation potential of Mix VMA, possibly explains why this occurs. However Mix VMA still results in a larger crack area compared to Mix Ref. The lower tensile strength capacity of Mix VMA is believed to be the resulting cause of the larger crack area.

6.9 Recommendations

From the knowledge gained in this study, several aspects hold potential for future research and include the following:

- The current method of determining capillary pressure build-up proved adequate; however the reliability of the sensors after numerous testing becomes a factor. Development of a new robust, wireless capillary pressure sensor system with chargeable batteries will assist in easing the measurement of capillary pressure in fresh concrete. Furthermore, the wireless system will allow measurements to be conducted on construction sites in real world conditions. This will also push towards standardising capillary pressure monitoring in the construction industry.

- Capillary pressure measurements should be conducted in cracking tests in order to obtain a more accurate air entry time.

- An investigation into the mechanism responsible for crack area reduction through the addition of fibres in plastic concrete can be explored using the direct tensile setup together with plastic shrinkage and cracking tests.

- Initial curing procedures should be explored in greater detail using a wider variety of curing times and admixtures. This together with a more suitable quantification of relaxation may assist in producing a possible cracking model. Furthermore, cracking tests should be divided into pure plastic settlement and pure plastic shrinkage cracking tests in order to obtain better cracking observations.

- The development of a rheological tool box which provides a link between yield stress and workability may be useful towards standardising the use of rheometers on the construction site

References

Abel, J., & Hover, K. (1998). Effect of Water/Cement Ratio on the Early Age Tensile Strength of Concrete. Transportation Research Record: Journal of the Transportation Research Board, (1610), 33-38.

ACI 116R-90. (1990). Cement and concrete terminology. Detroit,USA: American Concrete Institute.

ACI 201.1R. (2008). Guide for conducting a visual inspection of concrete in service Farmington Hills: American Concrete Institute.

ACI 224R-80. (1984). Control of cracking in concrete structures (224R-80). Detroit,Michigan: American Concrete Institute.

ACI 231R. (2010). Report on early-age cracking: Causes, measurement, and mitigation. Farmington Hills: American Concrete Institute.

ACI 308R. (2001). Guide to curing concrete. Farmington Hills: American Concrete Institute.

Aldea, C., Shah, S. P., & Karr, A. (1999). Permeability of Cracked Concrete. Materials and Structures. Materiaux Et Constructions, 32(219), 370-376.

Al-Qassag, O., Darwin, D., & O'Reilly, M. (2016). Effect of a Rheology Modifier on Settlement Cracking of Concrete (No. 116a), Kansas, USA: The University of Kansas Center for Research.

ASTM C125-93. (1993). Standard definitions and terms relating to concrete and concrete aggregates. West Conshohocken,USA: American Society for Testing and Materials.

ASTM C1579. (2006). Standard test method for evaluating plastic shrinkage cracking of restrained fiber reinforced concrete. West Conshohocken, Philadelphia: American Society for Testing and Materials.

ASTM C232. (2004). Standard test methods for bleeding of concrete. West Conshohocken, Philadelphia: American Society for Testing and Materials.

References

ASTM D971. (2004). Standard test method for interfacial tension of oil against water by the ring method. West Conshohocken, Philadelphia: American Society for Testing and Materials.

Banfill, P. (2006). Rheology of Fresh Cement and Concrete. Rheology Reviews, 2006, 61.

Bentz, D. P. (2007). Cement Hydration: Building Bridges and Dams at the Microstructure Level. Materials and Structures/Materiaux Et Constructions, 40(4), 397-404. doi: 10.1617/s11527-006-9147-3

Bentz, D. P., Peltz, M. A., & Winpigler, J. (2009). Early-Age Properties of Cement-Based Materials. II: Influence of Water-to-Cement Ratio. Journal of Materials in Civil Engineering, 21(9), 512-517. doi: 10.1061/(ASCE)0899-1561(2009)21:9(512)

Boshoff, W. P., & Combrinck, R. (2013). Modelling the Severity of Plastic Shrinkage Cracking in Concrete. (Cement and Concrete Research), 34-39.

Brunauer, S., & Copeland, L. (1964). The Chemistry of Concrete. Scientific American, 210(4), 80-93.

BS EN 206. (2013). Bs En 206: 2013+a1:2016. United Kingdom: BSI Standards Limited 2016.

CCIP-048. (2010). Non-structural cracks in concrete. (No. 048).The Concrete Society: A cement and Concrete Industry Publication.

Chhabra, R. P., & Richardson, J. F. (2008). Chapter 1 - non-newtonian fluid behaviour. In R. P. Chhabra, & J. F. Richardson (Eds.), Non-newtonian flow and applied rheology (second edition) (pp. 1-55). Oxford: Butterworth-Heinemann. doi: https://doi-org.ez.sun.ac.za/10.1016/B978-0-7506-8532-0.00001-9

Chryso SA. (2007). General catalogue (1st Ed.). Boksburg: Chryso South Africa.

Combrinck, R. (2016). Cracking of Plastic Concrete in Slab-Like Elements. Stellenbosch University. Faculty of Engineering. Dept. of Civil Engineering. Stellenbosch

Combrinck, R., & Boshoff, D. W. (2009). Plastic shrinkage cracking of fresh concrete. (No. ISI2009-31).

References

Combrinck, R. (2012). In Boshoff W. P., Stellenbosch University. Faculty of Engineering. Dept. of Civil Engineering. (Eds.), Plastic shrinkage cracking in conventional and low volume fibre reinforced concrete. Stellenbosch: Stellenbosch University.

Coussot, P. (2012). 1 - Introduction to the rheology of complex fluids. In N. Roussel (Ed.), Understanding the rheology of concrete (pp. 3-22) Woodhead Publishing. doi: https://doi-org.ez.sun.ac.za/10.1533/9780857095282.1.3

Cracolice, M., & Peters, E. (2006). Basics of introductory chemistry; an active learning approach (Third edition). Portland: Ringgold Inc.

Dao, V. T., Dux, P. F., & Morris, P. H. (2009). Tensile Properties of Early-Age Concrete. ACI Materials Journal, 106(6)

Delsaute, B., Boulay, C., & Staquet, S. (2016). Creep testing of concrete since setting time by means of permanent and repeated minute-long loadings doi: http://dx.doi.org.ez.sun.ac.za/10.1016/j.cemconcomp.2016.07.005

Domone, P., &Illston, J. (Eds.). (2010). Construction materials their nature and behaviour (4th Ed.). New York: Spoon Press.

Domone, P., Xu, Y., & Banfill, P. (1999, Developments of the two-point workability test for high-performance concrete. Magazine of Concrete Research. No.3, 171-179.

EFNARC. (2006). Guidlines for viscosity modifying admixtures for concrete European Federation of National Associations Representing for Concrete.

EN 196-3. (2005). Methods for testing cement - part 3: Determination of setting times and soundness. Brussels: European Committee for Standardization.

Germann Instruments. (2010). Product Catalogue – ICAR Rheometer. Illinois : Germann Instruments Inc. doi: http://germann.org/products-by-application/rheology-of-concrete/icar-rheometer

Hannant, D., Branch, J., & Mulheron, M. (1999). Equipment for Tensile Testing of Fresh Concrete. Magazine of Concrete Research, 51(4), 263-267.

Hanson, W. (2011). Report on early-age cracking. ACI Committee 231.

Jeknavorian, A. A. (2016). Viscosity modification admixtures: A handy chemical admixture for the concrete producer. Retrieved 20 November, 2017, from http://www.theconcreteproducer.com/how-to/concrete-production/viscosity-modifying-admixtures_o

Kasai, Y., Vokoyama, K., & Matsui, I. (1972). Tensile properties of early-age concrete. Proceedings of Conference on Mechanical Behaviour of Materials.

Khayat, K. H., & Mikanovic, N. (2012). 8 - viscosity-enhancing admixtures and the rheology of concrete. In N. Roussel (Ed.), Understanding the rheology of concrete (pp. 209-228) Woodhead Publishing. doi: https://doi-org.ez.sun.ac.za/10.1533/9780857095282.2.209

Koeler, E. P., & Fowler, D.W. (2004).Development of a portable rheometer for fresh Portland cement concrete. ICAR Report 105-3F. Aggregates Foundation for Technology, Research and Education (AFTRE)

Kovler, K., & Roussel, N. (2011). Properties of fresh and hardened concrete doi: https://doi-org.ez.sun.ac.za/10.1016/j.cemconres.2011.03.009

Kwak, H., & Ha, S. (2006). Plastic Shrinkage Cracking in Concrete Slabs. Part II: Numerical Experiment and Prediction of Occurrence. Magazine of Concrete Research, 58(8), 517-532. doi: 10.1680/macr.2006.58.8.517

Leemann, A., & Winnefeld, F. (2007). The effect of viscosity modifying agents on mortar and concrete doi: https://doi-org.ez.sun.ac.za/10.1016/j.cemconcomp.2007.01.004

Mehta, P. K., & Monteiro, P. J. M. (2006). Concrete: Microstructure, properties and materials (3rd ed.). New York: McGraw-Hill.

Neville, A. M. (1963). Properties of concrete. London: Sir Isaac Pitman & Sons, LTD.

Nguyen, D., & Dao, V. (2015). Tensile properties of early-age concrete. Proceedings of the 27th Biennial National Conference of the Concrete Institute of Australia in Conjunction with the 69th RILEM Week, Melbourne, Australia, 1314-1324.

Nguyen, D. H., Dao, V. T. N., & Lura, P. (2017). Tensile Properties of Concrete at very Early Ages. Construction and Building Materials, 134, 563-573. doi: 10.1016/j.conbuildmat.2016.12.169

Østergaard, L., Lange, D. A., Altoubat, S. A., & Stang, H. (2001). Tensile Basic Creep of Early-Age Concrete Under Constant Load. Cement and Concrete Research, 31(12), 1895-1899.

Owens, G. (2009). Fulton's concrete technology (9th Ed.). Midrand, South Africa: Cement & Concrete Institution.

Pane, I., & Hansen, W. (2008). Predictions and Verifications of Early-Age Stress Development in Hydrating Blended Cement Concrete. Cement and Concrete Research, 38(11), 1315-1324. doi: 10.1016/j.cemconres.2008.05.001

Powers, T. C. (1968). The properties of fresh concrete. New York: John Wiley & Sons, Inc.

Rame'-hart. (2014). Surface tension and viscosity. Retrieved November, 15, 2017, from http://www.ramehart.com/newsletters/2014-03_news.htm

Roziere, E., Cortas, M. & Ahmed L. (2015). Tensile Behaviour of early age concrete: New methods of investigation. Cement and Concrete Composites, 55, 153-161.

SANS 201. (2008). Sieve analysis, fines content and dust content of aggregates. Pretoria, South Africa: South African Bureau of Standards.

Sant, G., Dehadrai, M., Bentz, D., Lura, P., Ferraris, C. F., Bullard, J. W., & Weiss, J. (2009). Detecting the Fluid-to-Solid Transition in Cement Pastes.

Shetty, M. S. (2008). Concrete technology theory and practice (7th Ed.). New Delhi: S. Chand & Company PVT. LTD.

Slowik, V., & Schmidt, M. (2010). Early Age Cracking and Capillary Pressure Controlled Concrete Curing. Advance in Cement-Based Material,

Slowik, V., Schmidt, M., & Fritzsch, R. (2008). Capillary pressure in fresh cement-based materials and identification of the air entry value doi: https://doi-org.ez.sun.ac.za/10.1016/j.cemconcomp.2008.03.002

References

Tailhan, J., Rossi, P., & Caucci, A. M. (2014). Probabilistic Modelling of Cracking in Concrete Structures. European Journal of Environmental and Civil Engineering, , 1-10. doi: 10.1080/19648189.2013.878256

Troxell, G. (1956). In Davis H. E., Composition and properties of concrete New York, N.Y.: McGraw-Hill.

Uno, P. J. (1998). Plastic Shrinkage Cracking and Evaporation Formulas. ACI Materials Journal, 95, 365-375.

Wittmann, F. (1976). On the Action of Capillary Pressure in Fresh Concrete. Cement and Concrete Research, 6(1), 49-56.

Zhao, X., Wei, J., & Liu, Z. (2004). Durability of Concrete Under Multi-Damage Action. Journal of Wuhan University of Technology-Mater.Sci.Ed., 19(2), 73-75. doi: 10.1007/BF03000175